Proceedings
of

9th Annual Continuous Mixer and Extruder Users Group Meeting

June 2-4, 1997
Lincoln Harbor, New Jersey

Chairwoman for 97 Meeting:
Ms. Eileen Heider
Picatinny Arsenal, New Jersey

Co-Chairmen for Continuous Mixer and Extruder Users Group Meeting:
Mr. David F. Fair, Army
Mr. Kirk E. Newman, Navy

Hosted by:
Highly Filled Materials Institute
Stevens Institute of Technology
Castle Point Station
Hoboken, New Jersey 07030
Tel. (201) 216-5030 / Fax (201) 216-5601
dkalyon@stevens-tech.edu

Extruder Users Group Meeting; Program - June 2-4. 1997
Lincoln Harbor, NJ
Hosted by: HfMI/Stevens

June 2, 1997

SESSION I – 8:30 a.m. - 12:00 p.m.

Ms. Eileen Heider - Welcome

Introductory Remarks - Dr. Joseph A. Lannon
U.S. Army, Picatinny Arsenal

Moderator: Mr. Kirk Newman [8:45 a.m. - 12:00 p.m.]

1. — • David F. Fair, "Army Program Overview."

2. — • Mark Michienzi, "Continuous Processing of Composite Propellants (CPOCP): US Project Overview"

3. — • Jim Baker, "Production of Air Bag Propellant at UPCO".

BREAK - 10:00 - 10:30 a.m.

4. — • Vincent Gonsalves and Eileen Heider, Picatinny Arsenal, U.S. Army Base, "Processing Energetics Materials Using the Twin Screw Mixer/Extruder."

5. — • Richard Muscato, "LOVA Twin Screw Processing and Propelling Charge Development Gun Firing"

6. — • S. Railkar*, A. Lawal and D. M. Kalyon, "Three-Dimensional FEM Analysis of Regular Flighted Single and Twin Screw Extruder Screw Elements."

SESSION II [1:30 to 4:30 p.m.]
Moderator: Ms. Eileen Heider

7. — • R. E. Carter and G. J. Privett, "On A New Purpose-Built Capillary Extrusion Rheometer for the Study of the Rheology of Energetic Materials."

8. — • Fevzi Zeren, "A New Multiple-Slit Rheometers for Energetics Processing."

9. — • E. Kucukpinar* and D. M. Kalyon, "Viscoelastic Material Functions and Extrudability of BAMO/AMMO TPE."

BREAK - 3:00 - 3:30 p.m.

10.— A. Haaland, "Twin Screw Extrusion Processing of Gun Propellants at Thiokol."

11. —• Mitch Gallant, "Calibrated Microencapsulated Sensors (CAMES)."

DINNER AT SIT/FACULTY CLUB - 6:45 p.m. - 10:00 p.m.

SESSION III
June 3, 1997
Moderator: Mr. David Fair [8:30 a.m. - 12:00 p.m.]

12. — • Kirk Newman, Steve Jones, and Neal Cowan, "Correlation of Extruder Residence Time with Screw Speed."

13. — • Jianya Cheng, D. Bigio and R. Breyer, "On the Effect of Shear Flow on the Devolatilization of Filled Polymeric Materials."

14. — • Salvatore J. Monte, "Compounding and Shaping with Neoalkoxy Organometallics for Propellants and Explosives."

15. • James Kowalczyk, "Mechanisms of Wear and Materials that Enhance Wear Resistance in Mixers and Extruders."

BREAK - 10:00 - 10:30 a.m.

16. — • Kirk Newman, Steve Jones, Suzanne Williamson, Neal Cowan, and Jim Gusack, "Injection Loading of PBX into Various Munitions and Components."

17. — • S. Koven*, Z Cao, R. Yazici, S. Railkar, E. Kucukpinar and D. M. Kalyon, "Twin Screw Extrusion Based Recovery, Recycle and Reuse of Grains Using Energetic TPE Binder."

LUNCH 12:00 - 13:30 p.m.

SESSION IV

Moderator: Mr. Mark Michienzi [1:30 - 5:00 p.m.]

18. —• R. Yazici*, E. Birinci, D. F. Fair, W. Ansley and D. M. Kalyon, "X-Ray Based Degree of Mixedness Analysis of Extruded Grains: Ramifications for On-Line Control of Continuous Processing."

19. — • David Dillehay and David Turner, "Informal Comments on Black Powder Substitute Extrusion; Safety Factors."

20. —• H. McSpadden, "Demixing and Weld-Line Formation in Casting and Ramifications on Ballistic Properties".

BREAK

— • Panel Discussion on Process Control, Modeling and Sensors [3:30 - 5:00p.m.]

June 4, 1997

*Demonstrations at Stevens *[8:45 a.m. to 12:00 p.m.]*

8:30 a.m. - Meet at lobby of Ramada to go to Stevens.

8:45 a.m. - Start the tour; at 5th Floor Conference Room of McLean Chemical Sciences Bldg.

*A map of Stevens is attached. Please register with Kathy for the SIT tour.

Éric Giraud
Technologies Procédés

Direction Technologie Recherche
BP 62 - 33166 Saint-Médard en Jalles
Tél. 56.70.50.50
Télex : 560 784 SMNPE F - Télécopie : 56.70.50.52

SNPE

NSWC
NAVAL SURFACE WARFARE CENTER
INDIAN HEAD DIVISION

INDIAN HEAD DIVISION
NAVAL SURFACE WARFARE CENTER
PO DRAWER 160
YORKTOWN VIRGINIA 23691-0160

KIRK E. NEWMAN
Technology Manager
Energetic Materials Research & Technology
Code 9311

757-887-4717 Ext. 34 DSN 953-4717 Ext. 34 757-887-4766 (FAX)
Email: knewman@noclant.navy.mil

Technical Consultants, Inc.
107 Ashwood Terrace
Marshall, Texas 75672

Dr. David R. Dillehay
President

Phone: (903) 935-3930 Fax: (903) 935-9422
E-Mail: dillehay@prysm.net

Technical Consultants, Inc.
107 Ashwood Terrace
Marshall, Texas 75672

David W. Turner
Vice-President

Phone: (903) 935-3930 Fax. (903) 935-9422
E-Mail: dterapin@prysm.net Home: (903) 938-4627

SALVATORE J. MONTE
PRESIDENT

KENRICH
PETROCHEMICALS, INC.

140 East 22nd Street/PO Box 32
Bayonne, NJ 07002-0032
(201) 823-9000
(800) LICA KPI
FAX (201) 823-0691

Edgar J. Timmons
Technical & Marketing Consultant

U.K. Office
Tel: (44) 1543 250 379
Fax: (44) 1543 419 295

PRISM

U.S. Office
35, Manor Drive
Belle Mead
New Jersey
N.J. 08502
U.S.A.

Tel: (908) 874 5140
Fax: (908) 874 4704

Loïc MINGUET
Materials and Technology Department

BP 57 - 33166 Saint-Médard-en-Jalles Cedex - France
Tél. (33)
Tlx 560 784 FMNPEF - Fax (33) 56 70 51 90

SNPE PROPULSION

Indian Head Division
Naval Surface Warfare Center
Indian Head, MD 20640

Stuart A. Richman
Manager, Process Technology Branch

301-743-6463 301-743-4843 (fax)

Email: srichman@pilot.ih.navy.mil

ALLIANT TECHSYSTEMS

E. Hays Zeigler
Staff Engineer
Radford Army Ammunition Plant
Aerospace Systems
Tel 540 639-8101

Alliant Techsystems
Route 114
P.O. Box 1
Radford, VA 24141-0100
DSN 931-8101
Fax 540 639-8290
Hays_Zeigler@atk com

UPCO

JAMES J. BAKER, Ph.D.
Manager, Energetic Materials

UNIVERSAL PROPULSION COMPANY, INC.

Talley Industries

25401 N. Central Avenue
Phoenix, Arizona 85027-7899
(602) 516-3340
Fax (602) 516-3364
email: research@upco-inc.com

US ARMY
ARMAMENT RESEARCH, DEVELOPMENT AND ENGINEERING CENTER

EILEEN HEIDER
CHEMICAL ENGINEER

ARMAMENT ENGINEERING DIRECTORATE
PICATINNY ARSENAL, NJ 07806-5000
S~~MCAR-AES-P~~, BLDG. 321
AMSTA-AR-WEA

36 3 7
201-724-~~3239~~
FAX 201-724-3162

B&P PROCESS EQUIPMENT AND SYSTEMS

KENT H. McNIER
Product Manager Carbon Paste and ~~Baker~~ Energetics Mixers
1000 Hess St. • Saginaw, MI 48601 • USA
Tel: 517.757.1300 • DD: 517.757.1311 • Fax: 517.757.1301
Web Site: www.bpprocess.com • E-Mail: bpprocess@bpprocess.com

Bob Clift
WX4 (Energetic Materials) Division
Processing and Formulations
Research

Tel: 01959 515392
Fax: 01959 516055

DEFENCE RESEARCH AGENCY
Fort Halstead, Sevenoaks,
Kent TN14 7BP UK

PROCESS EVALUATION
HAZARDS ANALYSIS

HIGH ENERGY MATERIALS
HAZARDOUS TYPE PROCESSES

ERNEST D. BROWN
Engineer Consultant

3930 N. 650 West / Ogden, Ut. 84404 U.S.A. / (801)782-8974

SALVATORE J. MONTE
PRESIDENT

KENRICH
PETROCHEMICALS, INC.

140 East 22nd Street/PO Box 32
Bayonne, NJ 07002-0032
(201) 823 9000
(800) LICA KPI
TELEX 12 5023 KPI BAYO
FAX (201) 823-0691

Richard Muscato
Industrial Engineer
Code 9420D

Indian Head Division, NSWC
101 Strauss Ave., Bldg 695
Indian Head, MD 20640-5035

301-743-4272/Fax 4843
rmuscato@pilot.ih.navy.mil

UPCO

JAMES J. BAKER, Ph.D.
Manager, Energetic Materials

UNIVERSAL PROPULSION
COMPANY, INC.

Talley Industries

25401 N. Central Avenue
Phoenix, Arizona 85027-7899
(602) 516-3340
Fax (602) 516-3364
email: research@upco-inc.com

Mark Michienzi
Mechanical Engineer
Code 9420M

Indian Head Division, NSWC
101 Strauss Ave., Bldg 695
Indian Head, MD 20640-5035

301-743-4272/Fax 4843
mmichienzi@pilot.ih.navy.mil

Highly Filled Materials
Institute

A Business Resource at
Stevens Institute of Technology

Stevens Institute of Technology
Castle Point on Hudson
Hoboken, NJ 07030
http://attila.stevens-tech.edu/hfmi
Tel: 201.216.5014
Fax: 201.216.5601
email: srailkar@attila.stevens-tech.edu

Dr. Sudhir B. Railkar
Research Associate Professor
Chemical Engineering Science

Highly Filled Materials
Institute

A Business Resource at
Stevens Institute of Technology

Stevens Institute of Technology
Castle Point on Hudson
Hoboken, NJ 07030
http://attila.stevens-tech.edu/hfmi
Tel: 201.216.5030/8225
Fax: 201.216.5601
E-Mail: dkalyon@stevens-tech.edu

Dr. Dilhan M. Kalyon
Director and Professor of
Chemical Engineering

Mail Address:
3823 W. Hartford Ave.
Glendale, AZ 85308-4220 USA
Tel: +602-938-6234 FAX: 602-938-2053
E-mail: hmcspddn@aol.com

HUGH J. MCSPADDEN
Consultant

Alternate address: P.O.Box 2652, Flagstaff, AZ 86003-2652
Telephone: +520-526-6170

TRW Automotive
Occupant Restraint Systems

TRW Vehicle Safety Systems
Mesa II Facility
11202 E. Germann Rd.
Queen Creek, AZ 85242-9361
602.987.4564
Fax: 602.987.4836
E-Mail: krzykosj@inet.mesaii.trw.com

Jason Krzykos
Manufacturing
Engineer

Éric Giraud
Technologies Procédés

Direction Technologie Recherche
BP 62 - 33166 Saint-Médard en Jalles
Tél. 56.70.50.50
Télex : 560 784 SMNPE F - Télécopie : 56.70.50.52

SNPE

B&P PROCESS EQUIPMENT AND SYSTEMS

KENT H. McNIER
Product Manager Carbon Paste and [redacted] Mixers
Energetics
1000 Hess St. • Saginaw, MI 48601 • USA
Tel: 517.757.1300 • DD: 517.757.1311 • Fax: 517.757.1301
Web Site: www.bpprocess.com • E-Mail: bpprocess@bpprocess.com

MINGUET Loïc

BP 57 - 33166 Saint-Médard-en-Jalles Cedex - France
Tél. (33)
Tlx. 560 784 FMNPEF - Fax : (33) 56 70 51 90

SNPE PROPULSION

GENCORP
AEROJET

Dr. Edmund K.S. Liu
Chemistry Manager,
Propellant/Explosive and
Materials Technology,
Chemical Products

Aerojet

P O Box 13222
Sacramento CA 95813-6000

Tel: 916-355-5716
Fax: 916-355-2044
E-mail: liu_edmund@aphub.aerojetpd.com

PROCESS EVALUATION
HAZARDS ANALYSIS

HIGH ENERGY MATERIALS
HAZARDOUS TYPE PROCESSES

ERNEST D. BROWN
Engineer Consultant

3930 N. 650 West / Ogden, Ut. 84404 U.S.A. / (801)782-8974

Magna
Projects & Instruments Ltd

17, Braemar Close
Mountsorrel, Leicestershire
LE12 7ES UK

Tel: +44-(0) 116-237-4716
Fax: +44-(0) 116-230-3606
Mobile: +44-(0) 385-270- 068
Email: magna@rocarter.demon.co.uk

Roy Carter *MSc FIM CEng*
Managing Director

Gary L. Smith
Manager
Process Development

Autoliv

Autoliv ASP, Inc.
3350 Airport Road
Ogden, Utah 84405

Phone (801) 471-3015
Pager (801) 734-5581
Fax (801) 471-3333
Internet smithgl@autolivasp.com

TACOM-ARDEC

Overview of the ARDEC Program

By

David Fair

Warheads, Energetics, and Combat-support Armaments Center

2 June 1997

Continuous Mixer & Extruder User's Group

U.S. Army Tank-automotive and Armaments Command -Armament Research, Development & Engineering Center

Outline

- ARDEC Twin Screw *
- Goodness of Mixing
- Twin Screw At Radford AAP
- Longhorn AAP Twin Screw
- Zeren Research Rheometer
- Programs

Goodness of Mixing

- Past Work
  - M43 LOVA
  - M30A1
  - Bofors M39
  - AA-6 (Navy)
- Portable Goodness of Mixing Devices
  - Contract Awarded to Stevens Institute of Technology

Goodness of Mixing (Cont'd)

- Observations
  - Excellent Means to Screen Manufacturing Processes
  - Provides New Insight to Micro Structure of the Product
  - Will Be Applied to Evaluating
    - Continuous Mixer Process Parameters
    - Batch Mixer Process Parameters
  - Has Potential for On-line Quality Control

Twin Screw At Radford AAP

- Approved to Begin Design
- Prototype Production
  - Flexible
    - Nitrocellulose Based Propellants
    - Solvent & Solventless
      - Long Barrel / Short Barrel
  - Remote Feeding and Take Away

Longhorn AAP Twin Screw

- Longhorn AAP Twin Screw is Being Moved to Thiokol's Wasatch Plant
- Twin Screw belongs to Thiokol
- Army Owned Support Equipment is Being Transferred with the Machine
- Longhorn AAP Programs are Being Transferred to Wasatch Site
  - Explosive Development
  - Propellant Development
  - Black Powder Substitute Development

Zeren Research Rheometer

- Small Business Innovative Research Project
- Status
  - Demonstration Planned for June 1997
- Portable
- Designed for Use on:
  - ARDEC's Twin Screw Machine
  - 4 Inch Vertical Press

Zeren Research Rheometer (Cont'd)

- Series of 3 Rheometers
  - Variable Gap Section
  - High Shear Section
  - Variable Configurations
- Material Behavior Can be Captured at Extreme Conditions
  - 100,000 1/seconds
- Continuous Measurements
- Application to Non-energetic Materials

8

Zeren Research Rheometer (Cont'd)

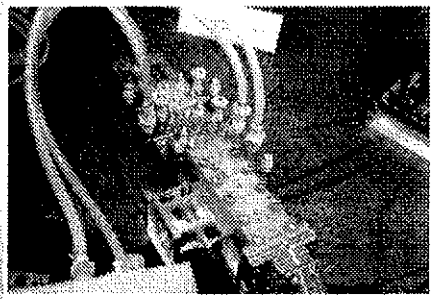

9

Zeren Research Rheometer (Cont'd)

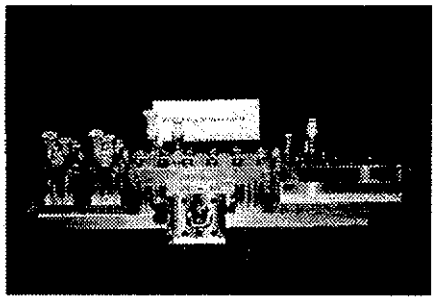

10

Programs

- PAX-2A
  - First Composition Developed to Be Processed in a Twin Screw
  - Superior Performance Characteristics
    - Insensitivity
    - Environmental Life Cycle
  - Qualification is in Progress
- TIME (Totally Integrated Manufacturing Enterprise)
  - Optimization & Modeling
    - Twin Screw Processing
    - Batch Slurry Mix Processing

11

Programs (Cont'd)

- Products
  - Validated Life Cycle Environmental Benefits
  - Demonstrated Product Quality
  - Demonstration of Remote Process Monitoring
  - Validation of Economics
- Team
  - Stevens Institute of Technology
  - Massachusetts Institute of Technology or other
  - Thiokol
  - ARDEC

12

Programs (Cont'd)

- ESTCP (Environmental Security Technology Certification Program)
  - Extension of Twin Screw Process Demonstrated on PAX-2A to Existing Pressable Compositions
    - Completely Closed System
    - Applicable to Latex Based Systems
    - Demonstrated High Degree of Uniformity

13

Continuous Processing of Composite Propellants

U.S. Project Overview

Connie Murphy
Project Manager

NSWC
Naval Surface Warfare Center
INDIAN HEAD DIVISION
Naval Sea Systems Command

Continuous Processing of Composite Propellants

U.S. Project Overview

Connie Murphy
Project Manager

NSWC
Naval Surface Warfare Center
INDIAN HEAD DIVISION
Naval Sea Systems Command

U.S. Project Team

Continuous Processing Team

Connie Murphy, Mitch Gallant
Rich Muscato, Mark Michienzi
Bill Newton, Sharp Johnson

Partners

The Highly Filled Materials Institute at Stevens Institute of Technology (HfMI/SIT)

University of Maryland at College Park (UMCP)

Applied Ordnance Technology, Inc. (AOT)

Accomplishments

- Finalized the feedstream scenario and conducted testing to optimize metering accuracy
- Completed the inert twin screw processing phase
- Demonstrated deaeration of the live propellant
- Initiated the development of a practical technique to understand mixing using CAMES
- Completed the NIR off line testing and model development

Accomplishments

- Characterized the rheology of several propellant formulations
- Validated the mathematical modeling approach for die design
- Completed the design and fabrication of the 2.75″ propellant grain extrusion die
- Manufactured inert propellant grains with the new 2.75″ extrusion die

Continuous Processing Facility

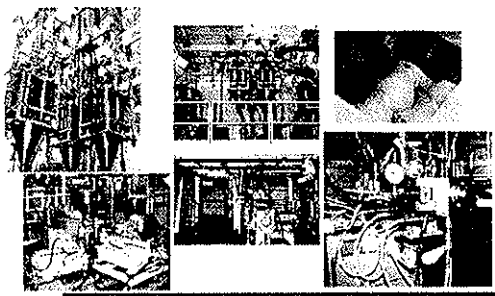

Extruded Composite Propellant Grain

- Propellant Grain
  - Nominal diameter of 2.42″
  - Nominal length of 30″
  - 11 point star perforation
- Propellant formulation
  - HyTemp binder
  - Bimodal AP distribution
  - Isocyanate cured
- Batch process uses approximately 10 - 15% solvent to manufacture

Cross-sectional View of Propellant Grain

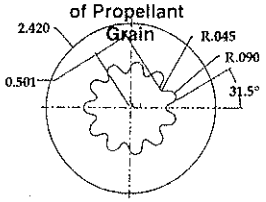

Feedstream Scenario

- Two liquid feedstreams
  - Bonding agent/plasticizer
  - Curative/plasticizer
- Three solid feedstreams
  - Hytemp coated with graphite
  - AP preblend
  - Mixed modifier preblend

Extruder Top View

HyTemp Feeding

- Most challenging material to date
  - Shear sensitive - particles rejoin easily to foul screws
  - Prone to bridging - very low hopper fills reduce this effect
  - 100% unfeedable in virgin form

K-Tron S-200 Feeder

- Solution
  - Cryogenic separation of elastomer with 2% graphite coating
  - Switched from twin screw to single screw feeder
    - Oversized feed tube (15 mm screw/27 mm tube)
    - Much higher hopper loads (up to 4 hours)
  - No agitator (evaluating an in-house design)

HyTemp Feeding Data

K-Tron S-200 Feeder Test Data

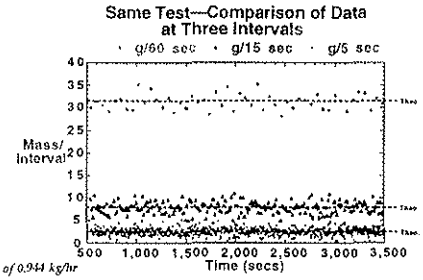

Feed rate of 0.944 kg/hr
Metal chute
Full hopper
No agitator

AP Preblend Feeding

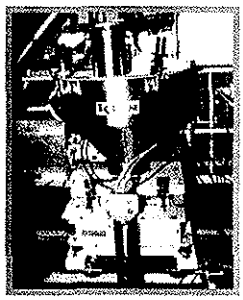

K-Tron T37 Feeder

- Features
  - Twin screw
  - Vertically agitated
  - Maximum feed rate of 100 lb/hr
- Conclusions
  - Electropolished finish on steel chute required
  - Chute vibration with cycling is necessary
  - Non dusting
  - No particle size segregation in hopper

AP Preblend Feeding Data

AP Feeding Study (60 lb/hr)

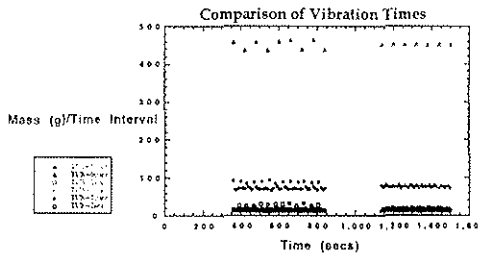

5 sec ON/35sec OFF *5 sec ON/10 sec OFF*

Mixed Modifier Preblend Feeding

K-Tron T20 Feeder

- Features
  - Twin screw
  - Horizontally agitated
  - Maximum feed rate of 10 lb/hr
- Conclusions
  - Achieving very low feed rates (<0.5 lb/hr)
  - No separation in blend
  - Minimal adhesion to electropolished chute
  - Vibration is not necessary

Inert Processing

- Staged mixing approach
  - Phase 1 - Binder Plasticization
  - Phase 2 - Filler Incorporation

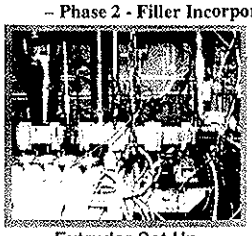

Extruder Set Up

- Objectives
  - Minimize solvent required
  - Define operating parameters for live processing
  - Optimize screw configuration

Phase 1: Binder Plasticization

Material Pressure Inside Extruder

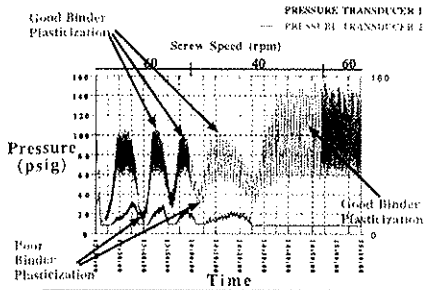

Phase 2: Filler Incorporation

- Successfully processed without solvent
- Developed an oatmeal purging technique
- Finalized the screw configuration for live processing
- Performed a design of experiments (DOE) to determine the effect of process parameters on mixing

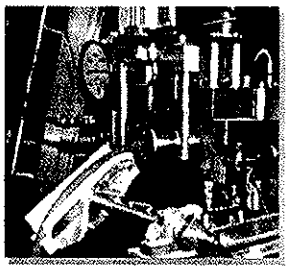

Extrusion of Inert Extruded Composite Propellant

Inert Processing Results

Temperature Rise in Filler Mixing Section

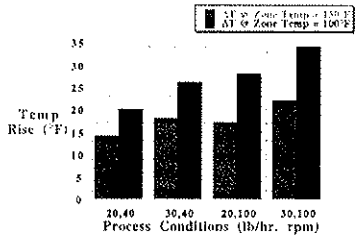

- Larger ΔT with:
  - Higher screw speed
  - Larger throughput

Live Processing

- Obtained management approval for live processing
- Conducted five solventless processing trials to date
- Manufactured propellant crumb for rheology characterization
- Successfully demonstrated deaeration
- Preliminary analysis has revealed a shift in burn rate
- First extrusion of a live 2.75" propellant grain is scheduled for June 1997

Extrusion of Live Extruded Composite Propellant

Understanding Mixing

Calibrated Microencapsulated Sensors (CAMES ™)

- Numerically characterize the effects of screw geometry
  - Residence time
  - Shear history
- Quantify process effects

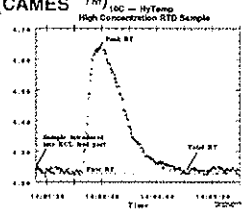

Capillary Rheology

- Modified ram extrusion press with seven capillary dies
- Controlled determination of pressure drop (ΔP) vs. volumetric flow rate (Q)
- Allows for the calculation of the shear stress over a wide range of temperatures and shear rates, $\eta(\gamma T)$
- Allows for the calculation of wall slip
- Inert and live testing completed

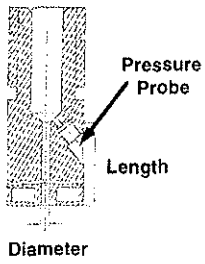

Rheological Characterization

Herschel-Bulkley Equation (for generalized Newtonian fluid)

Shear Stress at Wall (Corrected) versus Shear Rate at Wall (Corrected)

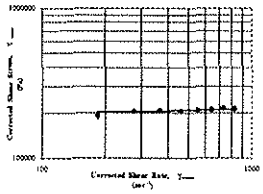

$$\tau_w = \tau_o + m\,\gamma_w^n$$

τ_w = shear stress at the wall
τ_o = yield stress
m = consistency index
γ_w = shear rate at the wall
n = power law index

Extruded Composite Propellant
@ T = 27°C (80°F): $\tau_w = 150{,}000 + 38{,}645\gamma_w^{0.1}$
@ T = 66°C (150°F): $\tau_w = 150{,}000 + 31{,}812\gamma_w^{0.1}$

Mathematical Modeling

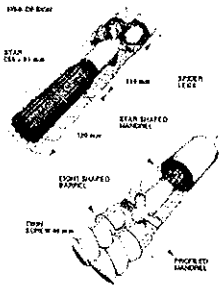

- FEM source code
  - Based on the HB constitutive equation
  - Used to design internal die profile to meet a target ΔP
- Extrusion die design
  - Validated methodology with small scale dies using inert twin screw processing data
  - Incorporated manufacturing considerations
- Die fabrication is complete

New Extrusion Die

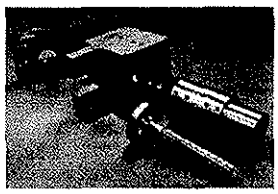

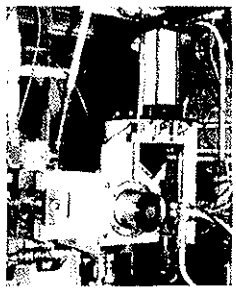

New Extrusion Die Testing

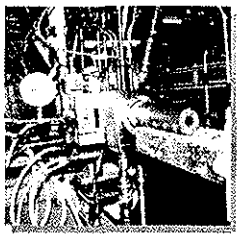

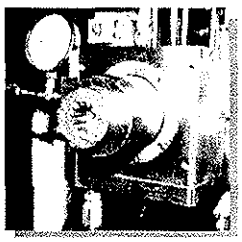

On-line NIR Spectroscopy

- Phase 1: Initial calibration and model development off line
- Phase 2: Testing and validation on line
- Phase 3: Development of process control strategies

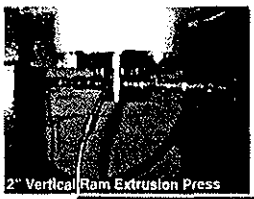
2" Vertical Ram Extrusion Press

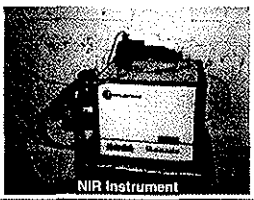
NIR Instrument

Summary of Results to Date

- Depth of penetration is 250μ
- Propellant does not foul probe sapphire lens
- Correlations developed between spectra and propellant properties
- NIR is sensitive to variations within a formulations

NIR Absorbance Spectra

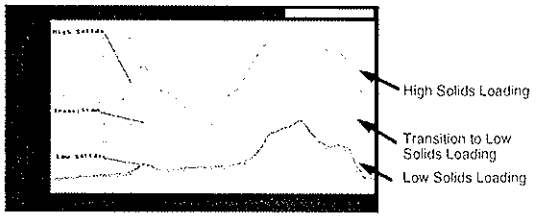

Third Year Plans

- SNPE
  - Manufacture rocket motors
  - Test rocket motors
  - Prepare final report

- IHDIV, NSWC
  - NIR system on-line and tested
  - Manufacture rocket motors
  - Test rocket motors
  - Prepare final report

Continuous Processing Facility

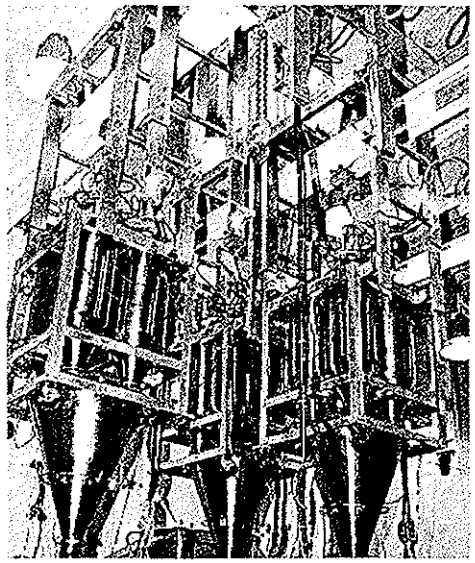

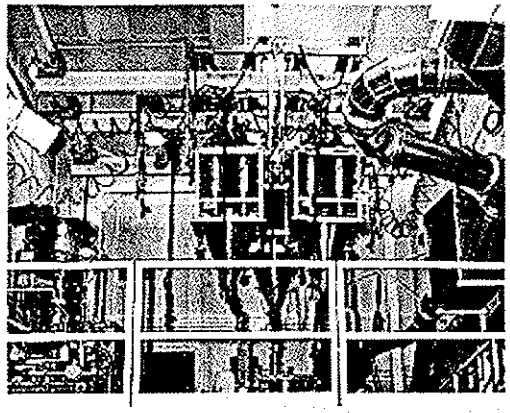

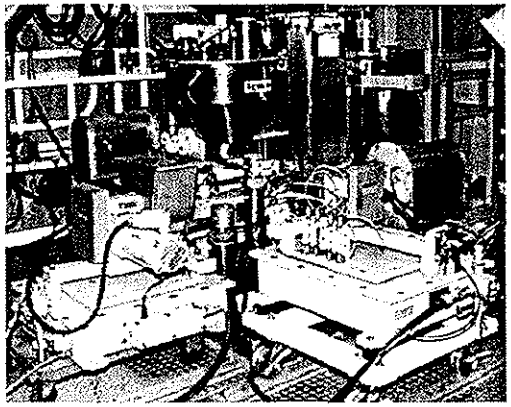

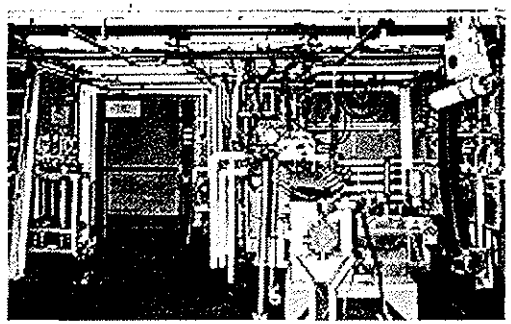

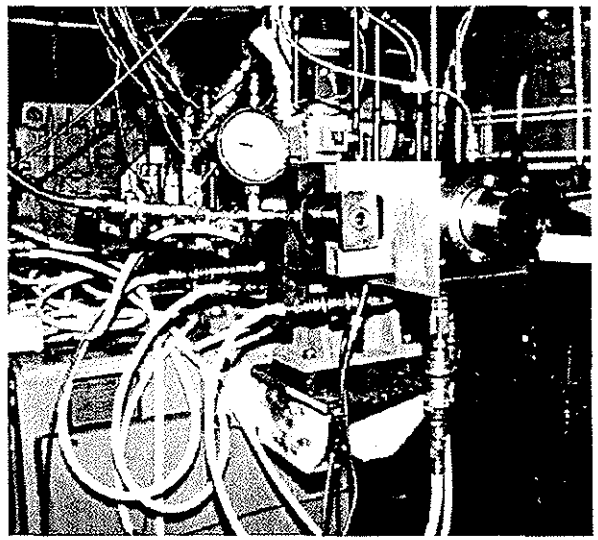

New Extrusion Die

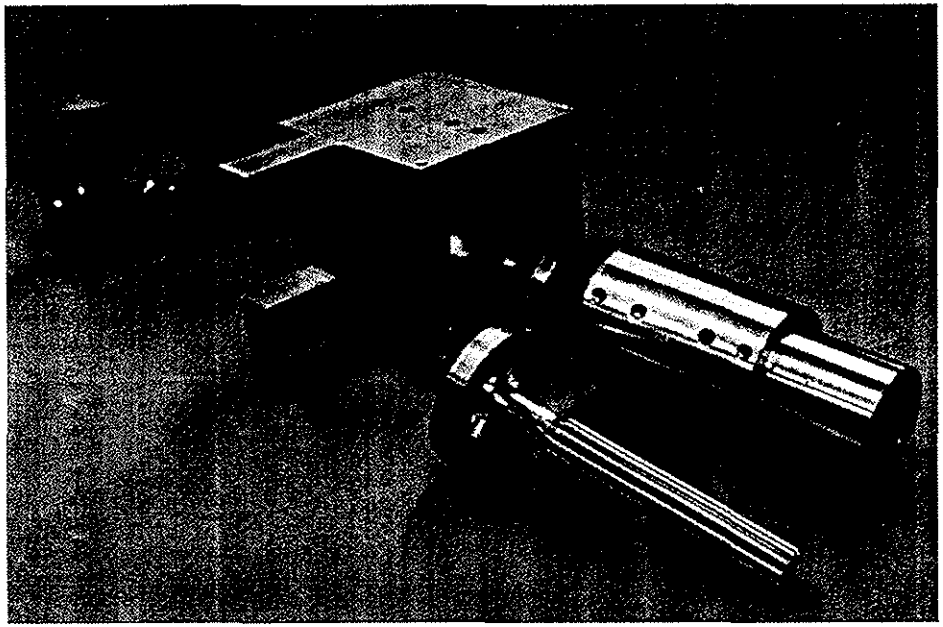

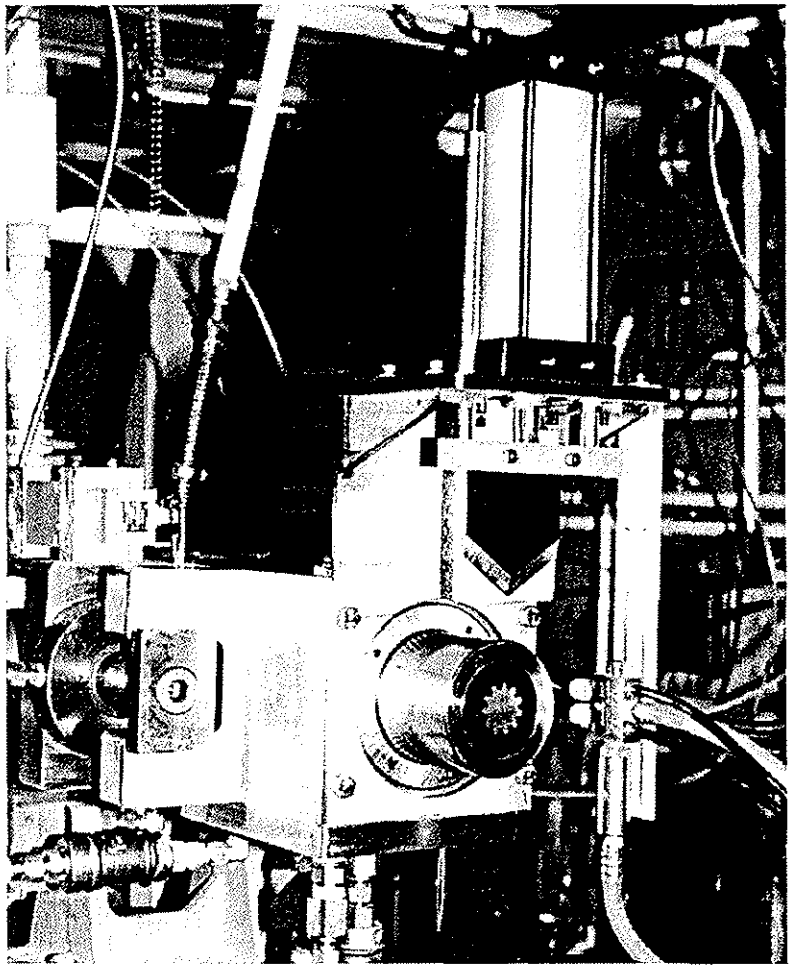

New Extrusion Die Testing

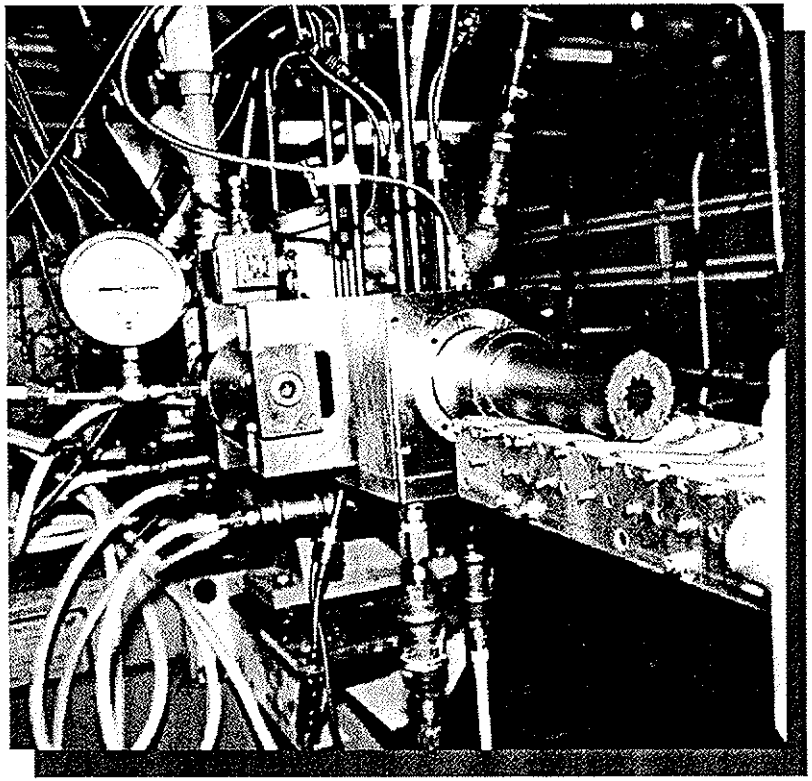

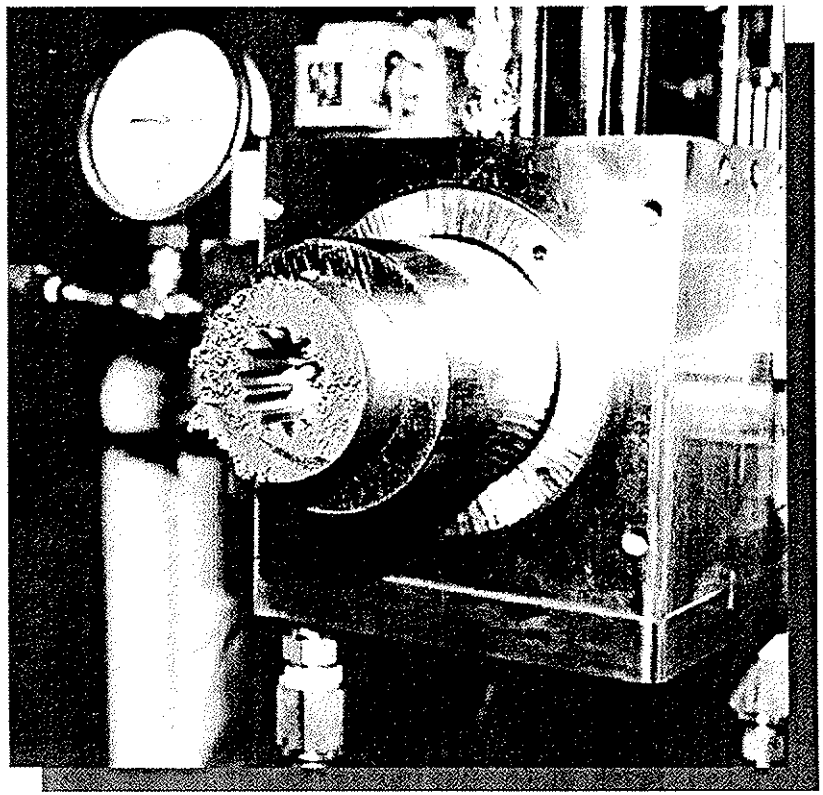

Production of Air Bag Propellant At UPCo

History of Facility

- Joint venture with Werner & Pfleiderer
- Compounder arrives 1987
- High Pressure Extruder arrives 1988
- First live 1989
- UPCo purchase 1993

What Have We Processed?

Live	Inert
– PVC/KP	– HTPB/KCl
– PVC/AP	– PBAN/KCl
– Smokey Devil	– PGA/KCl
– CTPB/AP	– CAB LOVA
– JA-2	
– TPE LOVA	
– TPE/KP	

What is the Composition?

- Potassium perchlorate
- PVC
- Plasticizer
- Stabilizer
- Chloride scavenger
- Opacifier

Flowchart

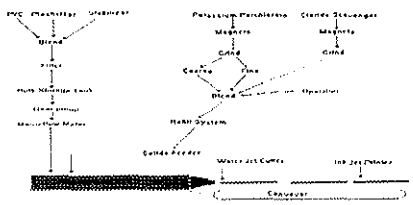

Walking the Tightrope

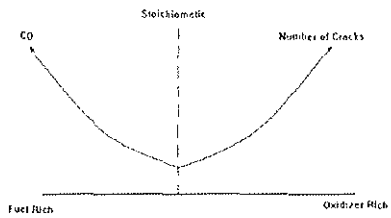

Compounder Sideview

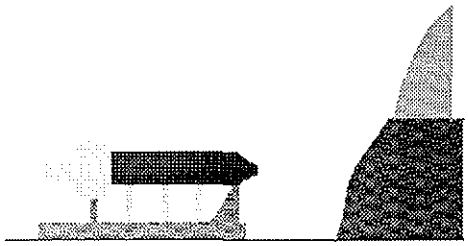

Facility Layout

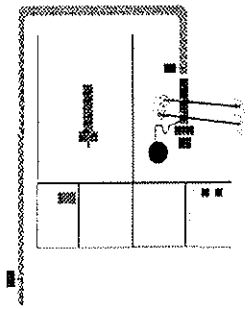

The Many Feeds Problem

- All feeders "hunt"
- Average composition is "right on the money"
- Individual portions of run may be "rich" or "lean"

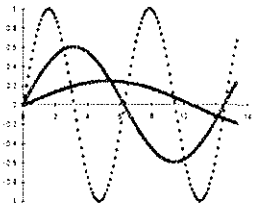

Conclusion

- UPCo's facility is "state-of-the-art"
- Fantastic mixing device
- Quality requirements determine number of feed streams
- Set-up and clean-up require large volumes
- For some products, there is no substitute

9th Annual Twin Screw Mixer/Extruder User's Group

June 2-3, 1997

Overview of Twin Screw Processing at TACOM-ARDEC

Presented by:

Ms. Eileen Heider
US. ARMY, WECAC, ASPD
Picatinny Arsenal, NJ
201-724-3637

BUILDING OVERVIEW

- Equipment
- Capabilities
- Deluge System
- Lightning Protection
- Waste Water Collection System

ARDEC FACILITY

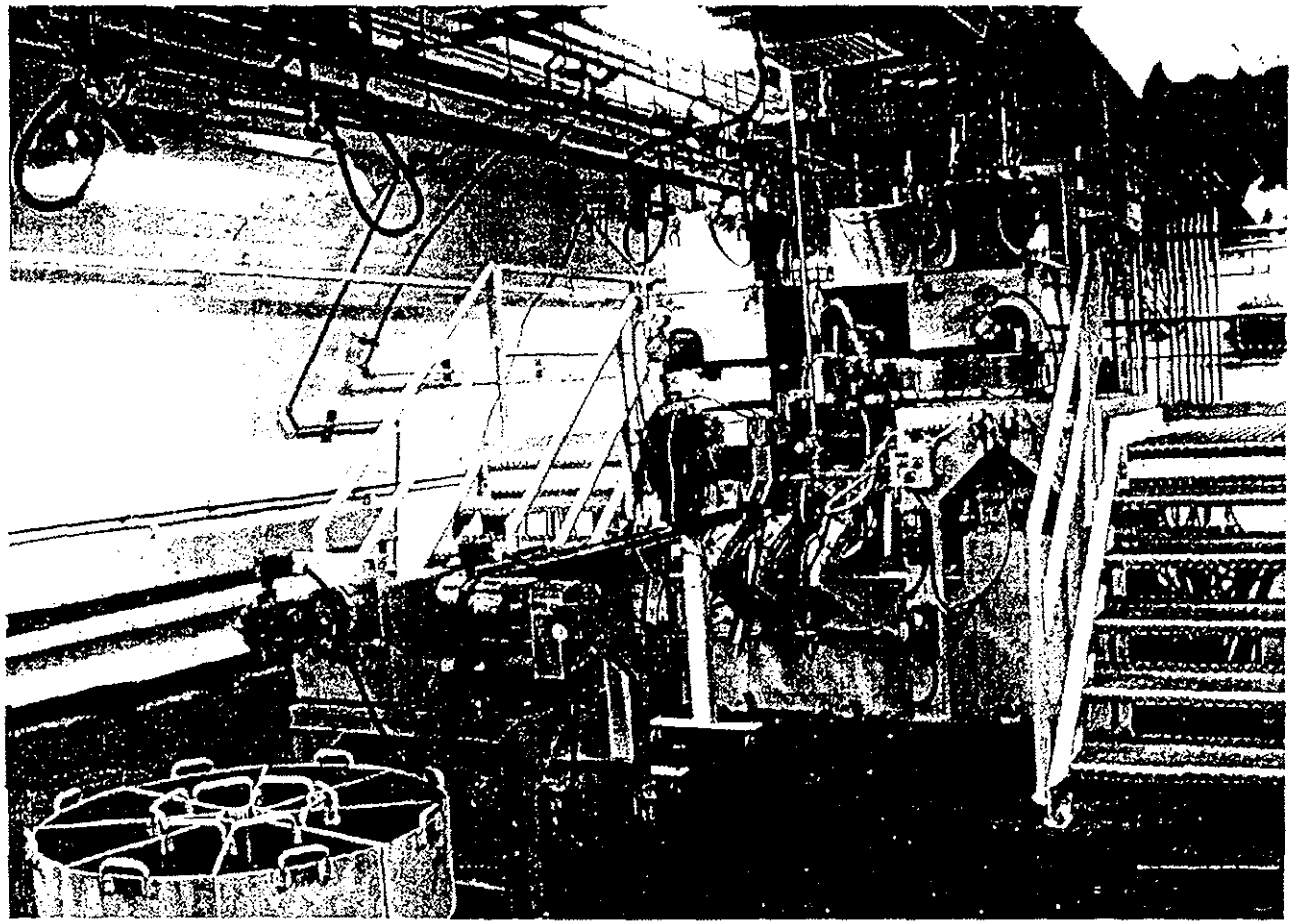

APV SE-1600 TWIN SCREW MIXER/EXTRUDER

- 40mm
- 16:1 L/D ratio
- Clam shell barrel design
- End bearing design with side discharge

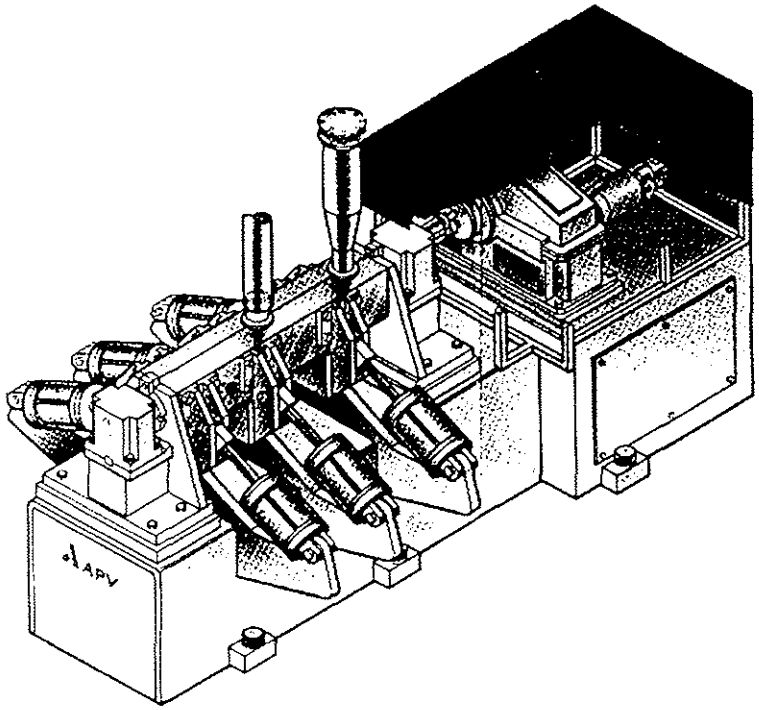

APV SE-1600 TSE (CON'T)

- 2 Solid Feed Ports
- 1 Vacuum Port
- 4 Zone Heating/Cooling Capabilities
- Separate Heating/Cooling for the Die
- 2 Liquid injection ports
- 5 surface temperature/pressure indicators
- 5 water Thermocouples

LOSS-IN-WEIGHT FEED SYSTEM

- AccuRate LIW Feeder
  - Three Solid Feeders
    - External Agitation
    - Single Screw Feed
    - Flexible Wall
      - Two feeders with 100lb capacity
      - One feeder with 44lb Capacity

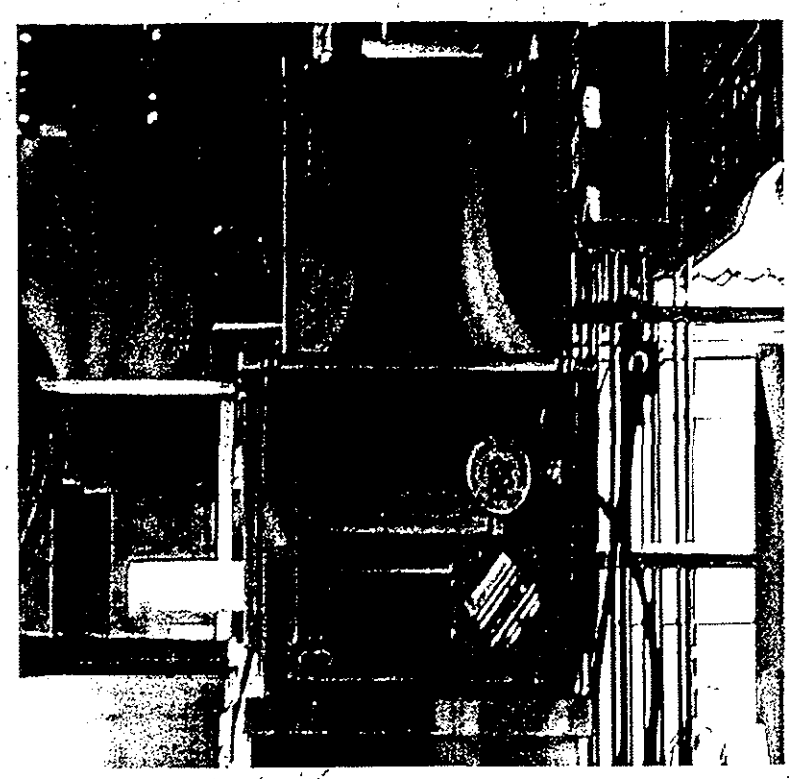

LOSS-IN-WEIGHT FEED SYSTEM

- AccuRate Liquid LIW
  - One Liquid Feeder
    - Designed for highly viscous material
    - Zenith Gear Pump
    - Ten Gallon Capacity

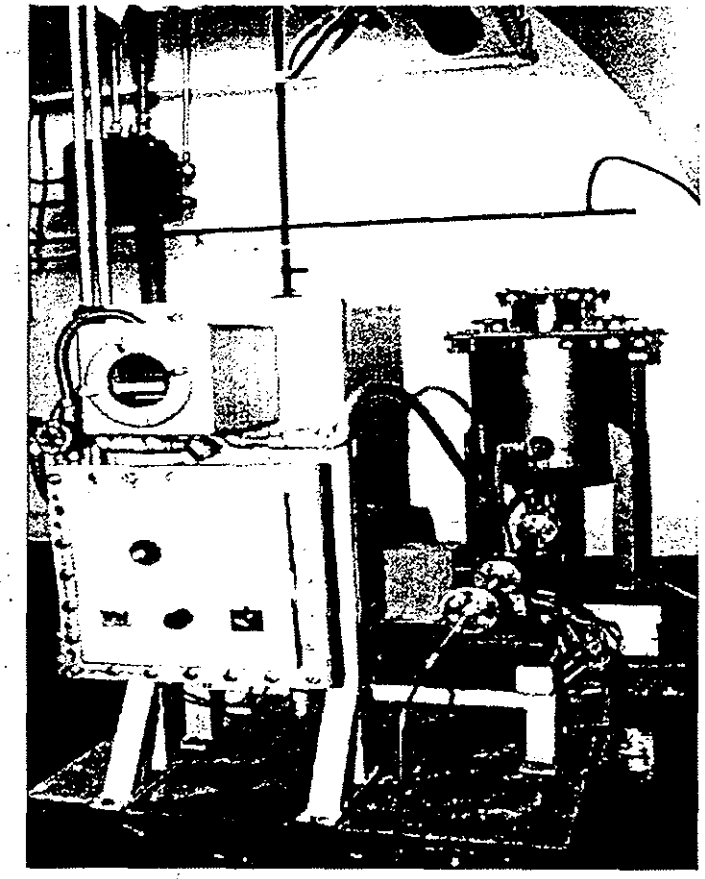

METAL DETECTION SYSTEM

- Safeline Design
- K-tron LIW Feeder
- Minimizes Operator Exposure
- Detects to 0.012" ferrous material

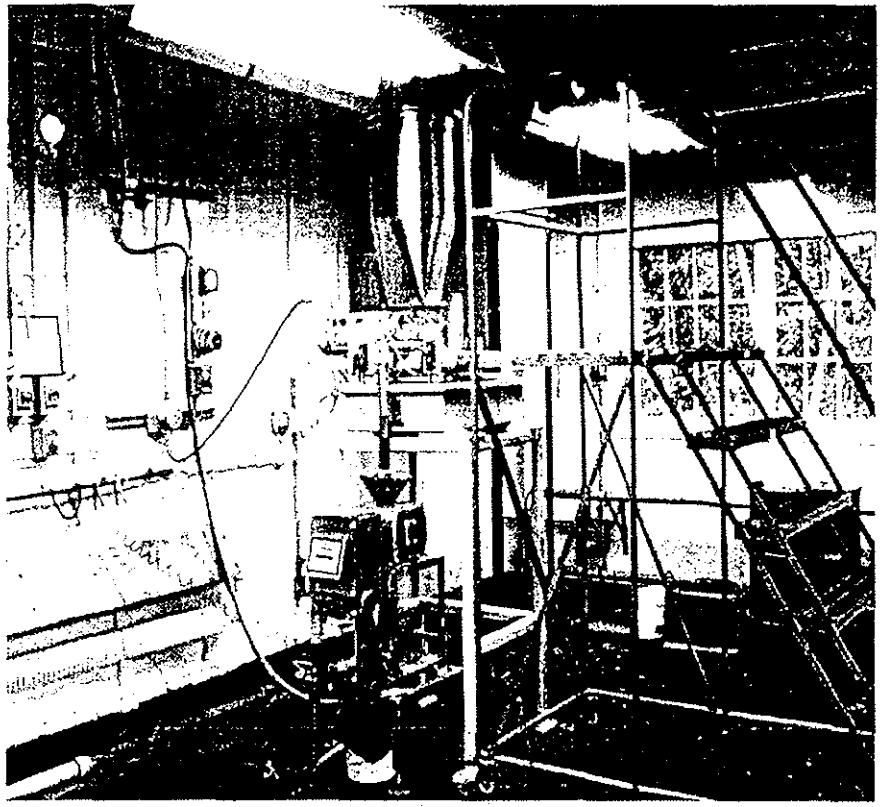

TAKEAWAY/CUTTER SYSTEM

- Guillotine Cutter
- Nobel Chematur Long Strand Cutter
- Nobel Chematur Short Strand Cutter
- Conveyor
- Rotary Collection System

CONTROL SYSTEM

- Allen-Bradley PLC-5
- WonderWare
- 3 Monitors and VCRs
- Editing Capabilities

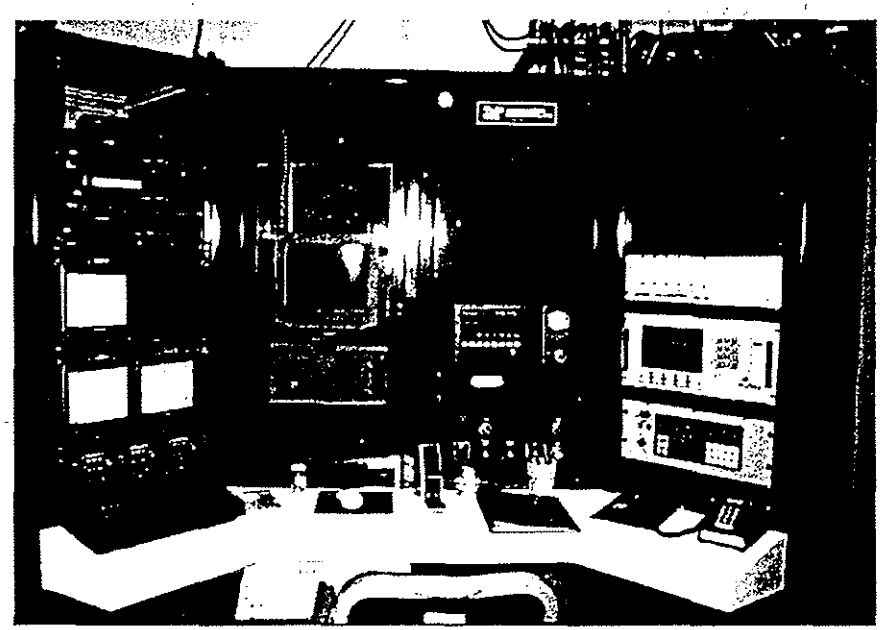

CURRENT MODIFICATIONS

Hydraulic Drive System Upgrade
Control & Metering Feeder Purchase
Control System Upgrade
X-Ray Diffraction On-Site Device
Task Order Contract with Stevens Institute of Technology
Zeren Rheometer
Re-Certification of the Deluge System

INERT PROCESSING STUDIES

- Material Characterization Study
- Lacquer Study
- Feeder Study
- Temperature/Pressure Study
- Mathematical Modeling of Process
- Screw Configuration Study
- Take-away/Conveying Study
- Die Design Study

LIVE PROCESSING STUDIES

- Feeder Study
- Temperature/Pressure Study
- Screw Configuration Study
- Mathematical Modeling of Process
- Product Analysis

CURRENT PROGRAM SCOPE AND OBJECTIVES

- An Integrated Product Development Team (IPDT) has been developed. Key members include:
  - TACOM-ARDEC
  - Thiokol Corp.
  - Stevens Institute of Technology
  - Lawrance Livermore National Labs
- The purpose of the team is to establish a methodology for the development and transition of Energetic Formulations to a flexible manufacturing Facility
  - Reduce Technology Transition Time
  - Improve Product Quality
  - Reduce Production Costs

Energetics Sub-Project Work Breakdown Structure

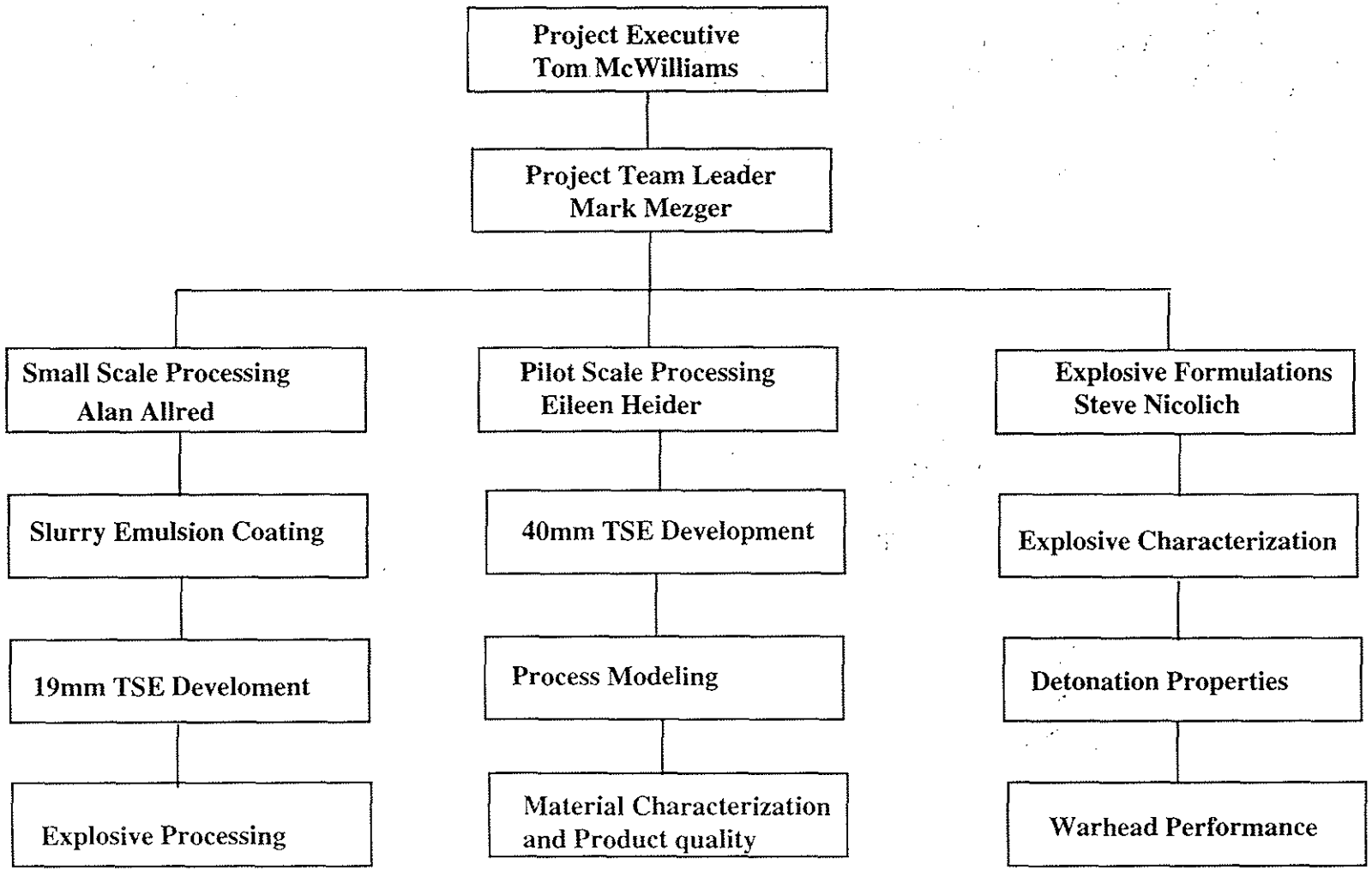

SUMMARY

- Automated Continuous Processing will enhance environmental compliance by reducing in-process solvent requirements, eliminate batch-to-batch variation, and minimize the waste or scrap material being produced.
- TACOM-ARDEC is committed to supporting the twin screw mixer/extruder technology and plans to continue the current liaisons that have been established for the TIME Program, and hopefully be able to expand the current team.

Naval Sea Systems Command

NSWC

Naval Surface Warfare Center

INDIAN HEAD DIVISION

Continuous Mixer and Extruder Users' Group Meeting
2 - 4 June 1997

Richard S. Muscato
IHDIV, NSWC

Continuous Mixer and Extruder Users' Group Meeting
2 - 4 June 1997

Richard S. Muscato
IHDIV, NSWC

Objectives

Batch vs. Continuous Processing Schematics

Solid Preblend Processing Technique

Experimental Approach

Test Results

Conclusions

- Develop a Solid Preblend Process
- Define Twin Screw Extruder Lower and Upper Processing Parameters to be used for Lova Gun Propellant Manufacturing
- Process a Sufficient Quantity of Lova Gun Propellant with a Twin Screw Extruder to Perform 5"/ 54 Propellant Charge Development Gun Firing

---

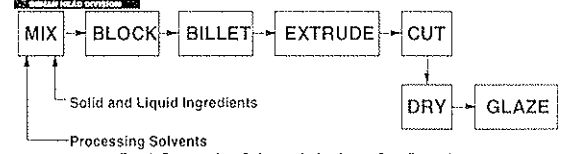

Batch Processing Schematic for Lova Gun Propellant

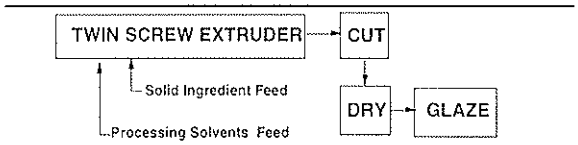

Continuous Processing Schematic for Lova Gun Propellant

Water Extraction Solid Preblending Process

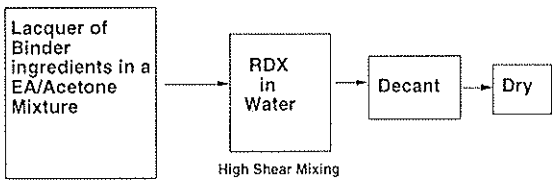

- Use Design of Experiments (DOE) Approach
- Extrude Through a 0.454 inch Die with 7 Perforations
- Manufacture 180 pounds for Propelling Charge Development Gun Firing in the 5 "/54 Navy Gun

DOE Processing Parameters:

- Total Throughput
- Solvent Percentage
- Screw Speed
- Temperature Profile

DOE Material Responses:

- Visual Homogeneity
- Scanning Electron Microscope (SEM)
- Temperature Rise
- Pressure Rise
- Torque Measurement
- Dimensionless Volumetric Flowrate Q*
- HOE, Density, Closed Bomb

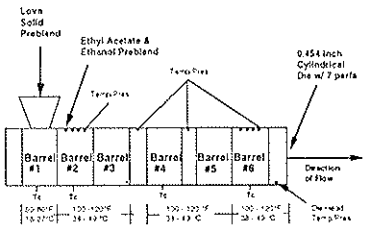

Parameters	Range	Final
Total Throughput (lb/hr)	15 - 30	30
Solvent Percent (by weight)	10.5 - 12.5	12.5
Screw Speed (rpm)	40 - 100	50
Temperature Profile (°F)	80/100 - 60/120	70/120

Test Performed	*Acceptable Range Batch*	*Results Twin Screw*
HOE(cal/gm)	955 +/- 10	955
Density (gm/cc)	1.63 - 1.66	1.657 - 1.659
Closed Bomb (in/sec at 40 Kpsi)	TBD (-6.2)	(-5.8)
Propelling Charge Development Gun Firing	TBD	See Graphs

- Successfully Developed a Solid Preblending Process
- Successfully Determined Lower and Upper Processing Parameters for Lova Gun Propellant using a 40 mm Twin Screw Mixer/Extruder
- Successfully Processed 180 pounds of M43 Gun Propellant for the 5 " / 54 Navy Gun
- Performed Propelling Charge Development Gun Firing Meeting Ballistic Requirements

Continuous Processing Facility

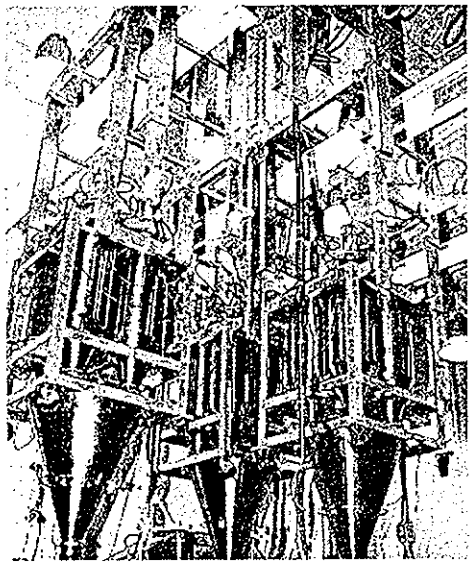

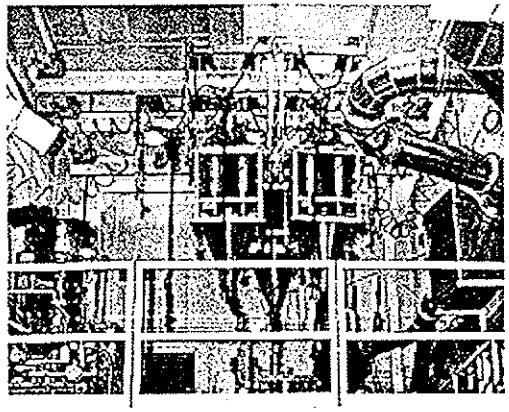

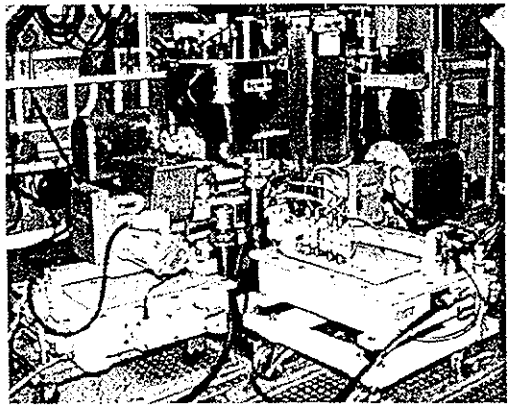

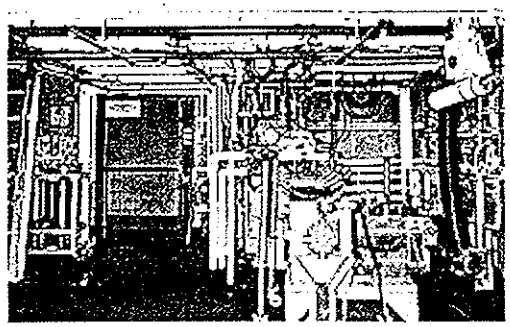

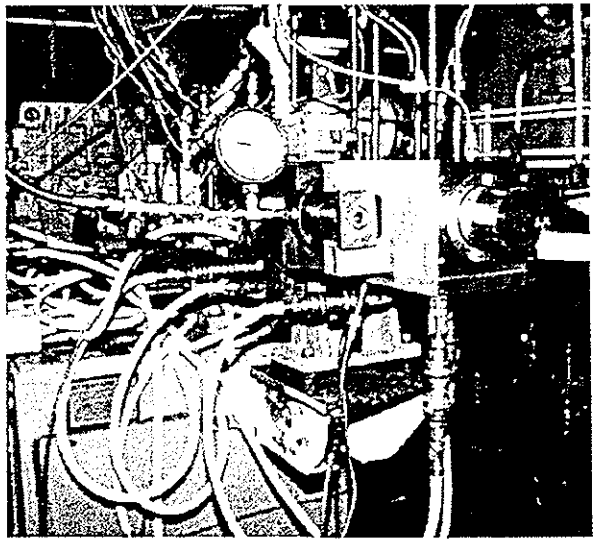

3-D ANALYSIS OF FULLY FLIGHTED SCREWS OF CO-ROTATING TWIN SCREW EXTRUDER

A. Lawal, S. Railkar, and D. M. Kalyon
Highly Filled Materials Institute
Stevens Institute of Technology
Hoboken, NJ 07030

There are two principal methods of mathematical modeling of the twin screw extrusion processing. In the first method Finite Element Method is used in conjunction with a mesh which duplicates accurately the channel geometry without unwrapping. This technique which our own research group has championed [1-5] in spite of the computational difficulties involved, has been successful in describing the flow and heat transfer occurring in such complex shaped screw elements as the lenticular kneading discs [1-7]. In the second method the channels are unwrapped and the conservation equations are solved employing either FEM [8-12] or methods like the Flow Analysis Method [13,14]. For the regular flighted screw elements of the co-rotating twin screw extrusion process the popular method has been the unwrapping of the screw channel [8-12]. Here we show how our FEM techniques can be applied to the simulation of flow and deformation occurring in the regular flighted screw elements of the twin screw extrusion process without unwrapping of the screws.

The co-rotating screw elements, used for the purpose of modeling, were double flighted and with relatively small flight width as compared with the channel width as shown in Figure. 1. The fully-flighted screw elements are considered to be a stack of infinitesimally small thickness kneading blocks staggered at almost zero stagger.

As consistent with our earlier work a single mesh is used and we differentiate between the fluid and the screw as a function of time as the screws rotate and as the boundary conditions change [1-5].

Flow Equations

The inertia effects can be ignored, because of the highly viscous nature of the materials generally processed in continuous processors and the creeping nature of the resulting flow. Here, we consider the isothermal creeping flow of an incompressible fluid in a twin screw extruder with two-tipped co-rotating screw elements as shown in Figure 1.

The penalty/Galerkin Finite Element Method is employed in the discretization wherein the continuity equation used as a constraint on the equations of conservation of momentum, and the pressure p is approximated by using a large positive number λ_p (penalty parameter) such that [1-5]:

$$p = \lambda_p \eta \left(\frac{\partial v_x}{\partial x} + \frac{\partial v_y}{\partial y} + \frac{\partial v_z}{\partial z} \right) \tag{1}$$

The equations of momentum are:

$$\begin{aligned} &\frac{\partial}{\partial x}\left[\lambda_p \eta \left(\frac{\partial v_x}{\partial x} + \frac{\partial v_y}{\partial y} + \frac{\partial v_z}{\partial z} \right)\right] \\ &- \frac{\partial}{\partial x}\left(2\eta \frac{\partial v_x}{\partial x}\right) - \frac{\partial}{\partial y}\left[\eta\left(\frac{\partial v_x}{\partial y} + \frac{\partial v_y}{\partial x}\right)\right] \\ &- \frac{\partial}{\partial z}\left[\eta\left(\frac{\partial v_x}{\partial z} + \frac{\partial v_z}{\partial x}\right)\right] = 0 \end{aligned} \tag{2}$$

$$\begin{aligned} &\frac{\partial}{\partial y}\left[\lambda_p \eta \left(\frac{\partial v_x}{\partial x} + \frac{\partial v_y}{\partial y} + \frac{\partial v_z}{\partial z} \right)\right] \\ &- \frac{\partial}{\partial x}\left[\eta\left(\frac{\partial v_x}{\partial y} + \frac{\partial v_y}{\partial x}\right)\right] - \frac{\partial}{\partial y}\left(2\eta \frac{\partial v_y}{\partial y}\right) \\ &- \frac{\partial}{\partial z}\left[\eta\left(\frac{\partial v_y}{\partial z} + \frac{\partial v_z}{\partial y}\right)\right] = 0 \end{aligned} \tag{3}$$

$$\begin{aligned} &\frac{\partial}{\partial z}\left[\lambda_p \eta \left(\frac{\partial v_x}{\partial x} + \frac{\partial v_y}{\partial y} + \frac{\partial v_z}{\partial z} \right)\right] \\ &- \frac{\partial}{\partial x}\left[\eta\left(\frac{\partial v_x}{\partial z} + \frac{\partial v_z}{\partial x}\right)\right] \\ &- \frac{\partial}{\partial y}\left[\eta\left(\frac{\partial v_y}{\partial z} + \frac{\partial v_z}{\partial y}\right)\right] - \frac{\partial}{\partial z}\left(2\eta \frac{\partial v_z}{\partial z}\right) = 0 \end{aligned} \tag{4}$$

In dimensionless forms of these equations the screw radius, R_S, screw rotational speed, ω, and the volumetric flow rate, Q, are used.

Results

Typical simulation results for the Bingham plastic fluid using a clearance between the screws and the barrel surface of 0.8 % of the screw radius are shown in Figure. 1. Here the velocity vectors are indicated by the arrows. The length of the arrow is proportional to the magnitude of the velocity vector and the directions are the same. The clearance was varied and the pressurization versus mass flow rate history was obtained. As the clearance is increased the pressurization ability of the extruder drops for a constant volume flow rate. Typical results were also obtained for the power law type generalized Newtonian fluid as a function of the power law index, n. The results were used for comparisons with analysis results where the channel was unwrapped [8-11]. The total flow rate, Q* is given as a function of the axial distance (not helical).

$$Q^* = \frac{Q}{2\pi R_s \omega \mathrm{Cos}\theta_b WH} \qquad (5)$$

and

$$\frac{dp^*}{dz^*} = \left[\frac{H}{2\pi R_s \omega \mathrm{Cos}\theta_b}\right]^n \frac{H}{m}\frac{dp}{dz} \qquad (6)$$

where, θ_b is the helix angle of the screw at the tip of the flights, W and H are the channel width and channel depth, and dp/dz is given along the axial and not helical channel direction and Q is the total flow rate.

Comparison of these results to earlier published two dimensional FEM solutions using unwrapping of the screw elements [8-11], reveals good general agreement between the 2-D and 3-D results explaining the reason as to why the 2-D approach has been so popular at least for screw geometries where the flight width is small in comparison to the channel width of the screw element. However, the 2-D approach is expected to break down for cases where the ratio of the flight width over the channel width becomes appreciable and the intermesh and the relative velocity between the two screws can no longer be ignored.

References

1. A. D. Gotsis, and D. M. Kalyon, *SPE ANTEC Technical Papers, 35,* 44-48 (1989).
2. A. D. Gotsis, Z. Ji and D. M. Kalyon, *SPE ANTEC Technical Papers, 36,* 139 (1990).
3. A. Lawal and D. M. Kalyon, *SPE ANTEC Technical Papers, 39,* 3397-3400 (1993).
4. A. Lawal and D. M. Kalyon, *J. Appl. Polym. Sci, 58,* 1501-1507 (1995)
5. A. Lawal and D. M. Kalyon, *Polym. Eng. & Sci, 35,* 1325-1338 (1995)
6. A. Kiani and H. J. Samann, *SPE ANTEC Technical Papers, 39,* 2758 (1993)
7. H. Yang and I. Manas-Zloczower, *Polym. Eng. Sci., 32,* 1411-1417 (1992).
8. C. D. Denson and B. K. Hwang, *Polym. Eng. Sci., 20,* 965 (1980).
9. D. M. Kalyon, A. D. Gotsis, U. Yilmazer and C. Gogos, Sangani, Aral, and Tsenoglou, *Adv. Polym., Techn., 8,* 337-353 (1988).
10. D. M. Kalyon, A. D. Gotsis, C. G. Gogos and C. Tsenoglou, *SPE ANTEC Technical Papers, 34,* 64 (1988).
11. R. Lai-Fook, A. Senouci, A. C. Smith and D. P. Isherwood, *Polym. Eng. Sci., 29,* 433 (1989).
12. A. Lawal and D. M. Kalyon, *Numerical Heat Transfer, 26, 103 (1994).*
13. W. Szydlowski and J. L. White, *Adv. Polym. Tech., 7,* 177 (1987).
14. Y. Wang and J. L. White, *J. Non-Newtonian Fluid Mech., 32,* 19 (1989).

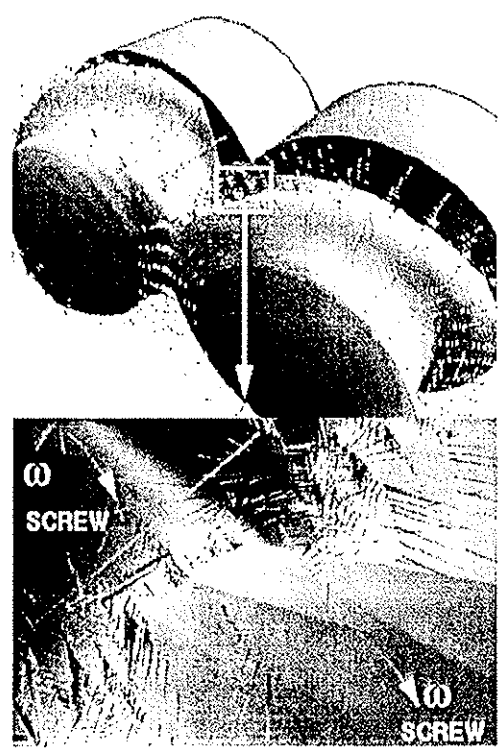

Fig. 1

ANTEC 97

VISCOELASTICITY AND PROCESSABILITY OF A BAMO/AMMO THERMOPLASTIC ELASTOMER

R. Esra Küçükpinar and Dilhan M. Kalyon
Chemical Engineering Department and Highly Filled Materials Institute
Stevens Institute of Technology
Hoboken, New Jersey

ABSTRACT

Various viscoelastic material functions of BAMO/AMMO based thermoplastic elastomer melt were characterized using small amplitude oscillatory shear, step strain and steady torsional flows. The relaxation spectrum and relaxation modulus data were used to fit the parameters of a K-BKZ type integral non-linear viscoelastic constitutive equation. The predictions of the constitutive equation were compared with the results of other viscometric experiments, including shear stress growth and relaxation, and were found to agree. The use of the constitutive equation to predict especially the shear viscosity material function over a broad range of temperatures and shear rates, i.e., to enable calculations regarding the processability of the thermoplastic elastomer in various molding and extrusion processes to be made, was also demonstrated.

INTRODUCTION

Thermoplastic elastomer based formulations are used widely in various applications, traditionally served by vulcanized rubbers and other thermosetting polymers. The ability to use conventional polymer processing equipment including injection and transfer molders and extruders and recyclability provide additional incentives. However, such processing operations also require detailed information on the rheological behavior of the thermoplastic elastomer and processability analysis. In this study, we provide extensive data on various viscoelastic material functions of a melt of a BAMO/AMMO based thermoplastic elastomer used in conjunction with a non-linear constitutive equation to enable predictions of rheological behavior and processability under conditions relevant to various molding and extrusion operations.

MATERIALS

A recently introduced thermoplastic elastomer based on a BAMO-AMMO copolymer was procuced from Thiokol Corporation. BAMO-AMMO is an alternating block copolymer obtained from the polymerization of BAMO and AMMO monomers. BAMO (3,3-bis(azidomethyl)oxetane) is a crystalline homopolymer forming the hard block and AMMO (3-azidomethyl-e-methyloxetane) is an amorphous homopolymer forming the soft block of the energetic thermoplastic elastomer. In this study BAMO-AMMO with a 25% BAMO is characterized. The melting temperature of BAMO-AMMO is 74.8 °C. This thermoplastic elastomer has a number average molecular weight of 10600 and a weight-average molecular weight of 45400, as reported by the manufacturer, Thiokol Corporation.

RHEOLOGICAL CHARACTERIZATION

The BAMO-AMMO thermoplastic elastomer was first characterized in terms of its linear viscoelastic properties, storage (G') and loss (G") moduli employing a Rheometric Scientific System IV in conjunction with 25-mm diameter parallel-plate fixtures. The experiments were carried out in the 85-100 °C range. The material is stable under the employed temperatures. The small amplitude oscillatory shear experiments covered the 0.01 to 100 rps frequency range. The magnitude of the complex viscosity, $|\eta^*|$ was determined from:

$$|\eta^*(\omega)| = ((G'/\omega)^2 + (G''/\omega)^2)^{0.5} \qquad (1)$$

The Rheometrics System IV was again used for steady shear, stress growth, and stress relaxation experiments, in conjunction with 25-mm cone and plate fixtures. Furthermore, a series of stress relaxation after sudden shearing displacement experiments were carried out in the 25-1200% strain range to determine the relaxation moduli, $G(t, \gamma_o)$:

$$G(t,\gamma_o) = \tau_{xy}(t) / \gamma_o \qquad (2a)$$

where $\tau_{xy}(t)$ is the shear stress and γ_o is the imposed shear strain. In these experiments parallel-plate fixtures were employed. The parallel plate data were corrected by employing (1,2):

$$G(t,\gamma_R)=G_a(t,\gamma_R)\left[1+\frac{1}{4}\frac{\partial \ln G_a(t,\gamma_R)}{\partial \ln \gamma_R}\right] \qquad (2b)$$

where γ_R is the strain at the edge of the disk, R, and t is time. The apparent modulus $G_a(t, \gamma_R)$ is given as:

$$G_a(t,\gamma_R) = \frac{2Y(t,\gamma_R)}{\pi R^3 \gamma_R} \qquad (2c)$$

and strain at radius R:

$$\gamma_R = \frac{\theta R}{H} \qquad (2d)$$

where θ is the angular displacement, R and H are the radius of the disk and the gap separation between the two disks, respectively, and Y is the torque exerted by the thermoplastic elastomer on the disk. The rise times involved in the imposition of the strain, γ_R, were not negligible in our experiments and varied between 0.1 to 0.8 s. The relaxation modulus values were corrected for the rise time on the basis of the procedure suggested by Laun (3).

CONSTITUTIVE EQUATION

To gain insight into the processing behavior of these engineering thermoplastics the experimental data were employed to determine the material-dependent parameters of the following integral type, network-based equation fitting the general form (4):

$$\tau = \int_0^\infty \left[M_1(s, I_1, I_2) C_t^{-1} + M_2(s, I_1, I_2) C_t \right] ds \qquad (3)$$

where C_t^{-1} and C_t are the Finger and Cauchy tensors, respectively, and M_1 and M_2 are the memory functions which are given as functions of the first, I_1, and second, I_2 invariants of the Finger tensor and the elapsed time s. Here we have followed Wagner's postulate (5) by setting M_2 to zero and assuming that the memory function, M_1 can be expressed as a product of two functions:

$$M_1(s, I_1, I_2) = M_o(s) h(I_1, I_2) \qquad (4)$$

where $h(I_1, I_2) \leq 1$ is the temperature-independent damping function which tends to unity for small deformations and $M_o(s)$ is the Lodge's rubberlike-liquid memory function (6):

$$M_o(s) = \sum_i (G_{oi} / \lambda_i) \exp(-(t - t') / \lambda_i) \qquad (5)$$

where G_{oi} and λ_i are the relaxation strength and time, respectively and (t-t') is the elapsed time, s. We have employed a double exponential dependence of the damping function to strain (3,5) namely,

$$h(\gamma) = f\exp(-n_1\gamma) + (1-f)\exp(-n_2\gamma) \qquad (6)$$

where f, n_1, and n_2 are material parameters. Various material functions predicted on the basis of this constitutive equation are reproduced here for convenience in Table 1.

RESULTS AND DISCUSSION

The storage and loss moduli of the BAMO-AMMO (25% BAMO) are shown in Figure 1. The data were collected at 85, 90, 95, 100 °C. Assuming that the material is a thermorheologically simple fluid, the variations in temperature basically corresponds to a shift in time scale. Accordingly, all relaxation times change with temperature proportional to the shift factor, a_T (7).

$$\lambda_i(T) = a_T \lambda_i(T_o) \qquad (7)$$

The relaxation strengths remain constant and the shift factor a_T is determined from the temperature dependence of magnitude of complex viscosity values determined at low frequency:

$$a_T(T) = \exp((E_a/R)(1/T - 1/T_o)) \qquad (8)$$

where E_a is the activation energy and R is the gas constant. The activation energy for BAMO-AMMO (25% BAMO) was determined as 13.9 kcal/g-mol on the basis of equation (8). A reference temperature, T_o of 90°C was selected. The discrete relaxation spectra for the resin were determined from the dynamic data employing a pattern search method that minimizes the objective function, F defined as:

$$F = \sum_{i=1}^{N} \left[((G'_{i,exp} - G'_{i,fit}) / G'_{i,exp})^2 \right] + \left[((G''_{i,exp} - G''_{i,fit}) / G''_{i,exp})^2 \right] \qquad (9)$$

where N is the number of data points, ($G'_{i,exp}$, $G''_{i,exp}$) are available from the dynamic experiments and $G'_{i,fit}$, $G''_{i,fit}$ denote the best fit values on the basis of Eqs. (11) and (12). The best fit of storage and loss moduli are shown in Figure 1 for the discrete spectra given in Table 2. The relaxation strengths G_{oi} represent the contribution to rigidity associated with relaxation times of the thermoplastic elastomer which lie in the interval $\ln\lambda$ and $\ln\lambda + d\ln\lambda$.

The results of the step strain experiments are shown in Figures 2 and 3. In these experiments the broadest 95% confidence intervals determined according to Student's t-distribution were observed for the modulus values determined at small strains. This observed scatter should be related to the relatively small torques measured in this range. In the linear viscoelastic region, the shear relaxation modulus values can be related to the relaxation spectrum through:

$$G(t) = \sum_i G_{oi} \exp(-t / \lambda_i) \qquad (10)$$

The relaxation moduli determined on the basis of Eq.(10) are indicated by the solid curve in Figure 2. The relaxation data pertaining to the linear viscoelastic range are further shown in Figure 3. The relaxation modulus values, which were determined according to Eq. (10) in the linear viscoelastic range, agree well with those determined employing step strain experiments.

The relaxation moduli values of BAMO-AMMO were determined up to a strain of 12, where the behavior is highly nonlinear. The relaxation moduli were separated into a time dependent modulus, G(t) determined in the linear viscoelastic range, and the strain dependent damping function, $h(\gamma)$, on the basis of Eq. (4). The damping function describes the destructive effect of the deformation in the entanglement density of the TPE melt. The damping function is given by the

vertical shift required to superimpose the curves of relaxation modulus at various strains on the reference curve representing the linear viscoelastic region. For this TPE the curves of nonlinear relaxation modulus as a function of time for different strain levels were generally parallel for all times, as required by the time and strain separability. The factorization of the nonlinear relaxation modulus requires that the slopes of $dG(t,\gamma)/dt$ be constant over the strain range. This is further elucidated in Figure 4 where the best fit of the damping function values collected at 0.25, 0.5, 0.75 s are compared. Mean values of the damping function values were also determined based on the best vertical shift of the nonlinear relaxation modulus curves over the entire experimental time range. The time dependence of the damping function is not strong. The three parameters of Eq. (6), which describe the strain dependence of the mean damping function values in shear flows, are reported in Table 3.

Figure 5 shows the typical comparison of the experimental shear stress growth behavior versus the predictions of the Wagner model. The comparisons of experimental and predicted stress relaxation upon the cessation of steady shear are reported in Figure 6. Overall, the agreement between the experimental and predicted time-dependent material functions is excellent. The predicted shear viscosity values are compared to the experimental values determined with cone and plate in Figure 7. The experimental magnitude of the complex viscosity values are also reported. According to the empirical Cox-Merz relationship (8), the magnitude of the complex viscosity approximates the shear viscosity at corresponding values of shear rate and frequency at relatively small deformation rates. The ability to predict the shear viscosity material function over a broad range of shear rates and temperatures, applicable to various molding and extrusion flows, provides the basis necessary to predict the rheological behavior and processability of the TPE under relevant processing conditions and geometries.

CONCLUSIONS

The rheological behavior of BAMO-AMMO (25% BAMO) was studied. The relaxation spectra and the damping function data were fitted in terms of a Wagner type BKZ model. The predictions of this model were compared with various viscometric material functions determined experimentally in this study. The reported experimental data and the model parameters should be helpful in defining the processing window of this elastomer and demonstrate techniques which are applicable to other types of thermoplastic elastomers.

ACKNOWLEDGMENTS

This research was funded by the Office of Naval Research under contract N00014-95-1-0770 and under the direction of Dr. Richard S. Miller. We are grateful for this support. We are also grateful to NSWC and Mr. F. Gallant for making the materials of this study available and to Thiokol Corporation for their valuable input.

References

1. R. Penn and E. Kearsley, *Trans. Soc. Rheol.*, *20*, 2, 227 (1976).
2. P. Soskey and H. Winter, *J. Rheol.*, *28*, 5, 625 (19840.
3. H. Laun, *Rheol. Acta*, *17*, 1 (1978).
4. B. Bernstein, E. Kearsley, and L. Zapas, *Trans. Soc. Rheol.*, *7*, 391 (1963).
5. M. H. Wagner, *Rheol. Acta*, *15*, 136 (1976).
6. A. Lodge, *Trans. Faraday Soc.*, *52*, 120 (1956).
7. J. Ferry, *Viscoelastic Properties of Polymers*, John Wiley, Third Edition, New York, 1980.
8. W. Cox and E. Merz, *J. Polym. Sci.*, *28*, 619 (1958).

Key Words: Rheology, Thermoplastic elastomers, BAMO/AMMO

TABLE 1

Small Amplitude Oscillatory Shear Flow and Steady Shear Flow:

$$G'(\omega) = \sum_i ((G_{oi}\lambda_i^2\omega^2)/(1+\lambda_i^2\omega^2)) \qquad (11)$$

$$G''(\omega) = \sum_i ((G_{oi}\lambda_i\omega)/(1+\lambda_i^2\omega^2)) \qquad (12)$$

$$\eta(\dot\gamma) = f\sum_i G_{oi}\lambda_i / (1+n_1\dot\gamma\lambda_i)^2 + (1-f)\sum_i G_{oi}\lambda_i / (1+n_2\dot\gamma\lambda_i)^2 \qquad (13)$$

Start-up Flow and Cessation of Steady Shear Flow:

$$\eta^+(t,\dot\gamma) = f\sum_i \frac{G_{oi}\lambda_i}{(1+n_1\dot\gamma\lambda_i)^2}\left[1-\exp(-t_{1,i})(1-n_1\dot\gamma\lambda_i t_{1,i})\right] + (1-f)\sum_i \frac{G_{oi}\lambda_i}{(1+n_2\dot\gamma\lambda_i)^2}\left[1-\exp(-t_{2,i})(1-n_2\dot\gamma\lambda_i t_{2,i}\right] \qquad (14)$$

where $t_{1,i} = \frac{1+n_1\dot\gamma\lambda_i}{\lambda_i}t$ & $t_{2,i} = \frac{1+n_2\dot\gamma\lambda_i}{\lambda_i}t$ and $\eta^+(t,\dot\gamma) = \frac{\tau_{12}^+(t,\dot\gamma)}{\dot\gamma}$

$$\eta^-(t,\dot\gamma) = \sum_i\left[(fG_{oi}\lambda_i)/(1+n_1\dot\gamma\lambda_i)^2 + (1-f)G_{oi}\lambda_i/(1+n_2\dot\gamma\lambda_i)^2\right]\exp(-t/\lambda_i) = \frac{\tau_{12}^-(t,\dot\gamma)}{\dot\gamma} \qquad (15)$$

TABLE 2

Relaxation Time λ_i and Strength G_{oi} at T=90 °C

λ_i,s	G_{oi}, Pa
1000	1.00E-04
100	2.00E-02
10	7.42E-01
1	1.82E+02
0.1	1.82E+03
0.01	2.38E+04

TABLE 3

Parameters in Double Exponential-Type Damping Function

f	0.0870
n_1	1E-05
n_2	0.1627

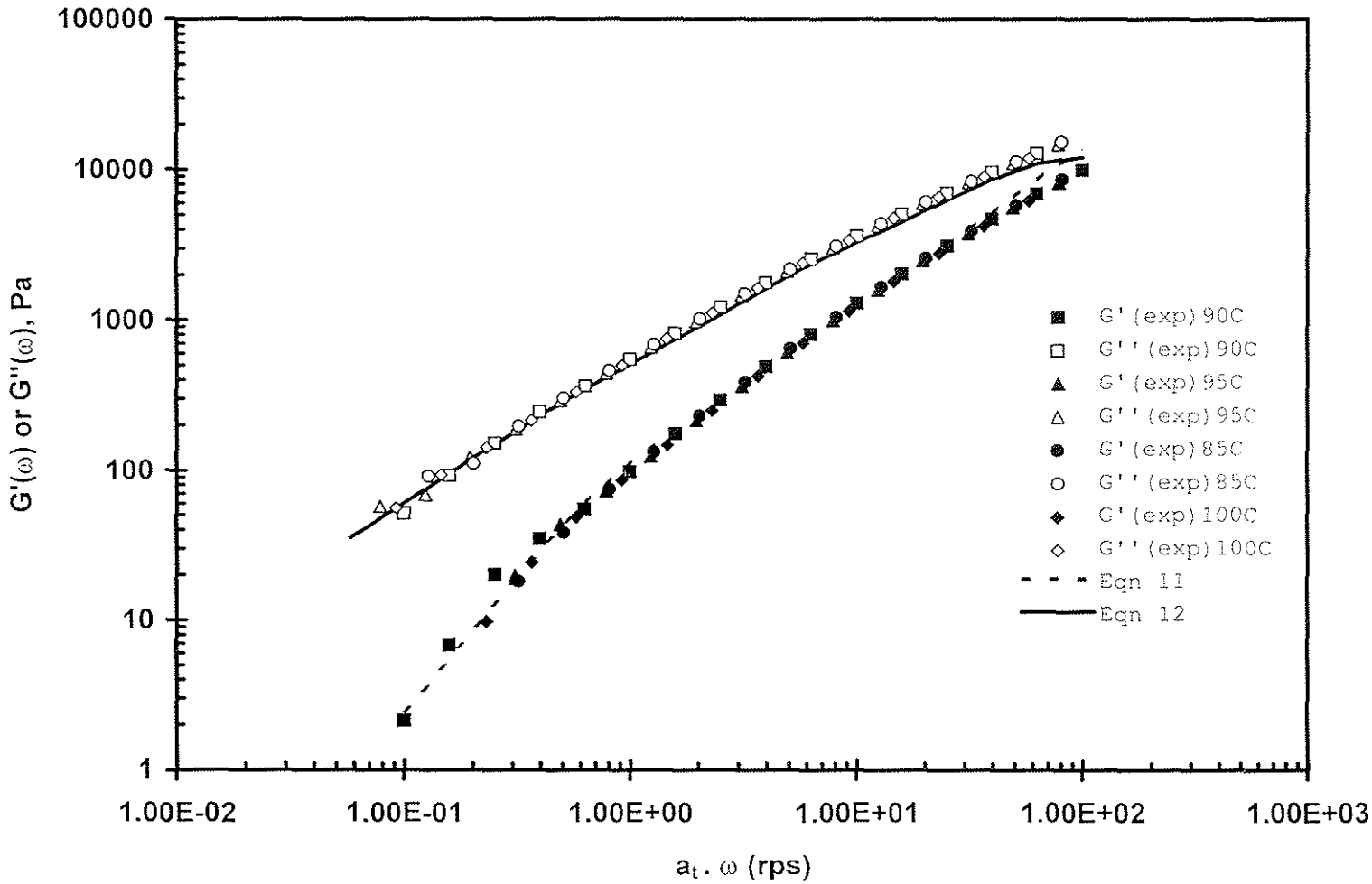

Fig. 1. Storage and loss moduli of 25% BAMO-AMMO

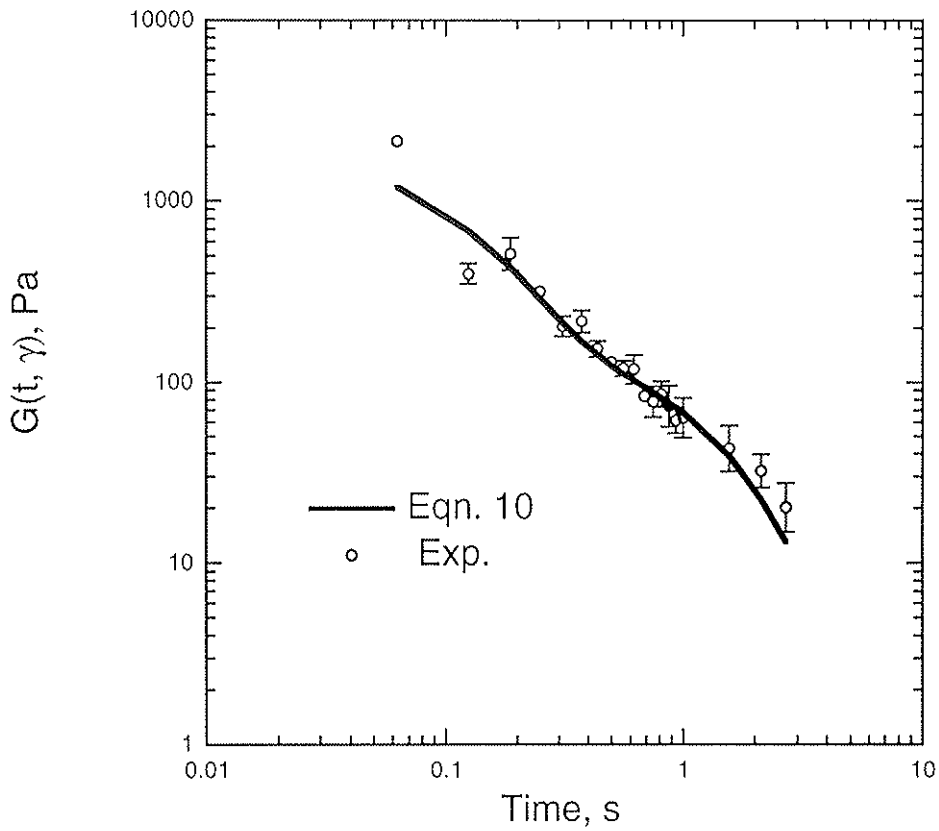

Fig. 2. Typical confidence intervals of the relaxation moduli in the linear viscoelastic range

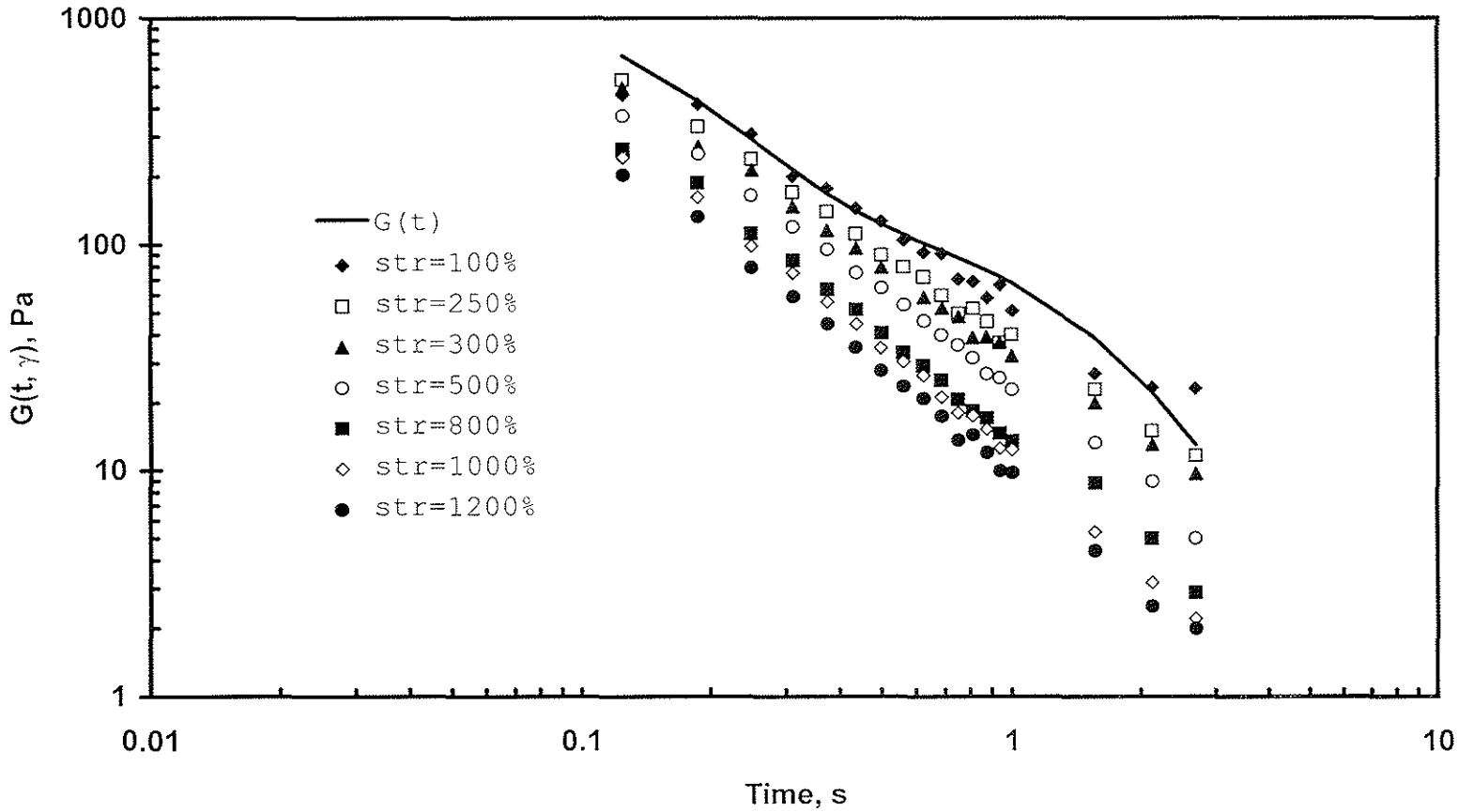

Fig. 3. Shear relaxation modulus of 25% BAMO-AMMO

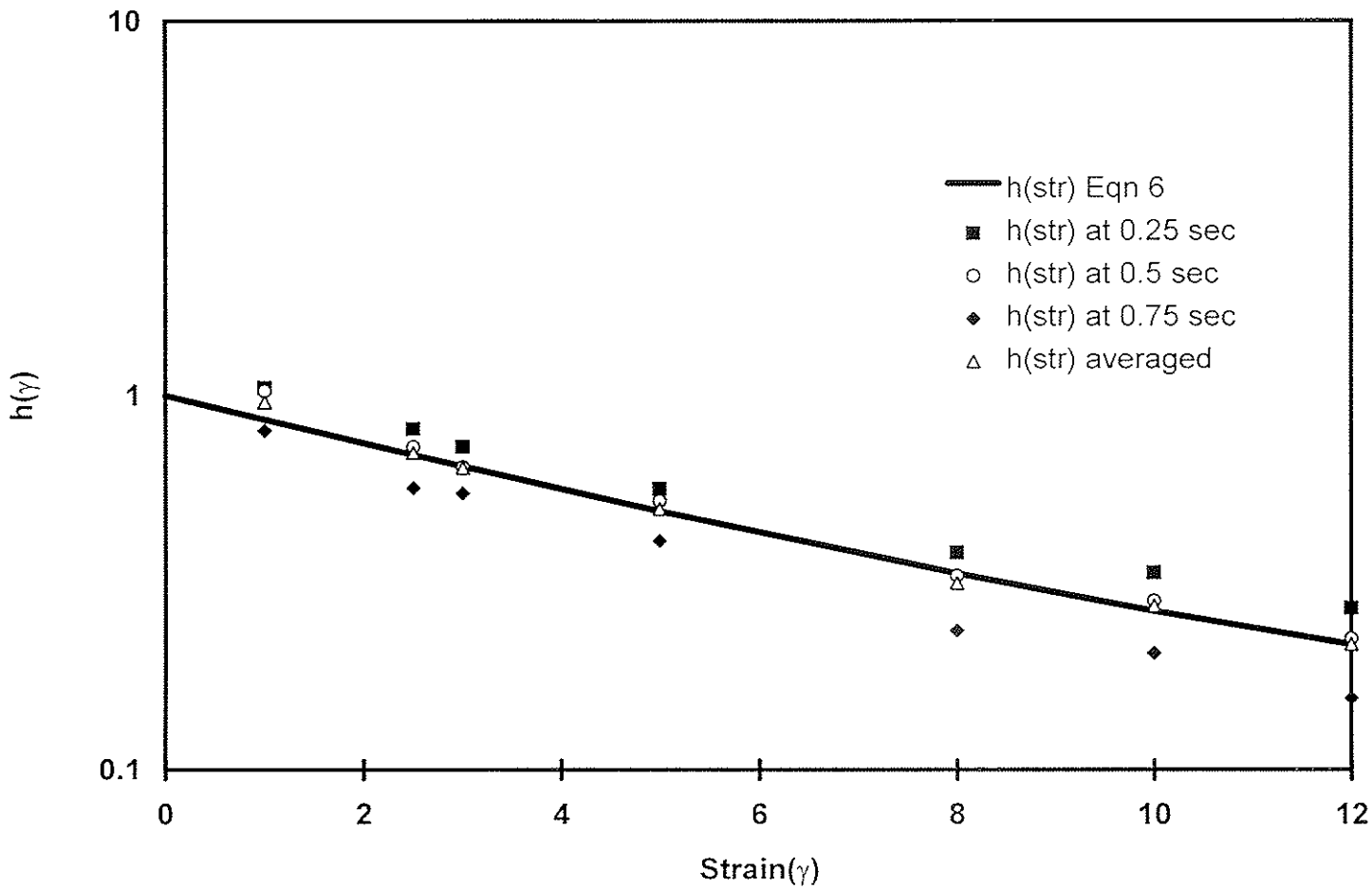

Fig. 4. Strain dependence of the damping function

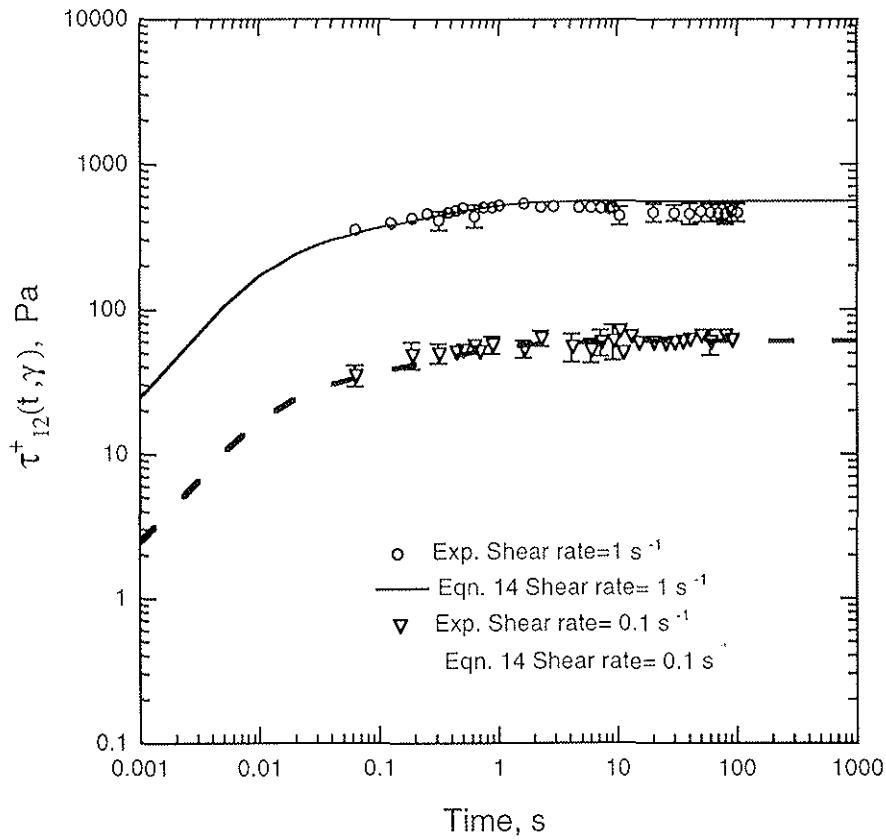

Fig. 5. Shear stress growth

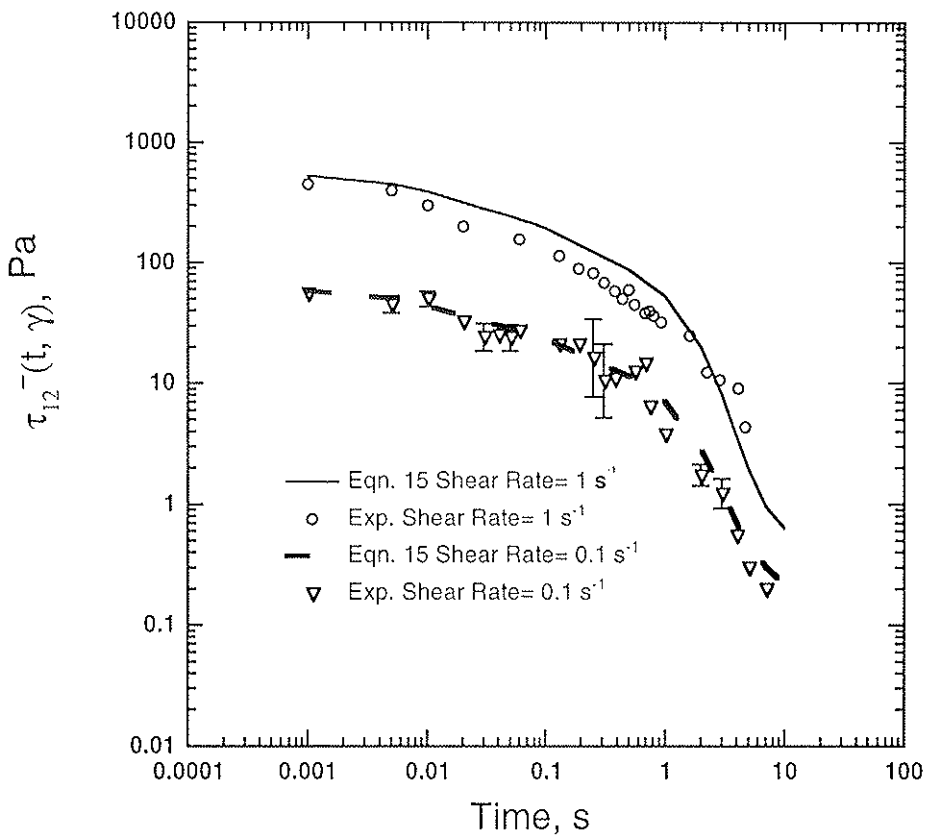

Fig. 6. Shear stress relaxation upon the cessation of steady shear

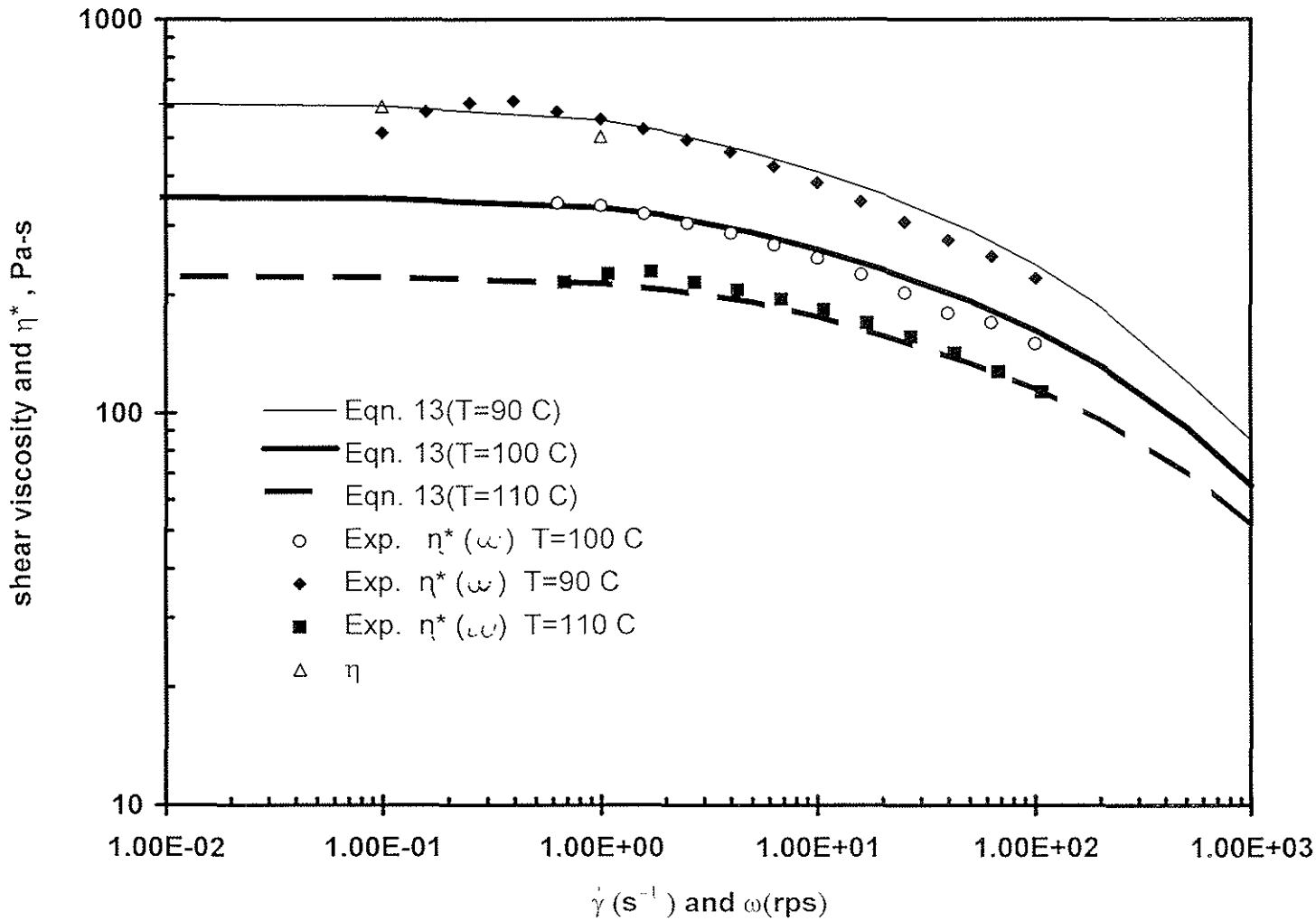

Fig. 7. Shear viscosity and magnitude of complex viscosity

Correlation of Extruder Residence Time with Screw Speed

Kirk Newman, Steve Jones, and Neal Cowan
Energetic Materials Research and Technology Department
Naval Surface Warfare Center
Indian Head Division
Yorktown, VA 23691-0160

and

Prof. David Bigio and Dr. Chi-Tai Yang*
Department of Mechanical Engineering
University of Maryland
College Park, MD 20742

The success of twin screw compounding and casting of plastic bonded explosives (PBX), or extrusion of composite propellants, is dependent upon process control. We demonstrated that the residence time of an extruder is a key component of process control algorithms, because it allows feeder data to be used in feed forward control strategies. However, the residence time of an extruder may not be constant for all materials and is definitely not constant for all screw speeds and designs. Therefore, a means of measuring or estimating the residence time as a function of screw speed would be useful for each screw design planned. If the extruder is to be utilized as an agile manufacturing facility, there may be numerous screw designs. We propose a two parameter correlation for residence time as a function of screw speed and volumetric flowrate. We conducted residence time experiments to fit the parameters of this correlation for one screw design we use for compounding and casting PBX at Yorktown. We have plans to continue this work for other screw designs. We believe that integration of a robust correlation for residence time estimation into our process control algorithm will produce significant cost savings in future process designs and demonstrations for new materials.

* Currently at Formosa Plastics, Corp., P.O. Box 320, Delaware City, DE 19706

Characterization & Correlation of Extruder Residence Time

A Cooperative Effort to Improve Process Control Algorithms

Kirk Newman, Steven Jones, and Neal Cowan
Energetic Materials Research and Technology Department
Naval Surface Warfare Center
Indian Head Division
Yorktown, VA 23691-0160

and

Prof. David Bigio and Dr. Chi-Tai Yang*
Department of Mechanical Engineering
University of Maryland
College Park, MD 20742

* Currently at Formosa Plastics, Corp., P.O. Box 320, Delaware City, DE 19706

Characterization & Correlation of Extruder Residence Time

A Cooperative Effort to Improve Process Control Algorithms

OUTLINE

INTRODUCTION
- [A] Process Development
- [B] Process Improvement

APPROACH
- [A] Correlate residence time with percent drag flow
- [B] Use correlation in process control algorithm

RESULTS (for a specific screw design)
- [A] Inert PBXs
- [B] Live PBXs

APPLICATIONS / DEMONSTRATIONS
- [A] SLAM ER warhead
- [B] 5"/54 ammunition

CONCLUSIONS

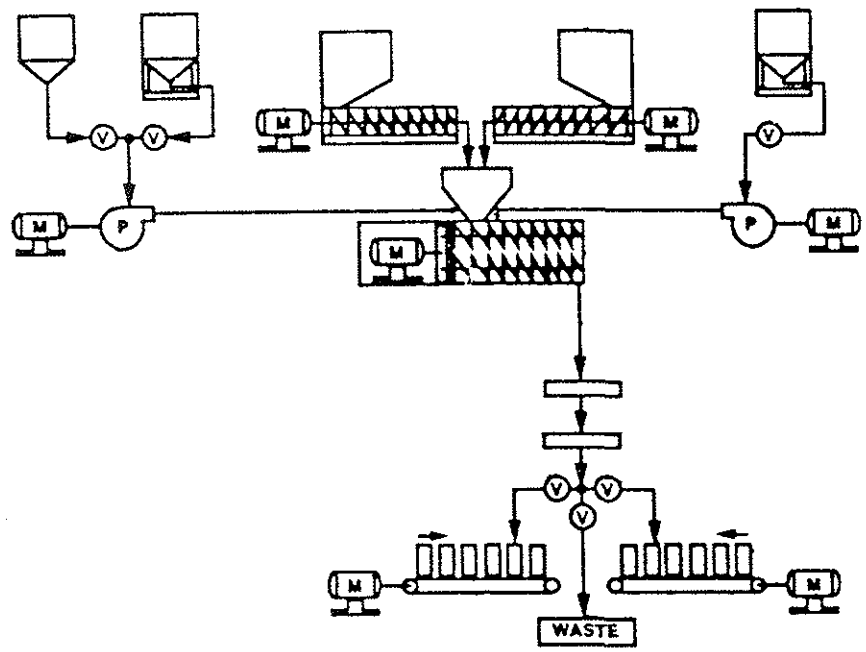

NSWC Twin screw compounding and casting process for PBX materials.

Continuous Processing

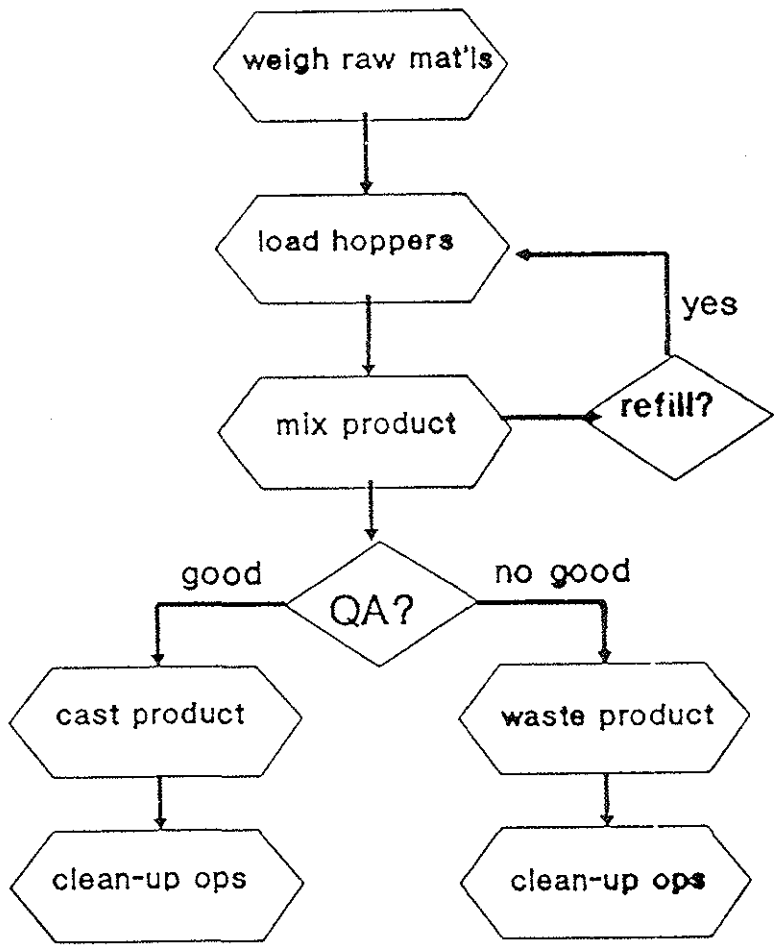

Characterization & Correlation of Extruder Residence Time

A Cooperative Effort to Improve Process Control Algorithms

INTRODUCTION

Process control algorithms for twin screw compounding and casting highly filled suspensions are dependent upon the residence time of the extruder.

Most users tend to assume that the residence time of their extruders is about constant for the parameters they use.

At best, most users tend to measure the extruder residence time as a function of the material being processed. And they try to force either the residence time, or the flow rate to be constant.

We propose a correlation that can be used to relate dependent variables, and provide dynamic processing limits for these variables in real time.

Therefore, we believe this correlation has potential to improve process control algorithms for agile processing facilities.

Typical feed forward strategy for process control of a twin screw compounding and casting (TSCC) operation based upon using loss-in-weight (LIW) feeder data and extruder residence time.

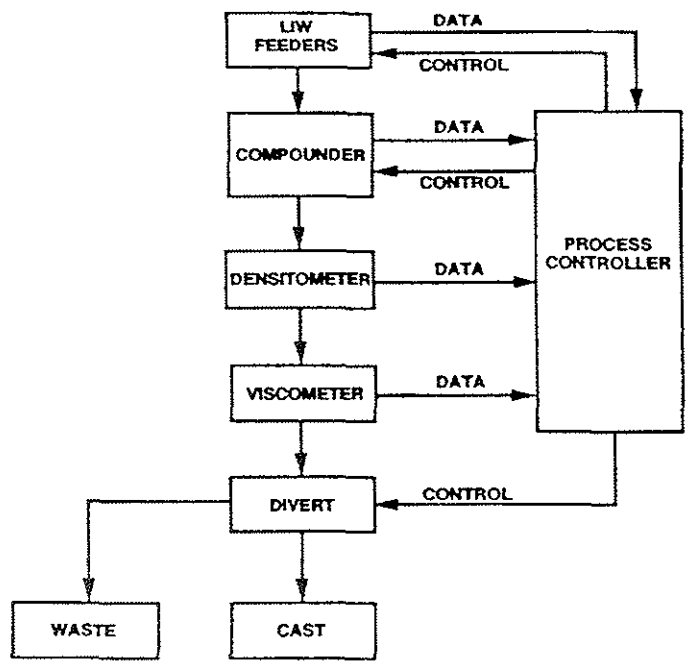

Characterization & Correlation of Extruder Residence Time

A Cooperative Effort to Improve Process Control Algorithms

PROCESS DEVELOPMENT

The twin screw compounding process for castable PBX was developed by NSWCIHD code 930 with NAVSEASYSCOM funding from the IMAD/HE program.

The process features a feed forward strategy and control algorithm based upon a running average of LIW feeder data, using the extruder residence time as the basis (U.S. Patent 5,114,630).

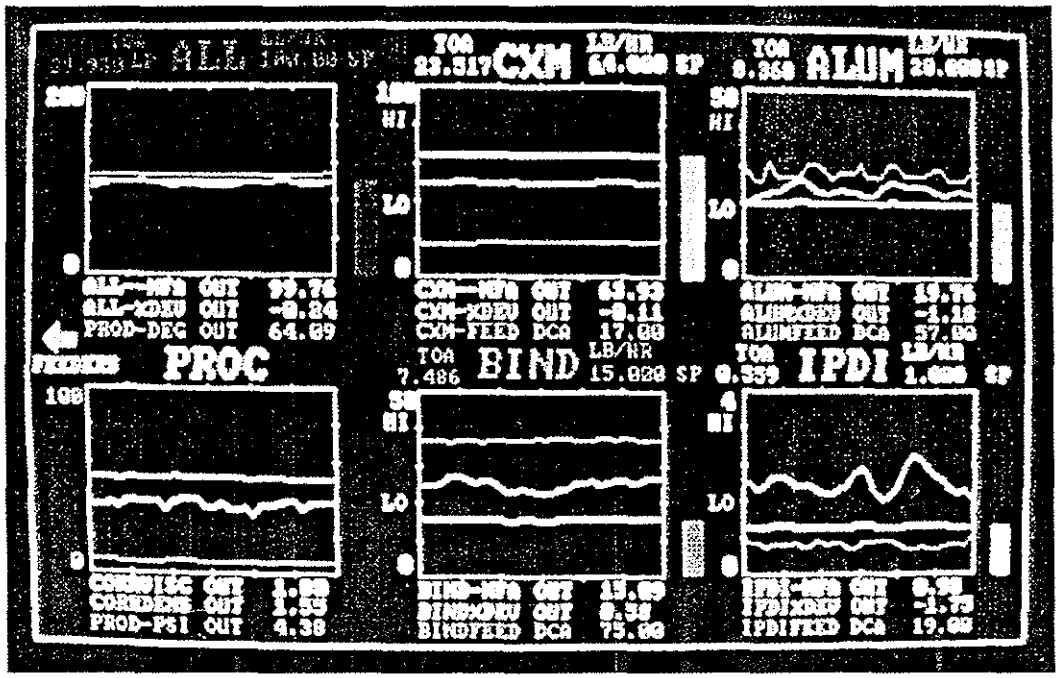

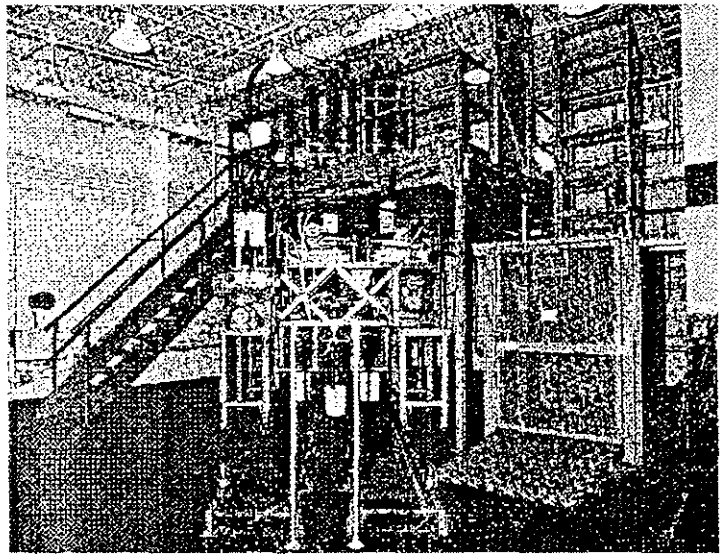

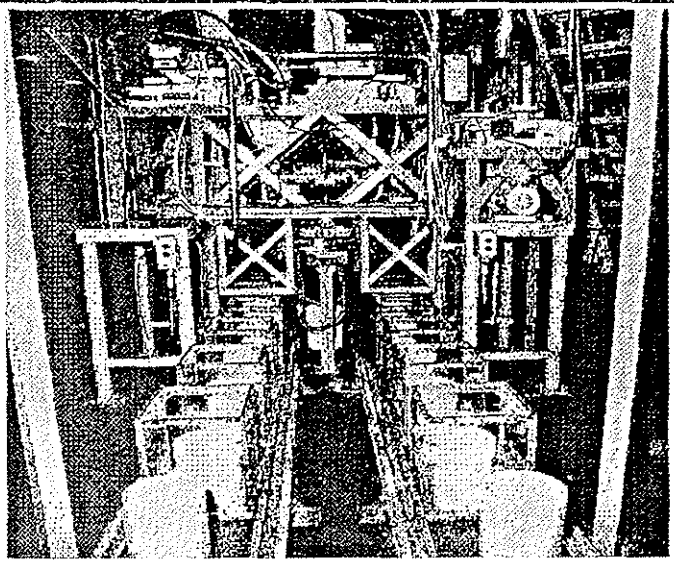

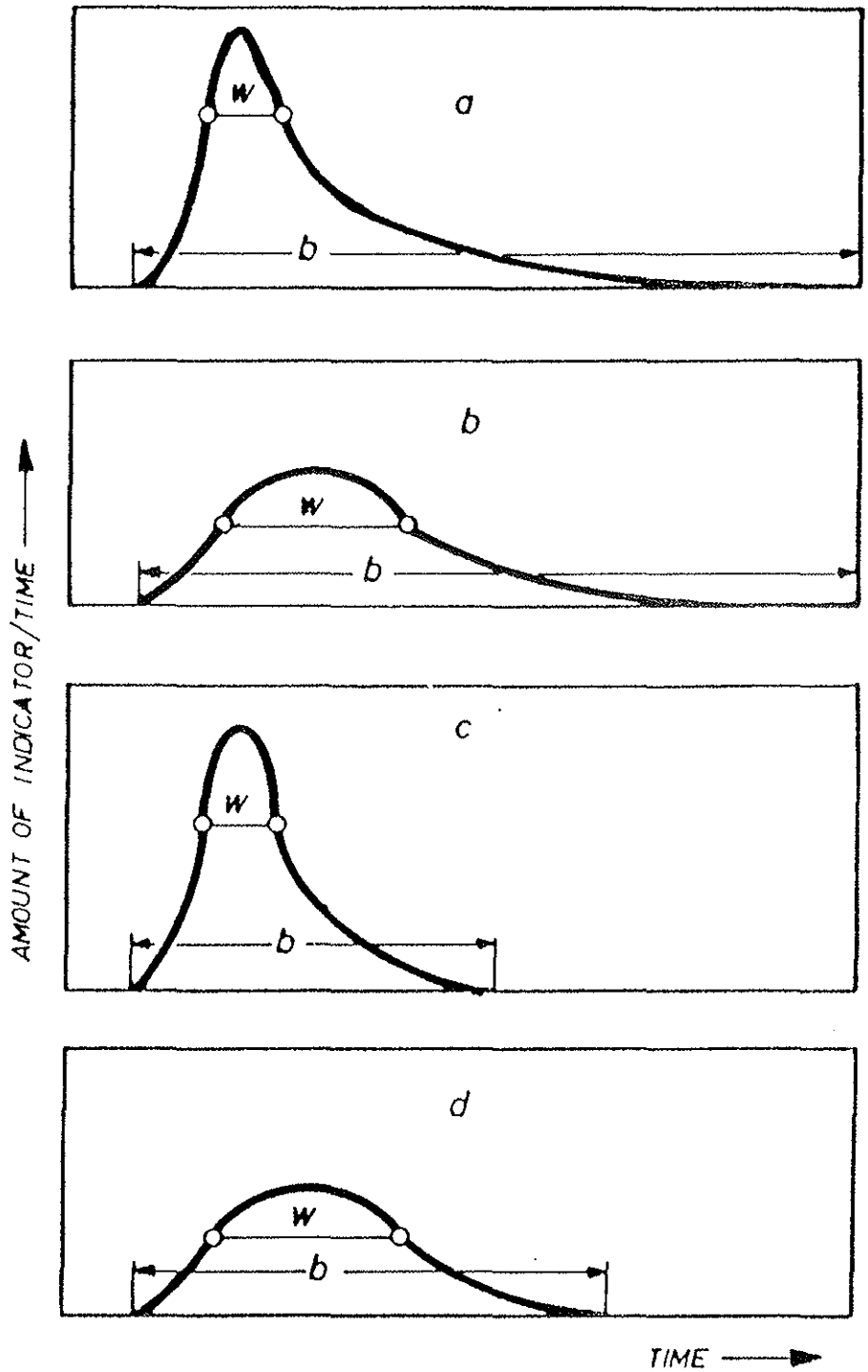

Figure 1. Four typical residence time curves for extruder processes (see text for discussion)

Characterization & Correlation of Extruder Residence Time

A Cooperative Effort to Improve Process Control Algorithms

NSWCIHD Code 930 has a process control algorithm for TSCC based upon a residence time of the form:

$$\tau = \varepsilon (V / Q)$$

where V is the volume of the twin screw compounder, Q is the volumetric flow rate of the product, and ε is the degree of fill of the compounder.

UMCP has proposed a new approach to analyzing residence time and mixing in a co-rotating twin screw extruder. This relation correlates residence time with screw speed and flow rate:

$$t = (a / Q) + (b / N)$$

This linear correlation is much easier to derive the residence time from experimental data, and it gives some information on the influence of processing variations.

PROCESS IMPROVEMENT

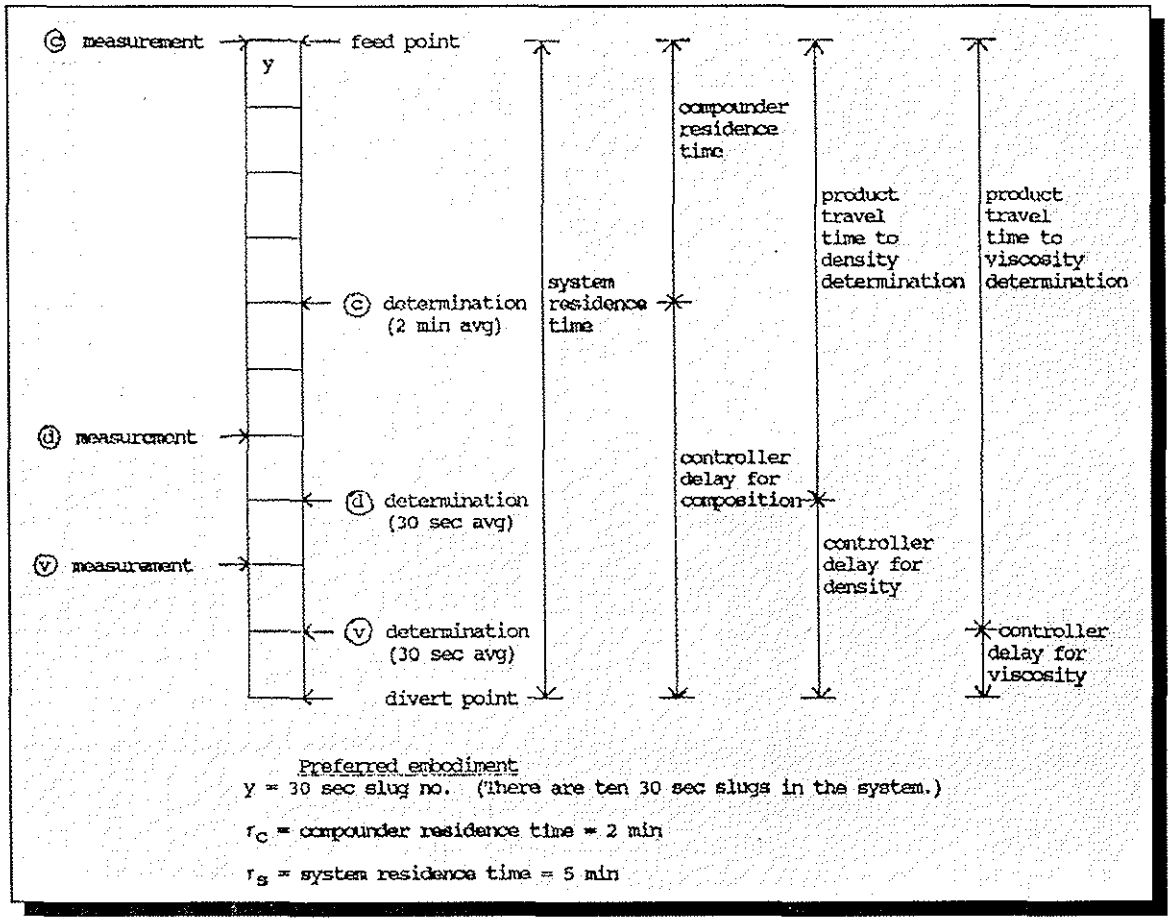

The existing algorithm for TSCC of PBX at NSWCIHD Code 930

APPROACH

Notional (or prototype) agile processing facilities being proposed (or developed) to produce energetic materials for future DOD acquisitions will probably be automated.

We believe that twin screw compounding represents a viable means to mix many of these energetic materials. The NSWCIHD Code 930 concept of a agile facility would have a twin screw compounding (TSC) operation as a fundamental unit operation. The TSC process then would be followed other unit operations, such as:
[1] extrusion
[2] vacuum casting, or
[3] injection loading,
depending upon the material and application.

We believe each unit operation should be controlled using a versatile PC/PLC architecture.

Therefore, we need to understand and describe the relationships between variables.

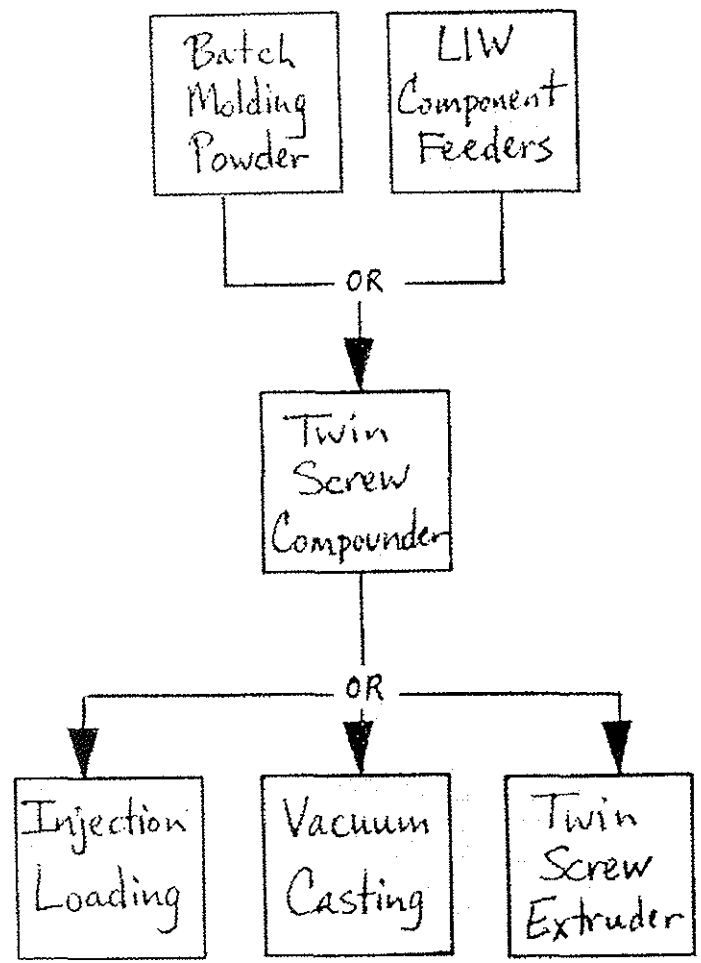

APPROACH

The experimental matrix for data collection is similar to most residence time studies, except that it can be accomplished with fewer data points.

[1] Bracket the processing range of interest in terms of N and Q.

[2] Determine the percent drag flow from an extruder design equation.

[3] Plot linear correlations for residence time.

[4] Attach physical meaning to the correlations, and use the results in the process control strategy.

CORRELATION OF RESIDENCE TIME WITH DRAG FLOW

The design equation for correlating twin screw compounders and extruders that has been expessed by Denson & Hwang (and others) can be simplified to give the 100 % drag flow condition as:

$$Q_{Drag} = [(2n - 1) / 2] \pi D N (\cos \theta) W H (F_{drag})$$

We use the ratio of (Q / N) as a measure of specific throughput (vol / rev), and we also consider it as a measure of channel fill. We calculate the specific throughput for 100 percent drag flow as:

$$(Q / N)_{100} = [(2n - 1) / 2] \pi D (\cos \theta) W H (F_{drag})$$

Therefore, we calculate the percent drag flow in terms of the specific throughput as:

$$(Q / N)_x = [(Q / N)_{100}] [x / 100]$$

USE CORRELATION IN PROCESS CONTROL ALGORITHM

Researchers at UMCP have noticed that the residence time increases with increasing drag flow. However, the material in the extruder tends to spend more time on the conveying elements and less time in the mixing zone. This indicates that:

$$\text{Degree of mixing} \quad \alpha \quad [\,\%\ \text{drag flow}\,]^{-1}$$

NSWCIHD Code 930 believes the % drag flow is useful in screw design and in defining operational limits. However, we believe the influence of Q and N upon extruder residence time is an issue for real time process control. Instead of assuming the residence time (t_{mean}) is constant, use the calibration curve to update the algorithm for on-line composition QA:

$$\text{Composition of component "i"} = [\,\Sigma\,(\text{MFA})_i\,] \,/\, [\,\Sigma\,((\text{scan rate})(t_{mean}))_i\,]$$

This could result averaging LIW feeder data over $\pm$ 6 scan times to determine if the PBX in the extruder will be acceptable or not.

RESULTS FOR INERT PBX

Screw Speed N (rpm)	Product Mass Flow Rate (lb/hr)	Time elapsed to first appearance of tracer t_{head} (sec)	Measured Residence Time t_{mean} (sec)
50	65	40	100
50	75	35	90
75	85	30	80
100	65	27	75
100	100	50	80

Screw Speed N (rpm)	Product Volumetric Flow Rate Q (ml/min)	Drag Flow (%)	N / Q (rev/ml)	$[(t_{mean})(N)]$ (rev)
50	307	21.26	0.16	83.3
50	354	24.53	0.14	75.0
75	402	18.54	0.19	100
100	307	10.63	0.33	125
100	472	16.35	0.21	133

Data for Residence Time Analysis of Inert PBX

"What is the effect of N and Q upon residence time?"

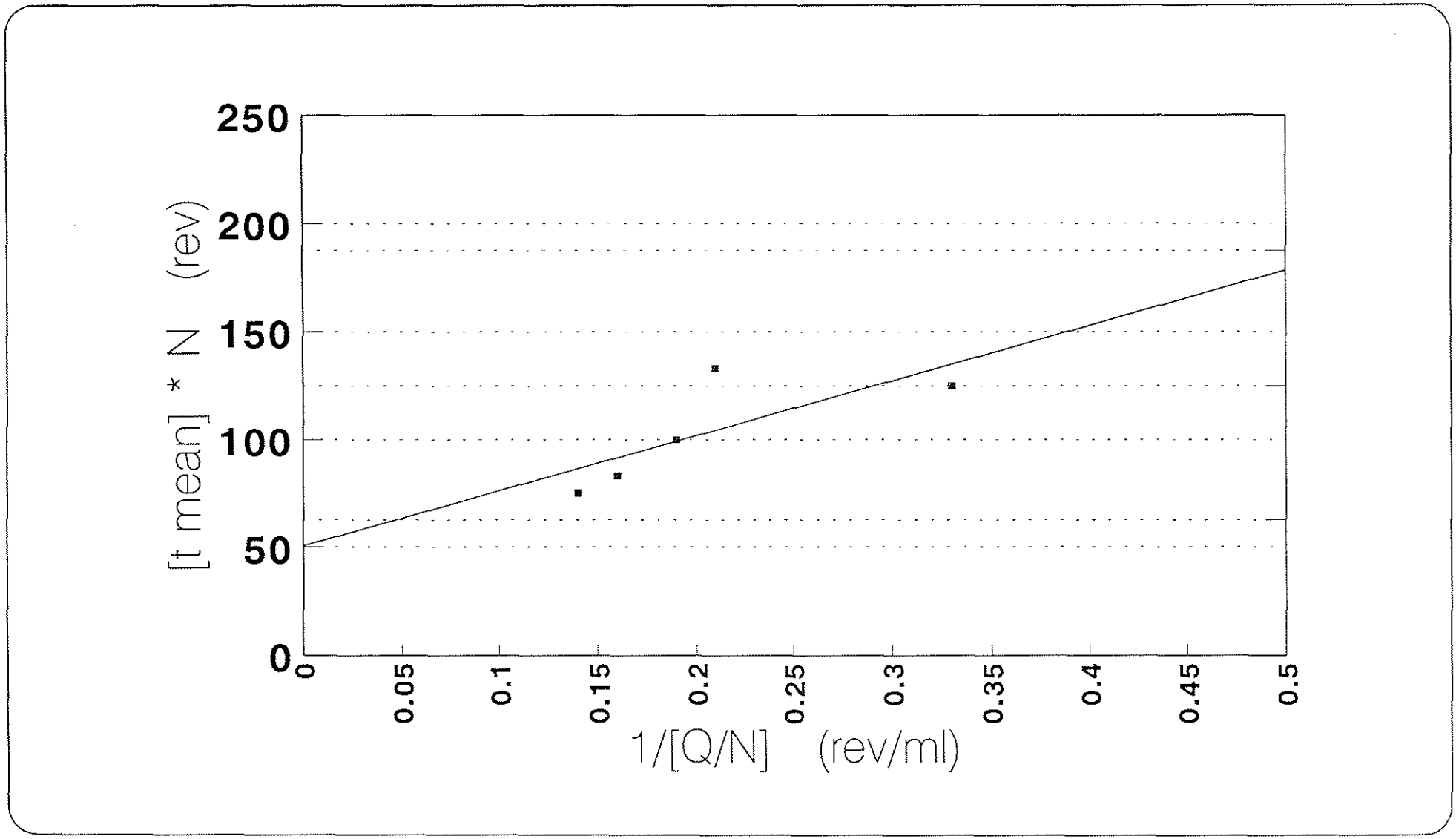

correlation = 0.75

Residence Time Screw Revolutions to Exit

RESULTS FOR PBXN-109

Screw Speed N (rpm)	Product Volumetric Flow Rate Q (ml/min)	Drag Flow (%)	N / Q (rev/ml)	[(t_{mean}) (N)] (rev)
50	307	21.26	0.16	150.0
50	354	24.53	0.14	137.5
75	402	18.54	0.19	156.2
100	307	10.63	0.33	266.6
100	472	16.35	0.21	200.0

Linear correlation is about 0.98 for the expression $t = (a / Q) + (b / N)$

RESULTS FOR PBXC-129

Screw Speed N (rpm)	Product Volumetric Flow Rate Q (ml/min)	Drag Flow (%)	N / Q (rev/ml)	[(t_{mean}) (N)] (rev)
50	307	21.26	0.16	179.2
100	307	10.63	0.33	208.3
100	472	16.35	0.21	200.0

Linear correlation is about 0.89 for the expression $t = (a / Q) + (b / N)$

Data for Residence Time Analysis of PBX Materials

"What is the effect of N and Q upon residence time?"

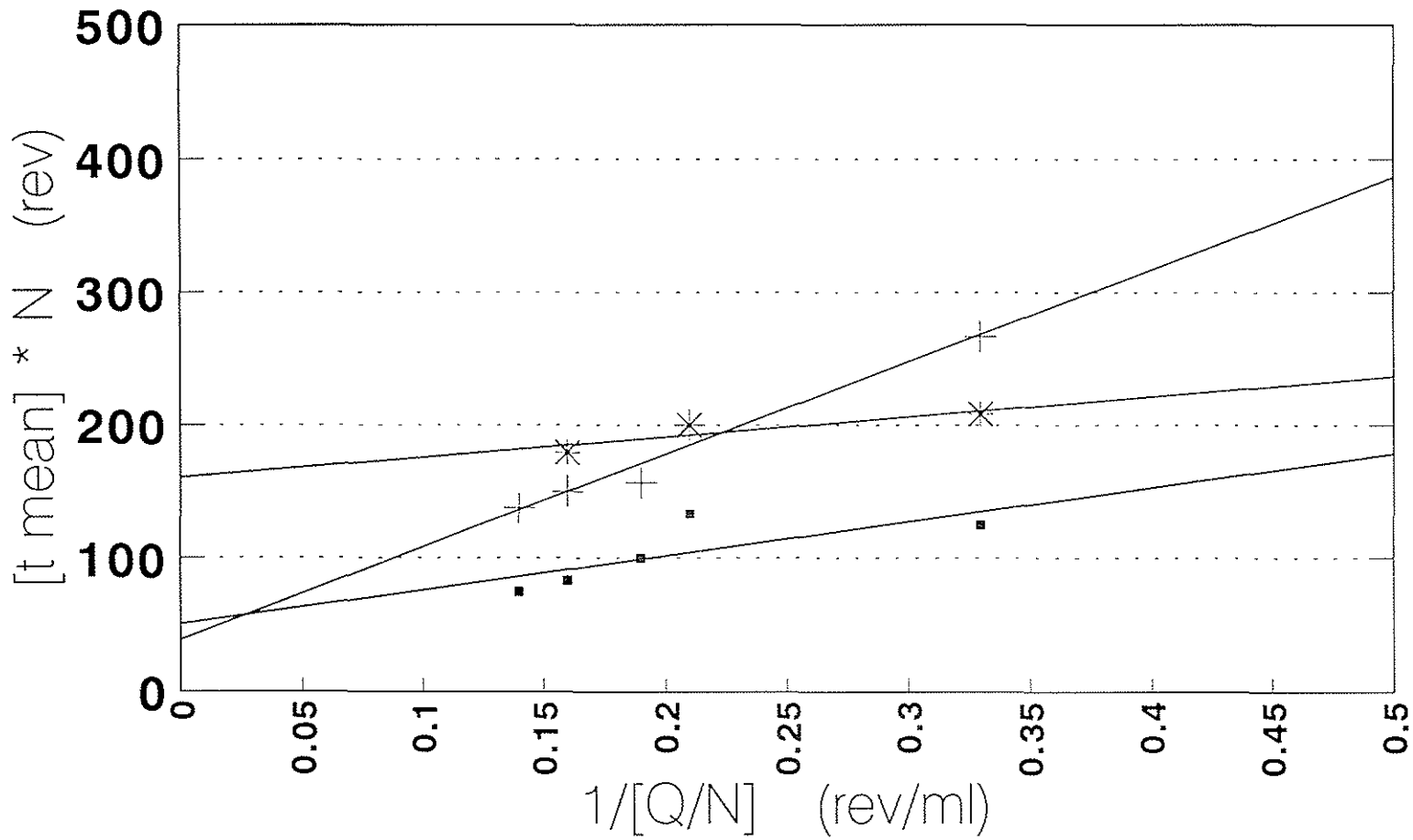

inert PBX PBXN-109 PBXC-129

Residence Time Screw Revolutions to Exit

RESULTS

The results for extruder residence time correlation for the three materials examined indicate that different materials behave differently, even if the screw design is the same.

Inert non-aluminized polyurethane PBX: $t = (255 / Q) + (51 / N)$

PBXN-109 (aluminized polyurethane filled with RDX): $t = (695 / Q) + (39 / N)$

PBXC-129 (non-aluminized polyacrylate filled with HMX): $t = (152 / Q) + (160 / N)$

APPLICATIONS

The Stand-off Land Attack Missile (SLAM) combines an imaging infrared seeker, inertial GPS-aided guidance, and data link control to provide stand-off precision strike against land targets and selective ship attack.

The Expanded Response variant of this missile (SLAM ER) will provide greater target coverage, destruction, penetration and range.

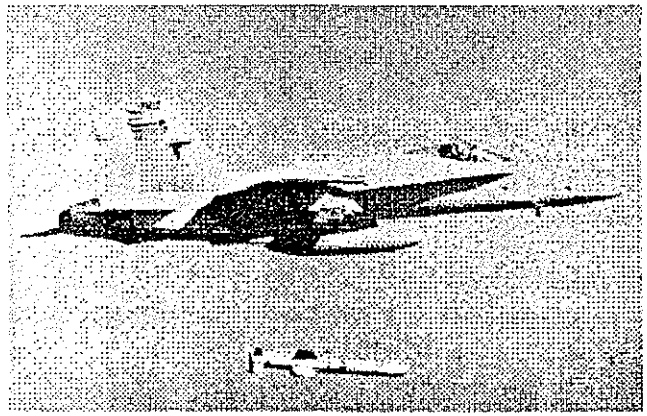

SLAM and SLAM ER provide the F/A-18 Hornet with precision strike capability

NSWCIHD Code 930 was asked to develop an automated pilot plant process to load the SLAM ER warhead with PBXC-129.

The automated twin screw compounding and casting (TSCC) process was then to be compared to a traditional vertical planetary batch mixing and casting operation.

The question of interest is: At what point is a TSCC process more economical than the traditional batch process ?

NAWCWPNDIV has solicited industry contractors to bid on the E&MD of SLAM ER.

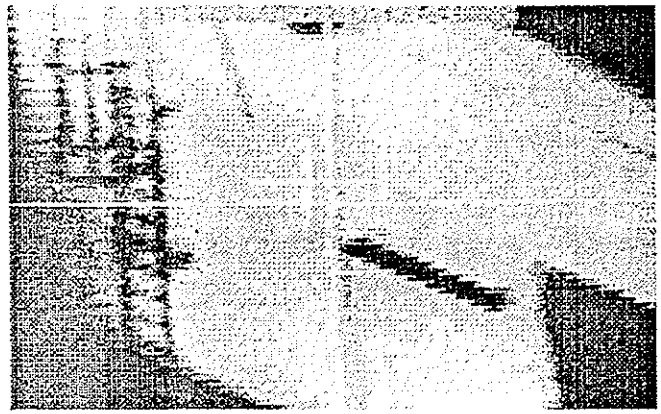

SLAM has demonstrated exceptional reliability and has combat-proven effectiveness in defeating a variety of targets.

Naval Surface Warfare Center
INDIAN HEAD DIVISION

Characterization & Correlation of Extruder Residence Time

A Cooperative Effort to Improve Process Control Algorithms

APPLICATIONS

The twin screw compounding process for castable PBXC-129 was recently developed by NSWCIHD code 930 with NAVAIRSYSCOM funding from the CMP program office.

In performing this project, we discovered that the residence time profile for this polyacrylate PBX was different than that for most of our previous work with polyurethane PBX materials.

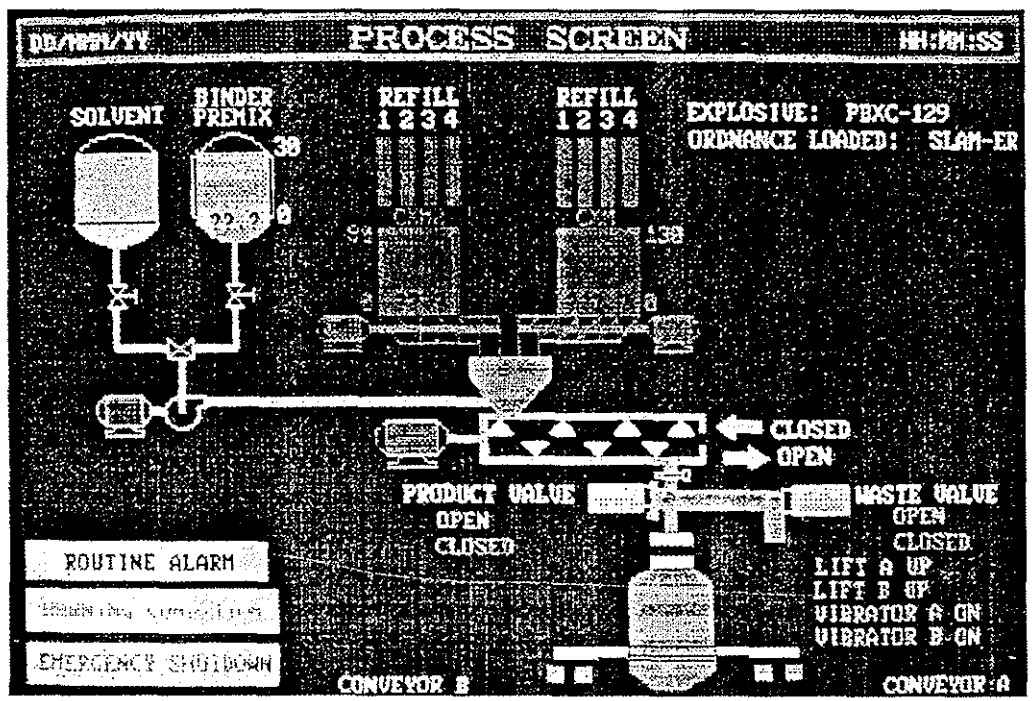

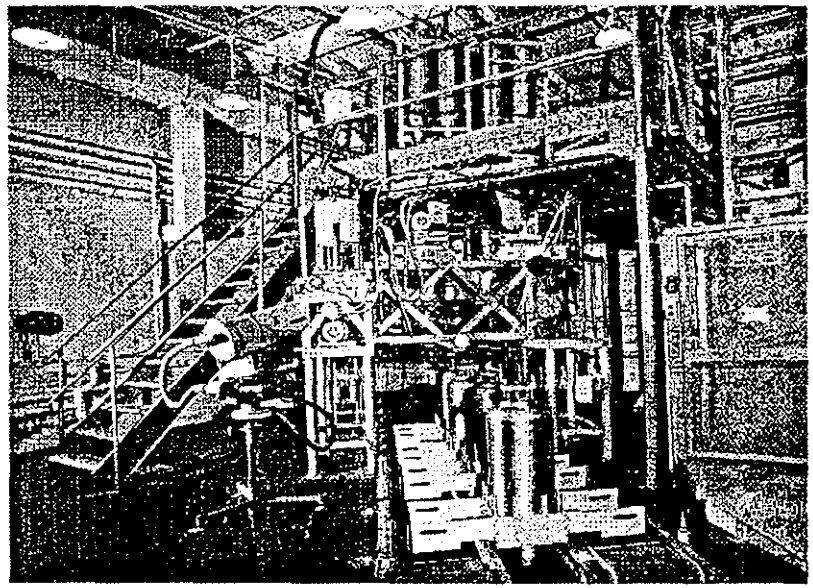

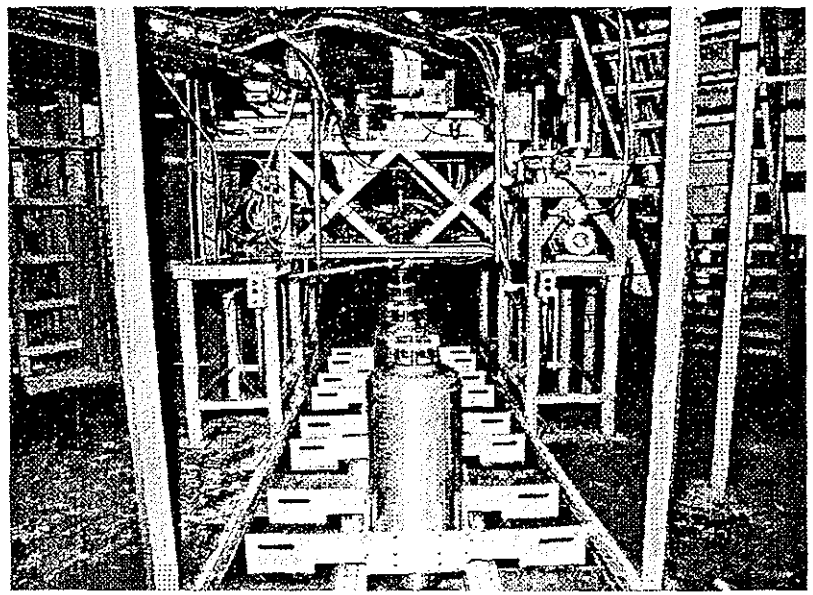

CAMPEP PROCESSING TECHNOLOGY ASSESSMENT

CONTINUOUS TWIN SCREW COMPOUNDING AND CASTING PBX

- *Using a special plumbing fitting, we can split the flow and still obtain empirical data for apparent viscosity during casting operations. This provides another data point for the process control algorithm.*
- *We maintain full vacuum in the warhead (and in the waste container), and use a PID controller for the product valve to maintain 25 psi pressure drop.*
- *We maintain a dynamic seal in the compounder using a new screw design based upon a NSWC solution to a set of design equations devloped by University of Delaware. The design equation for each section of the compounder is of the form:*

$$Q = f(N, \cos\theta, \eta, \Delta P)$$

where N is the screw speed, θ is the helix angle, η is the viscosity, and ΔP is the pressure drop. We measure η and ΔP. We control N to maintain constant calculated Q.

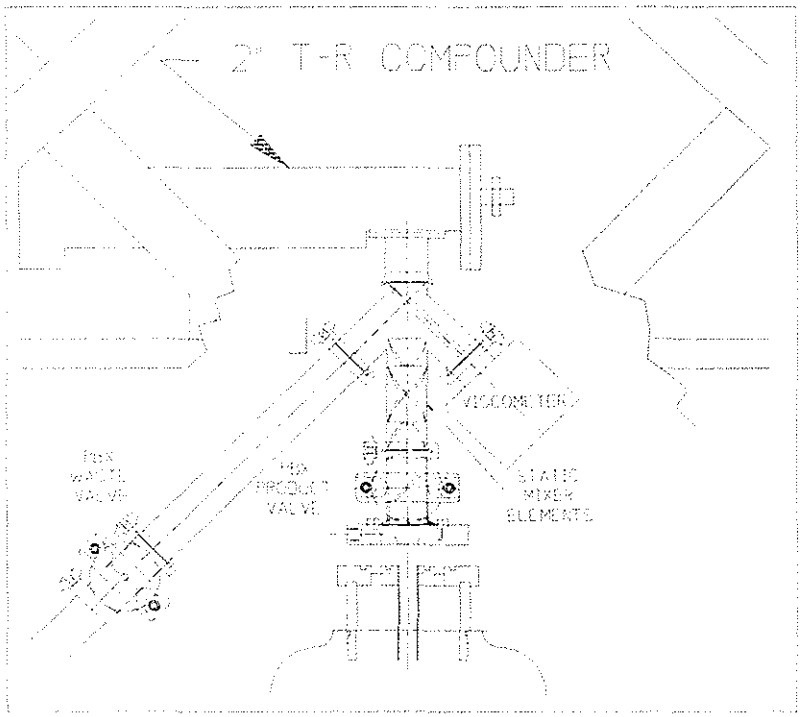

Naval Surface Warfare Center
INDIAN HEAD DIVISION

DEPARTMENT OF THE NAVY
SEA SYSTEMS COMMAND

CAMPEP PROCESSING TECHNOLOGY ASSESSMENT

CONTINUOUS TWIN SCREW COMPOUNDING AND CASTING PBX

- *Maintaining the pressure drop necessary for continuous vacuum casting by installing static mixer elements in the cylindrical plumbing.*
- *Volumetric flow to be modelled by:*

  $Q = [(\pi n r^3)/(3n+1)][(r\Delta P^{1/n})/(2Lm)]$

  for $n = 0.81$ and $m = 2.29$ kp, we need to maintain $\Delta P = 25$ psi to produce about 100 lbs/hr of PBX across a 10 inch run of 2 inch diameter plumbing.

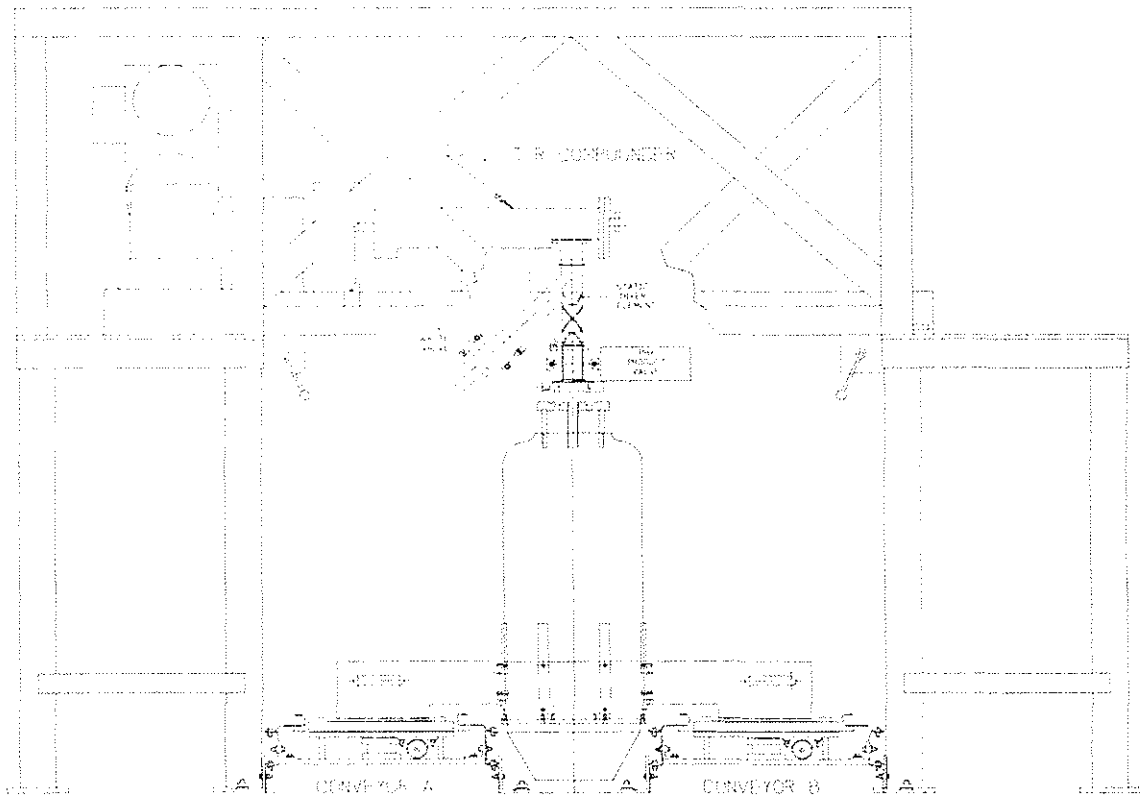

COMPARISON BETWEEN BATCH AND "CONTINUOUS" PROCESSING

Comparing 150-gallon VPM to 2-inch TSCC

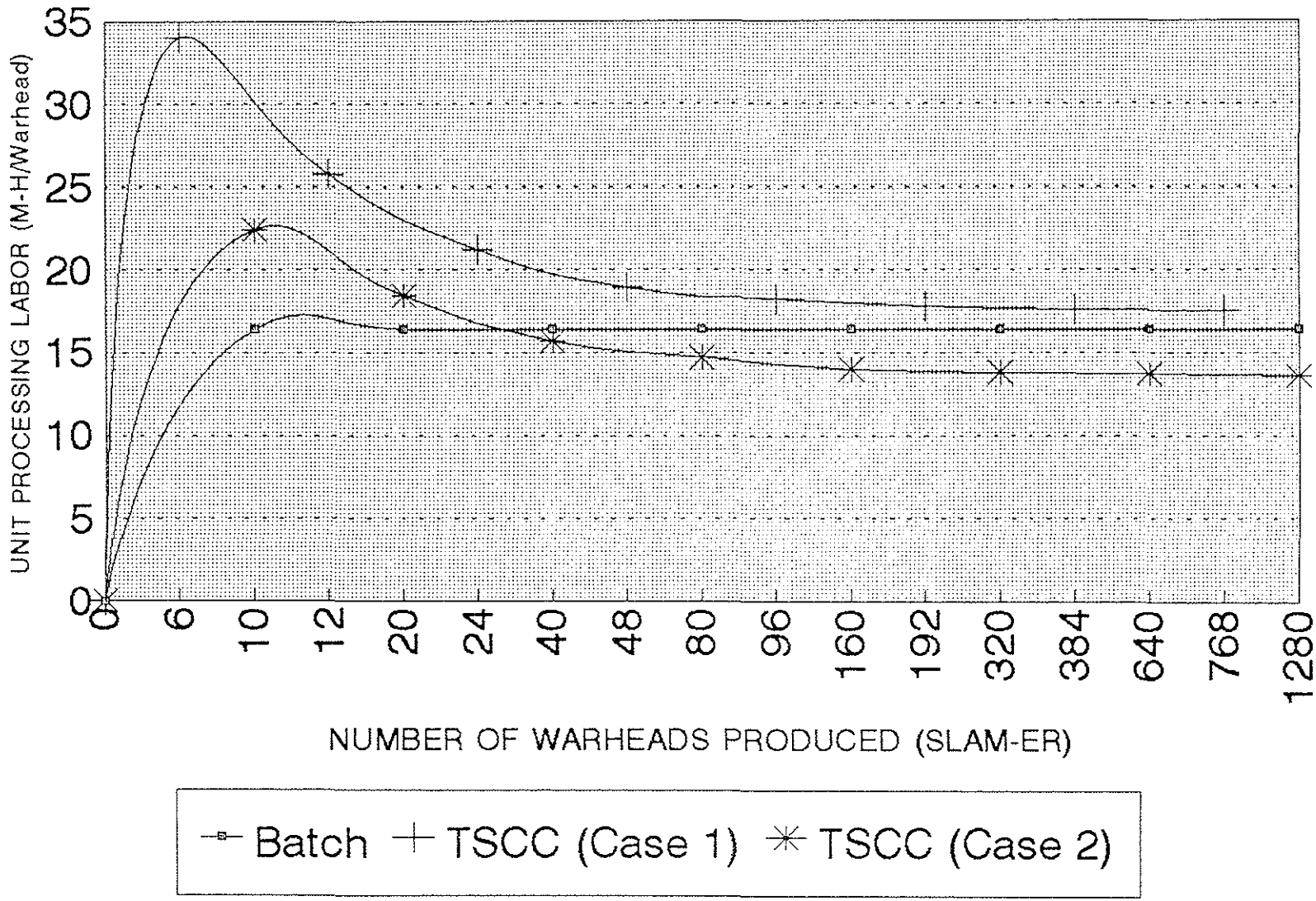

Estimate for NSWCIHD (Code 930) facilities
Case 1 = Interrupted TSCC
Case 2 = Uninterrupted TSCC

COMPARISON BETWEEN BATCH AND "CONTINUOUS" PROCESSING

Comparing 150-gallon VPM to 2-inch TSCC

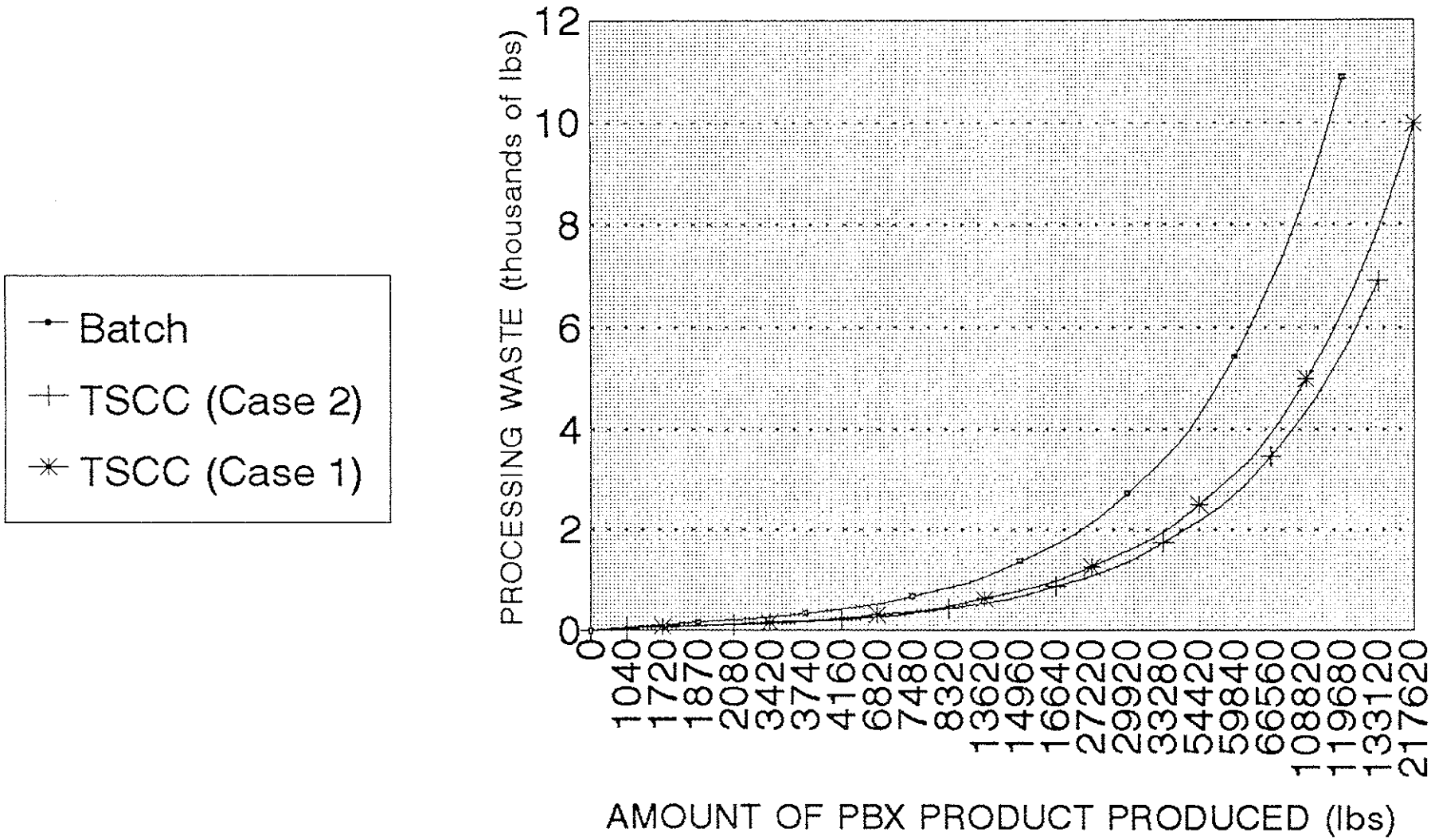

Estimate for NSWCIHD (Code 930) facilities
Case 1 = Interrupted TSCC
Case 2 = Uninterrupted TSCC

CONCLUSIONS

[1] The linear correlation of extruder residence time with Q and N is useful.

[2] The residence time is a stronger function of product than originally believed.

[3] The simulant used does not simulate either PBXN-109 or PBXC-129.

[4] Future work will be done to assess this correlation for different extruder screws.

[5] Future work will be done to assess the impact of this correlation upon on-line QA algorithms.

ON THE EFFECT OF SHEAR FLOW ON DEVOLATILIZATION OF FILLED POLYMERIC MATERIALS:

Jianya Cheng, David I. Bigio
Department of Mechanical Engineering
Robert M. Briber
Department of Nuclear and Material Engineering
University of Maryland, College Park, MD 20742

Abstract

This is the second part of a systematic program to investigate the onset and mechanisms of devolatilization of filled polymeric materials. The object of this work is to study the effect of shear flow on the devolatilization of filled polymers. It is found that shear flow enables abrupt foam growth at relatively high absolute pressure in comparison to the cases without shear flow. The shear flow also reduces the threshold pressure which distinguishes two regimes of gradual and abrupt foam. In addition, an oscillatory foam growth phenomena was observed. The foam growth and devolatilization efficiency are found to depend on the imposed shear rate .

Introduction

Devolatilization in polymer processing is used to remove residual volatiles. Extrusion processing of filled polymers has been used in a range of industries such as automobile, aerospace, etc. Specific aspects of filled systems such as orientation of solid particles, rheology of the system, interactions between particles and matrices, etc., are expected to make the devolatilization processing very complex. We have been performing in a range of experimental work to obtain comprehensive information to better understand the devolatilization process for filled polymers. The first part of the work was to investigate the effects of solid fill level, vacuum level, rheology of the matrix and mixture using a batch device without flow [1].

One of the factors which can influence the foam enhanced devolatilization in an extruder is the nature of flow field. Shear and extension flows are expected to change the process considerably. Flow and/or shear stress may induce bubble nucleation [2]. Shear and/or elongational deformation may change the early stage of foam growth by enabling quick detachment pre-existing bubbles from their surrounding [3,4]. Deformation imposed on bubbles is expected to generate more interfacial area for the transfer of volatiles from the matrix to bubbles. Deformation may also accelerate the bubble coalescence and rupture. Complex rheological behavior of filled polymers will tend to make the devolatilization process under flow more unpredictable.

One of the goals of this work is to simulate the devolatilization process during extrusion using a simple shear flow field and determine the effect of flow field on the onset of devolatilization for filled polymers in terms of the foam growth, bubble structure and devolatilization efficiency. This paper will report the results of experiments under simple shear flow.

Experimental

Experimental set-up

A concentric cylinder apparatus was used to impose a simple shear flow. The experimental set-up is shown schematically in Figure 1. The inner cylinder and outer cylinder were placed on a plate which was connected in the center to a rotational shaft. The rotation of the inner cylinder was driven by a AC motor through a series of gear-belt conveying systems. The bottom of devolatilization chamber was sealed using two bearings. The diameter of outer cylinder was 2.5''. Two different sizes of inner cylinders were used (2 1/8" and 1 1/2", respectively). The shear rate can be calculated from the following equation:

$$\dot{\gamma}_{r\theta} = r\frac{\partial}{\partial r}\left(\frac{v_\theta}{r}\right) = \frac{2\Omega}{1-\kappa^2} \qquad (1)$$

where Ω is the angular rotational speed and $k = d_{inner}/d_{outer}$. The d_{inner} and d_{outer} are the diameters of inner and outer cylinders, respectively.

The vacuum pressure level is controlled by side valve (A) and is measured by a vacuum pressure gauge (P) (see Figure 1). Foam growth behavior was videotaped and the variation of foam expansion volume with time was determined by analysis of the videotape. The fraction of volatile removal was measured by condensing the volatile vapor using a series of traps immersed in liquid nitrogen.

The samples were placed in the gap area between the two cylinders. The model Newtonian polymer matrix is polybutadiene with molecular weight of 2800 (viscosity μ = 84 poise at 25 ^{0}C, ELF Atochem). The inert solid filler is potassium chloride (KCL) with a mean particle size of 177 mm. The solid fill percentage used varies from 0 to 65 weight %. Toluene (ELF Atochem) was used as the volatile component. The volatile concentration ranged from 0 to 5 weight %. Samples were prepared by pre-mixing fillers into the matrix polymer already containing the volatile solvent. The air bubbles entrained in the polymer KCl mixture during blending were removed using ultrasound vibration and/or centrifugation. The removed volatile was condensed in the traps using liquid nitrogen.

Rheology of Filled Systems

Simple shear flow and small amplitude oscillation tests were conducted for both the Newtonian and viscoelastic matrix systems. The shear viscosity data for filled materials in the Newtonian polybutadiene matrix at different solid loadings are shown in Figure 2. The filled materials exhibit a shear independent viscosity up to 40% solid loading. As shown in Figure 2, the viscosity increases with increasing filler percentage. Shear-thinning behavior is observed for the 65% solid loading sample. At low shear stress, the viscosity at 65% solid loading is substantially higher than the viscosity of the 40% solid fill sample. This may be due to interparticle interactions [5]. Agglomeration of filler particles can result in a sharp increase of the low shear rate viscosity. The interfacial properties and particle size may also contribute to the viscosity increase. The shear-dependent viscosity observed for the 65% fill material can be represented by the Carreau-Yasuda four-parameter model [6]:

$$\frac{\eta}{\eta_0} = \left[1 + (\lambda \dot{\gamma})^a \right]^{(n-1)/a} \qquad (2)$$

The values of the regression parameters, η_0, λ, n and a, for fitting the data in Figure 2 by Eq. 2 are 208.5 (Pa.s), 0.314 (s^{-1}), 0.368 and -191.1. The Newtonian shear viscosity for 0% 20% and 40% solid loadings are 8.57, 12.43 and 20.87 (Pa.s)

In addition to shear thinning behavior, 65% fill Newtonian matrix material also exhibits elastic behavior. The primary normal stress difference is defined as:

$$N_1 = -(\tau_{11} - \tau_{22}) = \Psi_1 \dot{\gamma}^2 = m' \dot{\gamma}^{n'} \qquad (3)$$

Where N_1 is primary normal stress difference, τ_{11} and τ_{22} are the primary and secondary normal stresses, Ψ_1 is the primary normal stress difference coefficient and $\dot{\gamma}$ is the shear rate.

RESULTS AND DISCUSSION

Devolatilization experiments have been performed for 20, 40 and 60% filled polymers in a Newtonian matrix (polybutediane) at different vacuum levels under different shear rates. Typical foam growth volume expansion versus time is plotted in Figure 3 for 40% solid loading at 40 mm Hg. Without shear flow, the sample started to grow *gradually* after vacuum was applied. After about 2 min, the foam reached its maximum foam expansion volume. After shear flow was applied for a few minutes ($\dot{\gamma}_{r0}$ = 5 s^{-1}) foam would grow immediately upon the introduction of vacuum. The foam would then rupture after a short period of time (about 1 min). Then sample would have a second period of foam growth and collapse again. This oscillation phenomena remained for rest of the experiment with the amplitude of foam expansion dampening.

Similar phenomena was observed for same sample (40% solid loading) at vacuum of 80 mm Hg (see Figure 4). Without shear flow, the material grew very slowly after vacuum was introduced. The foam reached its maximum foam expansion volume after about 5 minutes. However, the foam started to grow abruptly under shear deformation at shear rate of 5 s^{-1} after the vacuum was applied. Within few seconds, the foam reached its maximum foam expansion volume and collapsed a short time later. This cycle of growth and collapse repeated but with a decreasing amplitude compared to the previous cycle.

Figure 5 shows the foam growth for 20% solid fill samples at 10 and 40 mm Hg with and without shear flow. The foam growth behavior for cases under shear at both 10 and 40 mm Hg is similar. Abrupt foam growth was observed under shear deformation with a shear rate of 5 s^{-1} at 10 and 40 mm Hg. However, gradual foam expansion was found at 40 mm Hg without shear. These results are similar to results obtained for 40% solid loading.

Next a set of experiments were conducted to determine the effects of shear flow on the onset of the threshold pressure that distinguish the different regimes of foam growth dynamics. During batch devolatilization we found that, for a given polymeric system, the material may not foam under very low level of vacuum pressure (e.g., high absolute pressure). After increasing the vacuum level, the material begins to foam. There are two distinct foam growth phenomena. One is called "*gradual growth*"

and other is "*abrupt growth*". For gradual growth, the bubbles start to form after vacuum was introduced to the devolatilization chamber and continue to grow gradually. In contrast to the gradual foam growth regime, the bubbles grew abruptly at higher vacuum levels. Then the foam reached its maximum expansion volume within very short time period (at most only few seconds). In previous batch devolatilization work, we found that, for a given polymeric material, there is a threshold pressure that distinguishes these two different regimes of foam growth. We also found that abrupt foam growth occurred at lower vacuum levels for a given filled material under shear flow in comparison to the cases without shear [1].

Figure 6 shows the dependence of the maximum foam expansion volume as a function of vacuum pressure for 65% solid loading in the Newtonian matrix at shear rate of 5 s^{-1}. As seen in Figure 6, abrupt foam growth induced by shear flow occurred even at 120 mm Hg vacuum pressure. In contrast to the cases without shear flow, even at 10 mm Hg vacuum, only gradual foam growth was observed for 65% solid loading. The maximum foam expansion volume $(\Delta V/V_0)_{max}$ observed for abrupt growth remained relatively constant at around 1.05, while the $(\Delta V/V_0)_{max}$ value decreased with decreasing vacuum pressure (e.g.: increasing the absolute pressure). When the absolute pressure excesses 360 mm Hg, no foam growth was observed for 65% solid loading samples. As mentioned previously, the foam growth was gradual even at 10 mm Hg vacuum without shear deformation. However, at 10 mm Hg vacuum, abrupt foam growth was observed for 65% solid loading under shear deformation with a shear rate of 5 s^{-1}.

The value of the maximum foam expansion volume for 20% and 40% solid loading in a Newtonian matrix varied over wide range (shown in Figures 7, 8). Abrupt foam growth for 20 % and 40% solid loading under shear flow was observed even at 300 mm Hg. Without shear deformation, the abrupt growth was observed for both 20% and 40% solid loading only at 20 mm Hg. This indicates that the shear deformation plays an important role in the foam growth process.

It was observed that shear flow tended to elongate and break bubbles aggressively in comparison with the cases without shear [9]. Shear flow may constrain the free growth of bubbles. Under shear, the bubbles are stretched and form long elliptical shapes. This occurs when deformation or elongation rate of the bubbles is large compared to that for large initial size of the bubbles. For small bubbles, the matrix fluid can still be considered a continuous phase and the flow field is close to that of a pure fluid. However, for the systems with large bubbles, the matrix may no longer be a continuous phase and the momentum flux can be very different.

One of the possible explanations may be the quick detachment of nucleated bubbles from their nucleation site under shear flow. The existence of solid fillers can provide sites for heterogeneous nucleation. A nucleated bubble in the cavity of rough solid surface may require a critical force to detach from its cavity [5,6]. The shear flow may provide this force. At a given vacuum pressure, shear flow will produce extra forces on the bubble, which can lead to detachment of the bubble. Without shear, some bubbles may not be able to detach at a given vacuum pressure. Biesenberger and Lee [3] also observed a similar phenomena in devolatilization of unfilled polymers in a drum type devolatilizer. They found that a large swarm of bubbles formed after drum started to rotate, compared to the case where no bubbles were observed without the rotation of the drum. Foaming time was also found to be shorter with increasing screw speed in an extruder for unfilled materials [4].

Deformation of a bubble in a flow field can give rise to a large interfacial area compared to the undeformed spherical bubble. This interaction between the bubbles may enhance interfacial renewal for volatile mass transfer from fluid matrix to bubbles. The tensile stresses in the highly filled samples may be enhanced at same shear rate relative to lower levels of solid fill due to the enhanced viscosity (see Figures 2 and 9). These tensile stress may enable the nucleated bubble to detach quickly Foam growth was observed due to the shear even without application of vacuum. This indicates that the shear flow does impose extra forces enabling the detachment of nucleated bubbles.

The maximum foam expansion volumes under shear flow is lower than that without shear. It was observed that shear flow tended to elongate and break bubbles aggressively in comparison to cases without shear [9] Shear flow may constrain the free growth of bubbles. After shear, the bubbles were stretched to form long ellipses. The deformation or elongation rate is considerably large than the initial size of the bubbles. We can use Tylor's deformation parameter, D: [10]:

$$D = \frac{l-b}{l+b} \tag{4}$$

where b is the minor axis of the ellipse. The values of deformation parameter, D, for small bubbles are considerably larger than for big bubbles. This phenomena may be induced by different flow fields for two different systems, even at same apparent wall shear rate.

The rheology of filled polymers may change under different flow conditions. The dependence of shear viscosity with filler percentage is shown in Figure 9. The shear viscosity remains constant for 0, 20 and 40% filled samples. However, the shear viscosity decreases considerably for the 65% filled materials with increasing shear rate. This change of rheological properties may contribute to the higher threshold pressure for the 65% filled samples.

The effect of shear flow on the fraction of separation is shown in Figure 10. The fraction of separation under shear flow is higher than without shear at a given time interval. This may be due to quick detachment of nucleated bubbles and large interfacial area due to the deformation of the bubble. The fast interfacial renewal under shear flow may also contribute to the higher values of the fraction of separation. the interfacial renewal will reduce the resistance of volatile mass transfer from matrix to bubbles.

CONCLUSIONS

Abrupt foam growth was observed under shear flow at the same vacuum pressure where the foam grew gradually without shear. This phenomena was found for all filled samples. Oscillatory foam growth was observed during the devolatilization of filled polymers under shear flow. The maximum foam expansion volume under shear was somewhat lower that without shear. Shear deformation was found to constrain the free growth of bubbles. The fraction of separation under shear is somewhat higher than without shear at same time interval. The maximum foam expansion volume under shear was somewhat lower than without shear. The threshold pressure, which distinguishes the different foam growth phenomena, is strongly dependent on the shear deformation. Without shear flow, the threshold pressure is much lower than shear flow. For 65% solid loading, abrupt foam growth was observed under shear deformation, in comparison to the gradual growth observed at low vacuum pressure without shear flow.

References

1. Cheng, J., Bigio, D.I., and R.M. Briber, *SPE ANTEC*, **53**, 365 (1996).
2. Han, J.H., and C.D. Han, *Polym. Eng. Sci.*, **28**, 1616 (1988).
3. Biesenberger, J., and S.T. Lee, *Polym. Eng. Sci.*, **27**, 510-517 (1987).
4. Tukachinsky, A., Talmon, Y., and Z. Tadmor, *AIChE J.*, **40**, 670 (1994).
5. Carreau, P.J., Chapter 7. in Transport Processes in Bubbles, Drops and Particles, Hemisphere Publishing, New York (1992).
6. Bird, R.B., Armstrong, R.C., and O. Hassager, Dynamics of Polymeric Liquids, John Willy, New York, (1987).
7. Blander M., and J.L. Katz, *AIChE J.*, **21**. 838 (1975).
8. Fisher, J.C., *J. Appl. Phys.*, **19**, 1062 (1948).
9. Canedo, E.L., M. Favelufis, Z. Tadmor and Y. Talmon, *AIChE J.*, **39**. 553-559 (1993).
10. Talor, G.I., *Proc. Roy. Sco.*, (*London*), **A138**, 41 (1932).

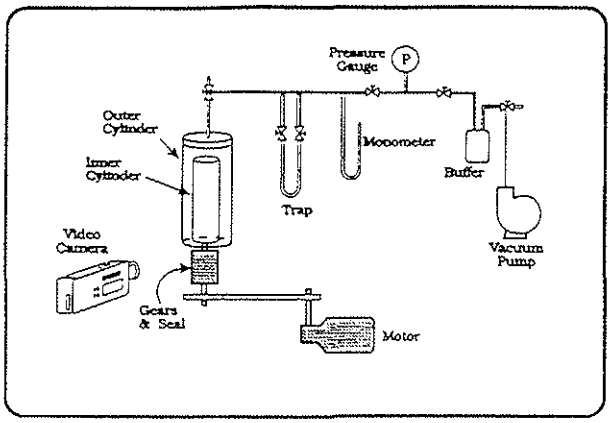

Figure 1. Sketch of Experimental set-up.

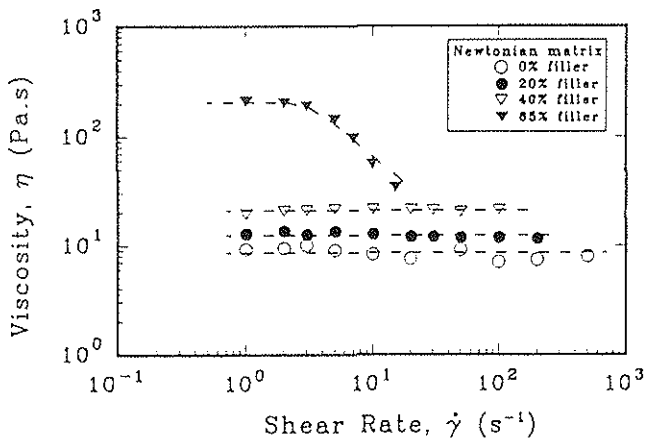

Figure 2. Rheology of the filled samples

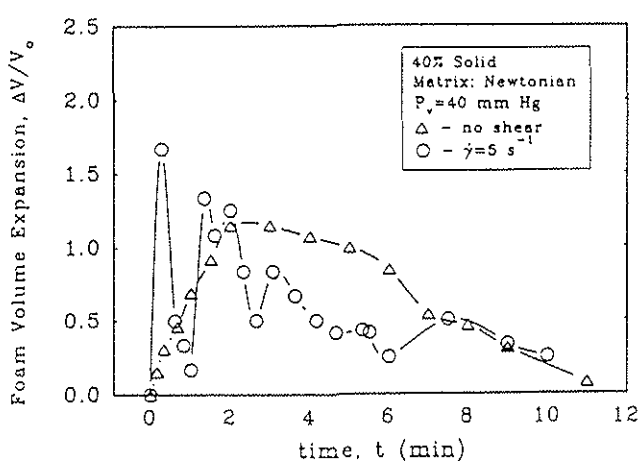

Figure 3. Effect of shear on foam growth for 40% solid loading at 40 mmHg.

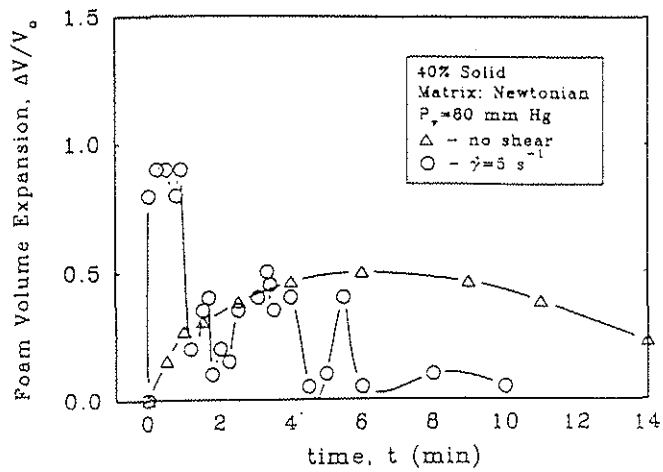

Figure 4. Effect of shear on foam growth for 40% solid loading at 10 and 80 mmHg.

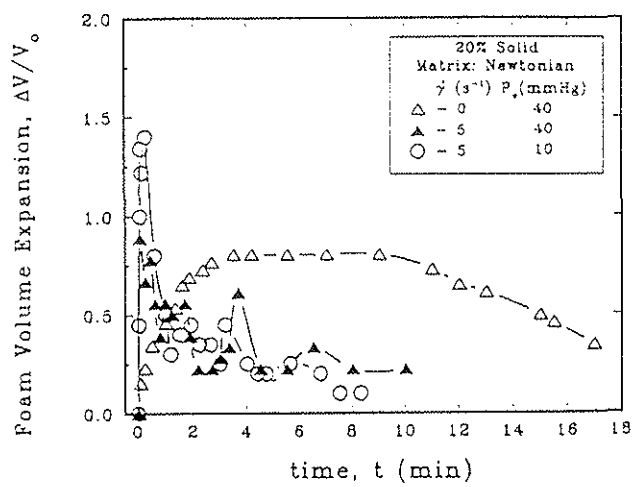

Figure 5. Effect of shear on foam growth for 20% solid loading at 10 and 40 mmHg

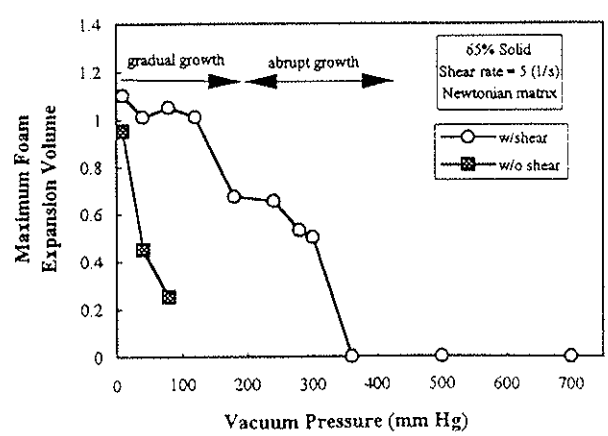

Figure 6. Dependence of maximum foam expansion volume with vacuum pressure for 65% loading

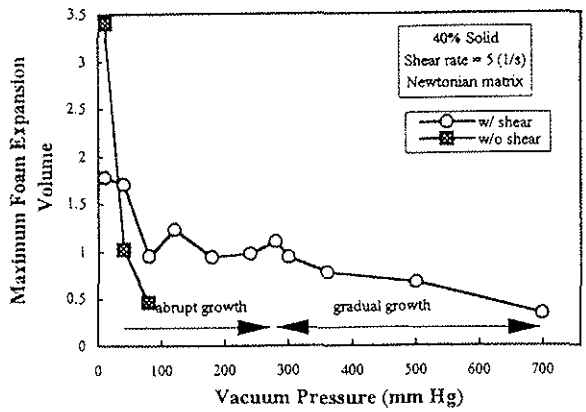

Figure 7. Dependence of maximum foam expansion volume with vacuum pressure for 20% loading.

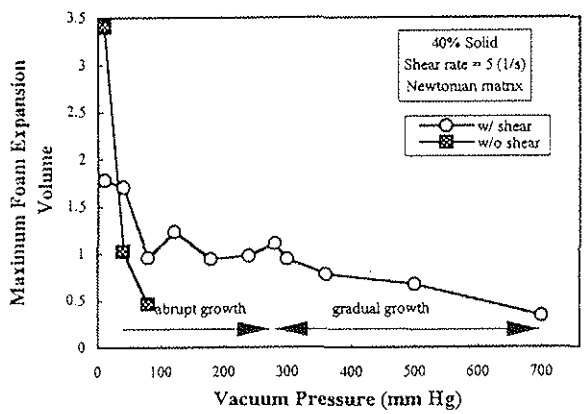

Figure 8. Dependence of maximum foam expansion volume with vacuum pressure for 40 % loading

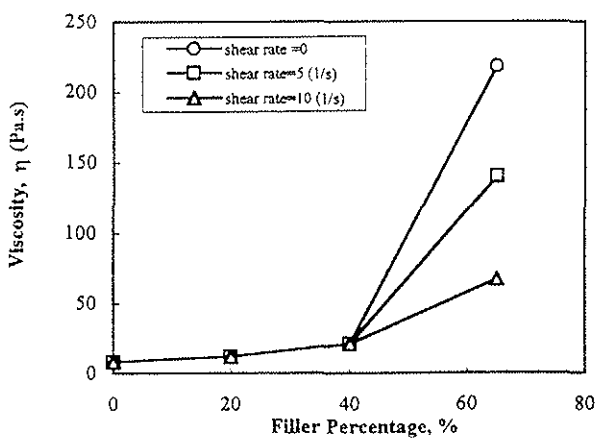

Figure 9. Dependence of shear viscosity on filler percentage.

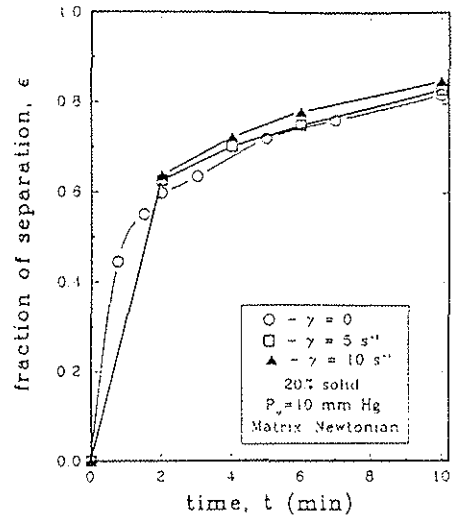

Figure 10. Dependence of fraction of separation on filler percentage.

COMPOUNDING AND SHAPING WITH NEOALKOXY ORGANOMETALLICS FOR PROPELLANTS AND EXPLOSIVES

by

Salvatore J. Monte
Kenrich Petrochemicals, Inc.
140 East 22nd Street
Bayonne, New Jersey 07002

ABSTRACT

Previous papers by the author proposed that minor amounts of thermally stable neoalkoxy titanates and zirconates (cf. Table 1) provide: a method for coupling (or bonding) via a proposed proton coordination mechanism to a wide variety of energetic and non-energetic particulate and fiber substrates heretofore considered non-reactive with silanes; and for in-situ metallocene-like repolymerization catalysis of the filled or unfilled polymer during the compounding, extrusion and blow or injection molding plastication phase resulting in significantly faster production cycles at lower temperatures of thermoplastic parts having better finish and equal or better mechanical properties. For example, both 40% $CaCO_3$ filled PP and unfilled PP compounds will experience 35.5% and 42% respective reductions in cycle time and 22% and 11% respective reductions in process temperature using 1% Ken-React CAPS L12/L.

The effect is not limited to CAB but to most polymers and is permanent and recyclable since the neoalkoxy titanate or zirconate ester remains permanently in the polymer as a repolymerization catalysis agent as opposed to Ziegler-Natta or metallocene (titanocene or zirconocene) derived polymers wherein the benefits are obtained when the monomer is only exposed to the mixed metal or biscyclodienyl derived titanium or zirconium complex catalyst during macromolecule formation (polymerization). For example, HDPE regrind from blow molding operations can be regenerated to virgin-like properties or PET/PC polyblended in a twin screw extruder will show significantly increased HDT, melt flow, tensile modulus and elongation using LICA 12 at 0.2% by weight of the polyblend against a control.

The discussion will also serve to review the commercial literature as to the 1200 references now in the ACS, CAS file discussing new and novel organometallic applications contained in significant technical papers or primary, first issued, non-subdivisional patents with an emphasis on new information not provided by the author in previous ADPA and JANNAF papers. For example, patent data will show use both as a catalyst to synthesize improved polyester polymers such as PET and PBT (Korea Institute of Science and Technology, Patent U.S. 5,237,042 dated August 17, 1993) as well as process aid and mechanical property improver in FR PBT (GE, Patent EP 0 547 809 dated June 23, 1993) wherein it is noted that the use of LICA 12 has the surprising effect of increasing melt flow and the stress strain properties of the polymer above the T_g thereby suggesting to this author that not only is improved rheology made possible but also controlled gas bubble formation at the activation temperatures of the nitrogen gas generator resulting in smaller bubbles and lighter and better foamed parts exhibiting a 2 to 22 fold increase in foaming agent efficiency. In addition to bonding characterization, changes in the morphology of energetic polymer binders such as CAB (Cellulose Acetate Butyrate) at explosive initiation temperatures containing titanates should be studied to better

understand LICA 12 performance in LOVA (US Army Patent 5472531 dated 05 December 1995) and High Energy Plastic Explosives (Union Espanola de Explosives SA ES2067367 dated 03 March 1995).

Data will be reviewed showing: up to 40% faster injection and blow mold and extrusion cycles at 10 to 15% reduced temperature on a wide variety of unfilled and filled thermoplastics; aromatic amino zirconate effects on adhesion of Kevlar to Phenolic; stronger graphite/epoxy propellant casings; fiberglass/epoxy bonding; aged caustic resistance of fiberglass/vinyl ester; a method for the sizing of graphite; significant viscosity reduction of particulate in water slurries (0.25% LICA 38 emulsified with an equal amount of ethoxylated nonyl phenol reduces 80% $CaCO_3/H_2O$ viscosity from 3,600,000 to 3,000 cps); and the viscosity reduction effect caused by varied efficiency of atomic monolayering on the particulate. It will be suggested that organometallic phosphatization in atomic monolayers on aluminum powder fuel during burn will allow control of burn rate and burn rate exponent to provide a new generation of more powerful (5X) and accurate solid rocket fuel.

INTRODUCTION

This paper is written as a supplement to References 1-10 and is divided into three segments: claimed performance benefits (why they are used); application considerations (how to use them); and characterization (why or how they work). Tables 3, 8, 9, and Figure 3 are repeated here from the SPE RETEC injection molding paper (cf. Ref. 1) so that this paper can stand alone or be read in conjunction with Reference 1.

DISCUSSION

Claimed Performance Benefits (Why They Are Used)

The following listed (numbered 1 to 10) performance benefits for the thermoplastics compounder and processor using subject neoalkoxy titanates and zirconates are based on years of experience obtained through research and development, plant trials, customer and investigator reports (patents, published articles, technical papers and private communications). For example, Table 2 is a summary of an ACS, Chemical Abstract Search for a typical one year period which has generated since 1974 over 1400 patents and technical papers reported by others using organometallics of the type invented by the author.

1. **Profit - Faster Cycles, less Energy** - 1% Ken-React CAPS L12/L (cf. Table 1 for description of pellet masterbatch form) on average will reduce injection and blow mold cycle times by 19% and process temperatures by 9% (cf. Table 3). Up to 40% cycle time reductions have been achieved.[1-5] Typically, a 4% cycle time reduction for a fully employed production capital equipment setup pays the cost of the additive and further reductions fall to the bottom line as profit (cf. Table 4).

2. **Quality - Stronger, Better Parts -** Mechanical properties and dimensional stability are maintained or improved because 0.2% Ken-React LICA 12 provides process rheology advantages by a claimed in-situ metallocene-like catalysis mechanism which Kenrich has patented worldwide under the title of "Repolymerization"(U.S. 4,657,988)[6].

   In the "Repolymerization" EP patent (European Patent Application No. 87301634.9-2109) peer reviewed by the EPO in Munich in November, 1996, examples 6 to 16 showed the

physical property effects of six neoalkoxy titanates (LICA's 01, 09, 12, 38, 44 and 97) and six neoalkoxy zirconates (NZ's 01, 09, 12, 38, 44 and 97) in powder form at 3 to 5 dosage levels in eleven thermoplastics (ABS, Acetal, Acrylic, CAB, Nylon 6, PC, PP, HDPE, PBT, PPO, and PS). The "best" titanate or zirconate and "optimum" dosage was reported (cf. Ref. 1 - Fig. 4). Table 5 compares the mechanical property effects of 0.3% CAPOW L12/H (equivalent to 1.0% CAPS L12/L) and 0.3% CAPOW NZ 12/H on the mechanical properties of the eleven aforementioned thermoplastics.

As a practical matter, most injection molders and thermoplastic processors handle many different polymers and prefer to handle pellets over liquids and powders. Accordingly, the 20% active masterbatch pellet form of the liquid coupling agent LICA 12 identified as CAPS L12/L dosed at 1 part per 100 parts of total polymer weight has become the general purpose commercially recommended additive for a wide range of polymers. For those compounders who cannot tolerate silica or who want to hold polymer carrier "contamination" to a minimum, a 60% active pellet form identified as CAPS L12/MPL-60 and 80% active powder form using Akzo Nobel's Accurel® MP series polymers was introduced in 1997.

Some other reported quality benefits are:

- Flatter surfaces for hot stamping derived from cooler processing temperatures (cf. Ref. 3 - Plant Trial #28).
- Better part definition such as sharper holes, indentations and texture to plastic surfaces from "complete mirroring" of mold designs due to improved flow (cf. Ref. 1 - Fig. 6).
- Elimination of shrinkage cracks along weld lines where there is usually little reinforcement (cf. Ref. 1 - Fig. 10).

3. **Use Less Plastic -** Use less plastic to equivalent strengths - particularly in blow molded thermoplastics where outer dimensions are unaffected by thinner gauging. For example, a HDPE marine fuel tank produced by Flambeau Corporation, Baraboo, Wisconsin, USA uses 1% CAPS NZ 12/L to reduce cycle time from 186 to 116 seconds at lower process temperature while reducing part weight from 1745 grams to 1500 grams to equivalent drop weight impact strength (cf. Ref. 1 - Fig. 14). The strength tests consisted of 3^+ meter drop-weight impact of water filled containers and two year Florida Everglades UV exposure of fuel filled containers.

Table 6 shows the use of 1% CAPS L12/L and alternately 0.3% CAPOW NZ 12/H for a 30 gal. (112 Liter) blow molded drum to allow the reduction of: average temperature of all zones 13% from 213 to 184°C; cycle time 21% from 191 to 151 seconds; and weight 8% from 6.0 to 5.5 kg. The drum passed proprietary internal pressure and external stacking tests.

Table 7 shows 1% CAPS NZ 12/L allows a blow molded HDPE container to have a cycle time reduction of 18% from 52.50 to 42.94 seconds (extruder speed increased 44% from 45 to 65 rpm). However, in this instance, average process temperature was reduced only 2.6% from 228 to 222°C.

4. **Process Engineering Plastics like Commodity Plastics -** Diamond Machinery Technology Inc. makes whetstones for knife sharpening using 40% fiberglass reinforced polycarbonate as a base (cf. Ref. 1 - Fig. 11) which they buy already formulated from a custom compounder.

Stanley A. Watson, Electroplating Manager/Chemist stated in a letter dated May 16, 1994 (cf. Ref. 1 - Fig. 10): *"This reply is in request to your query for feedback information regarding our sample requisition number K-70972 which contained one pound samples of Ken-React CAPS L12/E and KR 134S/K and sample requisition number K-71013 containing one pound samples of Ken-React CAPS KR 134S/K, NZ 44/E, L12/E, NZ 12/E, NZ 97/E.*

Our application is in molding 40% Fiberglass filled high molecular weight polycarbonate resin onto a perforated sheet of 16 gauge cold rolled steel. Our problem has been with shrinkage cracks along weld lines where there really is very little glass content - see enclosed examples. To aid our problem we've gone through a long process of mold solutions to change internal radii, hold down pin size, gate configuration, etc.

In general, we have seen a reduction in the severity of cracking with the highest degree of success being with L 12/E additive.

We have, as your Reference Manual indicates, experienced a significant decrease in barrel temperatures from as high as 580°F without coupling agent to as low as 370°F with agent. Our initial tests had such drastically altered rheology that most of our testing involved an attempt to regain prior flows and characteristics.

All our tests were done with coupling agent at 1% weight of CAPS and with red colored polycarbonate. We were able to reduce cure time by approximately 4 seconds with most of the agents".

On March 27, 1996 I met Mr. Watson in person for the first time when he visited our stand at MASSPLASTIC '96 in Fitchburgh, MA and he confirmed that after two years of product in the field, they are the best looking and best performing whetstones DMT has ever produced. The reduction of the injection mold temperature requirements of polycarbonate by 116°C from 304°C (580°F) to 188°C (370°F) reported by Watson with just 0.2% LICA 12 is significant.

In confirmation of Watson's work, a Ford 40% fiberglass/polycarbonate injection mold study of the effects of 0.2% LICA 12 on a 57 gram F-Series Fuse Cover (F2TB-15045D64; 4426-2056; PC-WSB-M4D627) truck part showed: a 60 to 45 sec reduction in mold cycle time; a 52°C reduction in process temperature; a 45% SPC (Statistical Process Control) reduction in out of tolerance measurements (i.e., improved dimensional stability); and an increase in minimum specific property requirements: tensile strength at yield (54.5 MPa), notched izod (44.6KJ/m^2) and melt flow (22.9 g/10 min.). Table 8 lists the control conditions for the fully automated injection molding machinery set-up and then the five (I to V) trial tests run to establish the new conditions for the 1% CAPS L12/E containing material.

Seven test runs were necessary for a PC electrical outlet plate cover (cf. Table 9) to achieve a cycle time reduction of 40% from 47.5 to 28.5 seconds, at half the injection pressure and at 15% lower temperature from an average of 267 to 223°C.

It would appear obvious to me that gas assisted injection molding technology would be synergistic with subject additive technology because polymer flow is facilitated at lower pressures.

Engineering resins such as polycarbonate need to be dried and are placed in a hopper dryer normally run at about 120°C. At these temperatures, CAPS made with EVA binder softened and created lumping problems for investigators such as Mr. Watson. A switch to 20 melt LLDPE binder solved the problem.

5. **Virgin-like Recycled or Regrind Parts -** "In-situ metallocene-like catalysis" or "repolymerization" catalysis regenerates recycled and regrind thermoplastics to virgin or better properties. A previous paper[7] on recycled plastics offered thermoplastic processing benefits for regrind and three examples are reviewed briefly here:

   a) Blow Molded HDPE (Regrind) Ski Boards - (cf. Ref. 7 - Table 10 and Figure 11) Results using 1% CAPS L12/E in Dow 25053P 100% HDPE regrind to produce blow molded HDPE ski boards showed the average temperature for the nine zones to be reduced 16% from 224 to 185°C while the cycle time was reduced 28% from 176 to 126 seconds. Also warpage was reduced or eliminated with the coupling agent; flash was removed easier; and the time needed to clean the molds was eliminated.

   b) Injection Molded ABS (Regrind) Carrier Case - (cf. Ref. 7 - Table 12 and Figure 13) An ABS Record Carrier Case made from 60% virgin and 40% regrind used 1% CAPS L12/E to reduce the average injection molded cycle 13% from 165 to 144 seconds while running the zones between 10 to 15°C cooler. In addition flash was removed much more readily from the parts containing the coupling agent.

   c) Extruded ABS (Regrind) Picture Frames - (cf. Ref. 7 - Table 13) 1% CAPS L09/K allowed for an 8% reduction in zone temperatures while the line speed was increased 16% from 17.5 to 20 meters per minute.

6. **In-Situ Copolymerization, Alloying or Compatibilization of Polyblends -** Thermally stable neopositioned quaternary carbon based (neoalkoxy) organometallic esters allow for "copolymerization" or "alloying" or "compatibilization" of dissimilar plastics such as in PET and PC blends. For example, 0.2% LICA 12 in a recycled PET/recycled PC - 80/20 blend provided a ten-fold increase in elongation and doubling of tensile modulus over a control blend. Jan Schut, senior editor of Plastics World summarized the data derived from a preview of a paper[8] in her report (cf. Figure 1) appearing in the September/October 1996 edition of Plastics Formulating & Compounding magazine and the December 1996 edition of Plastics World magazine.

7. **Synergize Blowing Agent Performance -** Endothermic and exothermic blowing agents are made significantly more efficient to produce lighter polymers with more uniform cell structure because, among other effects, titanates and zirconates at the elevated temperature where gas generation (blow) occurs maintain or increase polymer stress (force/area) properties while strain (elongation/unit length) properties are doubled or tripled. Thus, polymer bubbles do not break because of the greater stress/strain strength resulting in smaller and more uniform cell structure. Since the effect is based on polymer morphology, the source of gas or blow can

be diverse such as butane or RDX (cf. Table 2 for "High Energy Plastic Explosive" (ES 2067367) and "Insensitive Explosive Composition" (US 5472531)).

Other examples have been provided: Cell size variation is reduced from 6 - 48 micron to 9 - 15 micron in an exothermic azodicarbonamide foamed PE (cf. JP 58 75,713 Showa Denka Kk, Ref. 2 - pgs. 60 to 62 and Ref. 7 - Fig. 17); the density of an azodicarbonamide foamed flexible PVC is decreased threefold from 0.408g/cc to 0.129g/cc (cf. Ref. 4 - Fig. 3); the amount of endothermic sodium bicarbonate needed to foam SBR (Styrene Butadiene Rubber) is reduced twenty-nine fold from 15 phr of powder to 0.68 phr of a 75% active paste masterbatch containing a pyrophosphato titanate in the aromatic plasticizer phase (cf. Ref. 9 - Fig. 14).

Some practical foamed applications reported are: added dimensional stability to 100% regrind MDPE extrusion profiles; increased filler loads while not increasing density of recycled HDPE extruded lumber boards; injection molded $CaCO_3$ filled PP coat hangers having excellent memory (return to original shape); injection molded crates having low specific gravity and excellent strength (cf. Ref. 7 - Pg. 13).

Another obvious benefit for the compounder or thermoplastics processor would be using a combination of coupling and blowing agent for the elimination of sink marks as is shown in Table 10. Controlled blow eliminated sink marks at 12.9% lower temperature with just 2.5 parts of LICA 12 per 10,000 parts MIPS.

8. **Brighter, Better Aging Composites and Colors and Reduced Pigment Plateout -** Monomolecular layer of an organometallic titanate or zirconate makes inorganic and organic pigments and fillers hydrophobic and organophilic (cf. Ref. 2 - Pgs. 2, 3, 41 to 44) and eliminates air and water at the pigment/polymer interface resulting in better dispersion (Ref. 2 - Table 118), more intense colors (Ref. 2 - Fig. 47B) and other benefits such as increased adhesion[10], reduced plate-out of fluorescent colors[11] and better aging of filled and fiber reinforced polymers[12].

- For example, investigators from Osaka University concluded[10]: "*The effects of different coupling agents on the mechanical properties of the TiO_2 coated with a silane coupling agent were compared with composites prepared by dispersing titanate coupling agent-coated TiO_2 in epoxy. Young's modulus and flexural strength of the titanate coupling agent-treated composites were significantly better than those of the silane coupling agent-treated composites. Apparently a strong interfacial bonding between the filler and the matrix existed when the titanate coupling agent was used*".

  A fluorescent pigment manufacturer concluded[11]: "*Most efficient reactive additives were the Ken-React liquid and its powder grade equivalent. Other reactive additives effectively reduced plateout, but also caused brightness loss or blow molding problems.*"

9. **Functionalize Pigments and Fillers -** Coupling permits much higher loadings (cf. Ref. 2 - Fig. 126) and converts the filler to a catalyst support bed for reaction with the organic phase[12] to create a true continuous inorganic/organic matrix[13] for possible applications such as:

- Magnetic plastics or EMI/RFI shielding - Magnetic gamma ferric oxide loadings may be increased with significantly enhanced performance[14] and typically metal oxides and pigments dispersed in polymers exhibit decreased resistivity, i.e. 10^{10} (control) to 10^{5} (titanate) ohm-cm for a 60% loading of a $ZnO\text{-}Al_2O_3$ mixture in PP.[15]

- Non-toxic Flame Retardance - Phosphato and pyrophosphato functionality provides phosphato and pyrophosphato intumescent synergism and high loadings of non-toxic ATH^2 or $Mg(OH)2$[16]. For example, Robert Andy stated in U.S. 4,525,494: "*The present invention provides a polypropylene composition containing (64%) hydrated alumina which has high Izod impact strength, increased flow, increased elongation, increased deflection and increased Gardner impact values compared with the original polypropylene, without loss of tensile strength. The practice of this invention will give flame retardance to any polypropylene system while enhancing the strength of the product. For example, the practice of this invention has produced polypropylene products that have impact strengths which are increased four times and flow rates increased seven times over the starting material without loss of tensile or any other critical property*". Note the Alcoa hydrated alumina, Lubral® coated particulate exhibited improved mechanical properties only after in-situ reaction with the phosphato titanate.

- Impart "microwavability" or "X-ray detectability" to plastics due to high levels of $BaSO_4$. For example, 70% $BaSO_4$ filled PP fibers used as postoperative x-ray detectors in cotton swabs can be produced on a spinneret under virgin, unfilled PP conditions (Ref. 2 - Fig. 172).

- Couple or bond dissimilar substrates such as carbon fibre to PE[17] to make light but strong thermoplastics and, of course, thermosets.

10. **Transparent, Permanent, Non-Blooming and Non-Moisture Dependent Anti-Static Plastic -** The use of combined dissimilar thermally stable trineoalkoxy organometallic zirconates (Ken-Stat® KS MZ100) dispersed atomically into the polymer to form bipolar electrostatic dissipative layers so as to conduct electrons volumetrically through, as well as, along the polymer surface creates transparent, permanent, non-blooming and non-moisture dependent (U.S. and International Patents pending) antistatic parts.

    Unlike the catalytic effect of 0.2% LICA 12 which simply requires good stoichiometric distribution of its pellet masterbatch (CAPS L12/L) before the onset of melting and then shear to disperse the titanate in the injection screw melt phase, the antistatic effect of KS MZ100 often requires ten times as much organometallic (1 to 2% by weight of polymer). Optimum dispersion under high shear is needed to solubilize the combined zirconate esters into the insulating polymer to create a molecular bipolar electron conducting network. It is relatively easy to dissolve 1.0% KS MZ100 into xylene, then doctor blade the resultant mix on to a PE sheet and achieve a 2.7×10^{9} ohm-cm surface resistivity reading. It is more difficult to achieve the same electron transfer circuit in a non-polar (and therefore low solvating) polymer such as a polyolefin without intensive precompounding.

    Many times, a compounder or formulator wants merely to eliminate frictional static buildup caused by mixing. Just 100g of combined dissimilar thermally stable mononeoalkoxy

organometallic titanates (Ken-Stat KS N100) per 4,400 kilos of blended polyurethane painted sand eliminates separation problems caused by static electricity build-up differentials between pigmented sand containing conductive TiO_2 and non-conductive phthalo blue pigmentation used in the PU paint.

Table 11 is a summary of instructive work done in various polyolefins by Robert Kerr of Furon Inc. conveyed to me in a fax dated July 20, 1995 wherein mean surface resistivity measurements (six measurements per slab) using 0.5 or 1.0% Ken-Stat MZ100 for nine polyolefin resins were provided. A general improvement of 1×10^2 ohm-cm surface resistivity reduction was noted when Banbury mixing conditions were changed from 30 seconds drop after flux occurs at 50 rpm to 2 to 3 minutes mixing after flux occurs at 100-125 rpm thereby indicating a performance relationship of the combined organometallics to molecular distribution achieved via optimal mechanical dispersion conditions to achieve maximum work energy. More crystalline materials appear to show better results than their more amorphous counterparts.

An obvious application would be injection molded electronic packaging. Experience has shown that although Ken-Stat surface resistivity readings are sometimes higher than 10^{11}, the plastic is also volume conductive as well as surface conductive and, as a result, voltage discharge performance is often superior to packaging plastics using hygroscopic antistatic agents having 10^{11} surface resistivity readings. Initial tests have shown that injection molded containers containing Ken-Stat MZ100 exhibit significantly less voltage discharge than conventional antistats.

The foregoing are some of the claimed performance benefits of subject organometallic titanates and zirconates. Published efforts in metallocene (titanocene and zirconcene) chemistry by major polymer producers appear to be centered around olefin polymers and copolymers. Effects of neoalkoxy titanates and zirconates on metallocene derived polyolefins are incompletely determined. Catalysis effects of subject additives often vary by filler as well as polymer. For example, in wollastonite filled PP 1.6% LICA 38 outperforms 0.5% LICA 12 or KR TTS because of catalysis/mechanical property effects. Luo reported[18] work under the direction of noted rheologist Dr. Paul Han which showed at shear stresses above $200N/m^2$ for 50% $CaSiO_3$ filled Nylon 6 that 1% amino titanate (KR 44) treated filler composites exhibited melt viscosity at 230°C lower than pure Nylon 6 and that an amino silane (A-1100) had a similar but lesser effect. The same effect on rheology was not noted for titanates or silanes when $CaCO_3$ was substituted for $CaSiO_3$.

In any case, the titanocene or zirconcene catalysts used in synthesis do not remain in the polymer as do the titanate or zirconate ester forms to "anneal" scissored polymer chain lengths during processing. Also, metallocene derived HDPE and engineering plastics appear to be still off in the future while the titanate and zirconate esters appear to be efficacious to some degree in virtually all polymers synthesized via various routes.

Application Considerations (How to Use Them)

The application art of thermoplastics processing such as injection molding with neoalkoxy titanates and zirconates can be executive summarized with the general statement: "Tumble blend 1 part Ken-React CAPS L12/L additive with 100 parts of polymer compound material and then reduce injection mold machine temperature conditions by 10%". But as can be seen from Table 9, Edisonian efforts are often needed and dealing with side effects are not uncommon as seven adjustments were

necessary for the injection molded electrical outlet plate cover part in order to control splay, part dimensions and shear in the polymer melt.

Two principles govern the applications art: uniform distribution before the polymer melt phase and specific energy input for maximum dispersive work energy during the polymer melt phase.

Uniform Distribution Before The Polymer Melt Phase - Subject organometallics work on a stoichiometric catalytic principle and must be dispersed as thoroughly as possible throughout the unmelted polymer composite materials before the onset of melting whereupon catalysis is initiated as the titanate or zirconate solvates into the polymer organic phase. The pellet (CAPS) form is the simplest and best for the typical injection molding set-up. The liquid and powder forms of the coupling agent may also be used so long as there is no localization caused by polymer or filler surface physiabsorption of the additive. Localization upsets the stoichiometry subjecting the polymer to negative side effects from over or under catalysis. No amount of high energy dry powder blending such as post hi-speed Henschel type mixing can materially undo the capillary attraction forces created by physiabsorption of undiluted organometallic on to a filler. Dropwise addition of liquid coupling agent on to a fluidized (moving) bed of dry materials or dilution into a compatible liquid phase just prior to dry powder blending is the preferred use method. Even with pure polymer pellets, it is wise to add liquid coupling agent dropwise on to a fluidized bed of the pellets over a 2 ½ minute period.

We will discuss briefly some considerations of uniform distribution of titanates (and zirconates) on polymers and fillers:

Polymers - The CAPS pellet form usually insures uniform distribution after simple tumble blending with the polymer pellet. If the more efficient (higher % activity) CAPOW powder form is used, the polymer in similar powder form may work better. A principle of like to like - or pellet polymer to pellet coupling agent and likewise powder polymer to powder coupling agent should be considered. Although pellets respond well to tumble blending, it is usually better to high shear mix (Henschel, Pappenmeir, Wellex, Littleford, Patterson-Kelly, etc.) so as to intensively mix the powders before melting.

See the discussion in the fifth paragraph of Figure 1 for the differences between success and failure created by different compounding techniques in using LICA 12 as a copolymerization catalyst for a recycled PET/PC blend. Recently, in an evaluation of Ken-Stat KS MZ60S powder antistatic efficacy in PETG, significant (proprietary) performance differences were noted when the PETG was used in flake form (poor results) and in powdered form (good results).

Fillers - Reactivity with dry fillers such as $CaCO_3$ in the absence of any organic or polymer phase and the importance of solubilizing or finely emulsifying the titanate for uniform atomic distribution throughout the organic, polymer or water dispersion phase is demonstrated in Table 12. Water insoluble LICA 38 was made water emulsifiable by preblending with varying amounts of a water loving (hydrophilic), oxygen containing ethoxylated nonyl phenol (ENP), emulsified into the water with intensive stirring followed by addition of the $CaCO_3$. The viscosity reduction achieved from 3,600,000 to 3,000 cps is significant and underscores the need to obtain a fine emulsion of the titanate and further points to the atomic nature of their reactivity with the filler interface. The physics of mixing is as important as the chemistry of the interface.

From a compounder's standpoint, filler pretreatment with neoalkoxy type organometallics is not necessary because coupling/catalysis can take place in the polymer melt phase. See "Neoalkoxy

Evolution" for further detailed discussion. In some instances, the filler or reinforcement producer may want to "lock-in" performance by making the filler hydrophobic, organophilic and organofunctional with pretreatment. Most fillers such as $CaCO_3$ respond to a neoalkoxy titanate treatment technique of dropwise addition of coupling agent over 2 ½ minutes to a fluidized or moving bed (1800 rpm in a Henschel or Waring Blender will work) followed by a 30 second post mix. Spraying and dilution techniques increase the statistical probability of uniformity of pretreatment.

Table 13 shows the effects of pretreatment and in-situ treatment of LICA 12 WE33 (Water Emulsifiable 33% active LICA 12) on 1 and 5 micron $CaCO_3$. For example, 82% 1 micron $CaCO_3$ in water has a viscosity of 224,000 cps. Dropwise pretreatment with 0.5% LICA 12 WE33 reduces viscosity to 51,200 cps while in situ treatment technique gives 64,000 cps. In situ treatment in mineral oil yields 400,000 cps while Henschel pretreatment yields 192,000 cps and water slurry pretreatment yields 80,000 cps in mineral oil demonstrating how technique and solubility have different effects on coupling agent results. In Table 13, the water emulsifiable LICA 38ENP out performs the water soluble quat LICA 38J.

Table 14 provides further insight into treatment techniques. For example, 0.5% LICA 12 in situ treatment of $Mg(OH)_2$ reduces the control viscosity at 50% solids from 1,024,000 cps to 9,600 cps. Henschel pretreated $Mg(OH)_2$ using the same amount of undiluted LICA 12 dropwise added produces 640,000 cps as compared to 9,600 cps for insitu. A small amount of 1:1 dilution of LICA 12 with mineral oil provides significant pretreatment uniformity. For example, both 2 ½ minute and 4 minute dropwise addition of 0.5% LICA 12 to dry $Mg(OH)_2$ provided the same 640,00 cps viscosity response at 50% in mineral oil compared to 1,024,000 cps for the control. The same 0.5% LICA 12, diluted 1:1 with mineral oil and dropwise added for 2 ½ minutes produced a 64,000 cps viscosity response at 50% in mineral oil. The difference between 640,000 and 64,000 cps response to 0.5% LICA 12 is due to physics and not chemistry.

Specific Energy Input During The Polymer Melt Phase - Once the polymer begins to melt, work energy through mechanical shear creates the required intimate polymer/catalyst (coupling agent) mixing. The area under the power curve formed by a plot of torque vs. time is a measurement of the work energy or shear on the polymer/catalyst matrix. The most efficient polymer mix cycles generate peak torque in a short time. Torque is controlled by temperature, rpm's and back pressure. High torque creates high polymer shear rates. Polymers are non-Newtonian in flow and their melt viscosity decreases asymptotically with increasing shear. Under high shear rates, polymers exhibit the lowest viscosity with the least amount of variation as compared to greater polymer viscosity variation at lower shear rates - i.e. reproducible results. Most polymers (except for heat sensitive PVC) are not damaged by higher shear. Low shear rate melt indexes are not the way to measure the effect of subject additives.

Effects on torque reduction and dispersion were ascertained in a study comparing a titanate with conventional wetting agents in $CaCO_3$ - filled LDPE blown film. The samples were prepared in an electrically heated Brabender, wherein the LDPE, pigment, and wetting agents and the titanate (KR TTS) were charged as one blend into the mixing chamber having the following conditions: rotor speed 82 r.p.m.; temperature 93°C; 0.5 kg. weight on the ram. Torque readings in grams per square meter were performed every 30 sec. for 3 min., starting with an initial reading at 30 sec. elapsed time.

The resulting compounds were cooled and ground in a Wiley mill, employing a 60-mesh screen. The dry compound was dry-blended with a 2 melt index, high clarity, film grade LDPE in a

ratio of 9 to 1. Blown film of 1.5 mil thickness was produced from the dry blend on a 1.5 in. extruder at a 2.5 to 1 blowup ratio and temperature profile of 143 to 160°C. The resulting 1.5-mil film was examined for the number of undispersed pigment particles in 720 sq. in. of film. The results of this examination are summarized in Table 15.

The KR TTS treated $CaCO_3$/LDPE system reflects almost instantaneous torque reduction and short mixing cycles for optimization. Dispersion is excellent with only 33% of normal power requirements when compared to conventional systems. The dispersion of $CaCO_3$ treated with KR TTS in the LDPE would most likely have been improved if the temperature of the Brabender had been lowered to increase the torque and therefore the resultant area under the power curve which is a measure of the work energy. See the "Early Historical" discussion for references on the above work. In retrospect, it is now obvious to me that 0.2% KR TTS is having a catalytic effect of the LDPE and changing its intrinsic morphology independent of $CaCO_3$ content.

Typically in thermoplastic processing such as injection molding, machine rear zone temperatures are reduced 15% and front zone temperatures 5%. Generally, the injection molding plant trial begins by holding the injection molding machine's normal running conditions constant except for the temperature which we begin lowering in increments of about 10°C across all zones (front, middle and rear) until polymer flow is such that the part is incompletely filled--and then back off by raising the front and center zones until part quality is acceptable. But, every machine and every polymer behaves differently.

In the case of thermoplastic polyesters such as polycarbonate, the coupling agent's effect on temperature is very significant. Besides the bottom line 40% reduction in cycle times, a close examination of Table 9 shows the rear zone temperatures were reduced 20% from 258° to 202°C and the front zone by 12% while injection pressure was dropped 53% from 10360 kPa to 5500 kPa to achieve the desired part quality.

On occasion, injection pressure can be manipulated if temperature lowering does not fill the mold properly. Usually, when 1% CAPS is added to the polymer and the machine's conditions are "normal", injection will create excessive flash and the pressure will have to be dropped significantly if the temperature is not lowered. Since the cooling of the polymer compound in the mold is often the limiting time factor in injection molding, because of the low thermal conductivity of polymers, it makes more sense from an efficiency and non-Newtonian rheology standpoint to use the machine's high pressure capabilities by maintaining the pressure settings and alternately dropping process temperatures. High pressure assures less variability in the apparent melt flow of the shear dependent polymer.

Generally, rpm's and temperature are more dominate control parameters in extrusion processing as temperature and pressure would be in injection molding (I.M.). It is often a good idea to increase rpm's when using neoalkoxy titanates because a wider torque window (before reaching limiting Amps) is made possible. We usually do not adjust the rpm setting during I.M. plant trials. Of course, with the proper computer and software attached to an I.M. machine, the perfect balance of temperature, pressure and rpm's could be achieved for maximum efficiency. But, even with computerization, it is difficult for the human computer to handle more than two variables simultaneously so for injection molding the dominant condition of temperature is dealt with first, followed by pressure only when necessary and rpm's rarely.

Other Considerations - Many thermoplastic resins require thorough drying prior to injection molding or extruding to eliminate void formation or a degradation of the material at molding temperatures and continuous hopper dryers are often used. Our experience with the CAPS masterbatches has shown that EVA and Kraton/Styrenic binder systems often "gum-up" while a 20 melt LLDPE appears to work satisfactorily for most applications.

Table 15 shows that 1% CAPS L12/L enabled Pentaforma Manufacturers C.A., Venezuela to reduce the cycle time by 25% of an unfilled polypropylene syringe cylinder on a medium sized 250 Ton I.M. machine from 19.5 to 14.0 sec. while reducing the front and center zone temps. by 10%. In this plant trial, it was not practical to lower the rear zone temperature more than 3% because the feed pellets would not melt sufficiently when lowered below its normal setting of 185 to 190°C.

The biggest problem with this test run was that there was a slight yellowing of the part due to an assumed reaction of the titanate with the unidentified phenolic antioxidant (not Irganox 1010 or 1076) used in the undisclosed grade of PP. Titanates are usually used over zirconates because they are less expensive. However, all materials have inherent natural limitations.

An area of concern in using titanates is the possibility of undesirable color formation experienced when they come in contact with additives containing phenolic functionality such as heat and light stabilizers (antioxidants) used in thermoplastic vinyl and polyolefin systems, alkyds and urethanes. Phenolics are also used as chain stops in polyester systems, urethanes, alkyds and acrylics. In common with virtually all Titanium IV derivatives, titanate based coupling agents (including neoalkoxy and acetylacetonate) produce colored pigments on contact with phenolic containing free hydroxyl groups. The color intensity developed is proportional to the increasing concentration and conjugation of the phenolic hydroxyl from yellow through orange to red and burgundy.

Fortunately, since writing Reference 1 we have established that the LICA 12 titanate does not form color bodies with popular antioxidants and thermal stabilizers such as Irganox 1010 (CIBA-3.5-bis(1,1-Dimethylethyl)-4-hydroxy- benzenepropanoic acid, 2,2-bis[[3-[3,5-bis(1,1-dimethylethyl)-4-hydroxyphenyl]-1-oxopropoxy]methyl]1,3-propanediyl ester) widely used in PP and Irganox 1076 (CIBA-Octadecyl 3,5-bis(1,1-dimethylethyl)-4-hydroxybenzene-propanoate) widely used in HIPS. Not only are parts made with plastics using these antioxidants and LICA 12 neoalkoxy titanate good in color, but no discoloration is observed when LICA 12 is mixed directly with either Irganox 1010 or Irganox 1076 at 1:1 ratios.

Zirconates in general are not color body producers in contact with phenols other than nitrophenols. Both the organotitanate and organozirconate coupling agents do not interact with hindered amines (light stabilizers and/or antioxidants - HALS) under common operating conditions. Zirconates would appear to have greater thermal stability than titanates. For example, when equal amounts of CAPOW L12/H and CAPOW NZ 12/H were exposed to 235°C for 1 hour in a forced air oven, the titanate powder turned from white to black while the zirconate turned from white to very light tan. However, since the titanate is used at 2 parts per 1000 parts of heat sink polymer, thermal tolerance is higher than indicated in the forced air oven test.

In any case, since it was not appropriate to ask Mr. Ailen Austurias of Pentaforma to disclose the PP specifications for the material being tested, a plant trial using the zirconate was run 6 months later. In the less-than-laboratory perfect world of plant trials, the inside syringe plunger (and not the cylinder as in Table 16) was being run on a different machine. Table 17 shows the effect of the

zirconate (CAPS NZ 12/L) on the unfilled PP wherein the cycle time was reduced by 30% from 23 to 16 secs. while the temperatures on this machine were reduced 14% in the rear zone and about 5% in the front zone to get the proper balance of injection mold part quality for the polypropylene syringe plunger. The color problem did not occur with the CAPS NZ 12/L.

Grival LTDA did not run into any color problems when using 1% CAPS L12/L to injection mold PP toilet seats on an Asian Pacific Machinery Corp. (Model SM650) and was able to lower cycle times 16% on the first trial run setting (see Table 18). Leonardo Montano of Multiportes LTDA injection molded PP chairs on an Ingersoll Rand 500-2135 machine and was able to reduce cycle times 21% on the second trial (see Table 19). The chairs had good color also.

ABS parts run on an Engel injection molding machine at Unilemh LTDA had flow lines show up at irregular intervals. The use of 1% CAPS L12/L eliminated the flow lines and provided a better appearing part with higher gloss while reducing cycle time by one-third from 77 to 52 seconds at 5% average lower temperature (see Table 20).

Polytac LTDA injection molds heels for ladies shoes using HIPS and a trial as shown in Table 21 showed a 31% reduction in cycle time by the second trial. This result would have been wonderful for Humberto Pinilla if we had not encountered an incompatibility between the LDPE carrier in the CAPS L12/L and the HIPS. This incompatibility resulted in a loose film forming on the outside of the part. There was a definite separation of materials, especially when the part was cooled in water. Trials will have to be rerun using the CAPS L12/K to hopefully overcome the difficulty caused by the CAPS' LDPE binder.

Characterization (Why or How They Work)

Significant inventions rarely start with a full understanding and characterization of why or how they work. The Wright Brothers didn't understand all the principles or implications of their first or subsequent flights. They just flew. It's only with the luxury of time and retrospection that one begins to understand scientifically what's happening so that the art can be fully exploited.

Characterizing why or how they work can be done more effectively by reviewing the evolution of subject coupling agent technology from the early 1970's mindset of "bonding or coupling agent" to the current 1990's thinking of "metallocene-like catalyst".

At this point in time we perceive and advertise commercially (see Figure 2) the performance benefit effects to be functions of better bonding (or coupling) if fillers, pigments, reinforcements, fibers or dissimilar substrates are present in the composite and metallocene-like catalysis by the single site titanium provided by the thermally stable organometallic titanate's structure. A structure similar to the titanium provided in a metallocene catalyst such as a titanocene or the $TiCl_4$ of a Ziegler-Natta type catalyst.

Since the catalysis effect can occur in-situ in the finished polymer we have described the invention as "repolymerization"[6]. The following discussion is important since the full potential of and polymer processing with neoalkoxy titanates and zirconates can only be realized when large sums of money are dedicated to fully characterize answers to questions such as: their relative efficiency compared to other forms of catalysts; their effect on chain branching, molecular weight distribution, recrystallization time, glass transition temperature, etc.; and their current limitations so that new and improved titanates (zirconates and aluminates) can be synthesized.

Early Historical - In 1973, I had developed some interesting titanate esters such as KR TTS at Kenrich for the purpose of achieving high loadings (85%) of magnesium oxide and zinc oxide in napthenic process oils as part of a line of extruded bar (using a soap plodder) dispersions trade named Ken-Mag® and Ken-Zinc® meant for the rubber industry. 1973 was the time of the Arab oil embargo and people were trying to extend resin supplies with fillers.

At the time, Paul F. Bruins was Professor Emeritus of Chemical Engineering at the Polytechnic Institute of New York and my M.S. Polymeric Materials thesis mentor four years prior in 1969. S.J. Monte and P.F. Bruins, in a December, 1974 Modern Plastics magazine article entitled "New Coupling Agent for Filled Polyethylene", reported superior reduction of torque during compounding of calcium carbonate-filled LDPE (cf. Table 14). Work (cf. Ref. 1 - Table 2) was also done on mineral filled ($CaCO_3$, Clay, Wollastonite and $BaSO_4$) polyolefins using KR TTS.

It was Gordon Kline, the then Technical Editor of Modern Plastics, who applied the moniker "coupling agent" to the tetravalent titanate ester KR TTS for the December, 1974 article.

The term "coupling agent" had been applied previously to another group of additives based on tetravalent Si known as silanes. In the 1950's, silanes had been instrumental in producing successful fiberglass reinforced thermoset polyester composites such as the Corvette automobile. It was logical to apply the term "coupling agent" to an additive which increased the bonding of glass fiber or filler to polymer. A "filler/coupling agent/polymer" and "filler/wetting agent/viscosity reducer" mindset for the titanate esters was thereby established. But there was, and is, a big difference between silane "coupling" and titanate "coupling". For example, titanates work on $BaSO_4$ and $CaCO_3$, even in the water phase, while silanes do not.

Coupling - Plueddemann had stated[19]: *"It is fairly well established that silane coupling agents form oxane bonds (M-O-Si) with mineral surfaces where M = Si, Ti, Al, Fe, etc. It is not obvious that such bonds should contribute outstanding water resistance to the interface since oxane bonds between silicon and iron or aluminum, for example, are not resistant to hydrolysis. Yet, mechanical properties of filled polymer castings were improved by addition of appropriate silane coupling agents with a wide range of mineral fillers. Greatest improvement was observed with silica, alumina, glass, silicon carbide, and aluminum needles. A good but somewhat lesser response was observed with talc, wollastonite, iron powder, clay, and hydrated aluminum oxide. Only slight improvement was imparted to asbestine, hydroxyapatite ($Ca_{10}(OH)_2(PO_4)_6$), titanium dioxide and zinc oxide. Surfaces that showed little or no apparent response to silane coupling agents include calcium carbonate, graphite and boron"*. Recently, Dr. Ming J. Chen, research scientist with Witco Corp.'s OSi Specialties Group (Tel. 914-784-4860; Fax 914-784-4890) ranked silane substrate adhesion similarly.

A discussion of the six functional sites of titanate (or zirconate) as compared to a silane to explain performance differences may be represented as follows:

Titanate

$$\overset{(1)}{(RO\text{-})_n}Ti\text{-}(\overset{(2)}{\text{-}O}\ \overset{(3)}{X}\ \overset{(4)}{R'}\ \overset{(5)}{Y})\overset{(6)}{_{4-n}}$$

Silane

$$\overset{(1)}{(RO\text{-})_3}Si\text{-}(\overset{(5)}{\text{-}R'\ Y})$$

where,

(1) RO = hydrolyzable group or substrate reactive group.
(2) Ti, Si = Tetravalent titanium, zirconium or silicon. The Ti-O (or Zr-O) bond is capable of transesterification, transalkylation and other repolymerization catalysis mechanisms while the Si-C bond is more stable and unreactive.
(3) X = binder functional group (phosphato, pyrophosphato, sulfonyl, carboxyl, etc.).
(4) R' = thermoplastic functional group (aliphatic, napthenic or aromatic).
(5) Y = thermoset functional group (acryl, methacryl, mercapto, amino, etc.).
(6) 4-n = mono, di or triorganofunctionality. Hybrid coupling agents such as 1 mole of (3) carboxyl, (4) aliphatic isostearoyl and 2 moles of (3) carboxyl (5) acryl titanates (zirconates) are possible.

The function (1) concerns itself with filler/fibre substrate reaction mechanisms, while functions (2) to (6) are polymer/curative reactive. In its simplest terms, the titanate function (1) mechanism may be termed proton (H^+) reactive via solvolysis (monoalkoxy) or coordination (neoalkoxy) while the silane function (1) mechanism may be termed hydroxyl (OH^-) reactive via a silanol-siloxane mechanism.

The claimed neoalkoxy group/proton (H^+) coordination filler/fiber coupling mechanism appears to provide wider reactable substrate possibilities than the trisalkoxy group/hydroxyl (OH^-) dependent coupling mechanism attributed to silanes. Hydroxyl groups can be found on a limited number of materials such as silica, alumina, glass etc., but non-hydroxyl bearing particulates such as carbon black and $CaCO_3$ (the most widely used fillers in elastomers and thermoplastics respectively) and graphite, aramid and organic fibres (in fact, all materials) have protons on their surface.

Titanate Catalysis - Organic titanates (and zirconates) are well known catalysts [20,21] used in the manufacture of:

- Polyolefins[22,23]
- Polyesters[24-30]
- Polybutylene terephthalate[31]
- Polyurethanes[32-37]
- Polycarbonates[38-39]
- Polysiloxanes[40-47]

For example, reference 31 refers to U.S. Patent 5,237,042 dated August 17, 1993 issued to the Korea Institute of Science and Technology (KIST) entitled "Process for the Preparation of Polybutylene Terephthalate Based Polymer". It disclosed the use of a complex catalyst consisting of

antimony and titanium (KR 41B) compounds to produce a PBT polymer "*having excellent color, a small amount of side-product and a high degree of polymerization within a short time*". I was told by Y.C. Kwon during a personal visit to Kenrich's offices in 1994 that a KIST (Korean Institute of Science and Technology) study had been released, sponsored by seven South Korean PET fiber producers costing three million dollars and spanning five years, confirming KR 41B (tetrisopropyl di(dioctyl) phosphito coordinate titanate) to be the most efficient polymerization catalyst for PET.

Titanate Cross-linking - Titanates (and zirconates) are able to cross-link or cure a variety of polymers:

- polyolefins[48]
- polybutadienes[49,50]
- styrene-butadiene copolymers[51]
- polystyrene[52]
- polysiloxanes[53,41,54-57]
- epoxy[58-63]
- fluorocarbon resins[64-67]
- acrylic and methacrylic resins[68-77]
- polyvinyl alcohol[78]

For example, reference 48 is abstracted to read: "A *neoalkoxy trimethacryl zirconate* CAS # [PMN No. P97-77] crosslinked more effectively than a silane when used at 3 phr in a 0.5 phr dicumyl peroxide cured ethylene-vinyl acetate copolymer when immersed in 78°F (25°C) water for 72 hours".

Neoalkoxy Evolution - In 1984, neoalkoxy titanates were introduced to overcome objections from thermoplastic processors who were not equipped to pretreat fillers in a Henschel-type mixer to achieve the solvolytic reaction (isopropyl alcohol by-product) of the monoalkoxy titanate ester's isopropoxy group with the surface proton of the filler or reinforcement. The chemistry of the new neopositioned (neoalkoxy) quaternary carbon titanate esters provided sufficient thermal stability in the polymer melt phase for insitu addition directly into the polymer flux for subsequent filler coupling via a suggested proton coordination (no alcohol by-product) mechanism with the filler's surface protons (cf. Ref. 2 - Fig. 11B).

Repolymerization - Plant trials are the key to additive marketing success. Well, when additive salesmen and results oriented injection molders get together, success breeds more testing and some interesting results were coming in from the field as filled (and unfilled) compounds were tested at random as typified by the injection molded polypropylene weed wacker components shown in Figure 3. Examination of Figure 3 reveals that the use of 1% CAPS L09/E had 40% and 35.5% reductions in cycle time as average process temperatures were reduced from 197 to 168°C and 180 to 141°C respectively in the two 40% $CaCO_3$ filled PP compounds tested and surprisingly a similar 42% a reduction in cycle time and reduction in temperature from 184 to 163°C for the unfilled PP compound.

On examining the results of the weed wacker plant trial, it occurred to me (insight) that some sort of in situ Ziegler-Natta or metal catalysis effect was being evidenced from use of the titanate ester. "It didn't matter if the PP was filled or unfilled!" Classic coupling agent thinking had said that in a

filled polymer, the titanate formed an atomic monolayer on the filler surface to make it hydrophobic and organophilic and more readily deagglomerated under mechanical shear forces so as to achieve complete dispersion. Dispersion being defined as the complete displacement of air voids and moisture at the interface by the polymer to form a continuous filler/polymer phase. It had been thought that the "flow" was more attributed to a "wetting agent" effect on the filler than to a change in the morphology of the polymer itself. The coupling mechanism or chemical bridging between the inorganic filler and the organic polymer was said to be the result of the coupling agent's ability to transfer stress energy from the polymer matrix to the filler phase without bond rupture through van der Waals' entanglement via long carbon chains.

A shift in mindset resulted: "True, maybe the filler was now hydrophobic and organophilic as a result of the atomic titanate monomolecular layer formed, but now the filler also served as a catalyst support bed for titanium metal catalysis of the polymer". Promotional literature exclaiming: "Now deagglomerate, couple and catalyze...simultaneously!" (cf. Ref. 1 - Figure 3) was a result of the insight. By now, it was obvious to me that even when no filler was present, as long as the neoalkoxy titanate ester was uniformly dispersed into the polymer melt phase, organometallic titanium catalysis benefits could still be derived. Since Ziegler-Natta catalysis was well known and metallocenes were in development, I attributed the effects in the mid-80's to be the result of the titanate or zirconate's in situ Ziegler-Natta like catalysis. The rheology benefits heretofore noted in the literature were therefore more than likely not only the result of filler wetting but also catalysis, as in the case of unfilled polymers. We called it "repolymerization".

Plant trials to better understand and establish neoalkoxy titanate and zirconate injection molding process performance continued in the market place. Kenrich's corporate culture and laboratory equipment was oriented towards rubber chemical dispersions and plasticizers used in elastomers and flexible PVC. We could do things in our lab such as mix 1 part of AC617A (Allied Signal) low molecular weight polyethylene wax with 3 parts of mineral oil (Exxon Faxam 22) and observe the Brookfield viscosity increase from 22,400 cps to 3 - 7,000,000 cps with LICA 09, LICA 12 and NZ 12 (see Figure 4) or increase the efficiency of foamed PVC plastisols with LICA 38 (see Figure 5), but we were incapable of doing the necessary GPC, Tg, melt flow, dynamic rheology, recrystallization temperature determination, spectrographic and other characterization studies to completely understand what was happening. So, we learned as much as we could by trial and error doing plant trials with our customers.

Neoalkoxy Chemical Interactions Between Fiber Reinforcements and Polymers Such as PPS - Effects in glass reinforced epoxy, vinyl ester and PPS were reported by Patrick A. Toensmeier in a July 1988 Modern Plastics article entitled, "Coupling agents and modifiers: targeting upgrades performance" (cf. Ref. 1 - Figures 7, 8 and 9). Detailed property data effects comparing silanes, titanates and zirconates in reinforced (fiber glass, graphite and aramid) thermosets (epoxy, polyester, vinyl ester and polyurethane) were made available in a paper[79]. Another 1993 paper[80] outlined the adhesion and process advantages of NZ 37 in a Kevlar® reinforced Phenolic.

A December 14, 1987 private communication by me to Mr. John Gosse of Boeing offered seven potential catalytic reaction mechanisms of NZ 97 (neoalkoxy, triphenyl amino zirconate) with glass and PPS (cf. Ref. 1 - Figure 9):

1. Proton coordination between the glass and neoalkoxy group.
2. Proton coordination between the glass and the amino aroxy group.

3. PPS/NZ 97 ligand Exchange-End Thiol/Aroxy Interchange Generating Amino Phenol by-Product plus polymer bonded zirconate.
4. PPS/NZ 97 - Aroxy Insertion Reaction/Change Scission.
5. PPS/NZ 97 - Sulfide Insertion Reaction (Repolymerization).
6. PPS/NZ 97 - Amine/Sulfide Redox Alkylation.
7. Allyl Group Alkylation (Fridel-Crafts) and Crosslinking through reaction with secondary allyl group of the neoalkoxy function group.

In any case, it is clear that the addition of the neoalkoxy triphenyl amino zirconate has a significant catalytic or reactive effect resulting in the increased flow of the fiberglass reinforced PPS (as shown in cf. Ref. 1 - Figure 9). Recrystallization time effects with LICA 09 and other neoalkoxy structures are next discussed as extracted from U.S. Patent 5,340,861[81].

Neoalkoxy Catalysis - Reduction in the Recrystallization Time of PPS - A significant characterization which would help explain the reduction in thermoplastic processing and injection mold cycles would be an observed reduction in the recrystallization time of a polymer when a neoalkoxy organometallic is added to the control. A modified polyphenylene sulphide resin containing titanium organometallic compound (LICA 09) and molten polyphenylene sulphide resin was prepared[81]. "*The modified polyphenylene sulphide was compounded with a Werner & Pfleider twin-screw extruder (Model ZSK-30). The temperature of the screw die was maintained at 315℃. After the modified polyphenylene sulphide composition was evenly compounded, it was pelletized, dried, cooled, and monitored with a Perkin-Elmer Differential Scanning Calorimeter (Model DSC-7) to study the crystallization rate by measuring the isothermal crystallization time and crystallization temperature.*

It is evident that the addition of the titanium organometallic compound significantly improves both the isothermal crystallization time and the crystallization temperature of the polyphenylene sulphide resin. The isothermal crystallization time (at 250℃) was substantially decreased from 175 secs to 106 secs, and the crystallization temperature was increased by 8℃, with the addition of titanium organometallic compound".

Copolymerization - Titanate and zirconate coupling agents may act as compatibilizers via activation of both addition and condensation polymers[21]. When the activation occurs to more than one polymer simultaneously, in the absence or presence of filler or reinforcement (both inorganic and organic), or peroxide, said activation may result in repolymerization, or copolymerization (i.e. intermolecular rearrangement), or grafting, or other molecular modifications resulting in some other form of "alloying".

Activation of both addition and condensation polymers by selected organometallics may result in:

1. Rapid equilibration of molecular weights to produce near thermodynamic equilibrium distribution irrespective of starting compositions.

2. Randomization of most block copolymers except some aliphatic polyethers.

3. Reduction in polydispersity of molecular weight resulting in a narrower molecular weight distribution curve.

4. Controlled introduction of organofunctional groups for bonding enhancement.

5. Catalysis of a wide variety of reactions.

An example of subject organometallic effects on polymer blends (in addition to Jan Schut's discussion in Figure 1) was discussed in a Neste Oy Patent[82]: R. Holsti-Miettinen[82] overcame the difficulties of blending a polar liquid crystalline polymer (LCP) with non-polar polyolefins (PP and HDPE) using neoalkoxy titanates and zirconates. The art of recycling polymers often requires the blending of polar and non-polar ingredients and Example 1 from the patent is herein provided:

"Example 1 (WO 95) 3183):
PP/LCP and HDPE/LCP blends were prepared in a Berstoff ZE 25 x 33 D twin screw extruder. The melt temperature was at 240 - 245°C and "Polyblends" screw configuration was used. Rotation speed was 200 rpm and feeding rate about 9 kg/hr. The LCP component was predried before melt blending for 5 hours at 50°C. The prepared blends were predried overnight at 80°C before injection molding. Injection molded specimen were mechanically tested after 2 days of conditioning.

The materials used were the following:

- HDPE: NCPE 1515 supplied by Neste Oy,
- PP: VB 65 supplied by Neste Oy,
- LCP: Rodrum LC-3000 (a copolyester of p-hydroxybenzoic acid and poly-ethyleneterphthalate, supplied by Unitka Ltd.),
- Zirconate: neopentyl (diallyl) oxy, tri (dioctyl)phosphato zirconate, supplied under the name CAPS NZ 12/L by Kenrich Petrochemicals, Inc.,
- Titanate I: neopentyl(diallyl)oxy, tri(dioctyl) phosphato titanate, supplied under the name CAPS L12/L by Kenrich Petrochemicals, Inc.,
- Titanate II: neopentyl (diallyl)oxy, tri(N-ethylenediamino) ethyl titanate, supplied under the name CAPS L44/E by Kenrich Petrochemicals, Inc.
- Compatibilizer I: Lotader 8660 supplied by Norsolor and
- Compatibilizer II: a MAH-grafted PP supplied under the name Exxelor 1015 by Exxon Chemicals.

The recipes of the blends are given in Table 1 (Ref. 82).

Table 1. Recipes of polyolefin/LCP blends

Sample #	Isotropic polymer/wt-%	LCP/wt - %	Organometallic compound/wt-%	Compatibilizer/ wt - %
1	PP/69	30	Zirconate/1	-
2	PP/69	30	Titanate I/1	-
3	PP/69	30	Titanate II/1	-
4	PP/70	30	-	-
5	PP/69	30	-	Comp. I/1
6	PP/69	30	-	Comp. II/1
7	PP/68	30	Titanate I/1	Comp. I/1
8	PP/68	30	Titanate I/1	Comp. II/1
9	HDPE/69	30	Zirconate/1	-
10	HDPE/69	30	Titanate I/1	-
11	HDPE/69	30	Titanate II/1	-
12	HDPE/70	30	-	-
13	HDPE/70	30	-	Comp. I/1

Part of the samples were tested for orientation under drawing. Blends were extruded in a single screw Brabender extruder and immediately quenched in a water bath and drawn at different speeds of the take-up machine to form strands of different diameter. The draw ratio for each strand was determined as the ratio between the die and strand sections. The dimensions of the round hole capillary die were: length 30 mm and diameter 5 mm. The screw speed was kept at 100 rpm for all blends. The strands were tensile tested. The diameter of the rods was uneven but it was evaluated as an average of at least five measurements.

Results of mechanical and thermal testing are shown in Table 2 (ref. 82).

Table 2. Mechanical and thermal properties of LCP/PP blends

Sample #	Tensile Modulus (MPa)	Tensile Stress at Break (MPa)	Tens.Strain at Break (%)	Tensile Strength (MPa)	Flexural Modulus (MPa)
1	3260	39.7	2.5	39.8	3230
2	3030	37.7	2.6	37.7	3070
3	2680	34.5	2.4	34.7	2940
4	2900	36.8	2.7	37.0	2860

5	2930	38.0	2.7	38.1	2910
6	3070	37.8	2.4	38.0	2930
7	3010	38.1	2.6	38.5	3020
8	3150	38.6	2.6	39.0	3080
9	2810	38.3	2.8	38.4	2740
10	3060	38.7	2.5	38.8	2990
11	2780	36.9	2.7	36.9	2750
12	2560	36.8	3.1	36.9	2520
13	2350	36.1	3.2	36.2	2460

It is apparent from the results indicated in Table 2 (Ref. 82) that the addition of neoalkoxy zirconates improves the tensile modulus of both LCP/HDPE and LCP/PP blends. The improvement with neoalkoxy titanates was more pronounced in HDPE/LCP blends that in PP/LCP blends. It is worthwhile noticing that the mechanical strength of blend sample 8, which contained both a titanate and a compatabilizer (Exxelor 1015), was better than that of Reference Sample No. 4. This combination of modifiers also gave the best impact strength".

The Metallocene Analogy - Figure 2 shows the comparative chemical structure of the LICA 12 titanate and a titanocene. This is not to represent that the catalysts are the same. They are different. But, it is fair to say that both the metallocenes (titanocenes and zirconocenes) and the organometallic esters (titanates and zirconates) are titanium and zirconium complexes.

Beyond specific chemistry, one big difference is that the metallocene catalysts function during the synthesis of the polymer to produce the desired new generation olefin or copolymer while the titanate or zirconate ester is permanent in the plastic. The metallocene does not remain in the polymer and even metallocene derived polymers are subject to the subsequent negative effects of chain scissoring during recycling and reprocessing.

Virgin and recycled plastics and other art will benefit from full characterization and understanding of the effects of subject neopositioned quaternary carbon derived organometallics. Why does both HIPS processed at 175°C and Nylon 6.6 processed at 270°C experience the same 13% reduction in cycle time with 0.2% LICA 12 additive (see Figure 6)? Why does the 5.0 melt index of an HDPE with LICA 12 additive at 0.2% remain unchanged after 5 repeat passes through a twin screw extruder while the untitanated control climbs to 20.0? The neoalkoxy titanate effect appears to be catalytic and results in a self annealing polymer since its presence above the melt temperature inhibits chain scissoring caused by high shear polymer processing.

CONCLUSION

This paper claims ten significant benefits for compounding, extruding or injection and blow molding thermoplastics based on observations that minor amounts of thermally stable neoalkoxy titanates and zirconates provide a method of in situ metallocene-like repolymerization catalysis of the polymer during the compounding, extrusion and blow or injection mold plastication phase resulting in faster production cycles at lower temperatures of thermoplastic parts having better finish and equal or better mechanical properties. The effect is permanent and recyclable since the neoalkoxy titanate or

zirconate ester remains permanently in the polymer as a repolymerization catalysis agent as opposed to Ziegler-Natta or metallocene derived polymers wherein the benefits are obtained when the monomer is only exposed to the mixed metal or biscyclodienyl derived titanium or zirconium complex catalyst during macromolecule formation (polymerization).

Some applications considerations were discussed and a need for further characterization was expressed.

REFERENCES

1. Monte, S.J., "Injection Molding with Neoalkoxy Titanates and Zirconates", SPE/RETEC Conference "Polymer Additives for Injection Molding and Extrusion Applications", Whitehaven, PA, USA, October 19, 1995.
2. Monte, S.J., Kenrich Petrochemicals, Inc., "Ken-React® Reference Manual - Titanate, Zirconate and Aluminate Coupling Agents", Third Revised Edition, March, 1995.
3. Monte, S.J., "Increased Productivity of Thermoplastics Using Organometallic Titanate and Zirconate Coupling Agents", SPE ANTEC, New York, May 1-3, 1989.
4. Monte, S.J., "Coupling Agents Increase PVC Productivity", Plastics Compounding Magazine, November/December 1989.
5. Glaysher, W.A., D.R. Haff, H.H. Schlaubitz and S.J. Monte, "The Use of Organometallic Coupling Agents As Process Aids In Blow Molded HDPE", SPE RETEC, High Performance Blow Molding Conference, Oct. 9-10, 1990, Hamilton Hotel, Chicago, IL.
6. Kenrich Petrochemicals, Inc., U.S. 4,657,988 - 4/14/87.
7. Monte, S.J., "New Opportunities in Recycled Plastics With Neoalkoxy, Titanate and Zirconate Coupling Agents", SPE Recycle RETEC, October 31, 1989, Charlotte, NC.
8. Monte, S.J., "Titanium and Zirconium Esters as Couplers and Single Site Catalysts for In-Situ Repolymerization and Copolymerization Useful for Recycled Polymeric Compositions", Paper #57, ACS Rubber Division, Louisville, KY, October 8-11, 1996.
9. Monte, S.J., "More Efficient Manufacture of Better Foamed, Filled and Unfilled Polymer Compounds With Titanate and Zirconate Coupling Agents (26 pgs., 44 Tables, 69 Figures)", Northeast Regional Rubber & Plastics Exposition, September 21-22, 1994, Mahwah, NJ.
10. The Institute of Scientific and Industrial Research, Osaka University, "Effects of coupling agents on the mechanical properties improvement of the TiO_2 reinforced epoxy system", Mater. Lett. (1996), 26(6), 299-303 Coden:MLETDJ; ISSN:0167-577X.
11. Technical Bulletin No. 27, "Additives to Reduce Plateout of Day-Glo® zx-Series Pigments", Day Glo Color Corp., subsidiary of Nalco Chemical Company.
12. Monte, S.J., "Better Bonding and Metallocene-like Catalysis Benefits for Elastomers", Rubber Technology International '96, UK & International Press, a division of Auto Intermediates Ltd.
13. E. White, "Additives Give Better Bonding", Reinforced Plastics June 1996, 0034-3617/96 Elsevier Science Ltd.
14. Fuji Photo Film Co., LTD., US 4,444,850.
15. Ajinomoto, JP 63268767 - 11/7/88
16. Mitsubishi Cable Ind., US 4,769,179 - 9/6/88.

17. Yeh, J.T.; Chen, B.J.; Lee, H.M. "Impact properties of Carbon Fibre Reinforced Liners & Short-Chain Branched Polyethylenes", Polymer Bulletin 33 (Springer-Verlag, (607-614 (1994), National Taiwan Institute Technology.
18. Luo, Hong Lie; Han, Chang Dae and Mijovic, Jovan, "Effects of Coupling Agents on the Rheological behavior and Physical/Mechanical Properties of Filled Nylon 6", J. of Appl. Polym. Sc., Vol. 28,3387-3398(1993).
19. Plueddemann, Edwin P., "Silane Coupling Agents", PG. 114, 1982 Plenum Press.

20. The Organic Chemistry of Titanium - R. Field and P.L. Cowe, Butterworth & Co., Washington, D.C., 1965 (213 pp. 791 references).
21. Monte, S.J.; Sugerman, G. "The Use of Organometallic Titanates & Zirconates as Reactants and Compatibilizers in Polymers", Compalloy '90, New Orleans, LA, 3/9/90.
22. Asahi Chemical Ind. Co., J59 164,309 9/17/94.
23. Asahi Chemical Ind. Co., J60 60,116 4/6/85.
24. Nissan Chemical J 76-530, 1/6/76.
25. Teijin Ltd. J76,530, 1/6/76.
26. Hitachi Chemical, J77 81,346, 7/7/77.
27. Dainippon Ink & Chemical, J74 129,725, 12/12/74.
28. Kao Soap Co., J57 121,030, 2/28/82.
29. Teijin Ltd., J82 23,628, 2/6/81.
30. Showa Electric W & C Co., Ltd., J82 96,057, 6/15/82.
31. Korea Instit. of SC and Tech., US 5,237,042, 8/17/93.
32. Union Carbide, US 3,222,305, 12/7/65.
33. DuPont, US 3,426,025, 2/4/69.
34. Nippon Polyurethane Industry, J 58 113,260, 6/7/83.
35. Cemedine Co., Ltd., J 84 26,542, 6/28/84.
36. Center of Research Industrial Quebec, EP 128,060, 12/12/84.
37. BASF Corp., US 4,889,903, 12/26/89.
38. Juiles, Goudrons et Derives, FR 1,286,718, 3/9/62.
39. Eastman Kodak, US 2,789,969, 4/23/57 (See also: U.S. 2,789,967 and 2,789,970).
40. M. Kronstein, US 2,680,723, 6/8/54.
41. Dow Corning, EP 122,137, 10/17/84.
42. General Electric, EP 175,134, 3/26/86.
43. C.J. Gaillissen and A. Gancberg, US 2,732,320, 1/24/56.
44. G.W. Madaras, J. Soc. Dyers and Col., 74 pp 834-41 (12/58).
45. General Electric, US 3,014,826, 12/26/61.
46. Dow Corning, US 3,647,846, 3/7/72.
47. Dow Corning, US 3,015,637, 1/2/62.
48. Donald W. Kelley, US 4,837,272, 6/6/89.
49. DuPont, US 2,875,919, 3/3/59.
50. DuPont, US 2,876,207, 3/3/69.
51. ESSO Research & Engineering, US 3,025,259, 3/10/62.
52. Grillo-Werke, GER., 1,941,328, 3/4/71.
53. Goldschmidt, GER., 3,214,986, 6/2/84.
54. Dow Corning, EP 68,671, 1/5/83.
55. Kansai Paint, J 60 186,486, 9/21/85.
56. Dow Corning, EP 28,880, 5/20/81.
57. Otsuka Kogaku, J 86-37,105, 8/22/86.

58. National Lead, US 2,742,448, 4/17/56.
59. General Electric, US 2,962,410, 11/29/60.
60. Ventron Corporation, US 3,860,622, 1/14/75.
61. Westinghouse Electric, US 4,117,361, 9/26/78.
62. General Electric, US 4,307,212, 12/22/81.
63. General Electric, US 3,776,978, 12/4/73.
64. DuPont, US 3,103,490, 9/10/63.

65. J.P. Stevens, GER 3,026,987, 2/12/81.
66. Asahi Glass, J 60-127,373, 7/8/85.
67. Dow Chemical, US 4,554,325, 11/19/85.
68. Pittsburgh Plate Glass Co., US 3,151,101, 9/29/64.
69. Ricoh, US 3,726,823, 4/18/73.
70. Mitsubishi Gas Chemical, US 3,904,572, 9/9/75.
71. Kansai Paint, GB 2,042,559, 7/24/80.
72. Union Carbide, US 4,524,201, 6/18/85.
73. Kansai Paint, US 4,385,097, 5/24/83.
74. Hoechst,GB 1,583,316, 5/24/78.
75. Kansai Paint, J 79-77,635, 6/21/79.
76. Suwa Seikosha, J 80-71,778, 5/30/80.
77. Kansai Paint, J 80-73,746, 6/3/80.
78. Titangesellschaft, GER 1,007,453, 5/2/57.
79. Monte, S.J. and G. Sugerman, Kenrich Petrochemicals, Inc.; S.M. Gabayson and W.E. Chitwood, General Dynamics, "Enhanced Bonding of Fiber Reinforcements to Thermoset Resins", 33rd International SAMPE Symposium, Anaheim, CA, March 7-10, 1988.
80. Subramaniam, N.; Blum,F.D.; Gopal, P.; Dharani, L.R., "Interface Characterization of Kevlar® /Phenolic Composites", SAMPE Quarterly, January, 1993.
81. Industrial Technology Res. Inst., Hsinchu, Taiwan, US 5,340,861, 8/23/94.
82. Neste Oy, WO 95/23183, 2/28/95.

NOTE: U.S. dating convention is month/day/year, therefore 1/2/62 means Jan. 2, 1962 and not 1 Feb. 1962.

CSPE/sd/97

MECHANISMS OF WEAR AND MATERIALS THAT ENHANCE WEAR RESISTANCE IN CONTINUOUS MIXERS AND EXTRUDERS

Presented at
The Ninth Annual Meeting of the Continuous
Mixer and Extruder User's Group
Lincoln Harbor, NJ
June 2 - June 4, 1997

Author
James E. Kowalczyk

Shear Tool, Inc.
5763 Dixie Highway
Saginaw, MI 48601

The World Book Dictionary gives the definition of wear as **"meaning to reduce or erode, as by use or friction."** Everything in the world is subject to wear: boulders are worn down by the ocean's waves with the help of sand and gravel, mountains are worn down by wind, rain, snow and ice, and the Grand Canyon was worn in the earth's crust by glacial movement. Wear in the broadest sense occurs on or in everything, eventually changing its size or form.

Likely, it is not possible to **stop** wear. What is possible, however, is reducing the **rate** at which things wear. Sometimes this can be done so successfully that the appearance will be as if no wear is occurring. In order to address a wear condition and effectively reduce the rate of wear, one must first understand the mechanisms that cause wear to occur. If the cause of wear in a particular occurrence can be identified, then it is quite possible to modify either the mechanism of wear or the components being acted upon to substantially change the rate of wear.

There are two common beliefs about reducing wear (regarding changing the materials subject to wear), that are not necessarily valid under many circumstances. These beliefs are:

1. harder materials are more wear resistant than softer materials
2. thicker wear resistant materials are better than thinner ones

(Typically the belief is that "if a little is good then more must be better.")

An application involving the principles of wear that illustrates the fallacy of these stereotypical concepts is the simple "Where the Rubber Meets the Road" story. Simply put, rubber tires are very soft and pliable, while the steel rims they are normally mounted on are very hard in relationship. Nominally, the rims are several orders of magnitude harder than the tires. However if you drive a car on the soft tires, considering today's tire technology, you can normally drive for tens of thousands of miles before the tires are **worn out**. On the other hand, if you take the tires off the rims and attempt to drive home, chances are you will never get there before the rims are **worn out**. This is especially true if you live more than a few miles from where you started. Why is this? How is it that soft materials outwear hard materials in certain situations? Interestingly enough -- the application is the same, but the mechanisms of wear acting on the different materials are not the same due to the differing physical characteristics of these materials. The illustration, however, proves that a softer material under the right set of conditions will wear at a much slower rate than a harder material. We will address the mechanisms of wear a little later in this paper, then it will become clearer why a softer material might outwear a harder material if the right conditions exist in the wear mechanism.

Wear is a very complex phenomena with poorly defined scientific approaches to solutions. This is most likely because there are many mechanisms that cause wear to occur, and most wear situations are a compilation of more than one mechanism with a variable percentage of impact by each. Several years ago, a new scientific data base was established to study the phenomena of wear. This science is called **Tribology**. Practically speaking, Tribology is the study of wear mechanisms and resultant conditions to mating surfaces subjected to wear. Currently the four most recognized wear mechanisms are Adhesive Wear, Abrasive Wear, Corrosive Wear and Surface Fatigue Wear[1].

---

[1] Materials Engineering Forum, "Wear and Galling Can Knock Out Equipment", W.J. Schumacher

Adhesive Wear: This type of wear is commonly known as galling wear and is the most common and troublesome type found in moving machinery. Also known as scoring or scuffing, adhesive wear is caused by the strong adhesive forces developed whenever an imbalance of electrons exists between two mating surfaces. At low stresses, minute junctions form at contacting surfaces and small fragments of the metal become detached with subsequent movement. If stress levels are low enough, mild wear will take place between the mating alloys, and a wear rate can be measured after a specified number of cycles. This "mild" wear may or may not be tolerable, depending on desired service life. Furthermore, much larger junctions are formed at higher stresses. In such cases, catastrophic galling and eventual seizure may occur subsequently freezing the parts and stalling the equipment.

Abrasive Wear: This type of wear occurs when a much harder material cuts or plows grooves into a softer surface. The harder material may be one of the rubbing surfaces or it may be a third body introduced between the two mating surfaces. Qualitative definitions suggest three levels of severity (not three wear mechanisms) for abrasive wear.

1. Low stress abrasion (scratching) -- wear resulting from a cutting action by sliding abrasive, stressed below their crushing strength. The cut surface of the metal sustains little deformation. Consequently the surface does not work harden appreciably.

2. High stress abrasion (grinding) -- wear resulting from conditions of stress high enough to also cause plastic deformation of the ductile constituents.

3. Gouging abrasion -- high stress abrasion where sizable gouges or grooves are created on the wearing surfaces. These may be the result of sliding motion followed by impact.

Corrosive Wear: This type of wear stems from interaction of the wear surface and a corrodent. If an oxide film forms due to heating, wear may decrease or accelerate depending on the integrity of the film. Wear will be reduced if the oxide film adheres tightly and thus prevents metal to metal contact. On the other hand, a brittle oxide may spall and act as an abrasive. Corrosive wear may be minimized by selecting alloys that do not react with the chemical environment or with any lubricant that they might contact in service.

Fatigue Wear: This type of wear occurs without metal removal when a surface is stressed and unstressed repeatedly. This wear type predominates wherever there is rolling contact, as in ball bearings and gears. Cavitation due to vapor pressure will also induce fatigue. Fatigue is greatly affected by surface conditions such as microstructure, hardness, finish, residual stress and integrity. Design and fabrication techniques can be helpful here. Generous fillets and fine finishes reduce the high notch or stress concentration factors that generally accompany accelerated fatigue failures. Fretting wear is a form of fatigue wear. Fretting wear is the term used to describe material loss due to very small amplitude vibrations at mechanical interfaces. In fretting, various wear mechanisms combine and act together. Fretting involves an initial adhesion, metal transfer, the production of oxides and abrasive wear due to the oxide formation. Finally, the high oscillatory displacements lead to surface fatigue and thus fretting fatigue occurs.

Additionally, wear rate can be viewed on a macro scale as well as on a micro scale. Blindness to one or the other can produce a less than suitable answer when attempting to reduce tough wear problems. This is akin to not seeing the forest for the trees. On a macro scale, processes should be reviewed to better understand the wear mechanism(s) in play. One should also try to identify the key stimuli, and the magnitude of these factors, acting upon the materials relative to each wear mechanism type. Normally, reduction of the stimuli has the effect of reducing the impact of the wear mechanism, hence wear rate is reduced.

Key stimuli affecting the rate of wear are:

1. Cycles (key factor is differential velocity)
2. Slip velocity (key factor is adhesive characteristics)
3. Interfacial temperature (effected by both boundary conditions and overall process conditions)
4. Force (key factor is surface pressure, however note: that surface stress is only one resultant of surface pressure)
5. Chemical compatibility of the materials in contact with each other (this condition is highly affected by boundary conditions on a micro scale and by general process conditions on a macro scale)

Each of these stimuli can be either cause or effects of each other and each factor can effect wear differently based on both the magnitude of the stimuli and the type of wear mechanism involved in the process.

In the rubber tire and steel rim example, the tire has good adhesive properties in relation to the road surface providing little slip velocity. Hence the wear mechanism on the tire is primarily fatigue with cycles and force being the key factors in the life of the tire. The steel rim, on the other hand, has very poor adhesive characteristics and spins easily on the road surface. Hence the wear mechanism on the rim is primarily abrasive and the key factors governing life are slip velocity, force and interfacial temperature. The combination of these stimuli acting within the abrasive wear mechanism causes a wear rate on the rim several orders of magnitude higher than that on the tire subjected to primarily fatigue wear conditions. However, if the tire were on a race car where forces applied to the tire would cause it to overcome the adhesive characteristic (break the frictional grip) and spin at high velocity, then the wear mechanism would change to abrasive wear and the tire would wear at a much accelerated rate in comparison to the normal street tire scenario.

In mixers and extruders, the most common parts to experience wear are the agitator (or screw) components and the bores of the barrels (or casings that contain the screws). The problem of wear on mixer components has been escalating in terms of production costs due to several factors, some of the most notable are:

1. substantially increased production rates per barrel bore size
2. substantially increased horsepower per barrel bore size
3. substantially increased screw speeds
4. more aggressive agitator geometry's

5. more aggressive process materials in the form of chemistry, solids loading and physical composition
6. elevated temperatures of some processes

When addressing wear in a continuous mixing system and before spending large sums of money on exotic materials of construction, take time to review the process and look for opportunities to modify the process or the geometry of the mixer first. This is usually the most cost effective way to solve a wear problem, especially if it is inherent to a small section of the processing equipment. Before a company buys a piece of processing equipment in today's world, they usually run a process test at the perspective sellers "Customer Demonstration Center". These tests usually assure the prospective buyer that the equipment, as configured by the seller, will produce an acceptable product at an acceptable rate. However, it would normally be cost prohibitive for such tests to be run for a long enough period of time to produce acceptable wear data on a process. In most cases months or even years of continuous running are required to produce the desired wear data.

Usually wear problems are discovered in the field when unacceptable levels of parts replacements are required to sustain a particular process. When this occurs, the first reaction is to look for a more wear resistant material for the parts. Not many users would look at changing the geometry of the machinery or the process variables as these are considered sanctimonious once the process is working. However in many cases, changing these parameters will still produce an acceptable product while solving the wear problem.

As an example, several years ago a customer was mixing a polymer with fiberglass, calcium carbonate and talc. In the massing area where the polymer was being compounded, he was wearing out a section of the screw and barrel in a very short period of time. This area comprised a relatively short section of a barrel and screw. In the region of highest wear, the screw was configured of several 90° offset paddles. This is an extremely aggressive configuration which induces substantial energy (read "surface stress") over a very small surface area. These paddles were replaced with 60° offset forwarding paddles. A little feed screw length was sacrificed to allow for enough extra paddles to equal the total energy input of the 90° configuration, but this change spread the stress over a much larger surface area. Due to this change, the wear in this region was reduced to be equivalent with the rest of the barrel configuration. The feed screw length change did not hinder the process as previous dead stops showed this screw less than 30% filled under normal rate conditions. As a result the problem was resolved and special alloys were not required to correct the undesirable condition.

There may not always be a good process answer, but the lesson here is -- Do not look for a sophisticated materials answer until you have exhausted the possibility of a process resolution. Papers such as, Flow Distribution in a Co-Rotating Twin Shaft Continuous Mixer, authored by Mr. Bernard Loomans PE for the Compatibility and Processing Symposium of ADPA, April 1988, provides a good reference for identifying possible geometry changes to improve processing while reducing wear. *[See Exhibit A]* Another excellent reference for technical support on agitator and barrel configuration modifications to reduce wear, is groups like the Highly Filled Materials Institute @ Stevens. With their sophisticated computer modeling, they can optimize

geometry while leveling out surface stresses. They can also produce rheological data paramount to doing mathematical analysis of process behavior. As a general rule, optimizing process conditions normally promotes benefits, such as reductions in wear and other stresses sometimes problematic with twin screw mixers.

Once process conditions have been optimized and unacceptable wear conditions still persist, materials of construction can be scrutinized. A compilation of some of the most commonly utilized materials and processes for the construction of screw and barrel parts follows for your consideration.

Because there are so many wear mechanisms and stimuli, there cannot possibly be one wear resistant material combination that will economically combat all the forms of wear with the same positive results. In fact, in order to achieve optimum wear resistance, one would have to tailor a material specifically for each process situation. This type of application engineering in most cases would be too timely and cost prohibitive. Therefore, it is best to select standard materials based on history and market experience which will reflect reasonable wear resistance for a practical financial investment. This should be done in conjunction with investigating new concepts in materials for future improvements or for critical applications where the more common standard materials just won't do the job as required.

Following this logic, I would like to suggest that you consider the following: The most common forms of materials being used for abrasive wear resistance, where mild erosion is the norm, are the nitridable steels. These would most commonly include Nitraloy 135M and 4140 or 4340 heat treated steels. These materials offer a good core hardness combined with high tensile strength and toughness for a reasonable cost. They are also readily available in large volume and in an extensive variety of geometry's. All of these materials would have a core of about 28 to 32 RC and would be Ion Nitrided for maximum case depth and hardness. Typical surface hardness would range from around 52 to 62 RC and depth of case will vary from .002 inches effective case to .020 inches effective case, these characteristics being dependent on type of nitriding combined with temperature and time in process. *[See Exhibits B,C & D]*

Another common alloy used for mild abrasive conditions is 440C through hardened stainless steel. *[See Exhibit E]* This material offers some abrasive wear resistance, coupled with some corrosive wear resistance. It is commonly hardened to the mid 50 RC range with the barrel liners and screw elements having about a 4 RC point spread to help prevent galling. This hardness spread will also make the barrel (or liner) last longer than the screw parts. Traditionally screw parts are less costly than liner or barrel sections and are also much easier to replace. One must be careful when applying 440C, as minor changes in hardness above a certain level cause significant changes in the ductility of the material. The over hardening of 440C to achieve better wear characteristics will reduce toughness and can cause brittle fracture failure of components.

Still another family of materials that have been used very successfully for mild to medium wear resistance are the cast iron based alloys. Typically the Meehanite materials have been designed for wear, heat and corrosion resistant applications. *[See Exhibit F]* For typical non-corrosion wear conditions, Types W, WS and WSH materials are available. Type W offers

exceptional hardness with moderate shock resistance. Type WS offers high hardness, strength and toughness. Type WSH offers high impact strength. Additionally, the Thermoloy grade of HC-250 offers excellent abrasion resistance, and excellent heat resistance. *[See Exhibit G]* The caution here is that these materials when heat treated to acquire optimum wear resistance become very brittle and have little impact strength.

For medium wear conditions, mostly involving erosion due to abrasive wear, the current standard materials used on most twin screw mixer extruders are Crucibles CPM-9V and CPM-10V. *[See Exhibit H]* These materials have proved to be very effective on machines in a wide variety of applications. Both of these materials are produced from powdered metallurgy and the metal stock is formed by a process called Hot Isostatic Pressing. The metal powder is put into a vessel and vacuum is used to draw the material down so that it is at maximum density. The metal in the vessel is then melted and compacted at 50,000 PSI. The pressure is maintained in the vessel while the metal cools. The vessel is then cut away by chemical etching or by conventional machining methods. The remaining metal is then the raw bar or plate stock for the manufacture of barrel and screw components. These materials once machined can be through hardened to Rockwell levels in the 60 to 62 RC range. The normal concept is to utilize the CPM-9V for screw parts and the CPM-10V for the barrel liners. Approximately a 4 point RC spread is maintained between the screw and barrel parts for anti-galling and sympathetic wear considerations. When barrel and screw parts reach a certain size, the more practical approach is to HIP Clad the barrels and soft core the screw parts. This is achieved via the same method as forming the original bar stock, however in this case the vessel itself becomes the barrel or the screw core. HIP cladding of the barrels is, for the most part, a cost savings measure as only the bores need to be abrasion resistant. *[See Exhibits I&J]* From the standpoint of the screw parts, the softer ductile core prevents brittle fracture of the screw components when unplanned impacts are encountered in the system. However, it is not practical to soft core very small screw parts.

When wear in these applications contains an element of corrosion along with erosion, the CPM-420V alloy which is heat treatable (may be through hardened) while offering an element of corrosion resistance, is a good choice. *[See Exhibit K]*

Some manufacturers use D-2 (high chromium, high carbon cold worked tool steel) or other Tool Steels to advantage in medium wear applications. When through hardened and also nitrided they offer good wear characteristics for a reasonable price. D-2 can be through hardened to about 52RC. With nitriding it can produce a 72 RC surface, but at a very shallow case depth. The Crucible alternative to D-2 is their Cru-Wear material which normally offers better wear characteristics than D-2 or O-1 at a very comparable price. *[See Exhibit L]* This is because it contains 3.5% Vanadium Carbide and is heat treatable to a much higher level of hardness without sacrificing the toughness and strength of the Tool Steel. Cru-Wear is hardenable to 62RC and as such holds a nitrided surface of 72 RC at a much better case depth than D-2. Cru-Wear is also available as a HIP Clad material.

If one were looking to get a more wear resistant material into current machine designs on the market but was not yet prepared to delve into the very exotic alloys because of cost or other practical considerations, the next level up in wear resistance would probably be found in a new

alloy recently released by Crucible. That alloy is CPM-15V. *[See Exhibit M]* In many applications this alloy has been found to have more favorable wear resistant properties than the more well known CPM-10V. In this case, the best combination of materials would probably be barrel liners made from CPM-15V and screw parts made from CPM-10V. Consideration of HIP clad and hardness differential between the parts should be considered, the same as for the CPM-9V and CPM-10V combinations. This is done to minimize the possibility of adhesive wear.

The next step up in wear resistance, would be the HIP clad Colmonoy materials with Tungsten Carbide. The toughest of these materials is likely to be Colmonoy 88/w 40% Tungsten Carbide. *[See Exhibit N]* As these materials are 72RC as Hipped, they pose very specific manufacturing problems. Currently the best way to produce a finished product is by Electron Discharge Machining (EDM) and/or grinding. Each of these processes requires special machines and are quite costly. Therefore, the requirement to use such materials must be justifiable to the cost. Wear resistance on these materials is said to exceed that of almost any other production material on the market. This material can be custom tailored to contain any amount of Tungsten Carbide from approximately 15% to as high as 40%.

In addition to the HIP Clad materials, a wide variety of custom blended ceramics and metals can be employed to coat both barrel liners and screw parts using Fusion Deposition Processes. *[See Exhibits O&P]* These materials can also be applied to a wide variety of base metals providing many combinations applicable to corrosion, erosion and galvanic reaction. The Ceramics and Tungsten Carbides, in most cases, are extremely hard and abrasion resistant. The optimum process to be used with this type of application is high velocity impact deposition. With this process, the deposition gun generates 18,000°F plasma at controlled velocities between Mach 1 and Mach 4. The coating impacts the substrate in a plastic state and some fusion occurs. The bond is chemical/mechanical at the grain boundary level. The normal deposit of ceramics or carbides for wear is .005 to .007 inches thick, but for many other materials it is possible to build up the subsurface to .100 inches thick. The coating density can be controlled to present little to no interconnecting porosity.

Over recent years a family of complex buffer materials have been developed. These hybrid alloys act as buffers between the ceramic coating and the substrate material. This buffer coating allows the ceramic or carbide and substrate to expand and contract thermally at different rates without inducing stresses from one material to the other. A typical example of this application is the coated Titanium exhaust nozzle leafs on afterburners coated for aircraft manufacturers, as well as the government. (Typical users are McDonnell Douglas, G.E., Boeing, Pratt & Whitney, Rolls Royce, U.S. Air Force, Navy, etc.). The Air Force has extensively tested ceramic coated afterburner nozzles in Alaska on the F-15. These engines are started at -50°F and within 3-4 minutes, the afterburner nozzles reach 3000°F and glow white hot. The ceramic coatings on these nozzles have never failed.

To date over 10,000 exhaust nozzles have been manufactured with ceramic coatings for over a dozen aircraft engine manufacturers without a single failure of the ceramic coatings. Indications are that a stress free pure ceramic coating from .025 to .035 inches thick can be applied. Ceramic and metal hybrids can be deposited up to .200 inches thick. Currently, there are

over 200 formulations of ceramics and hybrids which are applied off the shelf. Suppliers can specially formulate almost any composition of materials to fit a unique application.

Ceramics have their own special problems -- the most significant being that they are very brittle, as it is the hardness which gives them exceptional wear resistance. In order not to crack or chip parts, special geometric forms on the substrate materials are required where the ceramic will be applied. Keeping the thickness of the coatings to the optimum nominal thickness required to do the job also reduces the probability of chipping and cracking. In some cases too thin a coating will cause it to chip or crack, in others too thick a coating will cause similar problems. The buffer materials give the coatings a better chance of impact survival as well as thermal stability. Another technique utilized to improve ductility is to alloy the coatings. Some ceramics are also very poor conductors of heat and if they are applied with a significant thickness, they will reduce heat transfer. However, there are a few ceramics which are very good conductors of heat. On the other hand, ceramics are generally poor electric conductors with high dielectric strength; this helps in applications where galvanic reactions occur. They can also be sealed with a wide variety of phenolics to increase dielectric strength. If barrels to be coated are not split, then 2.5 inches is about the smallest bore that can be coated evenly for any appreciable length. Bores smaller than this can only be coated about one length to diameter ratio. This is because the high velocity plasma heads used for deposition are too big to fit in a bore smaller than 2.5 inches. For the Ultra High Velocity Deposition processes (Modified HVOF), non split bores of less than 8 inches in diameter cannot be coated.

For optimum wear resistance, the following ceramics should be considered: Chromium Oxide materials for the barrel liners, on a base metal of 4140 heat treated or 4340 heat treated alloy steel. Base metals should be about 28-32 RC to give core toughness desired, the Chromium Oxide Ceramics would be 72-73 RC (Modified HVOF process). If the ceramics are to be used as coated, the optimum thickness would be .005 to .007 of an inch, if the surface is to be ground or lapped prior to use, then .008 to .010 of an inch would be the recommended thickness. To be compatible, screw parts should be of the same base metal, but coated with Gray Alumina Ceramic. This material has a coated hardness of 65-67 RC. Alternate materials for the screws might be Aluminum Oxides or Cobalt based materials.

From an economics standpoint going with as coated parts and avoiding the surface grinding or lapping is advisable. Post surface preparation is very expensive on these types of materials.

As for corrosive applications, the ceramics listed above are good choices, but other less expensive alternates are available. Where abrasive wear and adhesive wear are not a problem, simple 304 or 316 stainless steels are effective. For very aggressive corrosion problems, looking at more exotic nickel based materials such as the Hasteloys and Inconels may be a requirement. Where corrosion and abrasion are a collective problem, precipitation hardening stainless steels like 17-4-PH are a good choice. Where corrosion and adhesive wear are a collective problem, non-galling materials with corrosion resistance characteristics similar to Type 316 Stainless Steel are available, such as Waukeshaw Alloy 88 material. *[See Exhibit Q]* Where strength, wear and corrosion are all simultaneous problems, Duplex Stainless Steels are popular remedies. The most

well known of these materials are the Armco Nitronic materials such as Nitronic 60 and the HTM Division, Cabot Corp. materials such as Ferralium 255. *[See Exhibits R&S]* Both of these materials offer high strength and are hardenable while providing good corrosion resistance. They can also be coated with ceramics to enhance their wear resistance.

An interesting approach utilized in some batching processes to overcome the most difficult wear problems could be entertained for twin screw extruders as well. The novel approach is to run the very aggressive material primarily against itself. An example is a molten salt bath. The process salts when heated to 1800°F temperature are very active and aggressive both from an abrasion and a corrosion standpoint. While there are materials that will stand the corrosive affects of the chemical attack at this elevated temperature, almost nothing will withstand the combination of heat/corrosion/abrasion. The novel answer to this problem, was to heat the salt bed internally to melt it, and cool the vessel walls creating a film of solid salt on the internal wall surfaces and hence making the process material the inner shell of the vessel. A similar concept can be used in a twin screw mixer/extruder by rifling the barrel. The grooves fill up with the process material which runs against itself primarily as the basic wear surface. The drag flow of the machine is also enhanced as the compatibility of the process material against itself promotes good adhesion and reduces wall slip.

As we discussed, there is almost an infinite number of materials and combinations of materials that can be utilized to improve wear resistance. These represent but a small part of what is available to the industry today. However, these are probably the most commonly used for applications involving twin screw mixers and extruders. Possibly this information will prove to be of some use to your present and future development plans.

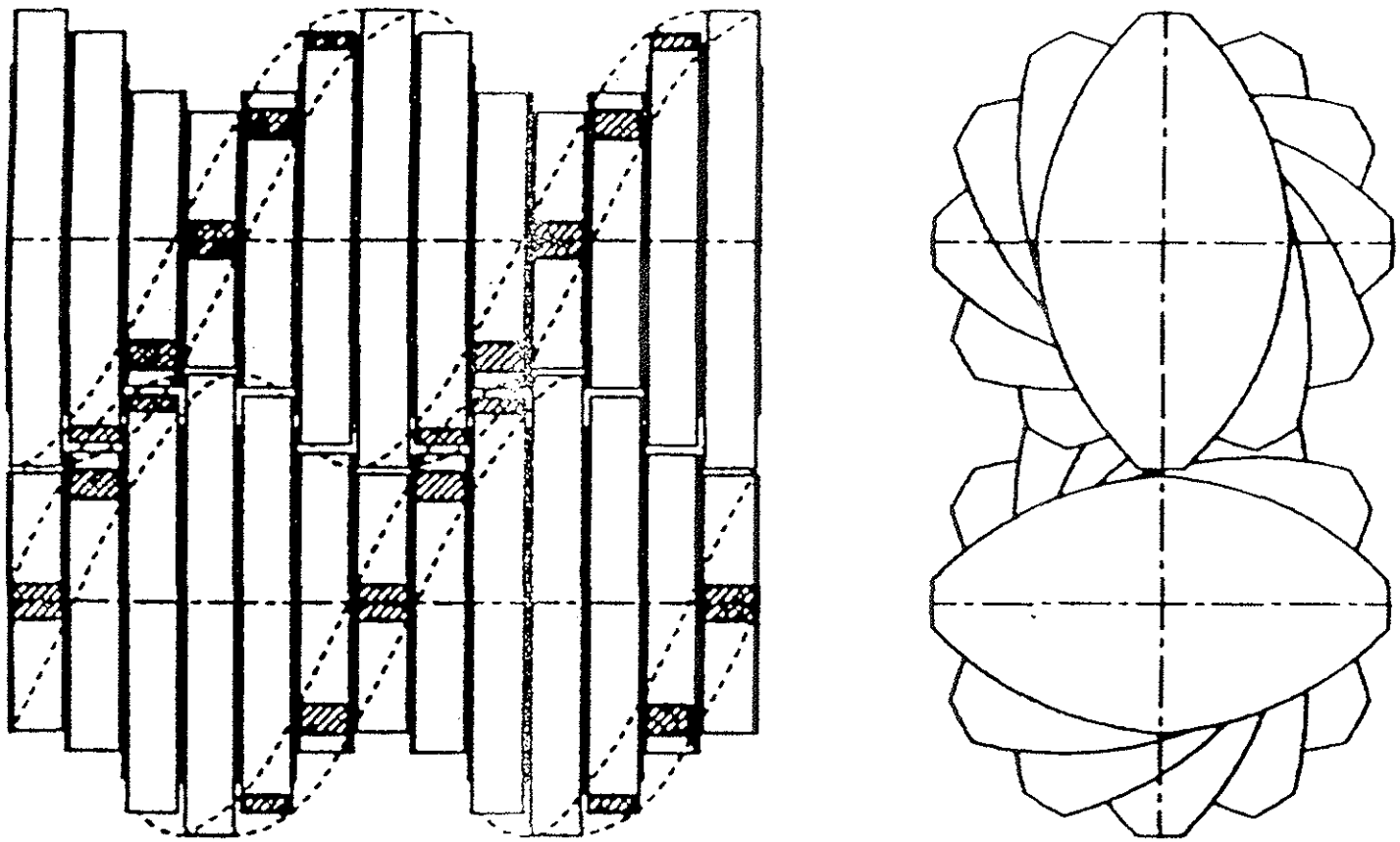

MIXING ELEMENTS HELICALLY OFFSET
FORMING A MIXING SECTION

FIG. 3

FIGURE A-1

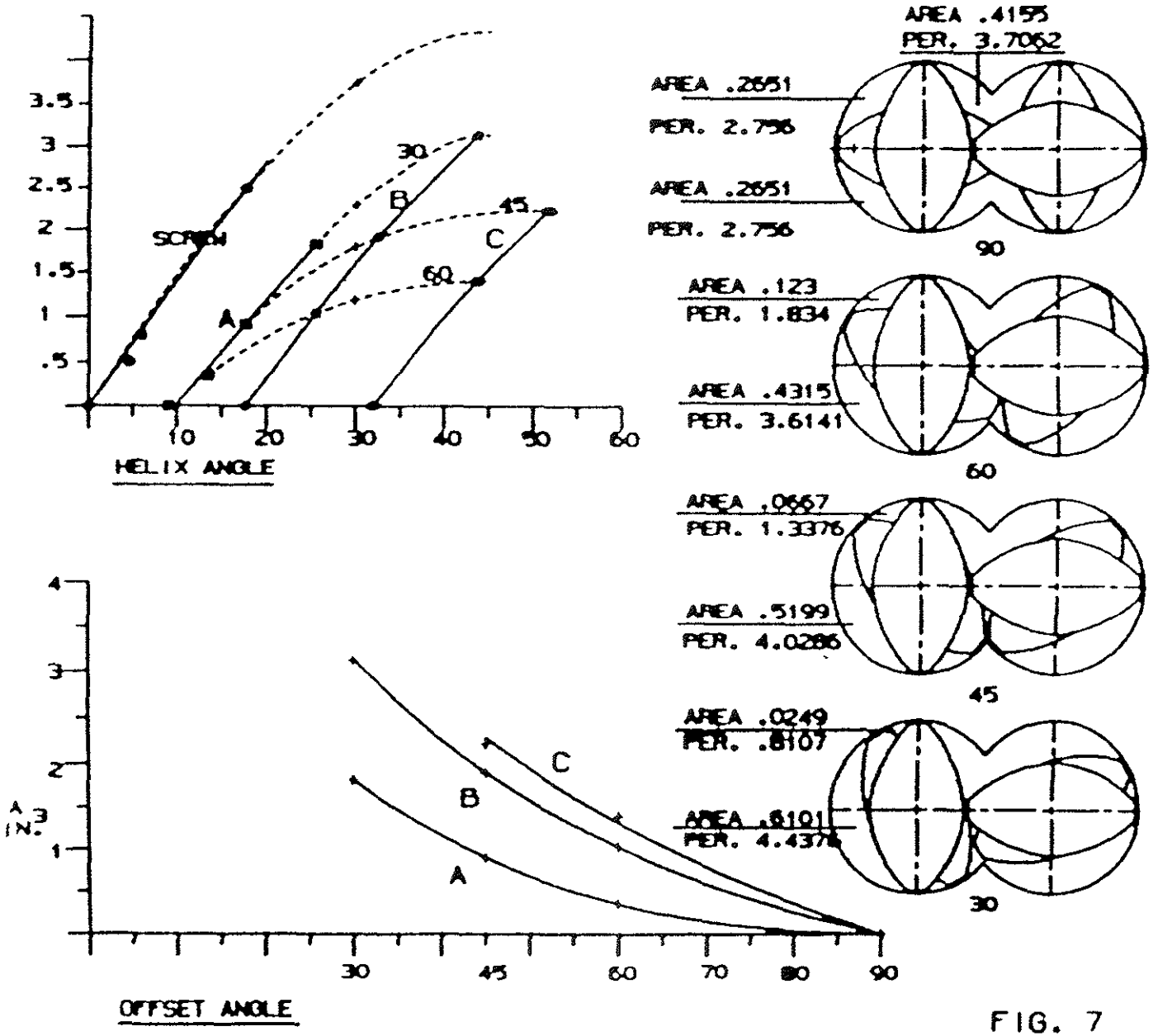

FIG. 7

FIGURE A-2

ionprocessing™

Surface

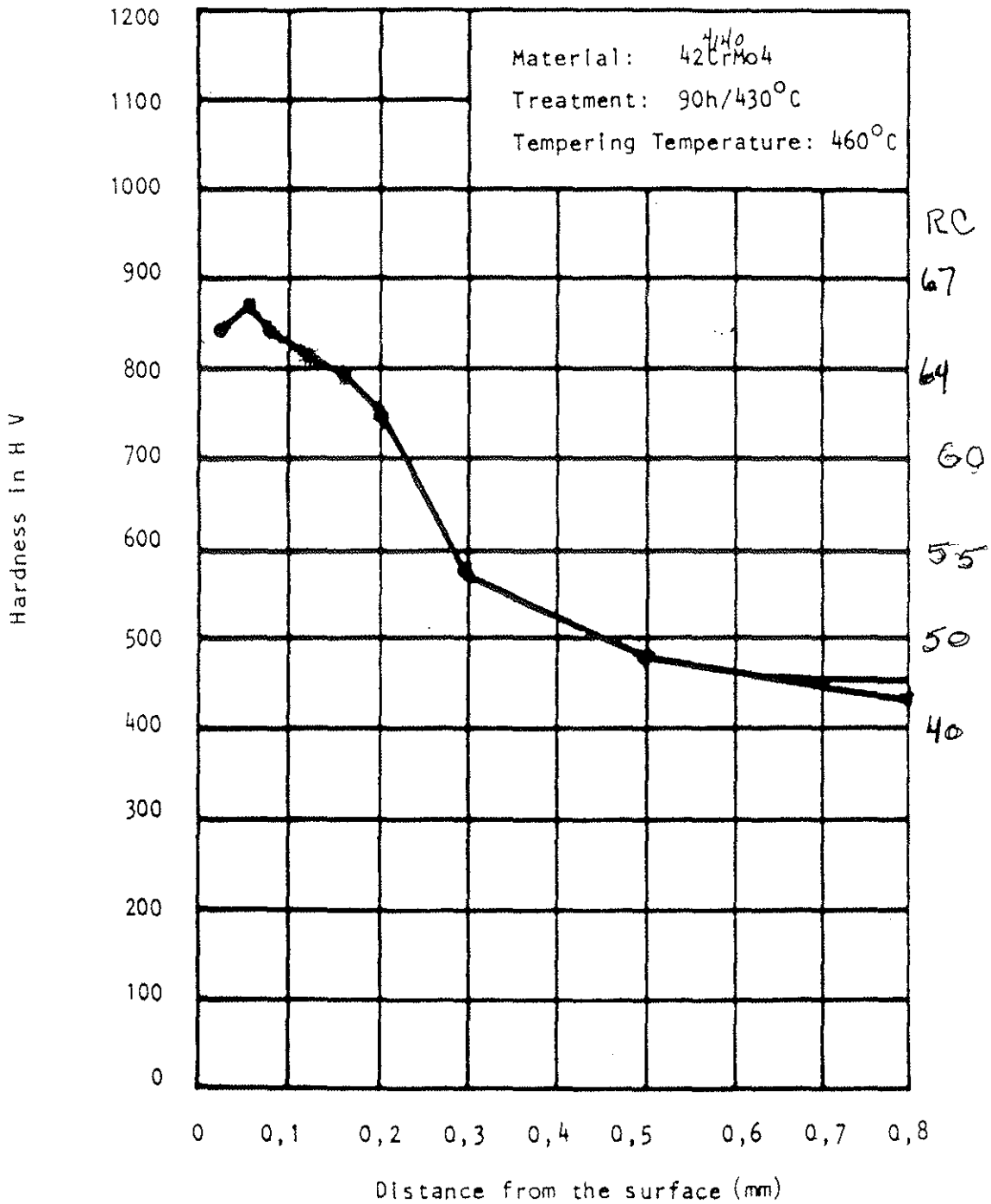

[illegible]

MIDLANDROSS

EXHIBIT B

ionprocessing™

Surface

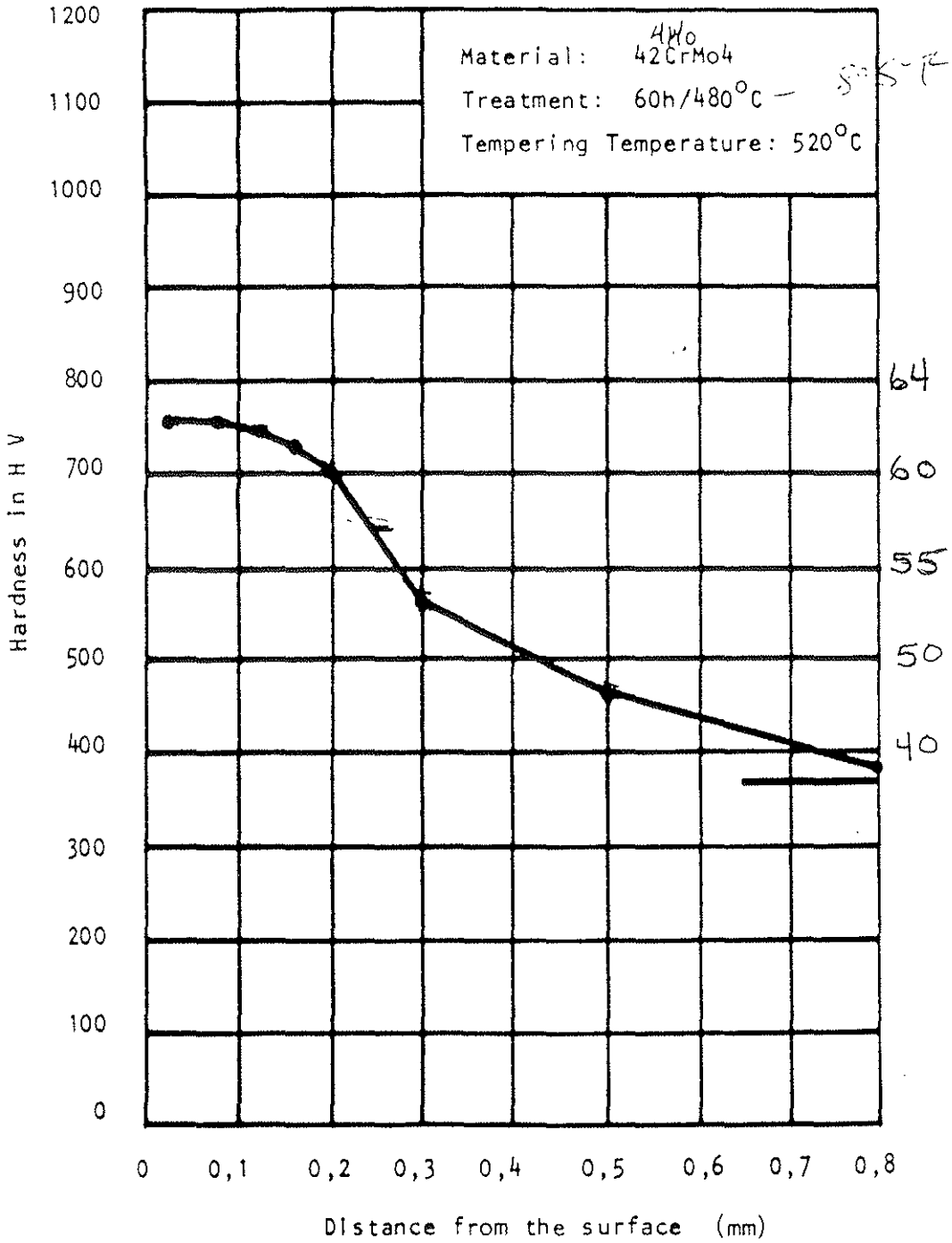

Name Date Page

The reserve all rights pertaining to this technical specification, including such as are related to the patent or patents or the registration of designs without prior notice. This technical specification must not be reproduced, made available to third parties or otherwise wrongfully used by the recipient or by third parties. Offenders shall be liable of damages and may be liable to prosecution.

MIDLAND ROSS

EXHIBIT C

Surface

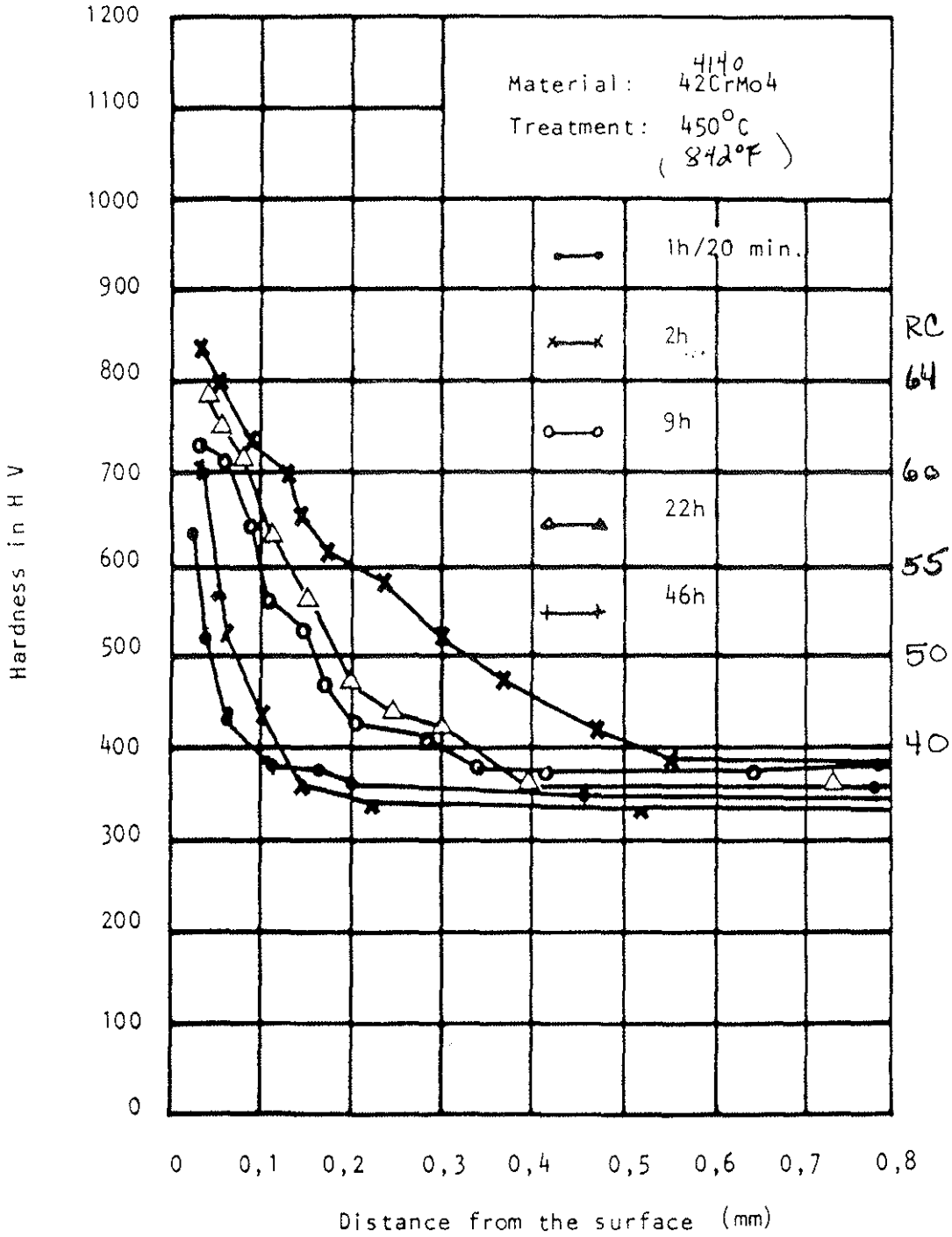

Name Date Page

We reserve all rights certain to this technical specification, including such as are related to the grant of patents or the registration of designs. Without our prior approval this material can neither be reproduced, made available to third parties or otherwise used for the benefit of other parties. Offenders shall be liable for damages and may be liable to prosecution.

MIDLAND ROSS

EXHIBIT D

COMPARATIVE WEAR RESULTS (DRY RUBBING TEST)

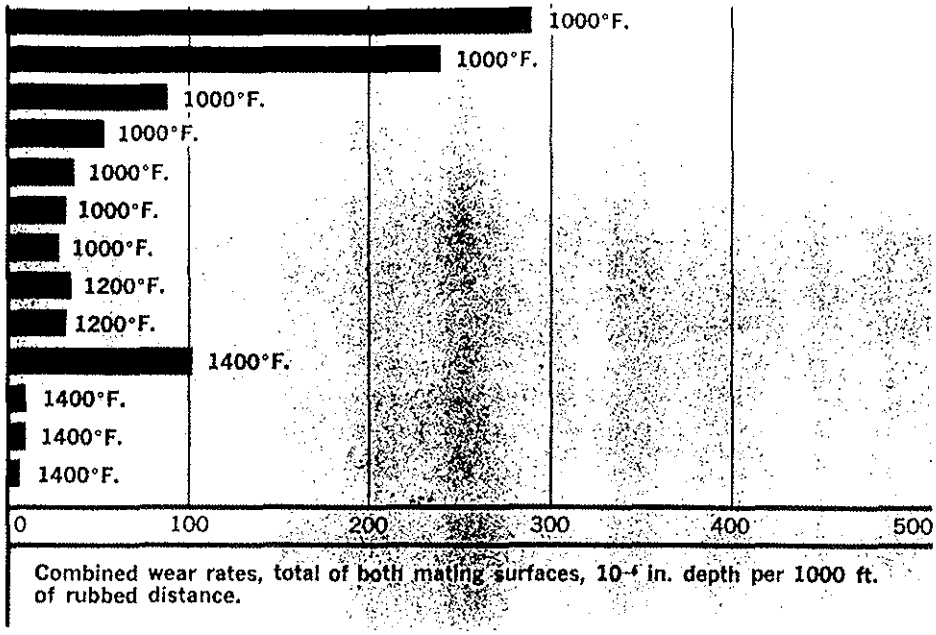

Combined wear rates, total of both mating surfaces, 10^{-4} in. depth per 1000 ft. of rubbed distance.

COMPARATIVE WEAR RESULTS (WET ABRASION TEST)

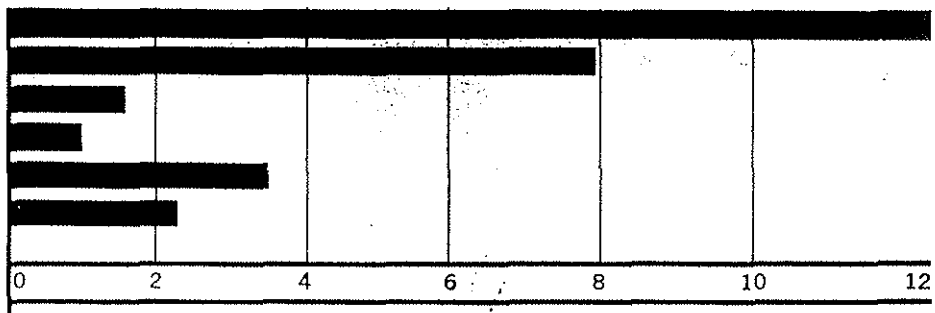

TAP WATER PLUS ABRASIVE DUST WAS ONLY LUBRICANT

Combined wear rate, total of both mating materials, MG./HR.

SERVICE CONDITIONS — COATING RECOMMENDATIONS

Environment	Impact and Vibration	Cutting	Abrasion
Near Neutral Fluids	LW-1N40	LW-1	LW-1
Alkaline Fluids	LC-1B55	LW-5	LW-5 LC-1C
Water-Steam to 1200°F.	LC-1B55	LW-5 LC-1C	LW-5 LC-1C
Woody and Fiberous	LW-1N40	LW-1 LW-5	LW-1 LW-5
Air to 1000°F.	LW-1N40	LW-1	LW-1
Air to 1200°F.	LC-1B55	LW-5	LW-5
Air to 1600°F.	LC-1B55	LC-1C	LC-5 LA-2
Air to 2000°F.	LC-1B55	LC-1C	LC-1C
Foods, Fruit Juices, Meat	LC-1B55	LW-5 LC-1C	LW-5 LC-1C

EXHIBIT E

WEAR-RESISTING TYPES

		U.T.S.	Yield	Elongation %	Brinell Range	Impact Ft.Lbs. / J	FATIGUE LIMITS [2]ROTATING BENDING Notched	Unnotched
WA	PSI N/mm²	50,000 345			250/350 (as-cast) <550 heat-treated			
W1	PSI N/mm²	50,000 345			500/600	[3]30-50 [4]40-68		
W2	PSI N/mm²	50,000 345			500/600	[3]40-60 [4]54-80		
W4	PSI N/mm²	50,000 345			400/700	[3]40-70 [4]54-95		
W.S.	PSI N/mm²	60,000 410	50,000 345	2-4	400/525	[3]<180 [4]<200		
W.S.H	PSI N/mm²	100,000 690	75,000 517	4-10	350/500	<120 <120		
A.Q.S.	PSI N/mm²	80,000 550	70,000 480	1-3	225/500	[1]1-3 [1]1-4		
K295	PSI N/mm²	130,000 900	100,000 690	8-12	280/360		270	440
K325	PSI N/mm²	145,000 1000	112,000 770	5-8	300/350		320	466
K405	PSI N/mm²	175,000 1200	140,000 965	2-5	<380		350	510
Symbol		Rm	Rpo.2	A5	HB30		$\sigma_{g.w}$	$\sigma_{g.w}$

1 Charpy 10mm² V Notch
2 Wöhler Rotating Bending Fatigue Test using a 10.6mm diameter test piece.
3 Ft. Lbs.
4 Joules

TABLE 1

EXHIBIT F

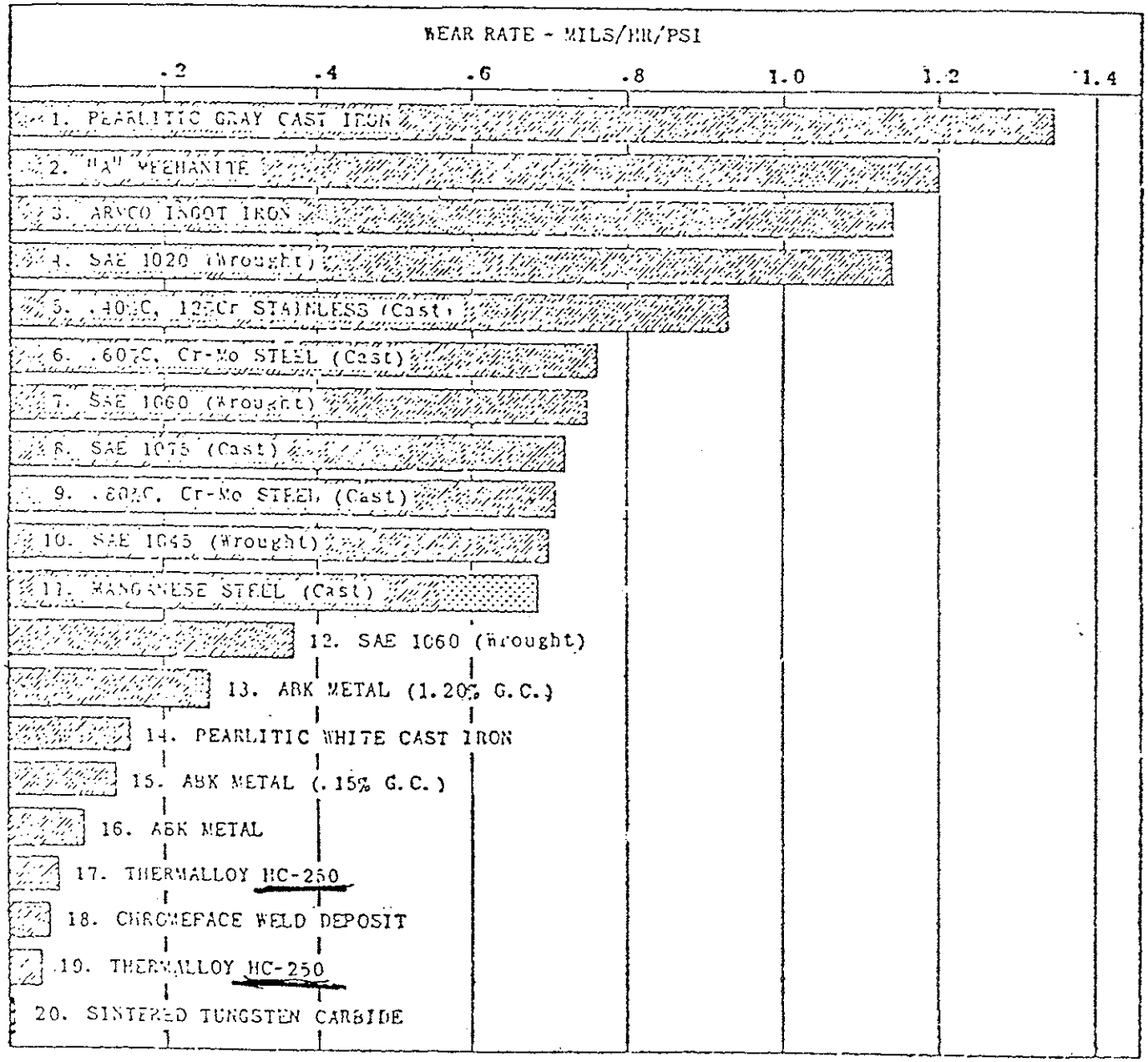

MAT.	HEAT TREATMENT	ABRASION FACTOR*	WEAR RAT (Mils/Hr/Psi
1	As-Cast	1.41	1.35
2	As-Cast	1.25	1.20
3	As-Rec'd	1.49	1.14
4	Annealed	1.33	1.13
5	Norm. and drawn	1.14	.93
6	Norm. and drawn	.83	.76
7	Annealed	.95	.75
8	As-Cast	.88	.72
9	Norm. and drawn	.84	.71
10	Norm.	1.00	.70
11	Quenched	.75-.82	.56-.69
12	Quenched and drawn	.41	.38
13	As-Cast 3" Block	.23	.26
14	As-Cast 2 Heats	.20	.16
15	As-Cast 3" Block	.16	.14
16	As-Cast 1" Block	.12	.10
17	As-Cast	.075	.061
18	As-Welded 2 Welds	.061	.050
19	Norm.+Avg. of 10 Csts.	.044 (.052-.025)	.040 (.057-.022
20	As-Rec'd	.013	.004

*SAE 1045 = 1.0

Fig. 17 Relative Performance in Dry Sand Abrasion of Various Materials

EXHIBIT C

Wear Resistance

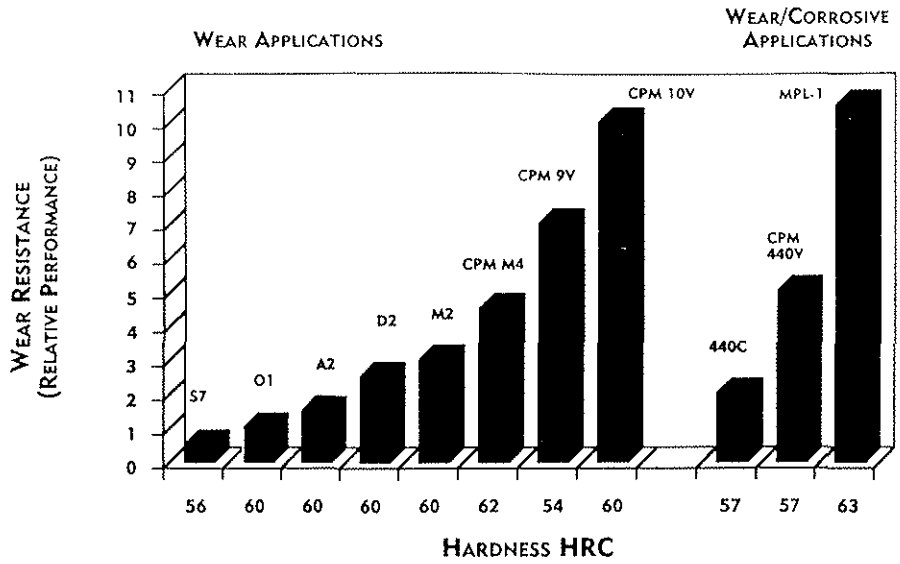

Crucible CPM 10V and MPL-1 provide exceptional hardness and wear resistance.

Toughness

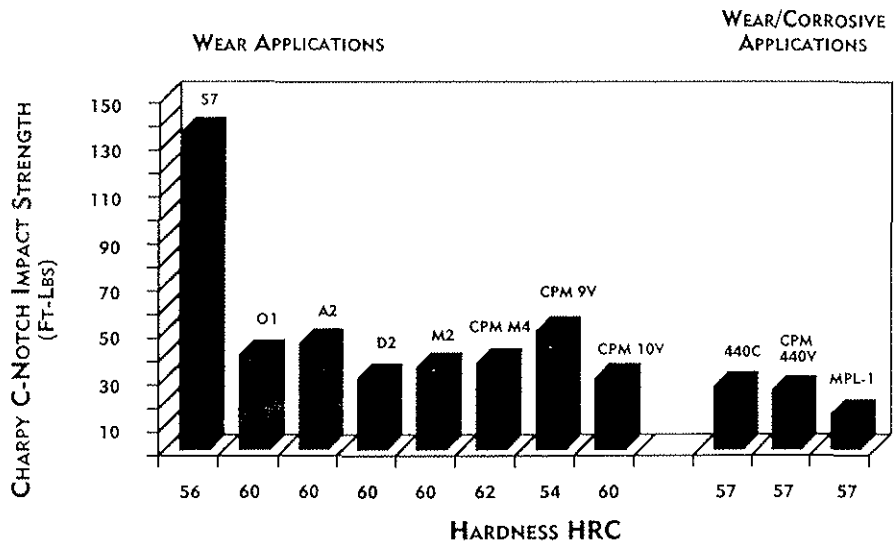

Crucible CPM 9V and 10V also exhibit toughness comparable to many other less wear resistant tool steels.

High vanadium screw segment with ductile steel core.

	Composition, WT %				
Grade	C	Cr	V	Mo	W
CPM 9V	1.78	5.25	9.0	1.3	—
CPM 10V	2.45	5.25	9.75	1.3	—
CPM M4	1.40	4.0	4.0	5.0	5.50
MPL-1	3.75	24.0	9.0	3.0	—
CPM 440 V	1.9	17.5	6.0	1.0	—
CPM 420 V	2.17	13.0	9.0	1.05	—

Note: Properties shown in this data sheet are typical values. Normal variations in chemistry, size and conditions of heat treatment may cause deviations from these values. For additional data and metallurgical engineering assistance, please call your Crucible technical service representative, at (412) 923-2670.

EXHIBIT H

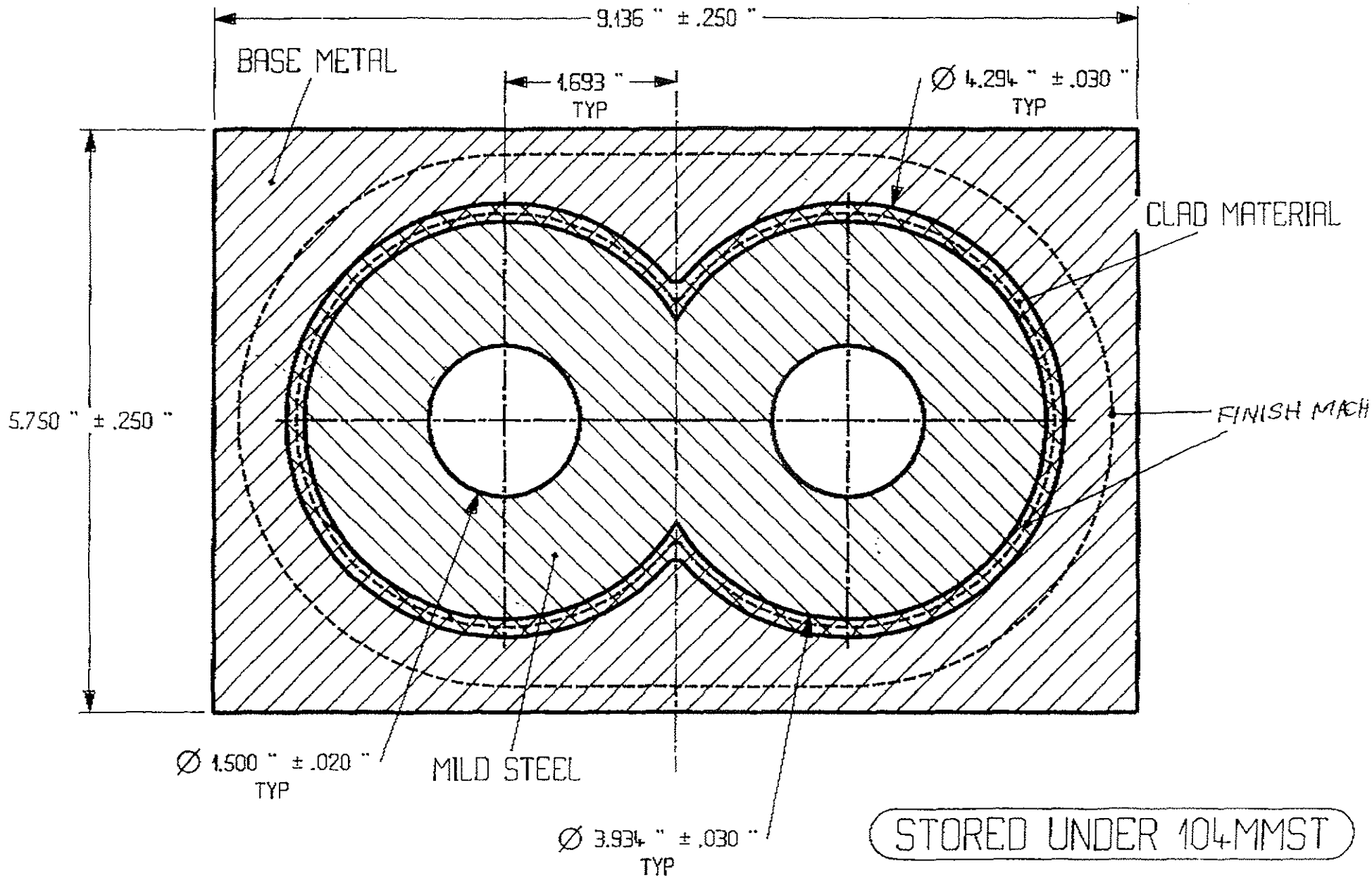

STORED UNDER 104MMST

EXHIBIT I

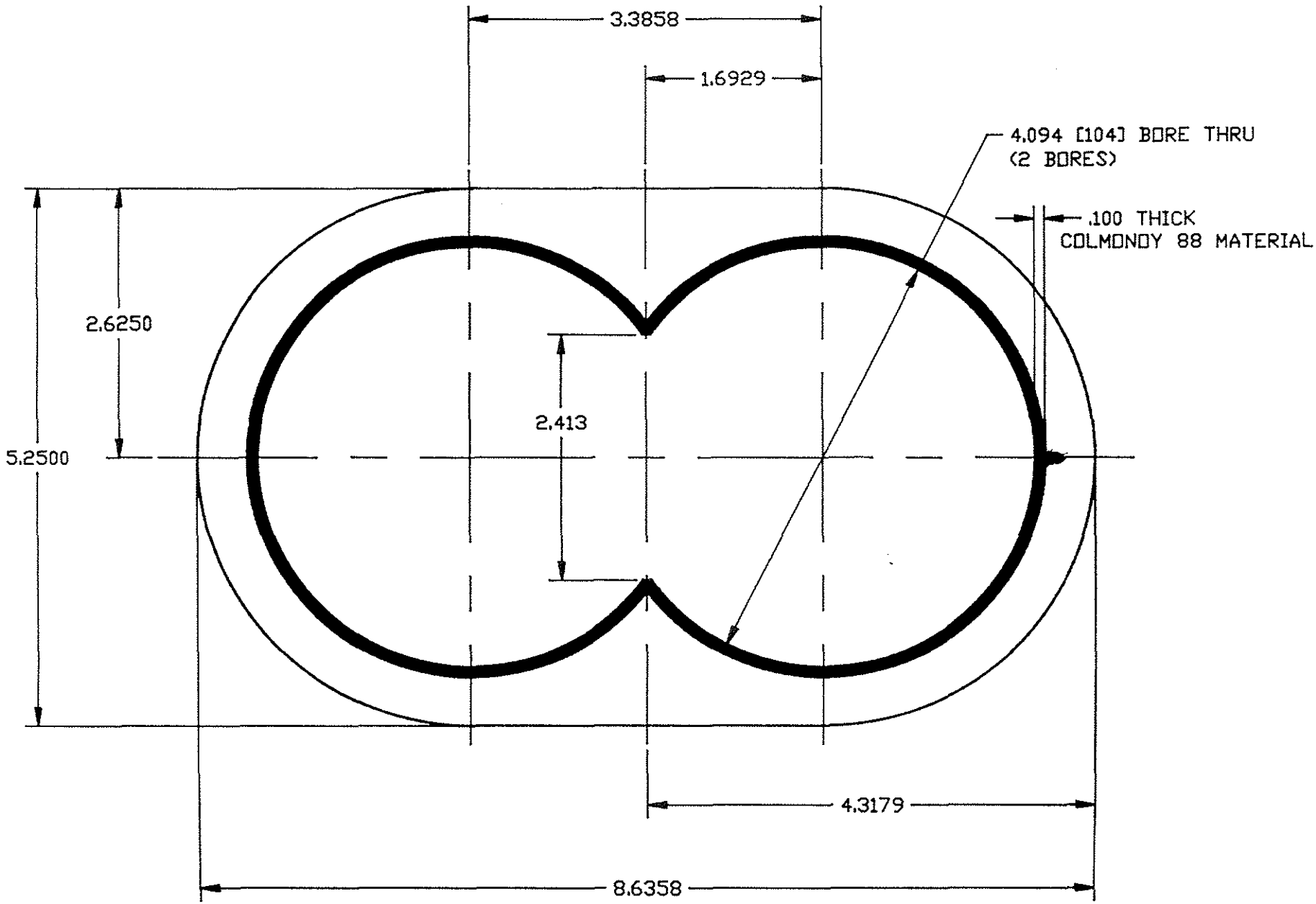
3.3858
1.6929
4.094 [104] BORE THRU
(2 BORES)
.100 THICK
COLMONOY 88 MATERIAL
2.6250
2.413
5.2500
4.3179
8.6358

EXHIBIT J

CRUCIBLE DATA SHEET

CPM 420V is a unique tool steel made by the Crucible Particle Metallurgy process. It is designed from a martensitic stainless steel base analysis, with high vanadium and carbon added for exceptionally good wear resistance. CPM 420V offers significant improvements over CPM 440V and other high chromium P/M and conventional tool steels in both wear and corrosion resistance.

The wear and corrosion resistance of CPM 420V make it an excellent candidate to replace CPM 440V or AISI 440C, where increased wear is a primary concern, as well as D2 or other tool steel applications where improved corrosion protection is of benefit.

Typical Applications

Plastic Injection and Extrusion Feedscrews
Gear Pumps
Non-return Valve Components
Gate and Nozzle Inserts
Pelletizing Equipment
Injection Molds and Inserts
Industrial Knives, Slitters and Cutters
Long-wearing Specialty Cutlery
Bearings, Bushings, Valves,Rolls
Wear Components for Food and Chemical Processing

Note: These are some *typical* applications. Your *specific* application should not be undertaken without independent study and evaluation for suitability.

Mechanical Properties

Wear Resistance:

In wear testing, CPM 420V has shown 25% to 50% better wear life than CPM 440V. Both grades offer several times better wear resistance than standard 440C.

Impact Toughness:

CPM 420V offers similar impact toughness (Charpy C notch) to CPM 440V and standard 440C at comparable hardnesses.

Mechanical properties

	Hardness HRC (1)		Impact Toughness(2) Ft-lbs	(Joules)	Wear Resistance Adhesive(3)	Abrasive(4)
CPM 420V	55/56	A	22	(30)	30/35	55/65
CPM 420V	57	B	12	(16)	35/40	50/60
CPM 440V	55	A	18	(24)	15/25	70/85
CPM 440V	58	B	13	(17)	20/30	60/70
440C	56/57	C	26	(35)	3/4	---
D2	59	D	22	(30)	3/4	---

Notes:
(1) A = Hardened 1950 F (1065 C),
B = Hardened 2050 F (1120 C), double tempered 600 F (315 C)
C = Hardened 1900 F (1040 C), double tempered 600 F (315 C)
D = Hardened 1850 F (1010 C), double tempered 600 F (315 C)
(2) Charpy C-notch impact test
(3) Crossed-cylinder adhesive wear test (higher number = better wear resistance)
(4) Pin abrasion wear loss (lower number = better wear resistance)

Crucible Service Centers

CRUCIBLE CPM® 420V

Issue #1

(AISI 420 modified with high vanadium)

Carbon	**2.2%**
Chromium	**13.0%**
Vanadium	**9.0%**
Molybdenum	**1.0%**

Physical Properties

	English Units	Metric Units
Elastic Modulus	31 x 10^6 psi	215 GPa
Specific Gravity	7.40	7.40
Density	0.27 lbs/in^3	7400 kg/m^3 (7.4 g/cm^3)
Thermal Conductivity @ 200 F (65 C)	10 BTU/hr-ft-F	17.3 W/m-K (0.041 cal/cm-s-C)

Coefficient of Thermal Expansion

°F	(°C)	in/in/°F	mm/mm/°C
70-400	(20-200)	6.1 x 10^{-6}	11.0 x 10^{-6}
70-600	(20-315)	6.4 "	11.5 "

Machinability and Grindability

Machinability in the annealed condition is similar to CPM 440V. Grindability will be slightly more difficult due to the higher vanadium carbide content. Similar grinding equipment and practices are acceptable. "SG" type alumina wheels or CBN wheels have generally given the best performance with the CPM steels.

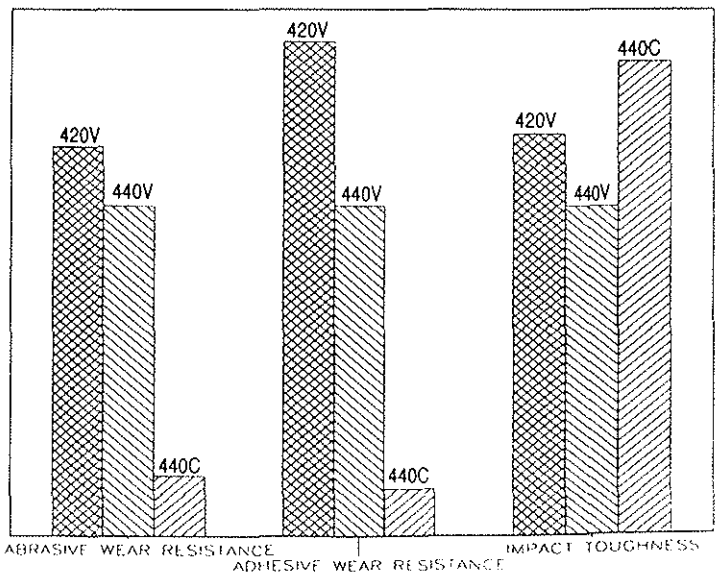

Relative Wear and Toughness Properties, CPM 420V vs 440V and 440C.

Note: Properties shown throughout this data sheet are typical values. Normal variations in chemistry, size and conditions of heat treatment may cause deviations from these values. For additional data or metallurgical engineering assistance consult your local Crucible Service Center.

EXHIBIT K

CRUCIBLE DATA SHEET

Issue #

CRU-WEAR is an air hardening tool steel possessing an excellent combination of high wear resistance and toughness. This grade is readily machined in the annealed condition and exhibits minimal distortion in hardening. The normal heat treatment is compatible to a wide variety of surface coatings such as nitriding, tin coating, etc.

CRU-WEAR excels in applications that require higher wear resistance than D2, greater toughness than M-2 high speed steel, or in applications that require both.

The combination of wear resistance, compressive strength, and exceptional toughness make CRU-WEAR a great choice for a wide variety of demanding tooling applications.

Typical Applications

Punches	Blanking Dies	Knives
Thread Rolling Dies	Shear Blades	Rolls
Forming Blades	Planer Blades	Gauges
Wear Parts	Coining Dies	Trim Dies
	Lamination Dies	

Note: The above are some typical applications. Your specific application should not be undertaken without independent study and evaluation for suitability.

Toughness

Lowering the hardening temperature (underhardening), reduces the grain size and increases toughness.

CRU-WEAR

Typical Chemistry

Carbon	1.10
Manganese	0.35
Silicon	1.10
Chromium	7.50
Vanadium	2.40
Tungsten	1.15
Molybdenum	1.60

Physical Properties

Density, lb/cu in. 0.28
Specific Gravity 7.7
Specific Heat 0.1
Modulus of Elasticity, psi (Compression) .....30-32 x 10

Annealed Hardness - BHN 207/248

Surface Treatments

CRU-WEAR can be nitrided, steam tempered, or titanium nitride coated if desired. If the CVD TiN treatment is used care is required in vacuum hardening.

TOOL STEEL COMPARAGRAPH

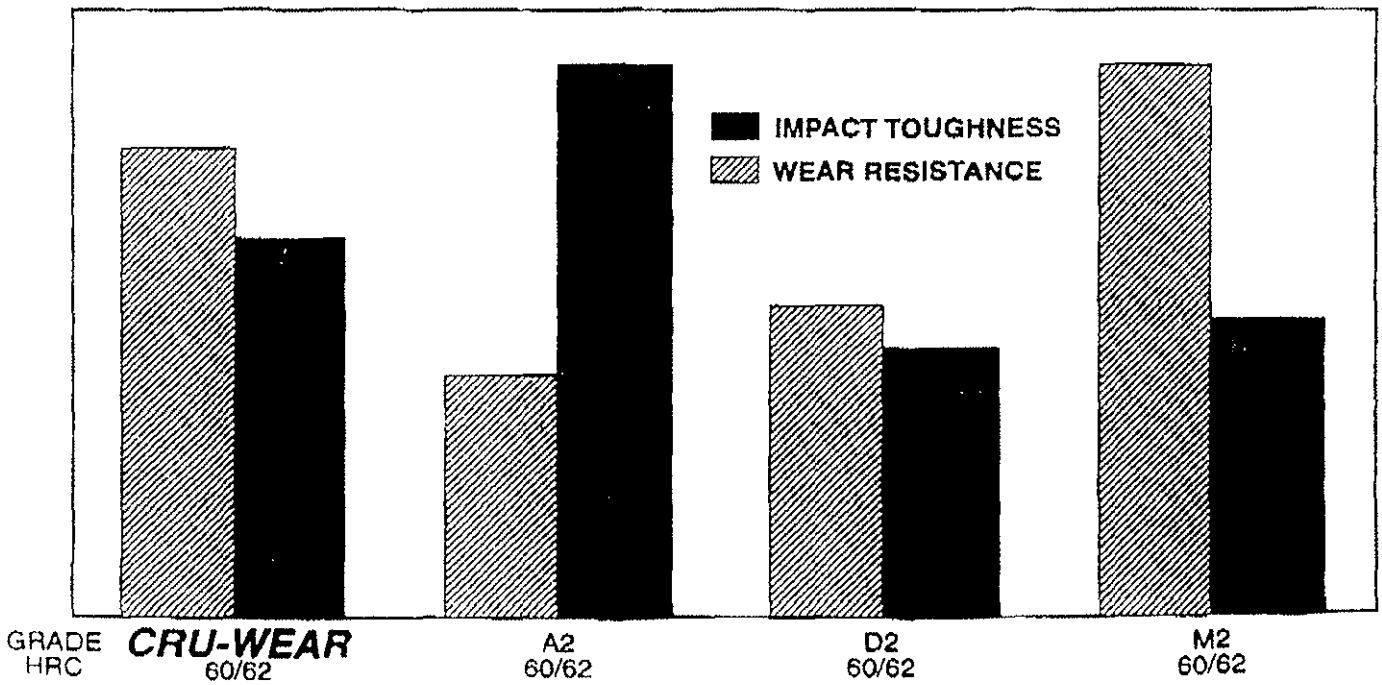

Crucible Service Centers

Note. Properties shown throughout this data sheet are typical values. Normal variations in chemistry, size, and conditions of heat treatment may cause deviations from these values. For additional data and metallurgical engineering assistance, consult your local Crucible Service Center.

EXHIBIT L

Crucible Service Centers

Tom Schleicher
Senior Sales Representative

Crucible Service Centers
A Division of Crucible Materials Corporation

A Division of Crucible Materials Corporation
1201 Piedmont
Troy, Michigan 48083
313/528-0332, WATS: 800/365/1133
FAX: 313/528/1977

TOOL STEEL
ALLOY STEEL
CPM HIGH SPEED
CONV HIGH SPEED

CRUCIBLE CPM® 15V

Preliminary Technical Information

Note: The following information represents the results of laboratory development work and preliminary commercial testing for a new grade, CPM® 15V. A full datasheet, including more detailed information, will be available upon commercial availability of the grade.

Relative Wear Resistance @ HRC 60-62
and Coded Toughness Guide

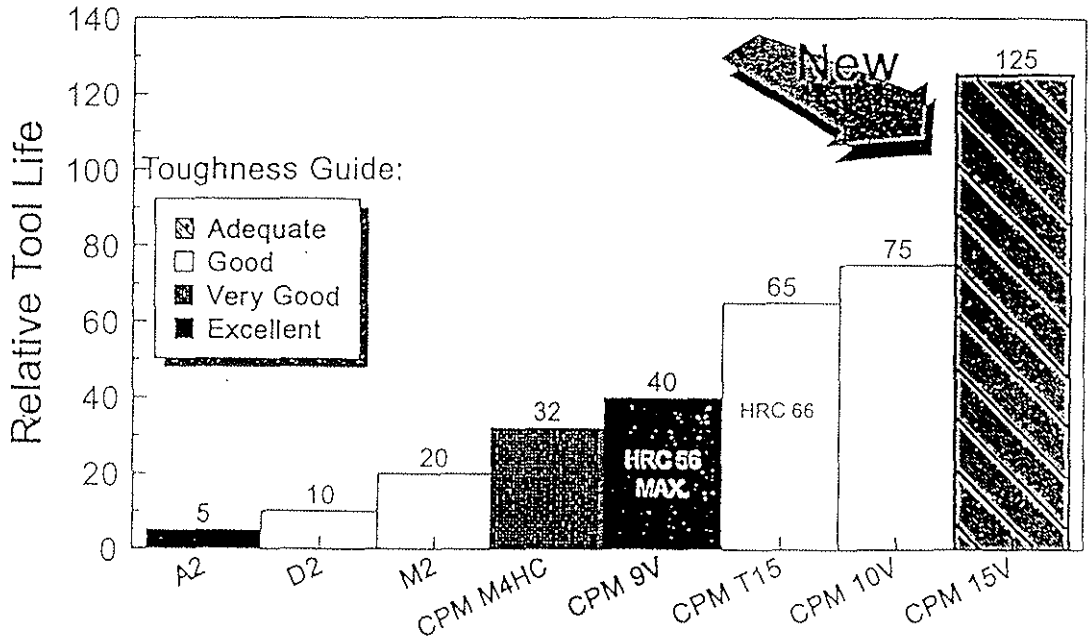

CPM 15V is a new tool steel made by the CPM (Crucible Particle Metallurgy) process. It is more wear resistant than our CPM 10V. It has about 50% more hard vanadium carbide in its microstructure than CPM 10V, to provide superior wear performance.

CPM 15V is intended for applications where wear is the primary concern. It is ideal for tools where CPM 10V is already successfully used, and even longer wear life is desired. CPM 15V is also recommended for any long wear life application where carbide tooling is too brittle.

The CPM process produces very homogeneous steel microstructures, which are characterized by better toughness and machining characteristics than conventionally produced steels of similar alloy content. However, when considering appropriate applications for CPM 15V, it is necessary to keep in mind that CPM 15V will be slightly less tough than CPM 10V, and machinability and grindability are expected to be at least 50% more difficult, because of the additional 50% carbide volume in the steel.

EXHIBIT M

COLMONOY® technical data sheet

Wall Colmonoy Corporation, 30261 Stephenson Hwy., Madison Heights, Mi 48071-1650
Tel 810-585-6400 Fax 810-585-7960

No. Ni-4.4B

COLMONOY No. 88

A Patented* Hard-Surfacing Alloy With Bi- and Tri-metallic Hard Phases for Maximum Wear Resistance

NOMINAL COMPOSITION

Carbon	0.8%
Chromium	15.0
Boron	3.0
Silicon	4.0
Iron	3.5
Tungsten	17.3
Nickel	Balance

PHYSICAL PROPERTIES

Hardness (Rockwell C)	59-64
Melting Point (approx):	
Solidus	1810°F (990°C)
Liquidus	2160°F (1180°C)
Density	9.89 gm/cc
Apparent Density	4.78 gm/cc

DESCRIPTION

Colmonoy 88 is a unique alloy containing fine, multiple hard phases which are uniformly distributed throughout a Ni-Cr-B matrix. These hard phases, comprised of complex bi- and tri-metallic borides and carbides, are precipitated during manufacturing, and are therefore an inherent part of the microstructure and not added externally as in conventional composite powders. The hard phases remain uniformly distributed during shipping, spraying and fusing to ensure consistent performance throughout the coating. They are an intimate part of the matrix and will not erode prematurely. Their fine size (5-10 microns) contributes to better finishing characteristics. The hard phases, along with the high-hardness Ni-Cr-B matrix, resist extreme abrasion and corrosion.

TYPICAL USES

Colmonoy 88 has proved successful in increasing the service life of glass mould plungers, where the alloy withstands wear from hot (1800°F), extremely abrasive, molten silica. Other applications include pump plungers and sleeves, valve seats, thermowells, centrifuges, plastics processing screws and barrels, wire drawing capstans, catalytic cracker components.

Photomicrograph (160X) of Colmonoy 88 shows the exclusive, finely dispersed bi- and tri-metallic hard phases distributed in the hard Ni-Cr-B matrix.

G-65 Dry Sand Abrasion Test

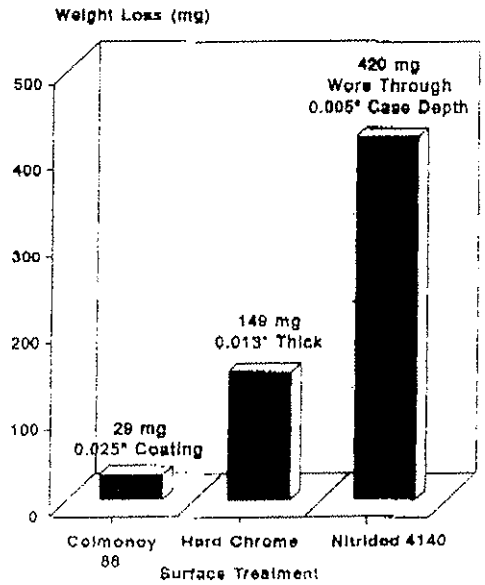

The chart shows the results of basic abrasion tests (ASTM-G65) comparing the wear resistance of Colmonoy 88 to typical hard coatings: ion nitriding and hard chromium plating. Colmonoy 88 is superior to the other coatings by a significant margin.

*U.S. Patent No. 5,141,571

TECHNICAL DATA BULLETIN

MATERIAL: Tungsten Carbide-Cobalt

DESCRIPTION: A dense, extremely smooth as-sprayed coating which generally does not require finishing and is highly resistant to fretting at low temperatures.

MATERIAL ANALYSIS:

1.	CHEMICAL COMPOSITION:	83% W 12% Co 4% C 1% Fe
2.	COATING DENSITY (G/CC):	13.6
3.	TENSILE BOND STRENGTH (PSI):	6,500
4.	TYPICAL MACROHARDNESS:	Rc 53
5.	TYPICAL MICROHARDNESS:	780 DPH
6.	COATING TEXTURE (AS SPRAYED):	250 micro aa
7.	COATING FINISH (GROUND):	7-8 micro aa
8.	COATING FINISH (LAPPED):	2.5-3.5 micro aa
9.	POROSITY (VOLUME %):	Less than 2
10.	SERVICE TEMPERATURE (LIMIT):	500 degrees F
11.	APPLICATION METHOD:	Plasma Spray

FSC 2071VF

TECHNICAL DATA BULLETIN

MATERIAL: Tungsten Carbide/Cobalt

DESCRIPTION: A virtually 100% dense, highly wear resistant coating, characterized by a very smooth, as sprayed surface. Hardnesses far exceed those previously obtained by conventional plasma spray methods. Very high resistance to wear by fretting and abrasion are demonstrated by this coating.

MATERIAL ANALYSIS:

1.	TENSILE BOND STRENGTH (PSI):	12,000
2.	POROSITY (VOLUME %):	Less than 1
3.	TYPICAL MACROHARDNESS:	Rc 70-72
4.	TYPICAL MICROHARDNESS:	1075-1245 DPH
5.	COATING TEXTURE (AS SPRAYED):	100-150 micro aa
6.	COATING FINISH (GROUND):	6-10 micro aa
7.	COATING FINISH (LAPPED):	1-2 micro aa
8.	SERVICE TEMPERATURE (LIMIT):	1000 degrees F
9.	APPLICATION METHOD:	HVOF Spray

FSC 22003

Waukesha Foundry, Inc.

CORROSION-RESISTANT, ANTI-GALLING WAUKESHA ALLOYS NICKEL BASE

Prevent Galling, Seizing In Metal-to-Metal Contact Where Lubrication is Restricted

No Galling

Galling

Microphotography shows effect of galling on structure of metal sample.

In machinery or equipment with moving parts, the action of one metal chafing or sliding against another metal without lubrication is likely to cause galling or seizing. Waukesha Foundry has developed several corrosion-resistant nickel-base alloys that work in contact with stainless steel, Inconel, Monel, chromium plate and many other metals without galling or seizing. These unique anti-galling alloys are used frequently in applications where daily cleaning or sterilization are required and where, as in pharmaceutical, food processing, and certain manufacturing operations, the use of lubricants is prohibited.

Such conditions as temperature variations, bearing load, mating materials, the type of product contacting the casting, and operating speed ordinarily determine which anti-galling alloy to use. Waukesha Foundry also conducts extensive tests on the corrosive effect of food products and chemicals on high alloy materials. Do not hesitate to consult with our metallurgists for specific recommendations.

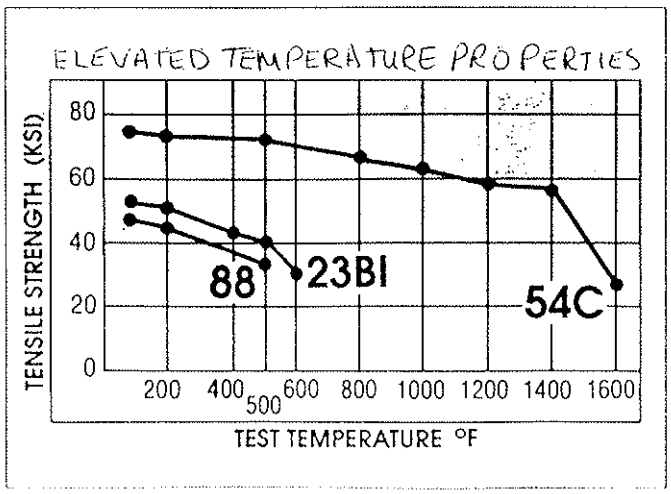

Please note that these anti-galling alloys cannot be hardened,or welded. They are used exclusively in the as-cast condition.

A Family of Anti-Galling Alloys

Not just one alloy, but a family of alloys provides superior resistance to galling or seizing in applications where metal-to-metal contact occurs without an additional lubricating element. Waukesha Foundry's nickel-based 23BI, 54C and 88 alloys are all anti-galling, but each has distinct differences, making proper selection imperative.

88 Alloy – Known as "the metal that mates", the 88 alloy is the workhorse of the anti-galling family. It offers good strength, superior corrosion resistance, and can be used at temperatures up to 500°F. It is ideal for use wherever close clearance with moving parts is required.

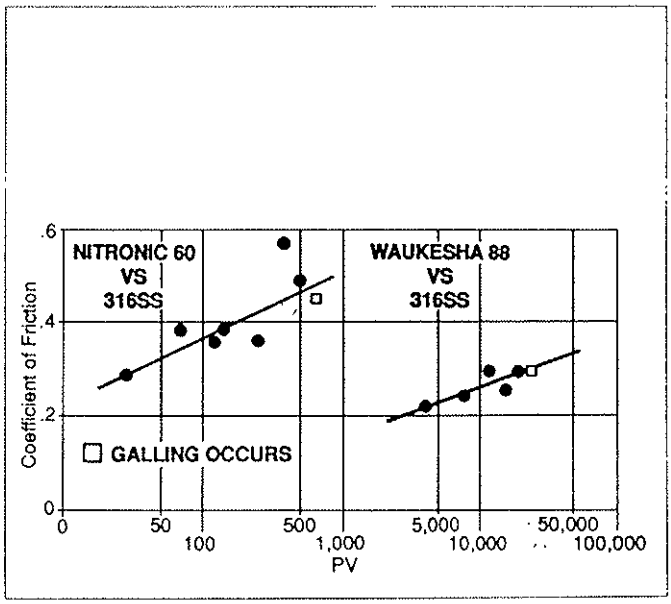

23BI Alloy – Offers somewhat similar strength, good corrosion resistance and can be used up to 500°F. The 23BI alloy has good hardness characteristics, is readily castable and machinable. The alloy was specifically developed for use in dairy equipment and other food processing machinery where sanitation is essential.

54C Alloy – This, our highest strength alloy, has good corrosion resistance and can be used at temperatures up to 1,600°F. The alloy's excellent self-lubricating qualities, due to the inclusion of silver, make it ideal for valve guides in aircraft engines that must operate in extremely hot temperatures. The 54C alloy affords exceptional wear resistance.

EXHIBIT Q

Here's The Stainless Steel That
Wears Up To Three Times Better
Than High Cobalt Alloys But Costs Much Less!

ARMCO NITRONIC 60

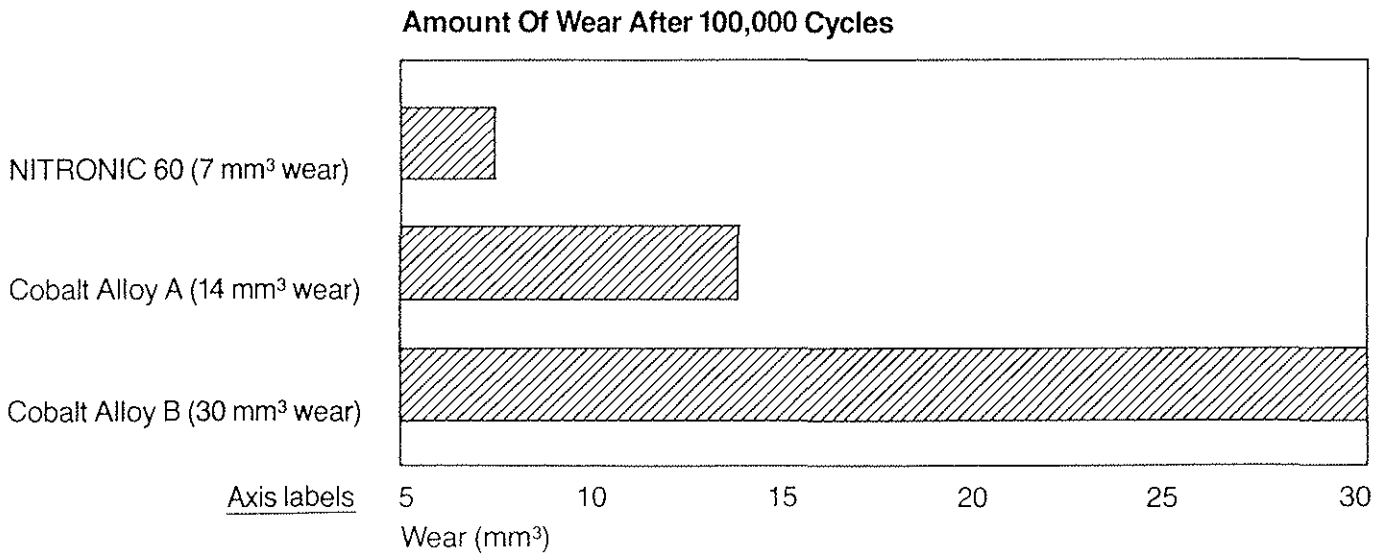

EXHIBIT R

FERRALIUM® alloy 255

A New High-Strength Super Stainless Steel

Outstanding Corrosion Resistance
FERRALIUM alloy 255 is a patented, ferritic-austenitic stainless steel containing approximately 26% chromium, 5% nickel, 2% copper and 3% molybdenum. It combines high mechanical strength, ductility and hardness with resistance to corrosion and erosion.

The corrosion resistance of FERRALIUM alloy 255, under most conditions of service, is superior to that of the fully austenitic type 304 and 316 stainless steels. It has excellent resistance to sulfuric, phosphoric, nitric, and many other acids and salts.

Alloy 255 is highly resistant to acetic, formic and other organic acids and compounds. It is particularly suitable for the higher concentrations and temperatures where pitting and preferential corrosion are common causes of failure with most conventional austenitic stainless steels in the presence of chlorides and other impurities.

Like the austenitic stainless steels, FERRALIUM alloy 255 is not generally suitable for handling hydrochloric acid and other severely reducing acids and chemicals.

Resists Chloride Stress-Corrosion Cracking
Alloy 255 has improved resistance to stress-corrosion cracking, crevice corrosion and pitting when compared to austenitic stainless steels such as types 304 and 316. It is highly-resistant to stress-corrosion cracking in sodium chloride, sea water and many other salt solutions.

Physical Metallurgy
FERRALIUM alloy 255 is a duplex alloy with approximately equal portions of austenite and ferrite matrix phases. The alloy has primary $M_{23}C_6$ carbides in the annealed condition and forms secondary $M_{23}C_6$ carbides when exposed in the 1000-2000 deg. F (538-1093 deg. C) temperature range. Aging or use of this alloy in the 1400-1600 deg. F (760-871 deg. C) range should be avoided since an abundance of an Fe-Cr intermetallic (sigma) phase is produced. Although the precipitation of the sigma phase does not have a significant effect on the corrosion resistance of alloy 255 in oxidizing environments represented by nitric acid and ferric sulfate tests, the ductility of the alloy is drastically reduced.

Heat Treatment
Optimum properties are achieved by a simple heat- treatment which does not involve martensitic transformation. FERRALIUM alloy 255 is solution heat treated at 2050 deg. F (1120 deg. C) and rapid cooled. The alloy can be hardened by a subsequent heat-treatment at 950 deg. F (510 deg. C) for 4 hours, air cool.

Availability
FERRALIUM alloy 255 is available from High Technology Materials Division in the form of sheet, strip, plate, bar, billet, welding electrodes, wire, tubing and pipe.

Applications
Because of its resistance to chloride pitting and stress-

FERRALIUM is a registered trademark of Langley Alloys Limited

EXHIBIT S

Injection Loading of PBX into Various Munitions and Components

Kirk Newman, Steve Jones, Suzanne Williamson, Neal Cowan, and Jim Gusack
Energetic Materials Research and Technology Department
Naval Surface Warfare Center
Indian Head Division
Yorktown, VA 23691-0160

The success of smart weapon systems has generated a need to process highly filled plastic-bonded explosives (PBX) through narrow flow channels. From a chemical engineering point of view, we need to understand the momentum transport and mass transfer phenomena of these viscous suspensions so that flow instabilities are minimized and adequate product quality is provided. These PBX materials are viscous suspensions containing multi-modal particle size distributions that are often at or very close to the theoretical maximum packing fraction. As a result, problems such as particle jamming, binder filtering, and shear induced particle migration can occur in some processes. Injection loading of highly filled PBX into various submunitions for smart weapons, or into weapon system components, or even into lengths of tubing for manufacturing detonation cords, requires an interdisciplinary approach. We present different engineering methods used to process PBX materials for all of these applications. We discuss some processing problems that can occur, and how they can result in product rejects. We then show how we utilize science based models for process design improvements and process control enhancements that can help to prevent processing conditions that create product rejects. We conclude that explosive selection for DOD applications must consider the rheology of the PBX, the geometry of the process, and the anticipated production rate of the product. Otherwise, producibility of a successful weapon system may be in jeopardy.

NSWC INDIAN HEAD DIVISION

INJECTION LOADING OF HIGHLY FILLED PBX MATERIALS

Kirk Newman, Steven Jones, James Gusack, and Suzanne Williamson

Program Acknowledgements IMAD/HE, SERDP/CAME, JSOW, TOMAHAWK, Surf Zone ATD, DOS, and TIP

Outline of Talk

[A] Introduction

[B] Injection loading of Submunitions

[C] Injection loading of Explosive Rope

[D] Injection loading of Initiation Systems

[E] Conclusions

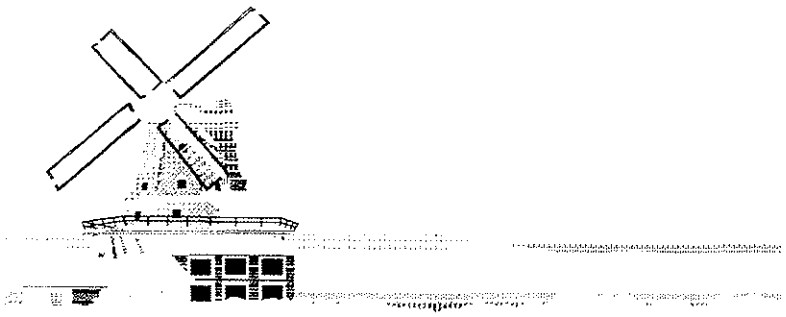

SMART PROCESSING OF SMART WEAPONS

(1) Pollution prevention through reduced reject rates made possible by process monitoring and control

(2) Process control using PC/PLC architechture

(3) Processing parameter selection is dependent upon good process design, and selection of robust materials

(4) Process design must consider material rheology and hardware constraints

(5) PBX formulation development and selection must consider application

PROCESS CONTROL

TO SIGNIFICANTLY REDUCE THE LIFE CYCLE POLLUTION BURDENS FOR ENERGETIC MATERIALS

CURRENT PROCESS CONTROL PARADIGM ("DUMB" Process Control):

[a] Expect no problems.
[b] Depend upon vendors, standardized specifications, and processing procedures.
[c] Not prepared for problems when they occur. Problems are disposed as wastes.
[d] Result is high reject rate and wasteful unit operations.

NEW PROCESS CONTROL PARADIGM ("SMART" Process Control):

[a] Murphy's Law applies. Problems will occur.
[b] Depend upon adaptive control that recognizes problems as they occur.
[c] Link anticipated disturbances to manipulative variables in the control strategy.
[d] Preemptively compensate for disturbances before material exits unit operation(s).
[e] Problem recognition invokes processing changes that prevent waste generation.
[f] Reduced pollution and "zero defects" munitions.

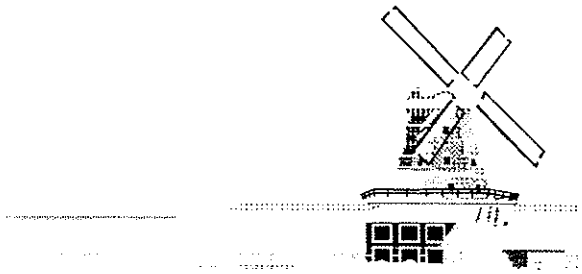

Naval Surface Warfare Center
INDIAN HEAD DIVISION

INTRODUCTION

[1] Smart weapons, distributed explosive nets, and Special Forces requirements necessitate loading small diameter munition components.

[2] Lethality requirements and Navy Insensitive Munitions (IM) goals necessitate using highly filled PBX materials having elastomeric binders.

[3] Better science and engineering data on PBX materials is required to describe flow behavior in process geometries.

[4] Automated manufacturing techniques, such as injection loading, must be used to perform real-time process control to produce zero defects.

INSENSITIVE MUNITIONS OFFICE
N★A★V★Y

DEPARTMENT OF THE NAVY
SEA SYSTEMS COMMAND

Naval Surface Warfare Center
INDIAN HEAD DIVISION

EVOLUTION OF PROCESSING EQUIPMENT

MELT-CAST LOADER AT KAAP

"Explosive Injection Molding Unit," MM&T Project 5824312, is designed to pump melt cast explosives at about 0 - 50 psig from a heated reservoir through eight horizontal injectors. Capacity is about 500 lbs/hr.

DAY & ZIMMERMANN, INC.
"A Leader in Munitions Production Technology"

DEAERATOR LOADER AT LLNL

"50 lb De-aeration Machine," Dwg 82-111206-00, is designed to degass and inject high viscosity explosive at about 100 - 300 psig and ambient conditions through one horizontal injector. Capacity is about 50 lbs/hr.

University of California
Lawrence Livermore National Laboratory

INJECTION LOADER AT NSWC

"Apparatus for Injection Molding High-Viscosity Materials," U.S. Patent 5,387,095, is designed to simultaneously degass and inject viscous plastic bonded explosives at about 100 - 200 psig and between 0 - 120 °C through one vertical injector. Capacity is about 200 lbs/hr.

INSENSITIVE MUNITIONS OFFICE
N★A★V★Y

Naval Surface Warfare Center
INDIAN HEAD DIVISION

EVOLUTION OF PROCESSING EQUIPMENT

MELT-CAST LOADER AT KAAP

- High volume, large capacity
- Eight simultaneous injectors
- No vacuum loading capability, only adequate for low viscosity explosives, like Cyclotol
- Multiple corner turns indicate potential for momentum and mass transfer problems
- Clean-up for anything but melt cast explosives is difficult
- Awarded a $14.5K contract in FY 87 to assess processing capability, resulting in failure to load PBX

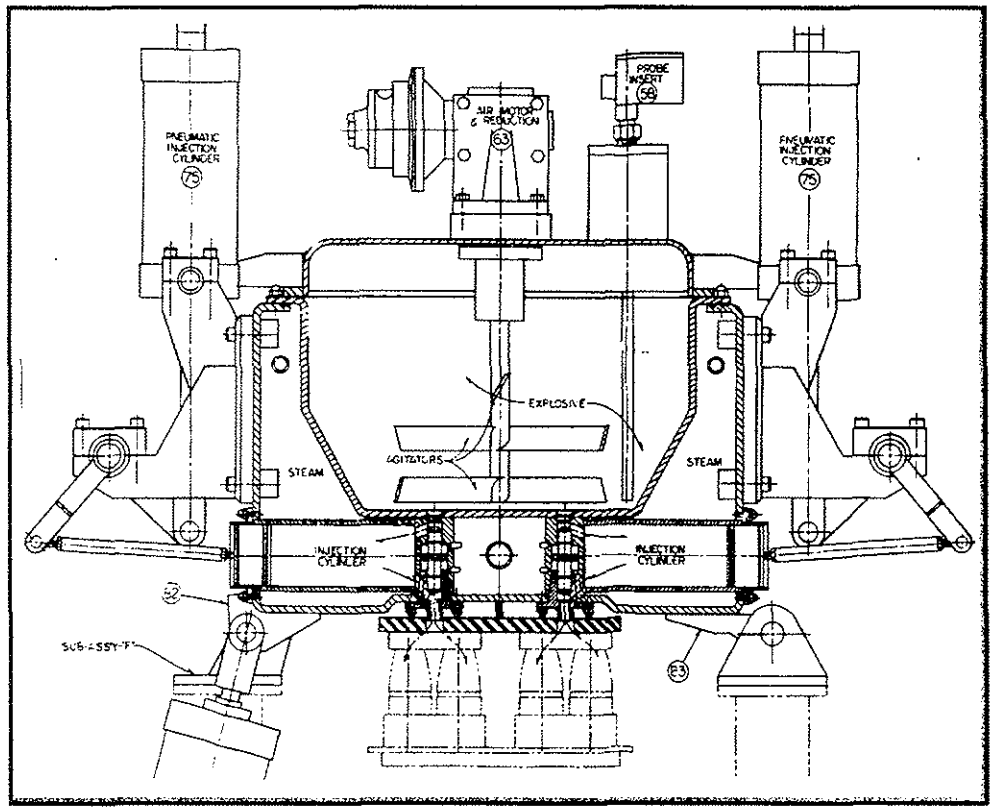

DAY & ZIMMERMANN, INC.

"A Leader in Munitions Production Technology"

Naval Surface Warfare Center
INDIAN HEAD DIVISION

EVOLUTION OF PROCESSING EQUIPMENT

DEAERATOR LOADER AT LLNL

- Low volume, R&D apparatus
- Single port injector
- Vacuum system is good for loading high viscosity extrudable explosives or paste explosives, such as ECX or PCX
- Severe corner turns indicate potential for momentum and mass transfer problems
- Cleanup operations are awkward and time consuming
- Witnessed loading of hemispherical charges in FY 87, resulting in decision to design something different for plastic bonded explosives (PBX)

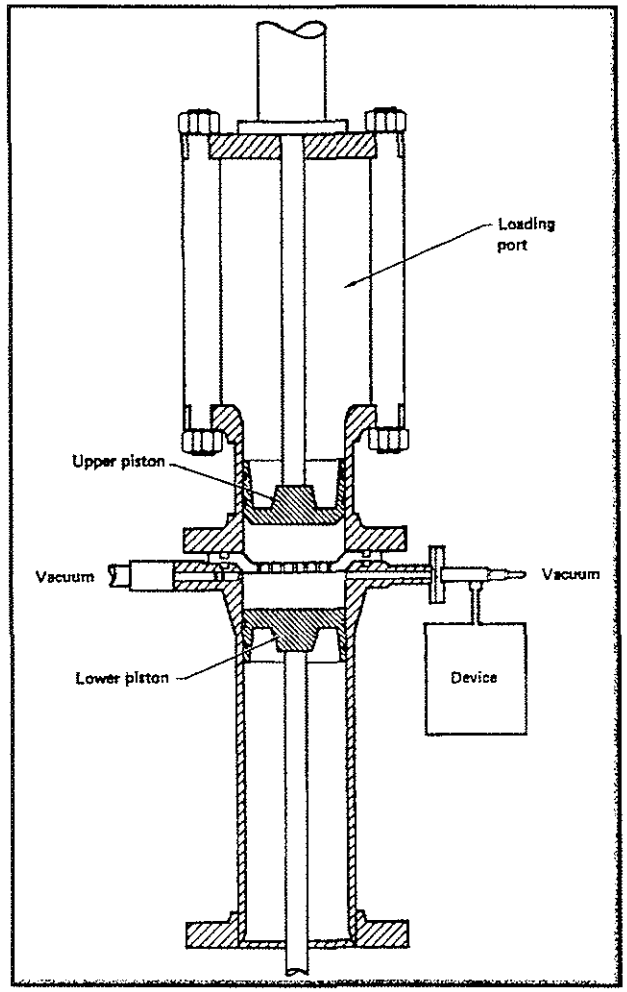

University of California
Lawrence Livermore National Laboratory

Naval Surface Warfare Center
INDIAN HEAD DIVISION

EVOLUTION OF PROCESSING EQUIPMENT

INJECTION LOADER AT NSWC

- Moderate volume, pilot plant apparatus
- Single port injector
- Vacuum system is good for loading moderate and high viscosity plastic bonded explosives (PBX)
- No corner turns, the machine rotates to align degassed PBX for injecting straight into evacuated submunitions, significantly reducing the potential for momentum and mass transfer problems
- Cleanup operations are relatively easy, and are not time consuming
- Demonstrated injection loading of several PBXs in various geometries and submunitions

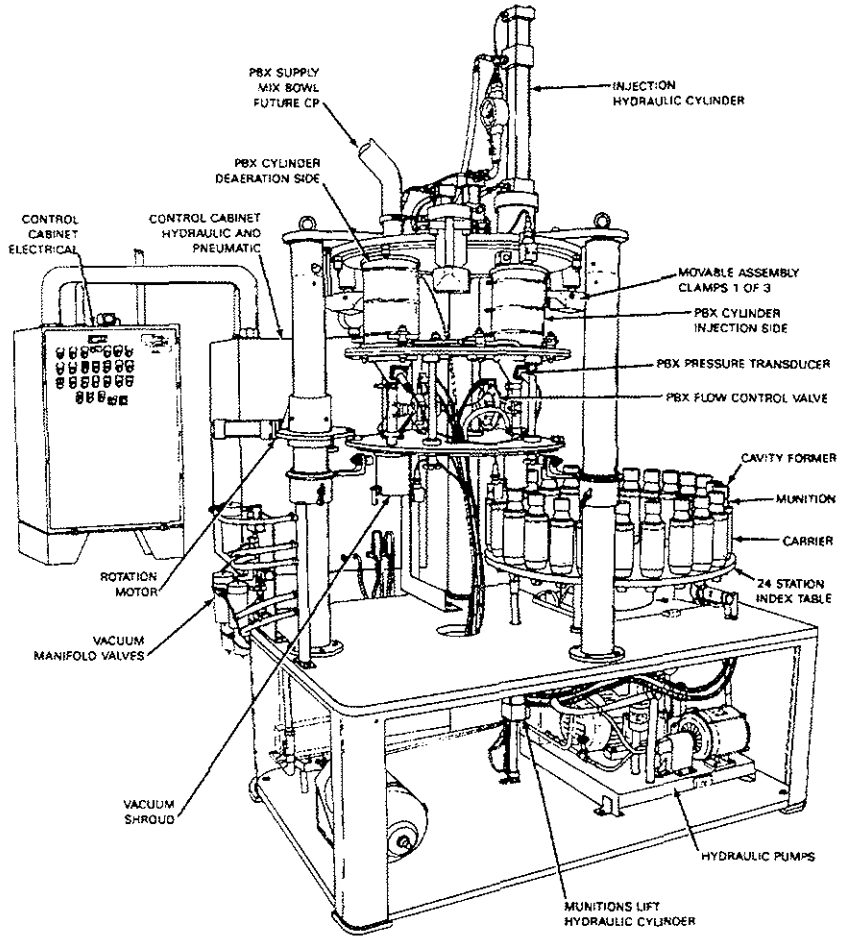

NSWC Injection Loading Apparatus at Yorktown

Naval Surface Warfare Center
INDIAN HEAD DIVISION

DEVELOPMENT OF COMPUTATIONAL TOOLS

LEVERAGING 10 YEAR ONR INVESTMENT IN COMPUTATIONAL FLUID MECHANICS & RHEOLOGY

From 1987 - 1997 ONR (Code 333, R. S. Miller) has invested $800 K - $1.0 M per year in computational fluid mechanics and rheology research at academic institutions, national labs, and Government activities to understand transport phenomena important to the development and processing of energetic materials.

Ballistic Missile Defense Organization (BMDO)

UMASS	(H. Winter)
MIT	(R. Armstrong, R. Brown)
Cal Tech	(J. Brady)
SIT	(D. Kalyon)
LANL	(A. Graham)
SNL	(L. Mondy)
NAWC	(T. Stephens)
Lockheed	(A. Chow, S. Sinton)

Strategic Environmental R&D Program / Clean, Agile Manufacturing of Energetics (SERDP/CAME)

MIT	(R. Armstrong)
Cal Tech	(J. Brady)
SIT	(D. Kalyon)
LANL	(A. Graham, J. Parkinson)
SNL	(L. Mondy)
NAWC	(T. Stephens)
NSWC	(M. Gallant, K. Newman)
LMMS	(A. Chow, S. Sinton)

Proposed Explosive Stand-off Minefield Breecher (ESMB)

LANL	(A. Graham, J. Parkinson)
SNL	(L. Mondy)
NAWC	(T. Stephens)
NSWC	(K. Newman)
LMMS	(A. Chow, S. Sinton)

Technology transition from R&D to production

COMPUTATIONAL MODELLING AND PROCESS DESIGN AT LANL

LANL uses theoretical and computational resources, as well as MIR facilities in NM and CA to:

[1] develop new "microstructual" theories for modelling flow behavior of highly filled suspensions

[2] develop experimental methods for validation of "microstructual" theories and appropriate constitutive equations

[3] develop numerical methods for solving flow fields using "microstructual" models

The Lovelace Institutes
Albuquerque, NM

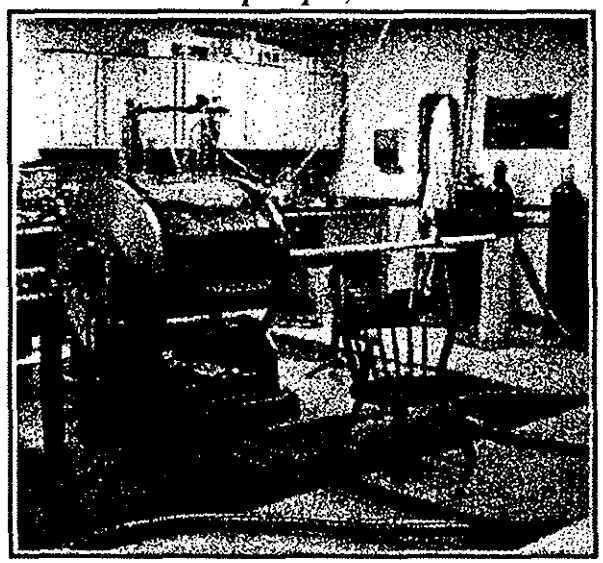

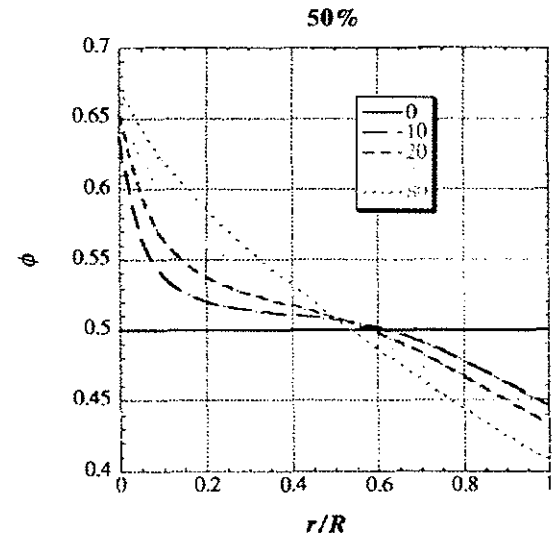

$$\frac{D\phi}{Dt} = a^2 K_c \nabla \cdot \left(\phi^2 \nabla \dot{\gamma} + \phi \dot{\gamma} \nabla \phi \right) + a^2 K_\eta \nabla \cdot \left(\phi^2 \dot{\gamma} \frac{1}{\eta} \frac{\partial \eta}{\partial \phi} \nabla \phi \right)$$

Phillips Diffusive Flux Model developed by MIT and LANL, Phys. Fluids, 4(30), Jan 1992

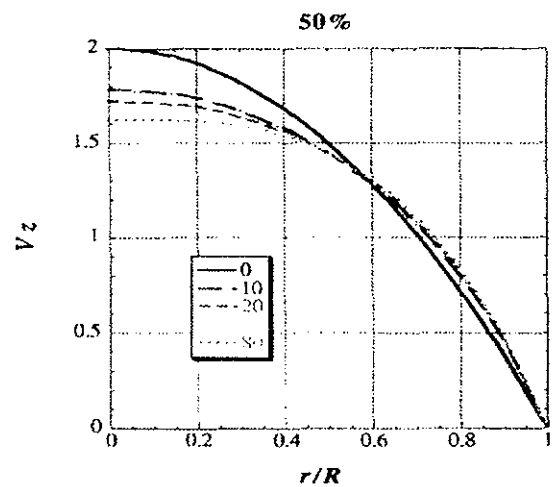

DEVELOPMENT OF COMPUTATIONAL TOOLS

PREDICTIVE AND EXPERIMENTAL RESOURCES AT SNL

The SNL experiments and predictive tools verify that initially well mixed suspensions demix during piston driven flow through a contraction. The particles migrate to low shear-rate regions of the flow field.

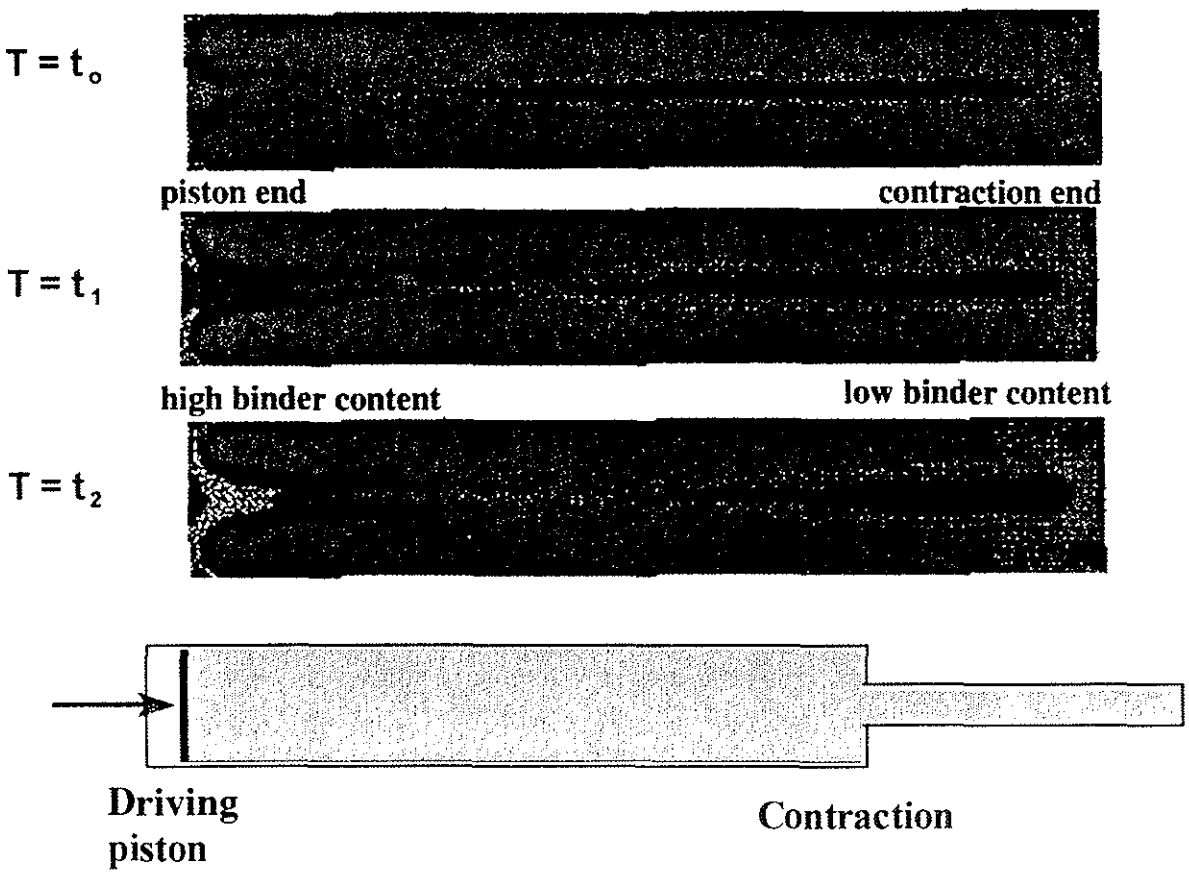

SNL uses MIR facilities at The Lovelace Institutes in Albuquerque to:

[1] image the phenomena of demixing that can occur during processing of filled suspensions

[2] examine piston-driven flow of suspensions through contraction and expansion geometries

[3] validate predictions of constitutive equations for real suspensions, such as inert Navy PBX

[4] enhance their own fluid mechanics codes, such as NACHOS and GOMA

Injection Loading of Submunitions

Momentum transport of PBXN-107 into submunitions such as the M73 Grenade and the BLU-97 is a difficult task. Traditional casting from a vertical planetary mixer yields excessive voids, while volumetric loaders designed in the food industry have yielded other problems.

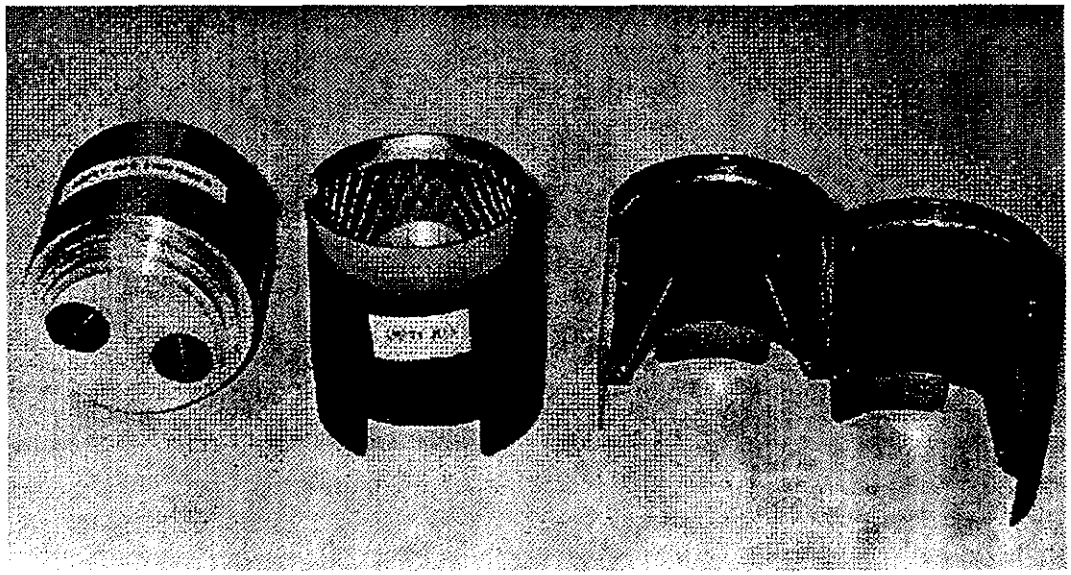

M73 Grenade loaded with PBXN-107 inert simulant

Cross-section of a PBXN-107 loaded BLU-97 bomblet

SERDP/CAME PROCESSING TECHNOLOGY ASSESSMENT

INJECTION LOADING OF BLU-97 SUBMUNITIONS

- *Joint Stand-Off Weapon (JSOW) has loaded 2,448 BLU-97 submunitions with PBXN-107 having an average reject rate of about 24% using a volumetric loader. The problems are due to particle jamming and binder filtration, as well as the geometry of the volumetric loader.*
- *TOMAHAWK Combined Effects Munition (CEM) is also planning to procure PBXN-107 loaded BLU-97 submunitions.*
- *Selection of an injection loading process with model-based and rule-based process control can resolve these processing problems. Resources include NSWC, NAWC, LANL, SNL, MIT, SIT, and Cal Tech.*

AIR DELIVERED WEAPONS

BLU-97 A/B
Combined Effects Bomblet

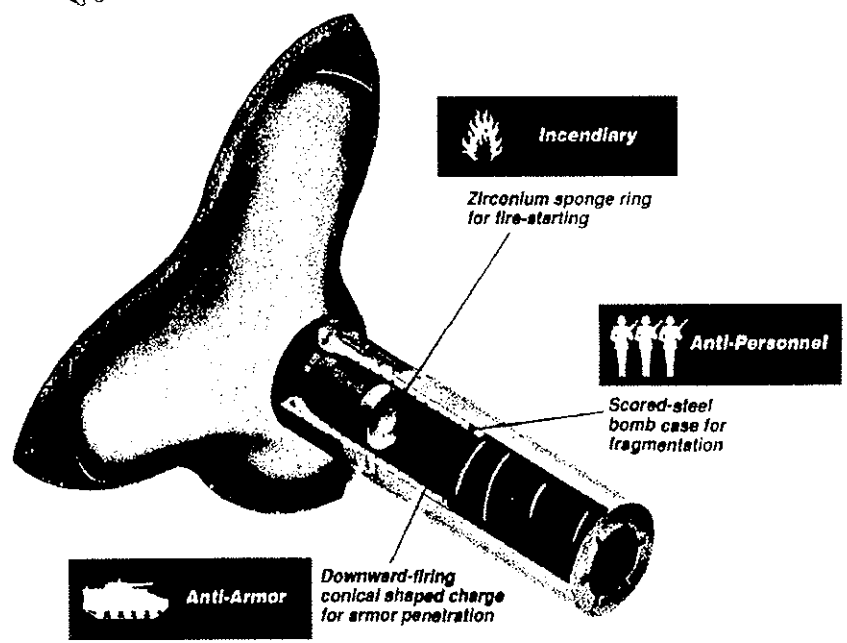

LOADING SMART WEAPON COMPONENTS WITH CASTABLE PBX THROUGH NARROW FLOW CHANNELS CAUSES QUALITY CONTROL PROBLEMS AND HIGH REJECT RATES

Joint Stand-Off Weapon (JSOW) Combined Effects Warhead has BLU-97 submunitions loaded with PBXN-107. The original end item requirements could not be satisfied using a volumetric loader having several 90-degree turns.

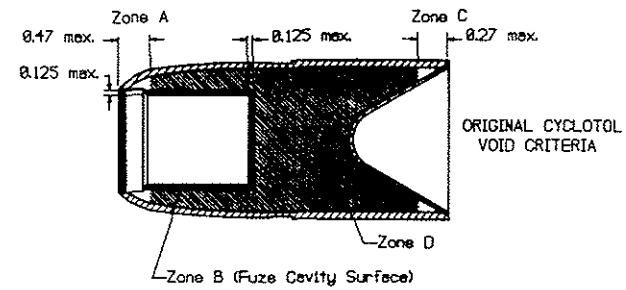

VOIDS	⇨	Due to inadequate control of binder viscosity
FILL HEIGHT	⇨	Due to inadequate control of momentum transport
GRADIENTS	⇨	Due to inadequate control of mass transfer

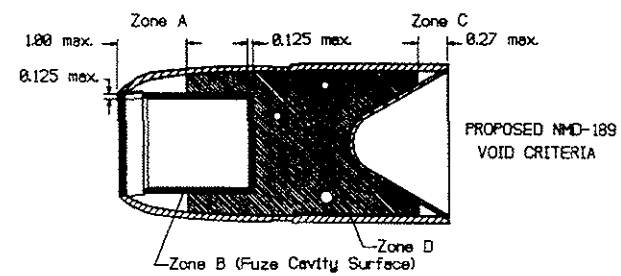

(All dimensions are in inches)

PROCUREMENT OFFICE ISSUES:

Less explosive in bomblet = reduced performance

Excessive pollution burden = estimated LCI indicates L/A/P wastes account for 30% of life cycle pollution

Explosive selection = PBXN-107 has a quad-modal RDX particle size distribution that contains 900 micron, Class 4 RDX.

Pollution Prevention

PROCESS CONTROL: FOR MOLD FILLING

TO SIGNIFICANTLY REDUCE THE LIFE CYCLE POLLUTION BURDENS FOR ENERGETIC MATERIALS

[1] Use apparatus described by U.S. Patent 5,387,095 to reduce momentum transport problems by eliminating all 90° corner turns.

[2] Eliminate fill height problem using NSWC BLU-97 endformer design.

[3] Use smart process control strategy based PLC/PC architecture.

[4] Use Arrhenius models for chemical reaction kinetics and viscosity dependency to process PBXN-107 at very cold temperature (5±5°C).

$$\eta\ (T) = A \exp\ (E/RT)$$

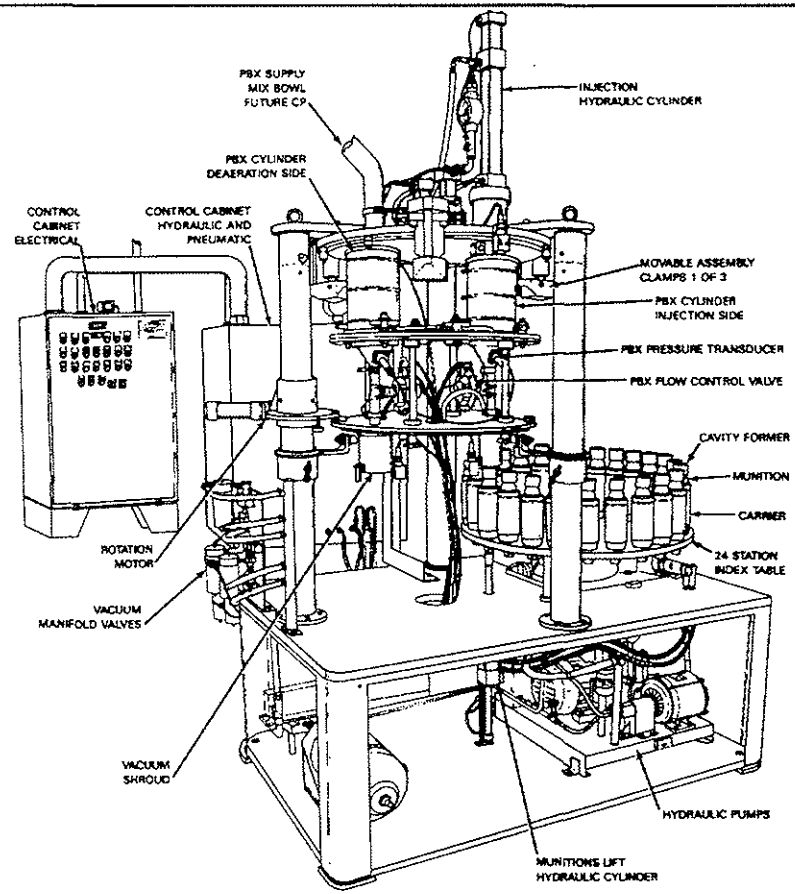

NSWC Injection Loading Apparatus

NSWC INDIAN HEAD Calculation Methodology for Shear Behavior of PBX's in the Code 930 Injection Loader Apparatus

The injection cylinder has an inside diameter of 4 inches and was nominally 12 inches from top to bottom. The nomenclature for spreadsheet data is the top of the cylinder is defined as 0 inch, while the bottom was 12 inches. For simplicity, we used to define R = 2.0 inches, L = 8.5 inches, and r = 0.25 inch. Now the injection loader is 18 inches from top to bottom and the contraction radius has been enlarged to r = 0.5 inch.

Capillary tester for volumetric flow rate

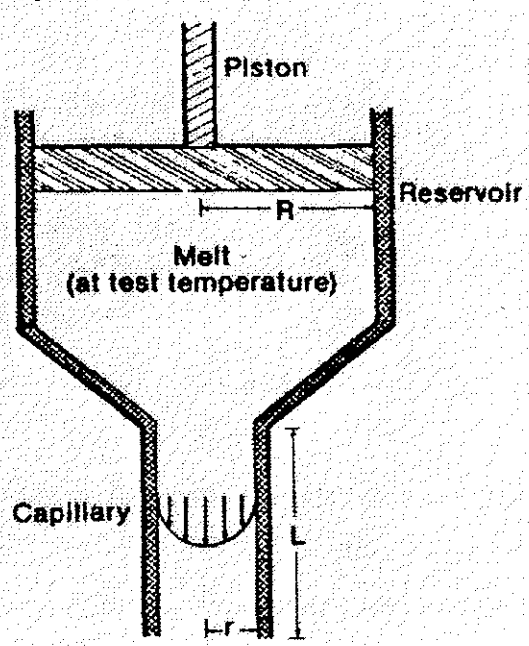

Calculating viscosity from flow-rate tests

$Q = \pi R^2 V$ (Eq. 1)

Q = Volumetric flow rate, in.^{3}/sec

R = Piston radius, in.

V = Piston velocity, in./sec

$\gamma a = \frac{4Q}{\pi r^3}$ (Eq. 2)

γa = Apparent shear rate, sec^{-1}

Q = Volumetric flow rate, in.^{3}/sec

r = Capillary radius, in.

$\tau = \frac{P \cdot r}{2L}$ (Eq. 3)

τ = Shear stress, psi

P = Pressure applied, psi

r = Capillary radius, in.

L = Capillary length, in.

$\mu = \frac{\tau}{\gamma}$ (Eq. 4)

μ = Viscosity, lb-sec/in.^{2}

τ = Shear stress, psi

γ = Apparent shear rate, sec^{-1}

PBXN-107 (loading BLU-97 submunitions)
Ram Displacement and Velocity vs Time

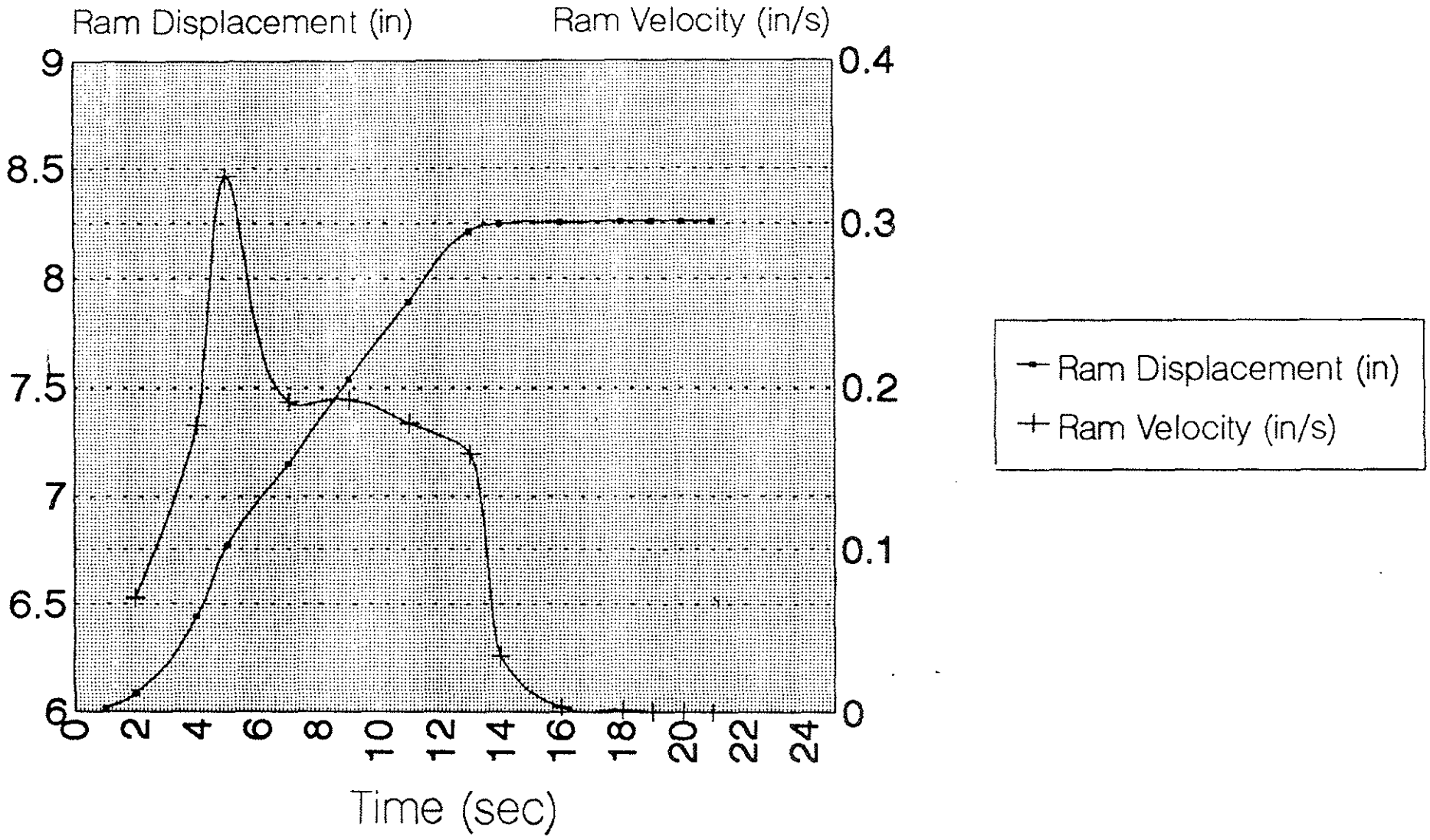

Injection Loading Run 1/22/93 (Increment #3)

PBXN-107 (loading BLU-97 submunitions)
Shear Rate and Shear Stress vs Time

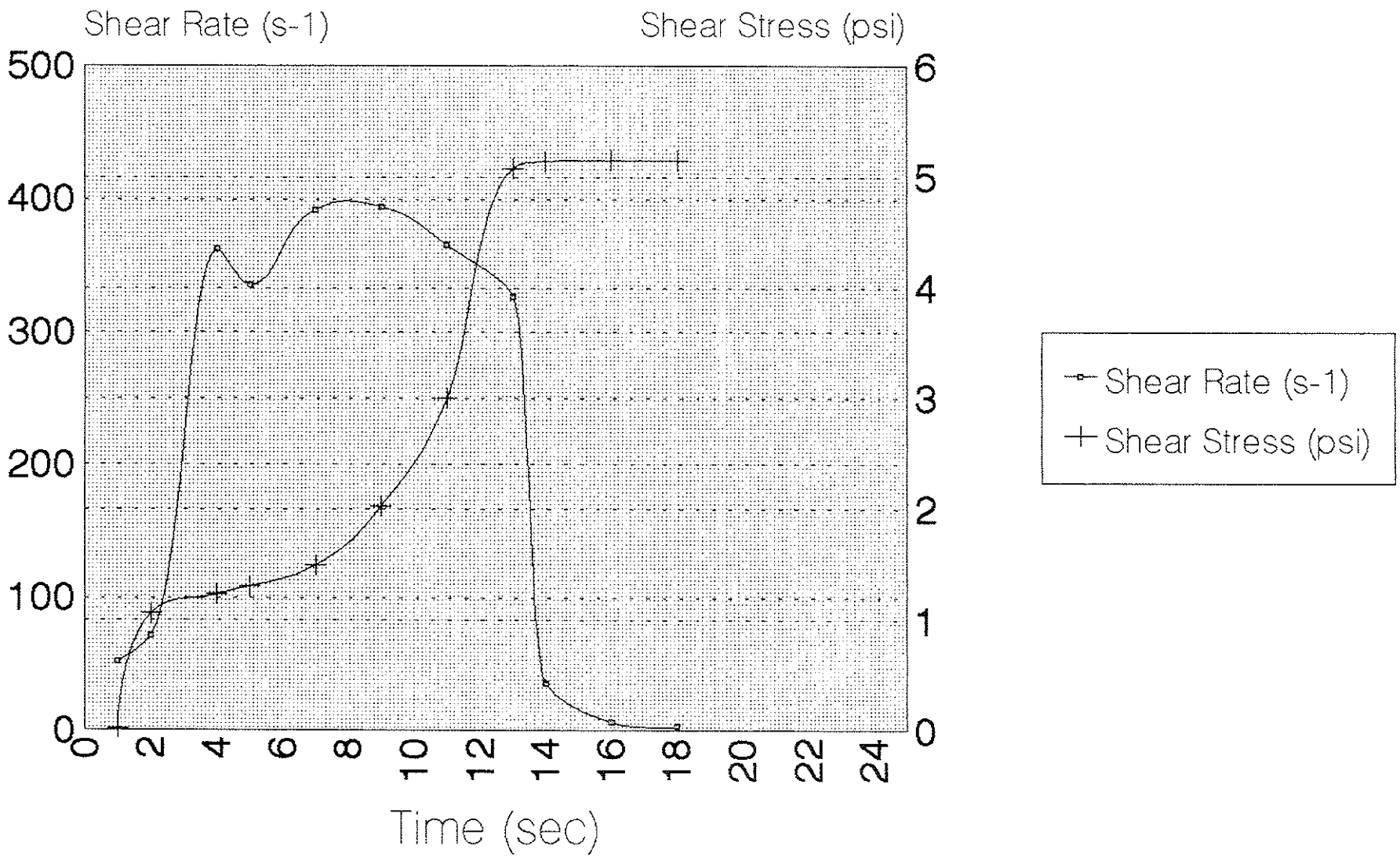

Injection Loading Run 1/22/93 (Increment #3)

PROCESS CONTROL: FOR MOLD FILLING

TO SIGNIFICANTLY REDUCE THE LIFE CYCLE POLLUTION BURDENS FOR ENERGETIC MATERIALS

NSWC has installed a gamma ray densitometer on the injection loader to demonstrate how "smart" process control can eliminate the voids observed during BLU-97 submunition loading with PBXN-107 via "dumb" process control.

This additional device provides another discrete input for the process control stategy to detect a disturbance early enough to take preemptive action of eliminating problems before they become waste.

"Dumb" Process Control

$Q = f(\Delta P)$

"Smart" Process Control

$Q = f(\Delta P, n, m)$

$\Delta Q = f(d(\rho V)/dt)$

Therefore NSWC is planning processing demonstrations to develop new processing data for reproducibly collapsing void structures, and will transition revised data profiles to LANL for neural net training.

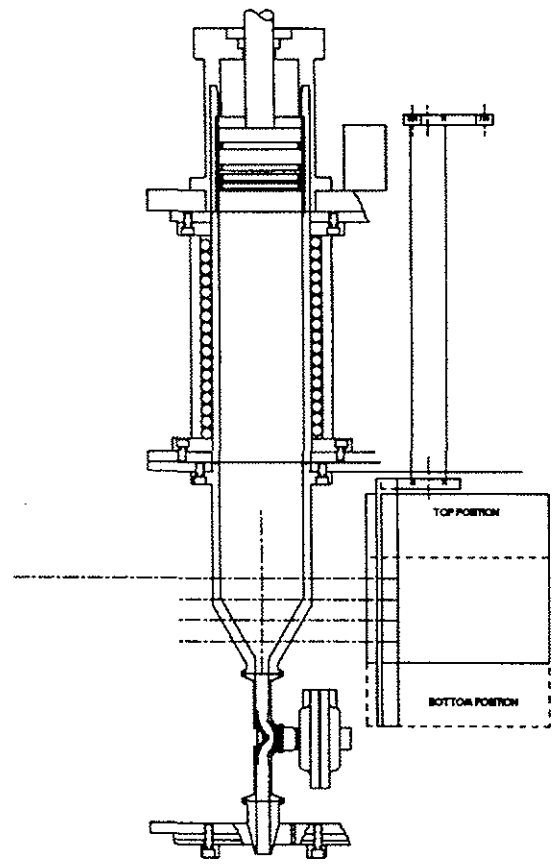

SERDP
Strategic Environmental Research and Development Program
Improving Mission Readiness Through Environmental Research

SERDP/CAME New processing techniques that reduce pollution

Pollution Prevention

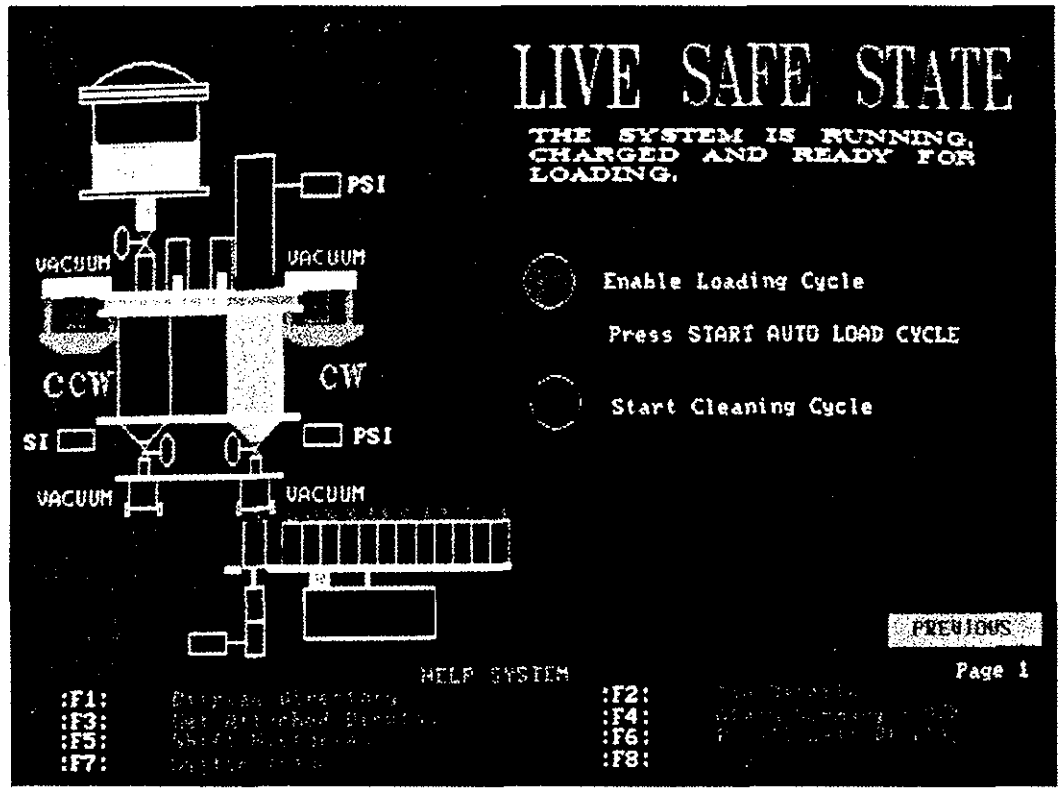

One of the process PC control screens for the injection loader at the NSWCIHD Code 930 facility showing simultaneous degassing and injeciton capability.

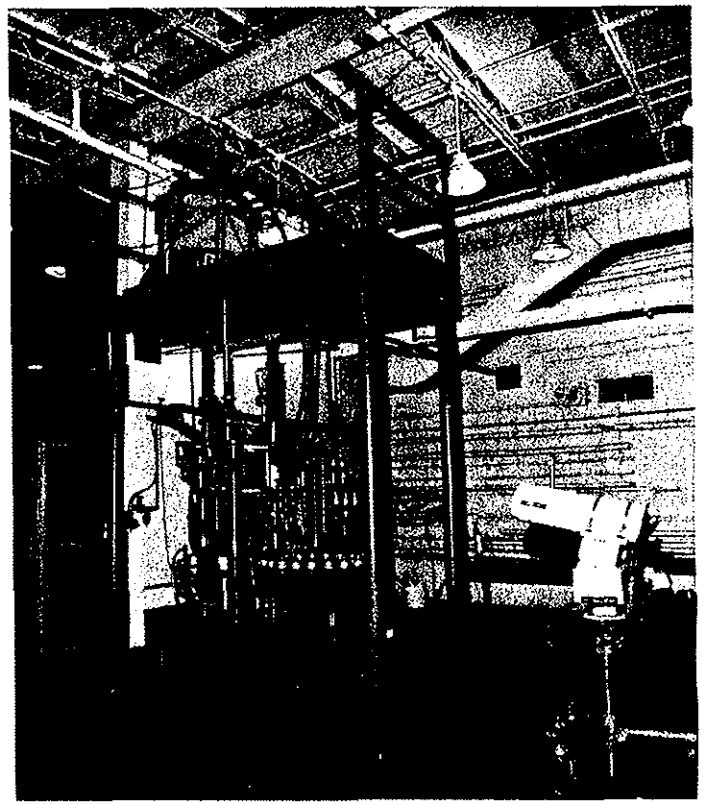

Actual injection loader apparatus with a 30-gallon vertical planetary mixer bowl on the mezzanine and BLU-97 submunitions on the lazy Susan index table.

We demonstrated a 100% improvement in the JSOW reject rate, and presented our results in FY 96 to the program office as well as the prime contractor.

NSWC
NAVAL SURFACE WARFARE CENTER
INDIAN HEAD DIVISION

Naval Surface Warfare Center
INDIAN HEAD DIVISION

DEMONSTRATION OF REDUCED REJECT RATES FOR JSOW

[1] Performed joint MIR experiments with NSWC to evaluate flow phenomena of inert PBXN-107 simulant, resulting in observation of some settling and shear induced particle migration in couette and pipe flow.

[2] Used NACHOS code, with MIT/LANL diffusive flux constitutive equation, to model piston driven flow through a contraction, resulting in shear at the ram and at the contraction. All the particle jamming is at the contraction.

[3] Used GOMA finite element code to predict free surface mold filling phenomena in BLU-97, resulting in minimum shear in the mold and very good agreement with NSWC density gradient analysis of sectioned BLU-97 submunitions.

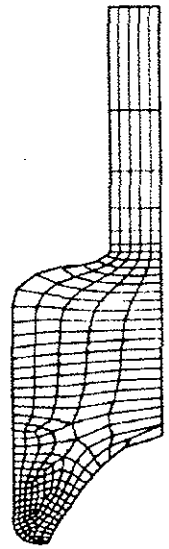

Mesh for GOMA code

Red is highly sheared fluid. Even though the shear rate is low in the BLU-97, the PBX entering it has been highly sheared.

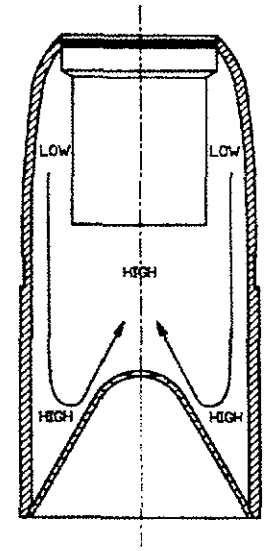

NSWC density analysis of sectioned BLU-97s loaded with PBXN-107 show RDX migration to region of least shear.

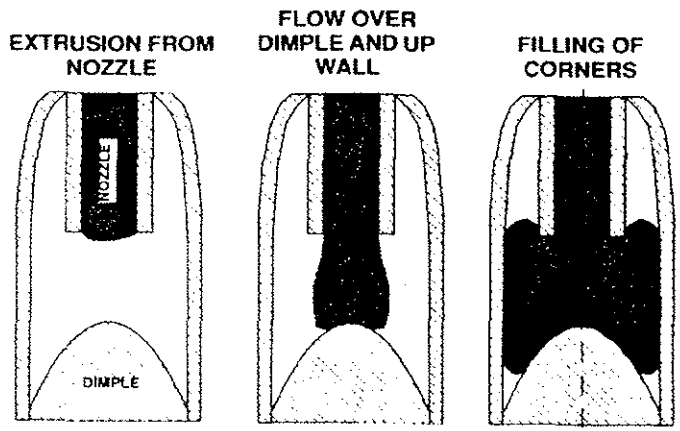

GOMA also properly predicts momentum transport problems. Filling of BLU-97 with PBX requires sufficient driving force to achieve required fill height

Sandia National Laboratories

Naval Surface Warfare Center
INDIAN HEAD DIVISION

DEMONSTRATION OF REDUCED REJECT RATES FOR JSOW

[1] Performed MIR experiments to evaluate when shear induced particle migration starts to occur in pipe flow, resulting in observation of shear induced particle migration at only 12 pipe diameters downstream of an in-line static mixer.

[2] Revised techniques for solving flow fields having short "entrance lengths," resulting in a recommendation to decrease the length of process plumbing and also decrease the L/D ratio of process geometry for large a/R scenarios.

[3] Used neural network code to fit NSWC injection loading data, resulting in the joint development of an adaptive process control system for injection loading PBXN-107 into BLU-97 that features a gamma ray densitometer.

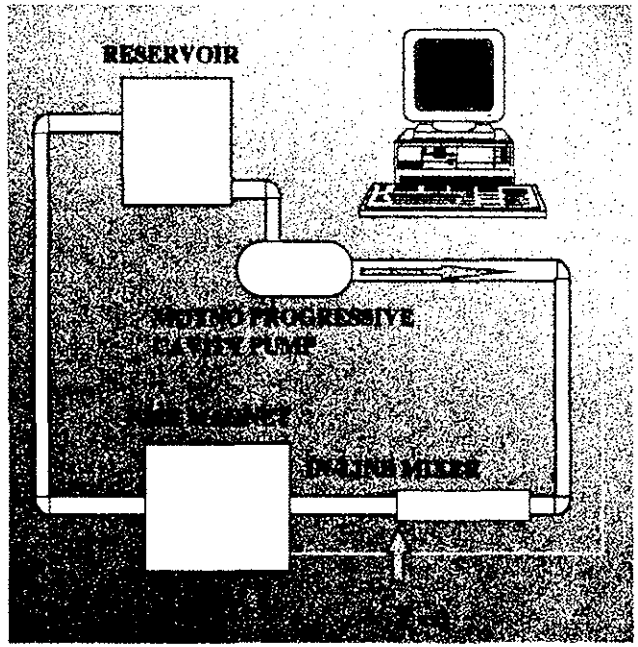

MIR experiment performed by LANL at The Lovelace Institutes used a 45% solids suspension at an average velocity of 20 cm/s.

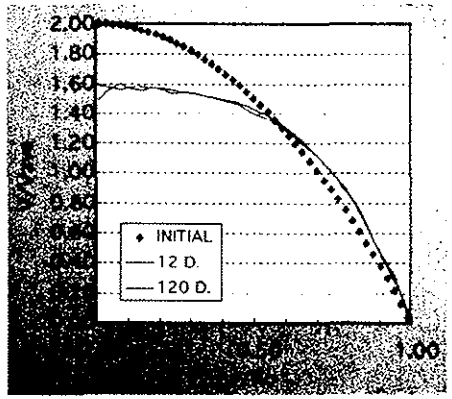

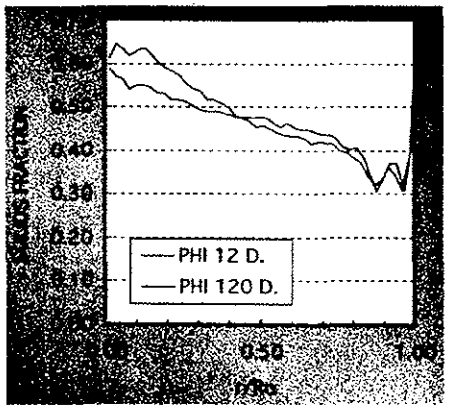

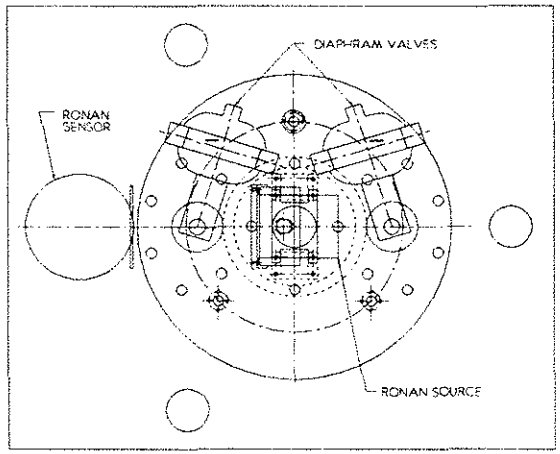

Cs 137 gamma ray densitometer can provide additional information about the response of PBX to piston driven flow. PBX appears to be compressable.

Los Alamos
NATIONAL LABORATORY
A US Department of Energy Laboratory

Naval Surface Warfare Center
INDIAN HEAD DIVISION

DEMONSTRATION OF REDUCED REJECT RATES FOR JSOW

[1] Performed MIR experiments in a vertical plane using the same contraction geometry of the NSWC injection loader, resulting in observation of the same shear rate and shear stress data NSWC reported for injection loading BLU-97 with PBXN-107 at constant applied pressure.

[2] Performed MIR experiments using new contraction geometry recommended by LANL and SNL, resulting in no apparent particle migration and substantially reduced shear rate.

LOCKHEED MARTIN

Lockheed Martin Missiles & Space
Advanced Technology Center

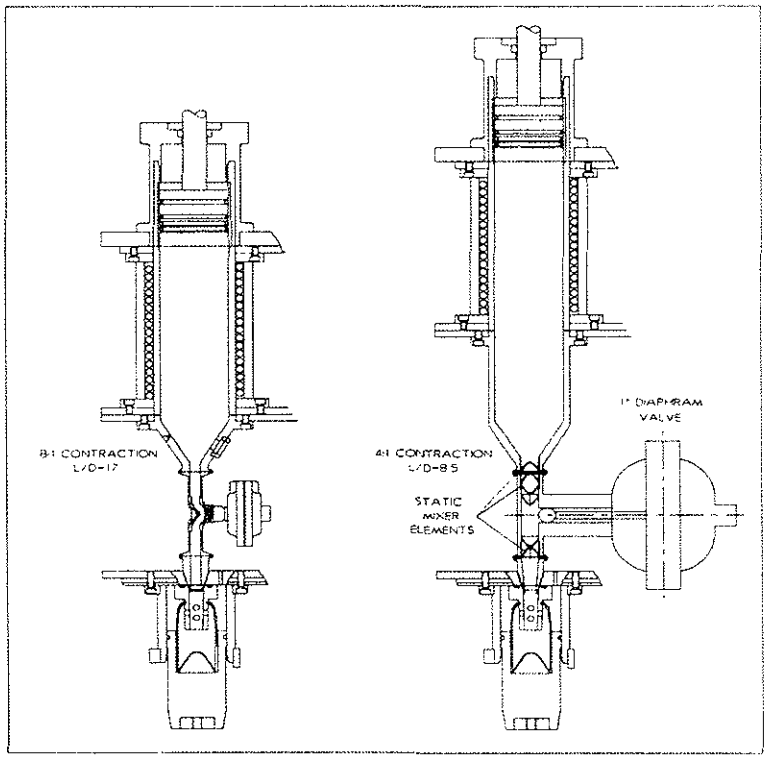

Results of NSWC process design changes. (The densitometer that was also added is not shown here.)

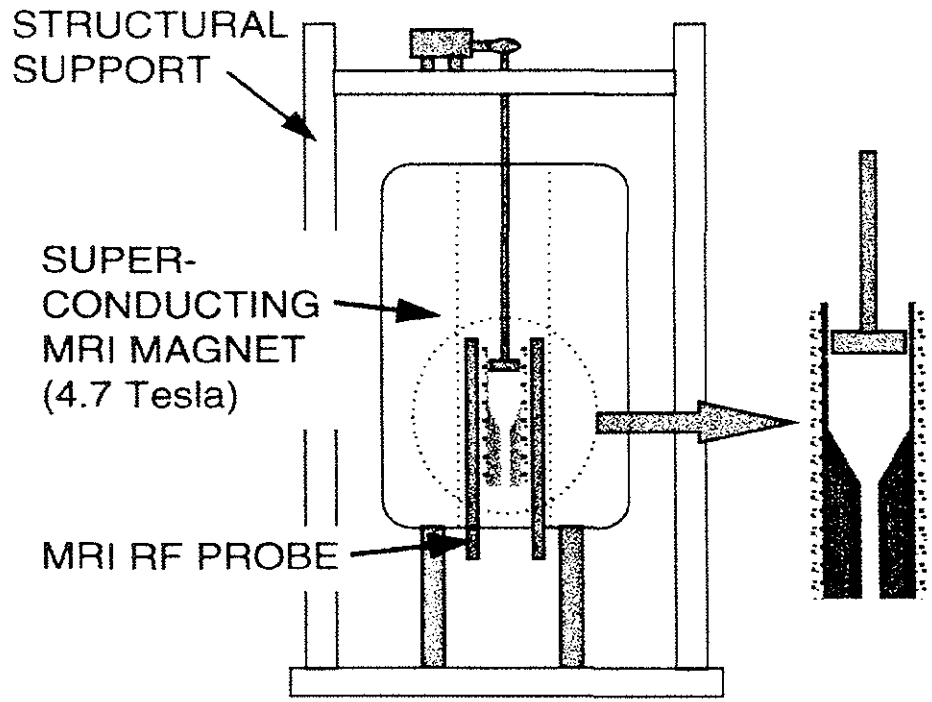

LMMS mock injection loader for MIR experiments

Naval Surface Warfare Center
INDIAN HEAD DIVISION

PLAN FOR ZERO DEFECT LOADING OF PLASTEC FOR ESMB

[1] Develop an inexpensive PBX having a tri-modal blend of RDX in an HTPB/IPDI polyurethane binder, resulting in the leveraging of IMAD/HE investment on PBXW-108 and a current projectile development task.

[2] Demonstrate injection loading of a prototype DEMNS #6 submunition with PBXW-108 Mod 2, resulting in no voids and no density gradients.

[3] Use successful SERDP/CAME fluid mechanics team to perform process design and control for simultaneous injection loading of multiple PLASTEC submunitions, resulting in a proposal.

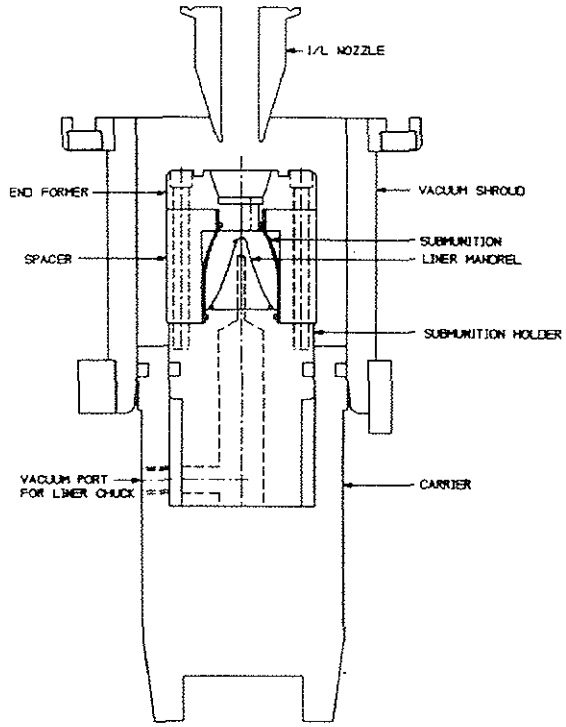

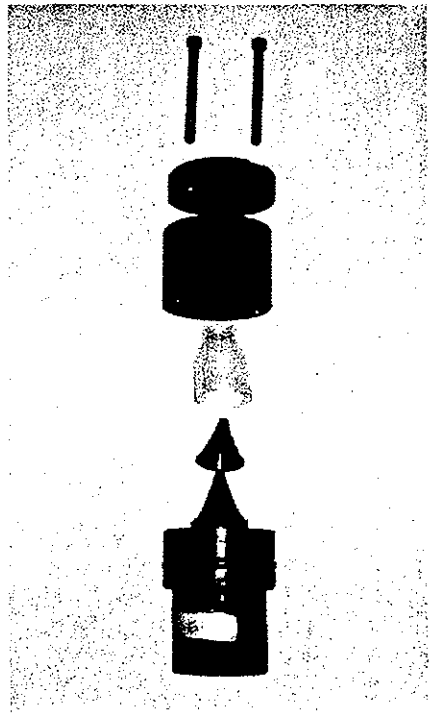

INSENSITIVE MUNITIONS OFFICE
N★A★V★Y

Six DEMNS #6 prototype submunitions have been successfully injection loaded with PBXW-108 Mod 2 (89% RDX) for performance testing. We have also loaded 13 LSGT and 10 VCCT tubes for qualification screening tests.

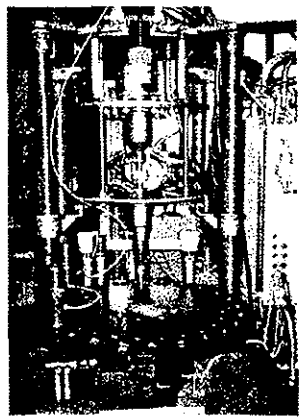

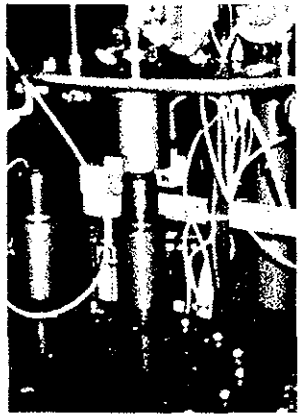

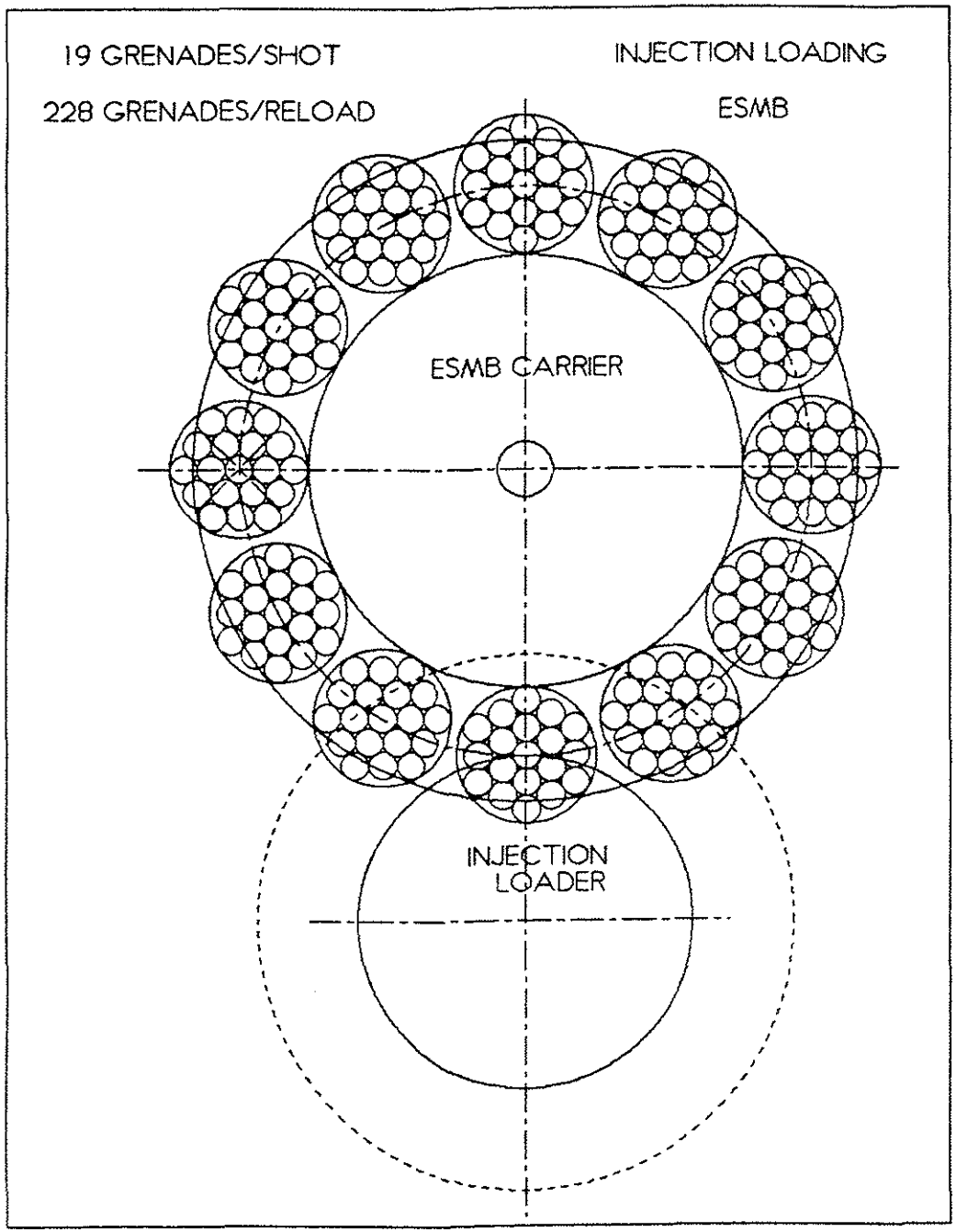
19 GRENADES/SHOT
228 GRENADES/RELOAD
INJECTION LOADING
ESMB
ESMB CARRIER
INJECTION
LOADER

INJECTION LOADING OF HIGHLY FILLED PBX MATERIALS

Injection Loading of Explosive Rope

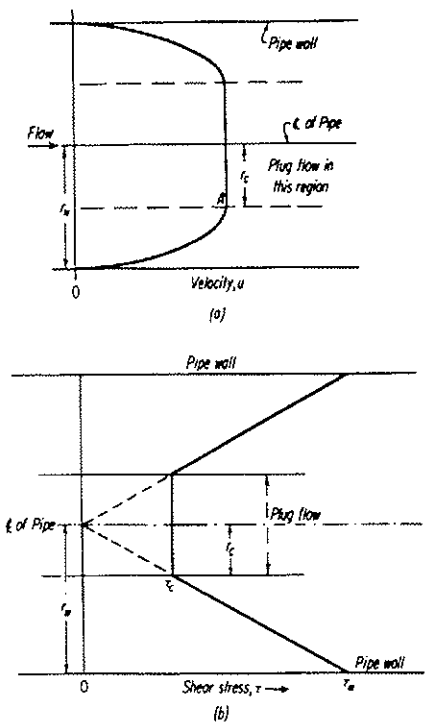

Lessons learned from injection loading of submunitions have led to the development of SMX-13 for the Surf Zone ATD program. SMX-13 is a polyurethane PBX having a very fine particle size filler and a high binder viscosity.

The average particle size of the filler (r) is very small compared to the cylindrical flow channel (R). As previously shown, when the ratio r/R is small, there is negligible shear induced particle migration ($d\phi/dt \sim 0$).

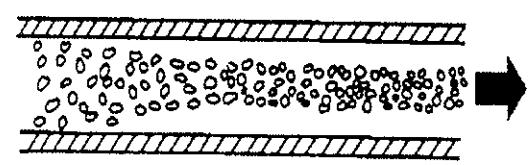

INJECTION LOADING OF HIGHLY FILLED PBX MATERIALS

Injection Loading of Initiation Systems

New ideas for initiating directed fragmentation warheads have lead to the development of new materials and different processing requirements.

Lessons learned from Navy IM and injection loading of submunitions have resulted in the development of PBX materials better suited for momentum transport in narrow flow channels.

PBXW-128 has a narrow particle size distribution of fine particle size nitramine in a polyurethane binder. It is not susceptible to shear induced particle migration because the ratio r/R is small.

CONCLUSIONS

Injection loading of highly filled PBX is a viable means to manufacture smart weapon system components, provided PBX material formulation and selection is based upon science and engineering data that includes :

[1] optimized particle size distribution of the filler in the chosen PBX,

[2] PBX flow behavior in geometries germane to the anticipated process,

[3] process design considerations for momentum transport and mass transfer phenomena between vessels, and

[4] end item product specifications.

DISSOLUTION STUDY OF BAMO/AMMO THERMOPLASTIC ELASTOMER FOR THE RECYCLING AND RECOVERY OF ENERGETIC MATERIALS

Zhihua Cao, Suphan Kovenklioglu, Dilhan M. Kalyon and Rahmi Yazici

Chemical Sciences and Engineering Department
and Highly Filled Materials Institute

Stevens Institute of Technology
Castle Point on the Hudson, Hoboken, New Jersey 07030

ABSTRACT

This study involves the characterization and dissolution of a thermoplastic elastomer copolymer used as binder in the new generation of energetic materials. The thermoplastic binder is an oxetane based elastomer manufactured by Thiokol Corporation. Since the binder encapsulates other components in an energetic material formulation, its controlled dissolution is crucial to the recovery and recycle of all the energetic material ingredients. The polymeric binder was found to be highly soluble in ethyl acetate and THF. The dissolution rate data obtained under well defined flow dynamics was satisfactorily correlated with the film model. External mass transfer resistance was found to be generally important but became negligible for Reynolds numbers above 6.0×10^4. The mass transfer coefficients calculated on the basis of the film model were found to be an Arrhenius function of temperature. The activation energy for the dissolution rates was estimated to be 4.8 kcal/mol.

Journal of Energetic Materials Vol. 15, 73-107 (1997)
Published in 1997 by Dowden, Brodman & Devine, Inc.

X-RAY BASED DEGREE OF MIXEDNESS ANALYSIS OF EXTRUDED GRAINS: RAMIFICATIONS FOR QUALITY CONTROL IN CONTINUOUS PROCESSING

Rahmi Yazici, Elvan Birinci and Dilhan M. Kalyon
HFMI, Stevens Institute of Technology, Hoboken, NJ,

David Fair
Picatinny Arsenal, Dover, NJ

and

William Ansley
NSWC/IHDIV, Indian Head, MA

Extruder Users Group Meeting - June 2-4, 1997

ABSTRACT

A wide-angle x-ray diffraction technique developed earlier at Stevens to characterize the degree of mixing in concentrated suspensions is applied to the quantitative characterization of the distributive mixing achieved in extruded LOVA grains, AA-6 double base propellants and various other formulations to demonstrate the applicability of the technique towards total quality assessment of energetic grains. The results presented in this publication include LOVA grains which were processed either in a batch mixer and ram extruded or processed and extruded using co-rotating twin screw extrusion, and AA-6 propellants which were either in sheet form or carpet rolled and ram extruded.

INTRODUCTION

The ingredients of energetic formulations have to be metered accurately and mixed adequately in order to secure their uniform distribution throughout the microstructure of the extruded grain. Inadequate mixing or segregation of the ingredients during processing lead to defect formation and production of inhomogeneous grains with localized "sensitive" regions which seriously degrade their performance characteristics. In order to improve quality and to reduce waste, reliable analytical techniques need to be developed and employed for "degree of mixing" and defect distribution analysis in extruded propellant grains.

Various theoretical and experimental methods have been developed to study the development of the microstructure and the degree of mixing in model materials[1-8].

Although some of these techniques are useful for understanding and modeling of the mixing process, their applicability in the industrial production environments is highly limited. Kalyon et al.[9] have employed magnetic resonance imaging, wide-angle x-ray diffraction and x-ray radioscopy for characterization of composite suspensions. Yazici and Kalyon[10-15] have developed and applied electron probe and x-ray diffraction techniques to the analysis of degree of mixing in concentrated suspensions. The magnetic resonance imaging and x-ray diffraction can provide detailed mixing analyses on any type of energetic material.

In this study, a wide-angle x-ray diffraction technique developed by the authors to assess the degree of mixing in concentrated suspensions is applied to the quantitative characterization of the distributive mixing achieved in extruded LOVA lots[13-14] and AA-6 double base propellants[16].

EXPERIMENTAL PROCEDURES

Materials Processing and Sample Preparation

LOVA: The formulation of the LOVA involved 30% by volume polymeric binder cellulose acetate butyrate (CAB) and 70% by volume solids. Same formulation was used in both the continuous and the batch mixing. The solid content was primarily cyclotrimethylene-trinitamine (RDX) that contained few volume percent octahydro-tetranitro-tetrazocine (HMX) as a by-product of RDX synthesis. The average particle size of the solid phase was approximately 4 microns. Both the continuously processed, i.e., twin-screw mixed and extruded, and the batch processed,, i.e., batch mixed and ram extruded grains, contained internal perfs as seen in Fig. 1 Sections of the extruded profiles each measuring 0.3" in diameter and 1" long, were randomly chosen from the continuous (C-1) and batch processed (B-1) lots. Each grain was sectioned as shown in Fig. 1b, prior to characterization with x-ray diffraction. In addition to the extruded profiles, samples of the raw ingredients that were used in the processing, i.e., CAB, plasticizer and RDX + HMX powder were also analyzed as reference materials.

AA-6 Double Base: Grain samples from various extrusion runs of AA-6 double-base (MK93) propellants were chosen for analysis. The nominal AA-6 double-base propellant formulation constitutes (by weight) 49% nitrocellulose (NC), 38.8% nitroglycerine (NG) 3.3% L-C salicylate, 1.5% aluminum and 7.4% of other ingredients and additives. Samples of the AA-6 double-base MK93 extruded grains were acquired through Extrusional CAD/PAD Division of Naval Surface Warfare Center, Indian Head. The samples of some of the raw ingredients i.e., NC, NG, and L-C salicylate were also acquired from Indian Head. A sheet AA-6 propellant sample of Radford Army Ammunition Plant, that was used in the production of MK93 propellant grains, was also provided by Indian Head.

The MK93 grains were processed by carpet rolling of AA-6 sheet propellant followed by ram extrusion. During this process the 14"± 3/4" diameter carpet rolls are stacked and conditioned at 130°F and extruded at 180°F in a vertical ram press to get the extruded annular profile of 4" OD (see Fig. 2 a and b). The propellant grain samples were received in transverse-sectioned form of 0.06" in thickness. Radial strips were cut from those cross-sectional samples prior to characterization with x-ray diffraction and electron microscopy (see Fig. 3).

Characterization of the Mixing Indices

Various mixing indices were determined at different scales of examination by varying the sampling area through alterations of the size of the x-ray probe by several orders of magnitude as shown in Fig. 1b. The relative volume-fractions of the ingredients was utilized as the basis for the measure of the degree of mixing of the grains. Here ϕ represents the volume fraction of a given ingredient.

$$CAB\,relative\ volume\ fraction\ in\ LOVA = \frac{\phi_{CAB}}{\phi_{CAB} + \phi_{RDX}} \qquad or \qquad (1)$$

$$NG\,relative\ volume\ fraction\ in\ AA-6 = \frac{\phi_{NG}}{\phi_{NC} + \phi_{NG} + \phi_{LC} + \phi_{Al}}$$

In general, the quantitative description of the mixing quality or goodness of mixing of a given mixture can be developed by comparison of the state of the mixture to the most complete mixing state attainable[17]. This complete mixing corresponds to statistical randomness of the ultimate properties of the ingredients being mixed which would follow the binomial distribution[18]. A basic measure of the homogeneity of a mixture is the extent to which the concentration values of the ingredients of the formulation found at various regions of the volume of the mixture differ from their mean concentration $\bar{c}$. The variance, s^2, arising from the individual concentration, c_i, measurements, provides such an index to quantitatively assess the degree of mixedness. Relative variability is defined with coefficient of variation, v, which is the ratio of standard deviation to the mean[19].

$$v = \frac{s}{\bar{c}} \qquad (2)$$

The maximum variance occurs if the components are completely segregated. Maximum variance is given by

$$s_0^2 = \bar{c}(1-\bar{c}). \qquad (3)$$

The intensity of mixing, I_{mix}, can be defined by normalizing the variance with its maximum value, and an amplitude of mixing or mixing index, MI, can be obtained by normalizing the standard deviation with its maximum value:

$$MI = 1 - \frac{s}{s_0} \qquad (4)$$

Both the intensity of mixing and the mixing index values range from zero, for completely segregated system, to one, for ideally homogeneous system. The objective of any mixing/processing operation, whether batch or continuous, is to homogenize the distribution of the components of the formulation; thus, to achieve mixing index values as close to one as possible at the desired scale of examination.

The Analytical Technique: Wide-Angle X-Ray Diffractometry

X-ray diffractometry has been successfully applied for both qualitative and quantitative phase analysis in multi-phase materials[20,21]. The technique and its application in mixing analysis have been reviewed elsewhere[10,13] and only a brief description will be given here. Upon irradiation with x-rays, a given substance produces a characteristic diffraction pattern. This is because the d-spacings between atomic planes and their distribution in space, ie., the crystal structure is unique for each material, the angular distribution of the diffraction peaks and their intensities is also unique for a particular material. Qualitative analysis by x-ray diffraction is accomplished by identification of the particular diffraction pattern of a crystalline substance from the standard diffraction tables[22]. In the amorphous materials, on the other hand, the atoms (and molecules) exhibit short-range order, in clusters of a few atomic (or molecular) distances, and lack long-range order. Such amorphous structures give rise to very broad x-ray scattering peak(s) centered around the corresponding characteristic interatomic (and intermolecular) distance(s). Identification of an amorphous material using the broad x-ray scattering pattern can be achieved by carrying out control x-ray scattering experiments with standard samples of the same material.

Quantitative analysis is possible, because the intensity of the diffraction pattern of a particular phase - in a mixture of phases - depends on the concentration of that phase in the mixture. Degree of mixing analysis is achieved by carrying out systematic "window" measurements at various locations of the extruded grains.

The relation between the integrated intensity I_x and the volume fraction ϕ_1 of a phase in a mixture depends on the absorption coefficient of the mixture, μ_m:

$$I_1 = K_1\phi_1/\mu_m, \tag{5}$$

where K_1 is a constant which depends on the material and the incident beam used but not on the concentration. The relative ratio of intensities from phases 1 and 2, however, is independent of μ_m

$$\frac{I_1}{I_1 + I_2} = \frac{K_1\phi_1}{K_1\phi_1 + K_2\phi_2} \tag{6}$$

K values can be determined either from the $I_x/I_{corundum}$ values listed by JCPDS[22] or by preparing standard samples of known composition.

In LOVA propellants, the relative volume fractions of the plasticized binder (CAB) and the fillers RDX and HMX were calculated from the relative intensity fraction values given by Eq. 6. These measurements were carried-out utilizing relatively high number of crystal-plane reflections of the crystalline fillers in order to eliminate texture effects and to increase accuracy, and for the amorphous plasticized CAB, the entire broad amorphous peak was utilized (see Fig. 5). Standard samples of the raw ingredients, i.e., the live RDX powder and the polymer binder were prepared and utilized to calibrate the measurements.

In AA-6 propellants, the relative volume fractions of L-C salicylate, aluminum and NC + NG were calculated from the relative intensity fraction values which are unique to each ingredient (see Fig. 4). For NC + NG, the entire broad amorphous peaks were utilized. The amorphous diffraction patterns of NC + NG were deconvoluted to separate the contributions of the individual ingredients NC and NG. As shown in Fig. 6, deconvolution of NG from NC was achieved by taking advantage of the unique shape of the diffraction pattern of NC. The amorphous peak of NG is positioned at the same 2θ angle (22°) as the NC amorphous peak and makes it impossible to apply conventional deconvolution peak intensity evaluation techniques. However, as shown in Fig. 6, the amorphous diffraction pattern of NC exhibits a unique "shoulder", at the higher 2θ

angles that extends up to 50°, in addition to the "head", at 22°. The ratio of the diffracted intensity values at the head (22°) and at the shoulder ($\sim 40^{o}$) locations of the NC pattern is constant for a given NC lot[23,24]. In this investigation, the shoulder intensity value was utilized to deconvolute NC signal from NG signal.

A software package by Rigaku, Images, was used for quantitative analysis. The contributions from the additives were considered in these calculations; however, the effects of the micro-voids and perforations were omitted. A Rigaku DXR-3000 wide-angle diffractometer system was used. Crystal monochromatized CuK_{α} radiation at 40 KV and 20mA was applied with 0.15 and 0.6 degree receiving slits. The x-ray probe sizes (defining the scale of examination) used were 1 mm^2 and 10 mm^2, respectively. The depth of penetration of the technique was in the order of 0.5 mm.

RESULTS AND DISCUSSION

LOVA Propellants:

A typical wide-angle x-ray diffraction (XRD) pattern of the extruded LOVA grains is shown in Fig. 4a. This is a convoluted pattern which includes diffraction peaks from all the ingredients present in the formulation. Computer search/match and identification/elimination methods were applied utilizing the documented crystallographic data, and XRD patterns listed in the JCPDS files[22]. The available diffraction patterns of RDX(I) and β-HMX are shown in Figs. 4b and 4c. In Fig. 4d, the x-ray diffraction pattern of the amorphous binder, i.e., plasticized CAB, is shown to demonstrate further the phase identification process.

The results of the quantitative x-ray diffraction analysis of the relative volume fractions of the binder and RDX from the systematic "window" measurements at two scales of examination are shown in Figs. 7 and 8, respectively. In both figures the data from the batch-mixed sample (B-1) is given in (a) and the data from the continuously-mixed sample (C-1) is given in (b), for comparison.

Table 1. Plasticized CAB Mixing Parameters

	Batch Mixed (B-1)		Twin Screw Extruded (C-1)	
	Scale of Examination		Scale of Examination	
	10 mm^2	1 mm^2	10 mm^2	1 mm^2
mean (vol.%)	24.73	24.71	25.1	25.5
s	2.183	6.321	1.98	3.44
v	.09	.26	.08	.13
MI	.95	.85	.95	.92

Table 2. RDX+HMX Mixing Parameters

	Batch Mixed (B-1)		Twin Screw Extruded (C-1)	
	Scale of Examination		Scale of Examination	
	10 mm^2	1 mm^2	10 mm^2	1 mm^2
mean (vol.%)	71.41	71.06	70.4	69.8
s	2.215	4.967	1.95	3.48
v	.03	.07	.03	.05
MI	.95	.89	.96	.92

The statistical analysis of these results are presented in Tables 1 and 2 for the relative volume ratios of the binder and RDX, respectively. Overall, the average volume fractions of the ingredients were very close to their target values in both batch (B-1) and continuously processed (C-1) lots. However, the amplitude of the dispersion or variance of the measured relative volume fraction values differed significantly. As can be seen in Figs. 7 and 8, the dispersion of the data is relatively narrow for 10 mm^2 scale of examination; however, when the scale of examination is reduced to 1 mm^2 the dispersion of the data increases substantially and the differences in dispersion between the B-1 and C-1 lots become pronounced.

The immediate inferences one can make from these results include the fact that the quality of mixing in the continuous mixed (C-1) lot is better than the batch mixed (B-1) lot. The quantitative comparison of the quality of mixing of C-1 and B-1 lots are shown

in the statistical parameters of the measurements listed in Tables 1 and 2. The parameters for the binder volume fraction at 1 mm^2 scale of examination show that the dispersion or standard deviation of the data is almost twice as large for the B-1 lot than the C-1 lot. Since the mean values for the two lots are almost identical, the coefficient of variation is also twice as large for B-1 than C-1, suggesting the superior distributive mixing achieved by the continuous processing method in comparison to batch mixing. The difference between the two lots is also evident in the index of mixing values. The relatively lower sensitivity of the index of mixing in differentiating the two lots is due, by definition, to its normalization with respect to the totally segregated state. The mixing index value for the continuously mixed (twin screw extruded) grains are greater than those of the batch mixed and ram extruded LOVA grains.

How significant are these results, which statistical parameter is more important and which scale of examination is more relevant? The answer to these questions can only come from the performance characteristics of extruded grains for a given application. However, the technique and the parameters generated can accurately classify a given extruded suspension with respect to ideally mixed and/or totally segregated states and quantify the "degree of mixing."

This comparative study was completed with no prior information about the two lots, and, only after presentation of the results some of the vital information related to the performance properties of the two lots were obtained from the sponsors. According to this information, the batch mixed B-1 lot had apparently failed the burn-rate-based performance test and was discarded. Therefore, the results that are presented in this study are very significant not only in determining the degree of mixing with quantitative parameters but also in indirectly providing information on the potential performance of a given energetic grain. The results indicate that the relevant scale of examination is 1 mm^2 (or lower) for the LOVA grains; and the index of mixing has to be significantly high (better than 0.90) at this scale of examination, for adequate mixedness and performance.

Double Base Propellants

Quantitative information on the volume fraction of the ingredients present was obtained from the XRD patterns by integrating the deconvoluted relevant peaks of the ingredients. Various computational methods were developed and used for quantitative studies. The contributions from the additives and the effects of the micro voids were omitted from these calculations.

The statistical parameters obtained from the degree of mixing analysis of the AA-6 propellant sheet stock are given in Table 3, for 1.2 mm^2 scale of examination. According to these results the mixing quality of NC and NG in the AA-6 sheet propellant is relatively poor, typically exhibiting mixing index (MI) of 0.87 and a coefficient of variance (v) of 0.16. The mixing quality of L-C salicylate was also poor with v = 0.17. The mixing quality of aluminum was worse, according to its unusually high v = 0.57 coefficient of variation. These findings indicated that the mixing process applied in the production of the AA-6 sheet propellant was inadequate, especially that of the solid ingredients.

Table 3. Degree of mixing parameters of the ingredients in AA-6 sheet propellant at 1.2 mm^2 scale

	NC	NG	L-C	Al
mean (wt.%)	49.0	39.0	3.3	1.5
s	5.7	6.2	0.6	0.9
v	0.12	0.16	0.17	0.57
MI	0.88	0.87	0.96	0.92

Table 4. Degree of mixing parameters of the ingredients in extruded AA-6 propellant MK93 grain #3, at 1.2 mm^2 scale.

	NC	NG	L-C	Al
mean (wt.%)	49.0	39.0	3.3	1.5
s	5.1	5.1	0.4	0.3
v	0.10	0.13	0.13	0.18
MI	0.89	0.89	0.97	0.97

The statistical parameters obtained from the degree of mixing analysis of a MK93 propellant grain are given in Table 4, at a scale of examination of 1.2 mm^2. According to these results the mixing quality of NC and NG in the extruded grain was improved considerably compared to the AA-6 sheet stock. The NC and NG ingredients exhibited MI = 0.89 and v = 0.13. The mixing quality of L-C salicylate remained about the same with MI = 0.97 and v = 0.13. The mixing quality of Al in comparison to the sheet stock improved to MI = 0.97 and v = 0.18.

The MK93 propellant grains are produced by carpet rolling followed by extrusion. The carpet rolling process involves the stacking of the AA-6 sheet propellant in layers in the radial direction and thus it effectively rearranges the inherent AA-6 mixing distribution. Furthermore, the extrusion step that follows, induces high shear deformations, which also contribute to the distributive mixing of the ingredients. The result, as the findings of this investigation indicate, is a better degree of mixing achieved in MK93 grains when compared to the AA-6 sheet propellant stock.

In order to determine the spatial mixing distribution of the ingredients as affected by the extrusion process, location specific x-ray diffraction measurements were carried-out on the cross section of the MK93 extruded propellant grain. A schematic description of these location-specific measurements are shown in Fig. 3. These location-specific measurements were taken systematically, one in every 2 mm intervals along the radius, from outer surface to the internal perforation. The results of the "mixing distribution" analysis are plotted in Figs. 9 and 10.

As shown in Fig. 7a, the regions close to the outer surface of the extruded MK93 grain are enriched in NG and depleted in NC. The reverse is true in the middle regions of the grain. According to these results, NG content decreased to a 30% level in the center of the propellant grains and increased to 47% level near the surface of the grain. Similar NG variation trends were also observed in the extruded M30 triple base propellant grains that were analyzed earlier at Stevens[24].

The migration of NG to grain surfaces from the interior could take place due to the thermo-mechanical history applied during extrusion of the propellants. In a previous investigation by Baker et al.[25] dielectric studies have shown that in NC+NG mixtures when the concentration of NG is above 27%, the interaction between the adsorbate (NG) and the adsorbent (NC) is considerably weakened. This weakening point approximately corresponds to the monolayer coverage of NC fibrular structure by

NG[25,26]. Addition of NG in excess of 27% leads to multilayer adsorption type of behavior where the NG molecules are more free to move than those in the first adsorbed layer. Furthermore, it has been shown that the amount of NG that goes into the adsorbed layer varies as a function of the level of nitration of NC, that is, the 27% NG adsorption monolayer value is characteristic for NC with 12.2% nitration and if the NC nitration is increased to 13.4%, the amount of the NG adsorption monolayer drops below 27% due to the decrease in adsorption sites on NC with higher nitration[27]. The NG molecules in excess of the monolayer adsorption maintain a "liquid-like" environment[25]. This means that NG in excess of 27% in a NC+NG mixture will act as an unbound liquid, and be prone to migration during processing such as extrusion. Such migration of the liquid phase has been documented by Kalyon and co-workers in die and extrusion flows[23,24].

The previous studies[25-27] are in good agreement with the findings of this investigation. In the (MK93) AA-6 double-base propellants that are investigated in this study, the NG content of the NC+NG mixture is 44%, substantially higher than the monolayer requirement of 27% and the excess NG is anticipated to be prone to migration during extrusion. The presence of other liquid ingredients and solvents could further aggravate NG migration by diluting NG in the adsorbed layer and making more NG available for migration.

The MK93 propellant grains are extruded with an annular die where the material flow with non-uniform shear rate $\gamma(r)$ and velocity $V_z(r)$ distributions and where the shear rate is higher near the die walls[30]. It is a well established fact that in such flow situations where a deformation rate distribution exists and where two immiscible polymeric fluids of different shear viscosity behavior are flowing, the separation of the two fluids is expected, whereby the less viscous ingredient migrates or "exudes" to the high shear rate region (towards the walls of the die) and encapsulates the higher viscosity ingredient[25,26]. This is probably the principal mechanism that causes the enrichment of NG near the extrudate surfaces. The excess NG (and the solvent) above the 27% monolayer formation level, acts as the less viscous fluid that migrates towards the walls of the grains. The extent and nature of the NG migration would, therefore, depend on the extrusion processing conditions applied. That is, the higher the extrusion rates the more pronounced the NG migration would be. Indirect evidence of such effects were found with dielectric and thermal analytical techniques[25,27] that showed the relaxation of low frequency "alpha peak" to be a function of the extrusion rate.

The particular MK93 propellant grain #3 analyzed in this investigation exhibited "rough surface" on the outside surface shown in Fig. 2b. This roughness, which is

indicative of flow instabilities may be due to the presence of excess NG at the surface regions during extrusion.

The mixing distributions of L-C salicylate (LC) and aluminum (Al) as a function of radial position are shown in Fig. 10. In this figure, logarithmic scale was employed in order to be able to show the mixing distribution of all four ingredients. According to Fig. 10, the distribution of LC is relatively uniform with tendency for enrichment from the middle (2.8%) to the surface (3.9%). This tendency is similar to NG migration and, therefore, might indicate an affinity of LC being carried with NG during extrusion. The distribution of Al, on the other hand, exhibit enrichment in the mid-radius zone of the grain up to 1.8%. Such enrichment may alter the burning rate distribution of the propellant grains.

CONCLUSIONS

Our degree of mixing analysis technique based on wide-angle x-ray diffraction was successfully applied to analyze extruded LOVA grains which were pre-mixed with batch and twin screw extrusion processes. The technique can: i) identify various components present in an extruded formulation, ii) quantitatively determine the volume fraction of each component at various locations in extruded profiles, iii) quantitatively characterize the degree of mixing of each component at the desired scale of examination for a given application.

In the LOVA grains studied, the average volume fractions of the ingredients were close to their target values in both batch and continuous mixed lots. At smaller scale of examination (1 mm^2) the quality of mixing of the binder and the energetic solid powder was significantly better in continuous mixed lot than batch mixed lot. The parameters defined, i.e., the variation coefficient and mixing index, were highly effective in quantifying the degree of mixing of extruded grains, which is related to their performance.

In the AA-6 double-base propellant formulation the principal components present, i.e., nitrocellulose (NC), nitroglycerine (NG), L-C salicylate and aluminum, were

identified, the weight fractions of each component were determined, the degree of mixing of each component was quantitatively characterized at 1.2 mm^2 scale of examination, and the mixing distribution of the ingredients across the MK93 propellant grains were quantitatively determined.

The degree of mixing of ingredients in the AA-6 sheet propellant was relatively poor especially that of Al and NG. The degree of mixing of ingredients in the MK93 propellant grain was considerably improved compared to the AA-6 sheet propellant. The mixing distribution analysis showed that in the MK93 propellant grain, NG was enriched at near surface regions and depleted towards the interior. The reverse was true for NC. The nature of the NG distribution indicated the unbound liquid-like behavior of the "excess" NG and its migration to the surface during extrusion of the grains.

ACKNOWLEDGMENTS

This research was supported by the contracts #N00014-904-I-0241 by U.S. Army Production Base Modernization Activity, managed by ONR with program directors Mr. David Fair and Dr. Richard S. Miller, and #N00014-904-I-0241 by NSWC Indian Head Division, with program director Mr. Jose Leon. We are grateful for these supports. The content of the information does not necessarily reflect the position or the policy of the government, and no official endorsement shall be inferred.

REFERENCES

1. J. M. Ottino, "The Kinematics of Mixing: Stretching, Chaos and Transport," Cambridge University Press (1989).
2. A. Morikawa, K. Min, and J. L. White, *Int. Polym. Process 4,* p. 23 (1989).
3. S.P. Rwei, I. Manas-Zioczower, and D. F. Feke, *Polym. Eng. Sci. 30,* p. 701 (1990).
4. B. David and Z. Tadmor, *Int. Polym. Process. 3,* p. 38 (1988).
5. M. N. Gokboro, "Mixing in Single Screw Extruders," Ph.D. Thesis, University of Bradford (1981).
6. K. Kubota, R. Brzoskowski, J. I. White, F. C. Weissert, N. Nakajima, and K. Min, *Rubber Chem. Technol. 60,* p. 924 (1987).
7. D.M. Kalyon, A.D. Gotsis, U. Yilmazer, C.G. Gogos, H. Sangani, B. Aral, and C. Tsenoglou, *Adv. Polym. Technol. 8,* p. 337 (1988).
8. D. M. Kalyon and H. N. Sangani, *Polym. Eng. Sci. 29,* p. 1018 (1989).
9. D. M., Kalyon, Yazici, R., Jacob, C., Aral, B., and Sinton, S.W., *Polym. Eng. Sci., 31*, p. 386 (1991).
10. R. Yazici, and D. M., Kalyon, *Rubber Chem. Technol., 66*, p. 527 (1993).
11. D. M., Kalyon, R. Yazici and A. Lawal, *Proceedings 1993 JANNAF Propellant Development and Characterization Subcommittee Meeting*, Livermore, CA, April 28, 1993.
12. R. Yazici and D. M. Kalyon, *SPE ANTEC Technical Papers 39*, p. 2845-2850 (1993).
13. R. Yazici and D. M. Kalyon, *J. Energetic Materials*, 14, p. 57 (1996).
14. R. Yazici, D. M. Kalyon and D. Fair, "Degree of Mixing Analysis in LOVA Propellants by Wide-Angle X-Ray Diffraction," US Army Report, ARPBM-CR-95001, p. 1-33 (1996).
15. R. Yazici and D. M. Kalyon, *SPE ANTEC Technical Papers 43*, p. 2076-2080 (1997).
16. R. Yazici and D. M. Kalyon, "Mixing Distribution Analysis in AA-6 Double-Base (MK93) Propellants," NSWC Progress report, Grant #N00014-174-95-K0063 (May 5, 1997).
17. D. M. Kalyon, in "Encyclopedia of Fluid Mechanics," Houston, TX, Gulf Publishing, vol. 7, Ch. 28, p. 887-926 (1988).
18. W.D. Mohr, "Processing of Thermoplastic Materials," E. Bernhard, Ed., Kreiger Publishing Co., Malabar (1959).
19. G. E. Dieter, "Engineering Design", McGraw Hill, New York, NY (1983).
20. B.D. Cullity, "Elements of X-Ray Diffraction", Addison-Wesley Pub., Reading, MA (1986).
21. L.E. Alexander, "X-Ray Diffraction Methods in Polymer Science", Kreiger Publ. Co., Malabar (1985).

22. International Center for Diffraction Data, JCPDS Files, Swathsmore, PA (1994).

23. Internal Report, Alliant Tech. Systems, Inc., Radford Army Ammunition Plant, Radford, VA (Feb. 1996).

24. R. Yazici and D. M. Kalyon, "Microstructure and Mixing Distribution Analysis in M30 Triple-Base Propellants", ARDEC Progress Report, (April 10, 1997).

25. F. S. Baker, M. Jones, T. J. Lewis, G. Privett, D. J. Crofton and R. A. Pethrick, *Polymer 25*, p. 815-820 (1984).

26. Y. M. Lotmensev and R. N. Schneerson, *Trudy Khimicheskoi Telnolog 1*, p.126 (1974).

27. F. S. Baker, M. Jones and G. Privett, *Proceedings ADPA, 3rd Int. Gun Prop. Symp.*, USA (1985).

28. U. Yilmazer, C. Gogos and D. M. Kalyon, *Polymer Composites 10*, 4, p. 242-248 (1989).

29. P. Yaras, D. M. Kalyon and U. Yilmazer, *Rheologica Acta 33*, p. 48-59 (1994).

30. D. M. Kalyon and M. Khemis, *Plastics and Rubber Proc. and App. 8*, p. 157-164, (1987).

31. G. Akay, *Rheol. Acta 18*, p. 256-267 (1979).

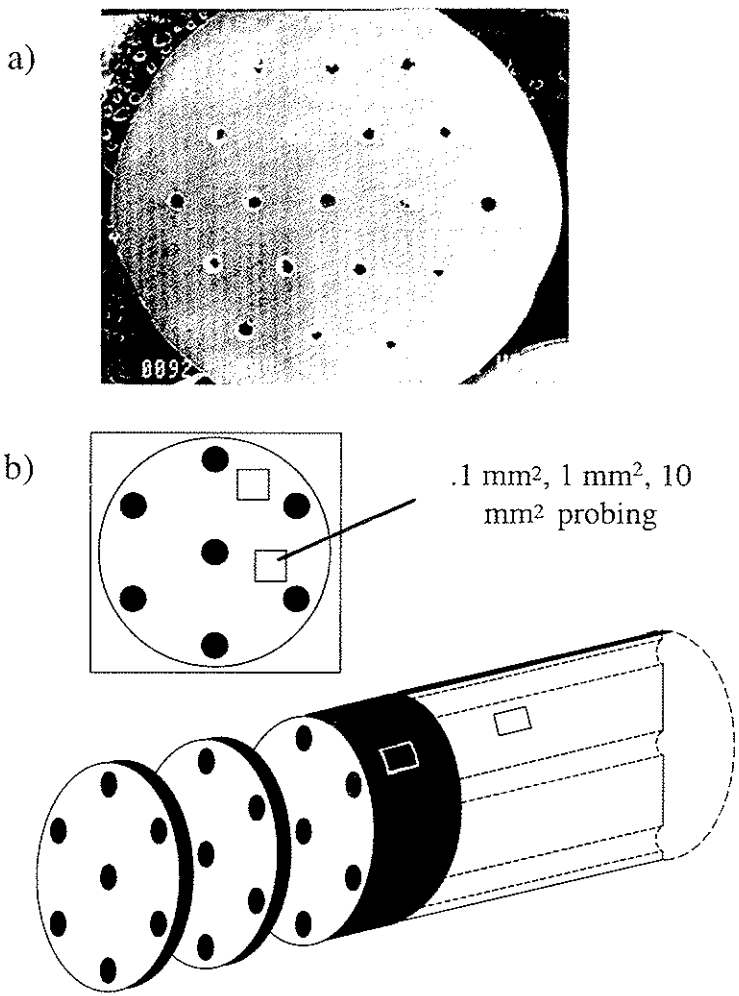

Fig. 1 Extruded grain cross section (a) and sampling (b).

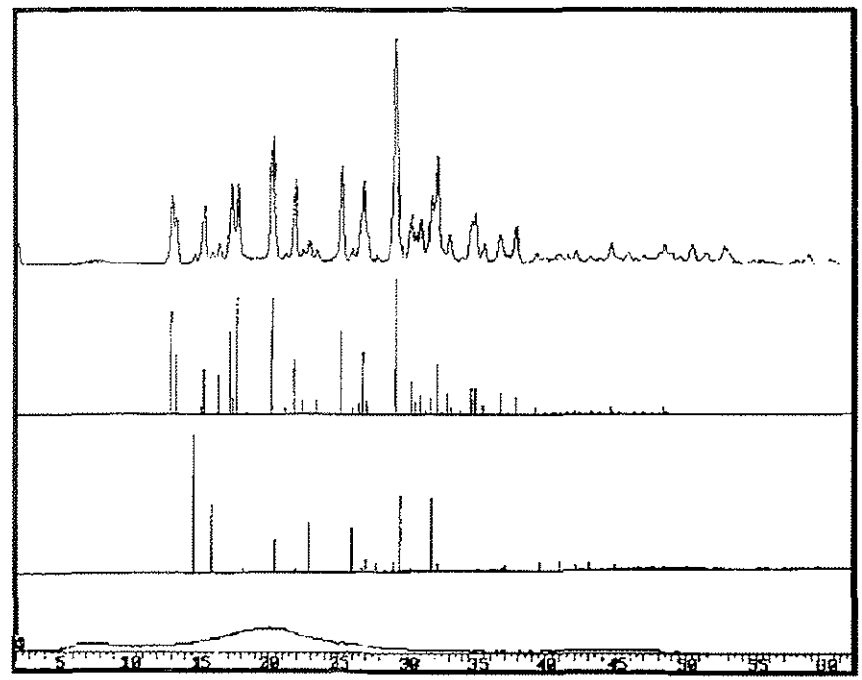

Fig. 4 X-ray diffraction patterns of the LOVA grains (a), RDX simulation (b), HMX simulation (c), and CAB (d).

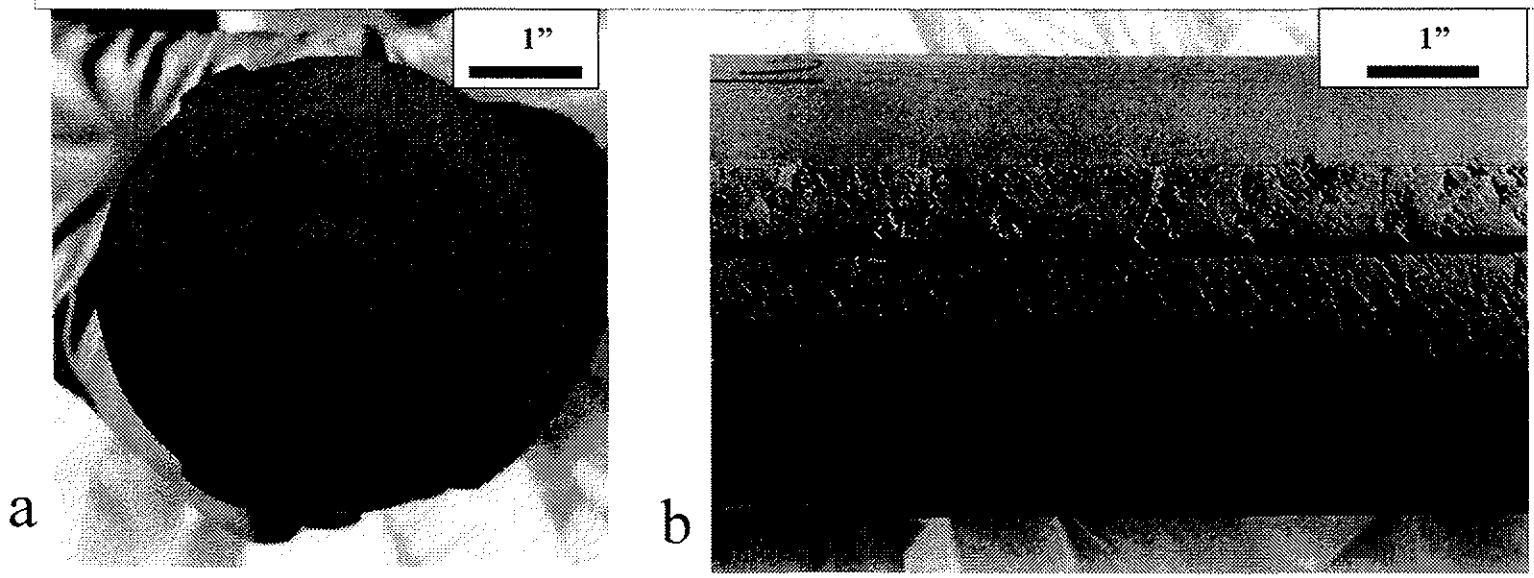

Fig. 2 MK93 extruded propellant grain: a) transverse cross section and b) longitudinal view with rough surface features.

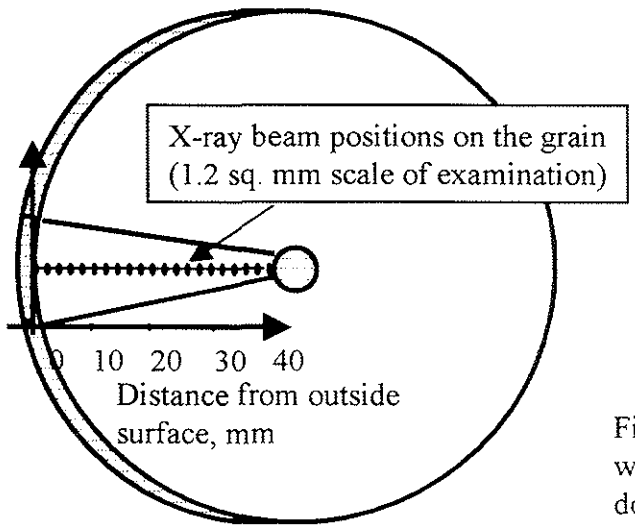

Fig. 3 Radial measurement of mixing distribution with wide angle x-ray diffraction on the cross section of AA-6 double base propellant grain (4" MK93)

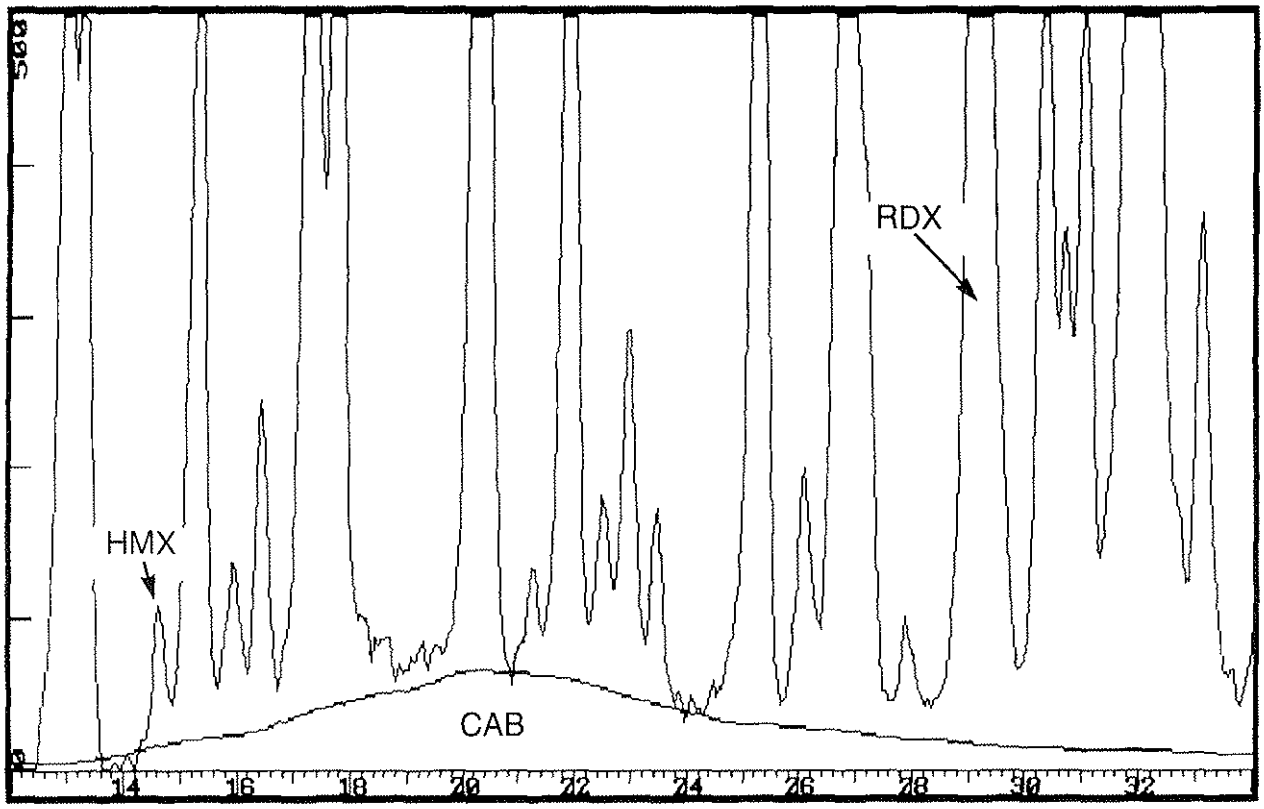

Figure 5. Deconvolution of a typical x-ray diffraction pattern of LOVA propellant where integrated areas of the peaks from different ingredients are marked.

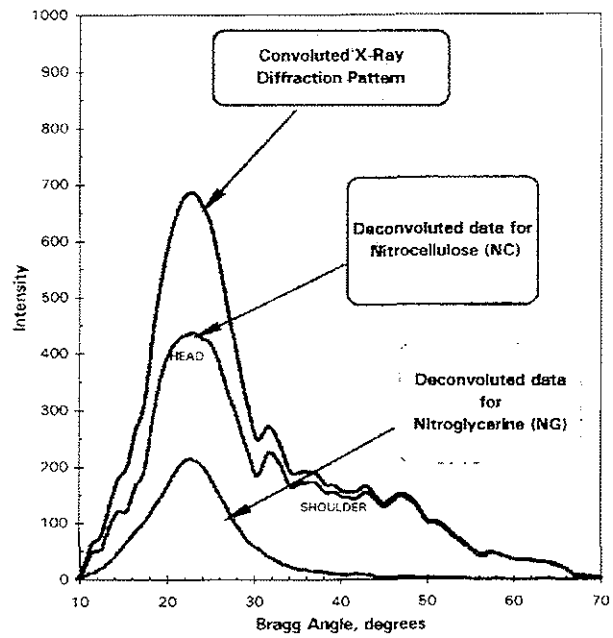

Fig. 6 Separation of the NC and NG signals from the convoluted x-ray diffraction pattern.

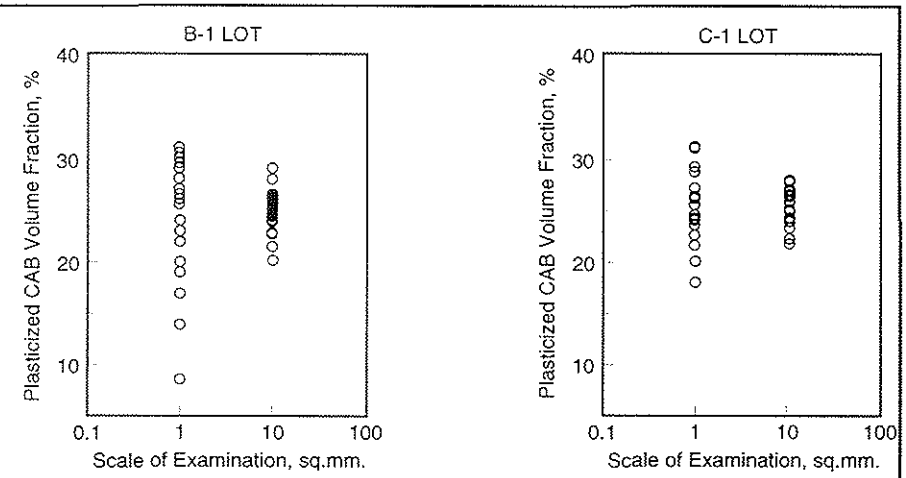

Fig. 7 Plasticized CAB volume fraction dispersion at two scales.

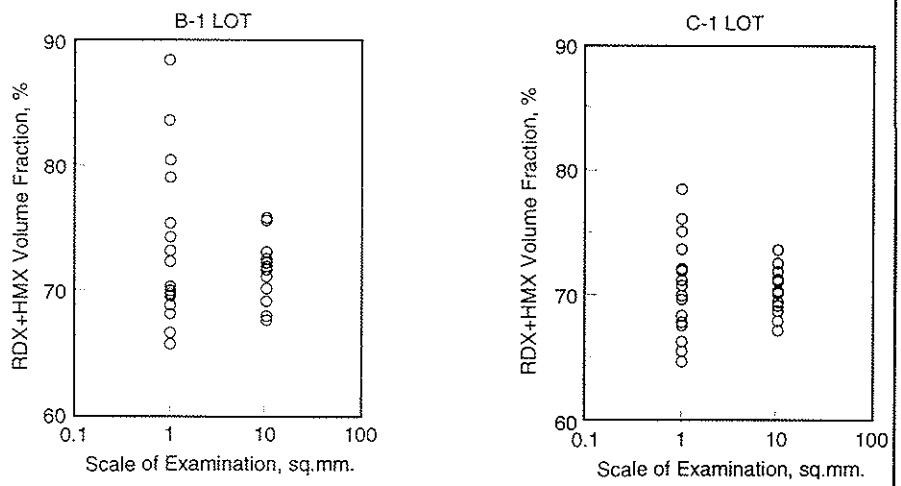

Fig. 8 RDX + HMX volume fraction dispersion at two scales.

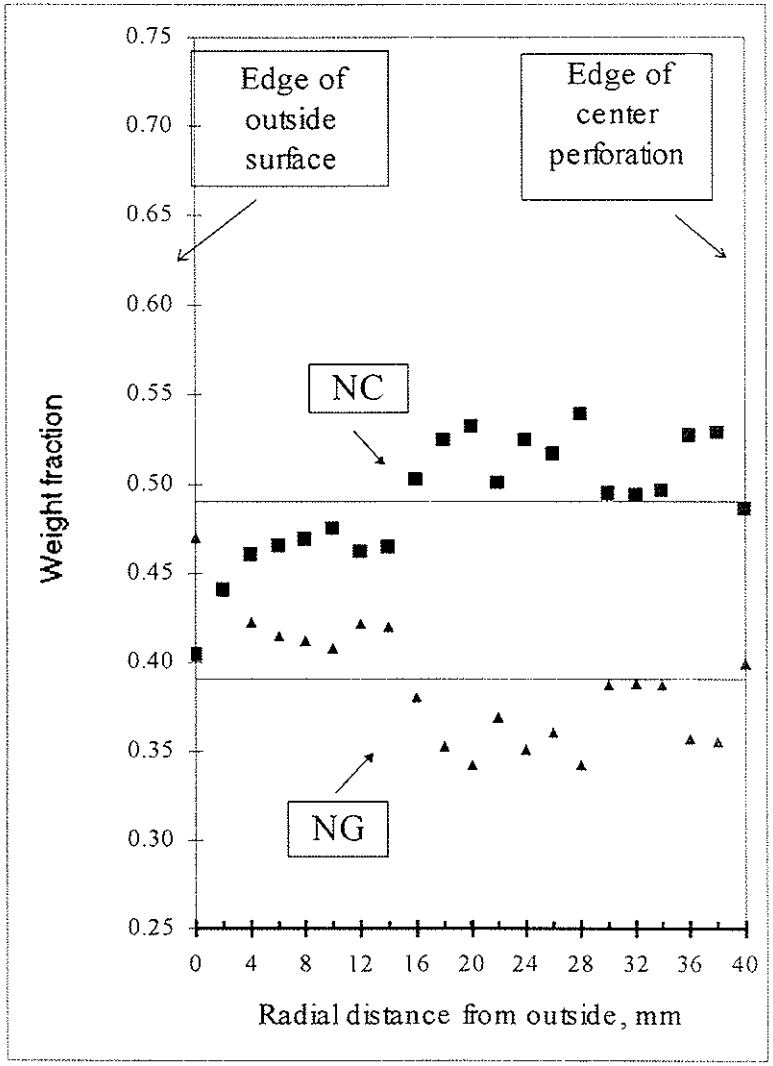

Fig. 9 Mixing distribution of NC and NG on the cross-section of AA-6 propellant MK93 grain.

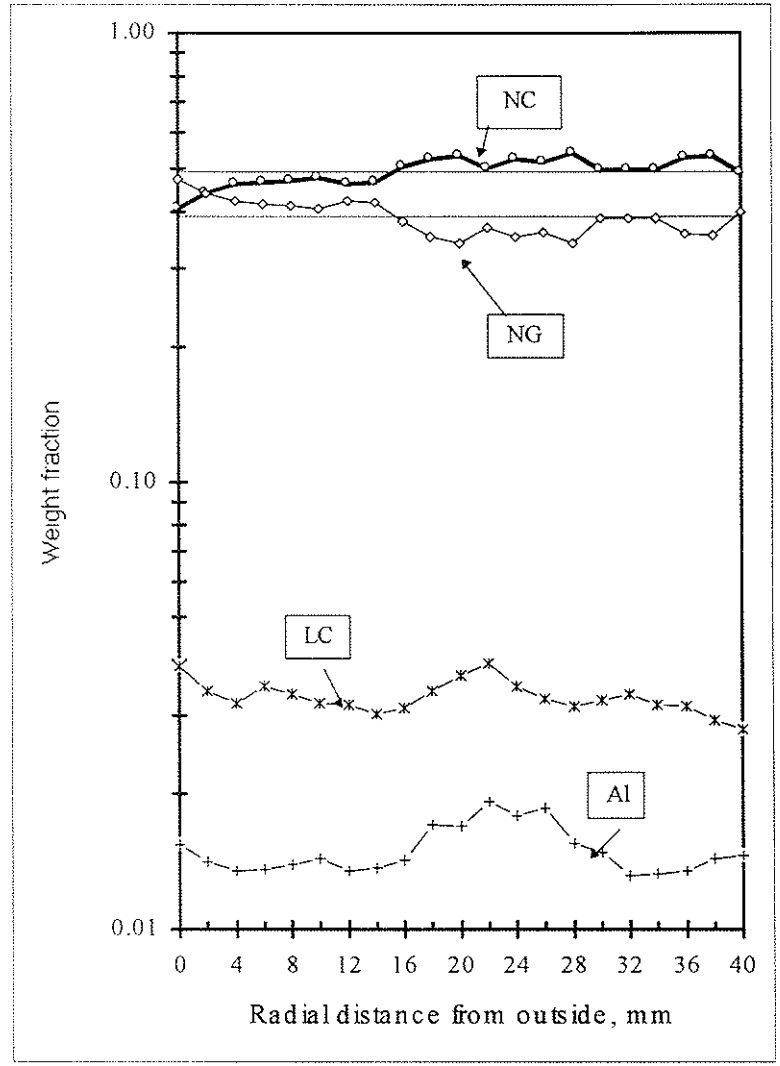

Fig. 10 Mixing distribution of NC, NG, LC salicylate and Al on the cross-section of AA-6 propellant MK93 grain.

Demixing.

Presented at:
9th Continuous Mixer and Extruder Users Group Meeting
2-4 June 1997, Weehawken, NJ

by
Hugh J. McSpadden
Consultant, Energetic Materials and Technology
3823 W. Hartford Ave., Glendale, AZ 85308-4220
Tel: 602-938-6234; Fax: 602-938-2053
E-mail: hmcspadden@juno.com or hmcspddn@aol.com

Demixing

A SMALL DISCLAIMER: I will not be presenting a mathematical treatment of demixing. I leave that to others who are much more skilled than I am.

Much of this paper is based on my personal experiences, also known as "been there, done that,..."

I have had many occasions to personally reencounter a definition of experience which I have used:

Experience is that event or knowledge
which tells you, you have made a mistake ---
again!!!

This paper will cover these topics:

1. What is demixing, and what does it do?
2. What causes demixing?
3. Why should you, or anyone, be concerned about demixing?
4. Examples of demixing from my experience.
5. Summary and conclusions

1. What is demixing, and what does it do?

1.1 Demixing is a physical process. It is result of something disturbing the randomness of a perfectly mixed, uniform propellant. Demixing occurs wherever the propellant contacts another surface forming an interface, whether the surface is the liner inside a rocket motor, or the mixer bowl, or the mixer blades, or casting tooling surfaces such as the mandrel, or even at the interface of the propellant with the air. Any interface creates a discontinuity within the propellant, extending from the interface into the propellant at least one-half the diameter of the coarsest particles within the propellant. Depending upon the origin of the demixing, the discontinuity may or may not be reatianed within the propellant mass.

For example, if the coarsest particles are ammonuim perchlorate at 200 microns, then the demixed, non-representative composition must extend at least 100 microns into the propellant. Assuming that a propellant, such as a castable HTPB-based one has adequate binder volume to fill the interstitial voids, then it is physically impossible to have exposed AP surfaces at the interface. Therefore, there is increasing binder and decreasing oxidizer as one gets closer and closer to the interface. Therefore this relatively thin film of oxidizer is not representative of the bulk, theoretical composition of the propellant, and is therefore properly called demixed propellant.

Even though the total effect on the bulk propellant, caused by the demixing at an interface, is small, it is a mathematical fact that the bulk composition is no longer exactly as specified, but is, in fact, slightly oxidizer rich, binder poor.

Because the demixing which I have mentioned here causes relatively little effect on the performance of the rocket motors, and can be compensated for by slight changes in the propellant formulation, I will turn now to more extreme forms of demixing.

1.2 Demixing segregates and/or separates propellant ingredients destroying the uniform distribution of the components. Demixing can cause cracks and insufficiently bonded areas within the propellant grains. The well-known "mid-web hump" is one example of ballistic changes caused by demixing.

1.3 Demixing can affect all sizes of propellant grains, and all types of propellants.

Examples of propellants which exhibit demixing:

* Nitrocellulose	Single Base, Double Base, without appreciable solids. Triple Base with added solids added (NQ) Composite Modified Double Base: AP + Al added
* TPE	Solids added (AP, Al, etc.)
* Castable:	Polysulfide, Polyvinylchloride, Polyurethane, PBAA, PBAN, CTPB, HTPB, GAP, NEPE, even the old polyester/styrene and asphalt based ones, etc.
* Extrudable	TPE, thermoset rubber, PVC plastisol

<u>OBSERVATION: No solid propellant is immune to demixing!!!</u>

2. What causes demixing?

Any external force acting upon a fluid, or semi-fluid propellant (that will ultimately become a solid propellant) has the potential to cause one or another type of demixing. A liquid solution such as the HAN-based gun liquid gun propellants will not show evidence of demixing. On the other hand, even single-base gun propellants will show demixing because the nitrocellulose molecules will align at the interface, such as inside a die, resulting in loss of some portion of the randomness of the bulk propellant.

The spiders that hold die pins in place are one source of mechanically-induced demixing. The spider legs, or the "wagon-wheel" spokes split the mixed propellant into multiple streams, and by reduction of the cross-section of the die reunite those stream after the propellant has padded the legs or spokes. Even after the individual parts of the propellant stream are pressed against each other, they may or may not weld back together. And, even if they weld together, the evidence of aligned particles will still be there, with a slight, but potentially noticeable change in both ballistics and in mechanical or physical properties.

In some cases, solventless double-base grains have failed to adequately weld together after flowing thru the die, resulting in grains that split apart into lengthwise segments after a length of time.

The flow of castable propellant through slit-plates, or through constricted casting ports, is well known to produce demixing. The magnitude of the demixing and the result upon physical, mechanical and ballistic properties is controlled by the specific formulation, the design of the casting tooling, and even the size of the rocket motor. Vacuum casting through slit plates, and aided by gravity creates ribbons of propellant that are demixed to some extent as they pass through the slits. The ribbons then fall into the evacuated

rocket motor chamber, and end up in a quasi-random arrangement, removing much of the effect of the demixing in many cases.

Another source of demixing is the decreasing viscosity of a liquid polymer at the beginning of a cure cycle, when the composite propellant has been mixed and cast at a temperature lower than the curing temperature. The result here is to have the oxidixer and metal fall under the influence of gravity, creating a gradient within the grain. The direction of the gradient depends on the physical position of the rocket motor during the cure cycle. The magnitude of this type of demixing depends on the type of polymer, the solids loading, and the temperatures used for mixing and for curing.

A fourth source of demixing is the composition of the polymer, and plasticizer. Polymers differ in viscosity, and in the solids loading required to meet the ballistic requirements. The plasticizer may have limited solubility in the polymer, and in time will move to the exposed surface(s) of the grain and show up as an exudate on the exposed surfaces of the grain. It may even migrate from the propellant into the liner.

One well-known missile utilized an expensive liquid burning rate catalyst and as plasticizer. The grain was an end-burning design. Unfortunately, when the liquid migrated into the liner, the result was a burning rate gradient from the center of the grain, outward, with the slower rate at the outside. This created a grain that progressively developed a conical burning surface, developing too much thrust, burning out prematurely, while having an extremely long tailoff. Collectively these results of demixing prevented the grain from doing the desired job.

2.1 EXTRUDABLE

* Flow through a die, whether the grain does, or does not, have one or more perforations within it creates a binder-rich skin to the extrudate, which is one result of the interface at the die inside surface.

* As mentioned previously, flow around spider legs, wagon-wheel spokes and mandrels may create a grain with segments not welded together. One result of the sliding of the flow along the legs and spokes is the formation of segments within the cross-section of the grain. This flow aligns the molecules of the polymeric binder and creates a binder-rich surface for each segment. The binder-rich surface may extend all the way from the inside to the outside, as well as extending the full length of the extrudate.

Properly designed dies will minimize the effects of the demixing. However, even the best designed die has absolutely no way to introduce remixing, because the best any die is capable of doing is shaping the material fed into it.

2.2 CASTABLE

* Flow through casting slits, or through casting ports results in moving the solids closer together within the local propellant stream, making the center of the stream oxidizer-rich, and surrounded by relatively binder-rich material.

In propellants with higher levels of castable binder, it is possible to create an outside to the propellant stream that is almost, or even totally free of oxidizer. This effect is most pronounced when large amounts of coarse oxidixer are used, in conjunction with higher binder levels. The RPI test motor mentioned in section 4 is one example of this effect.

As mentioned previously, the traditional use of slit plates for casting into a rocket motor both creates demixing, and at the same time does recreate some degree of randomness, if the motor is large enough.

Bayonet casting pumps a stream of propellant through a hose or pipe, and will introduce its own version of demixing.

2.2.1 RESULT OF DEMIXING IN CASTABLE PROPELLANTS

* In many cases the streams remain as laminae and never remix, even on a macro scale. One of the illustrations in section 4 will emphasize this point.

* Propellant becomes non-uniform in composition.

* Mechanical properties can change dramatically, with loss of elongation frequently occurring. In addition, there will be modulus gradients and even tensile gradients across throughout the grain.

* One result of these gradients is the loss of ability to temperature cycle.

* Ballistics can change from theoretical, resulting in rockets may burn too fast or too slow, thereby failing to meet performance requirements, and even undergoing catastrophic failure. In aircrew escape systems, there are ridgidly defined thrust limits which are a result of the limitations of the human body to resist acceleration forces.

2.3 THERMALLY CAUSED DEMIXING

Thermally caused demixing is the settling of solids inside the rocket motor during cure, and is caused by the reduced viscosity of the castable polymeric binder at the curing temperature. Historically, it has been encountered when high binder levels were used, whether dictated by the need for process fluidity, or dictated by the need for low burning rates, while still retaining adequate specific impulse.

Ballistic results of thermally caused demixing: (a) If cured vertically: then one end of the rocket burns fast, the other slow, with a high probability of case burn-through; and (b) if cured horizontally: one side of the rocket motor burns fast, the other slow. Either of these effects will shift the center of gravity of free-flight rocket, and may cause it to totally divert from its designed flight path. For example, if the rocket is flown as a sounding rocket, the flight path will show coning and/or wobble, and will not reach the designed altitude due to a number of factors. Even active guidance systems may not be able to totally compensate for c.g. shifts caused by demixing.

2.4 POLYMER PROBLEMS

Some polymers are, or have been, a blend of different molecular weight versions of the same basic, reactive polymer. The typical specification for a polymer used in propellants includes only those parameters which are measured on the bulk, or average composition of the polymer. Little or no requirements exist for the distribution of molecular weights, and for the distribution of functionality. Yes, there are, and have been, many investigations into polymer properties, with the results expressed as number average molecular weight, weight average molecular weight, and so on. These investigations and their results have not led to widespread establishment of more detailed specifications.

Others polymers are, or have been, a blend of functional and non-functional versions of the same polymeric backbone. If molecular weights differ too much, then separation can/will occur.

I. personally, have encountered a nominally di-functional polymer where much of the lower molecular weight fraction of the polymer mass appeared to be mono-, or di-functional, with the higher molecular weight fraction being tri-, tetra-, or even penta-functional. The ***average*** values were near the center of the specification range, but the polymer required a unique cure system --- one without cross-linkers, because the polymer was already capable of doing the cross-linking.

Selection of plasticizers with limited compatibility with the polymer will cause problems. It is well known that polymers have definite compatibility and solubility limits, which vary with the polymer and with the plasticizer. If these limits are exceeded, the liquid will become mobile and migrate. Migration into the liner can weaken the liner until it can no longer support the propellant grain, or the bond of the propellant to the liner can be catastrophically weakened. If the plasticizer migrates to the bore, or to the ends of the grain, ignition of the grain is delayed, or even prevented. Even if the grain ignites, the migration of the liquids may have left microscopic voids within the propellant, altering the apparent burning rate, and therefore altering the motor performance --- probably not in a favorable manner.

3. WHY SHOULD YOU, OR ANYONE, BE CONCERNED ABOUT DEMIXING?

3.1 Recognition of demixing

In order to be, or become, concerned about demixing you have to be able to recognize the presence or existence of demixing by the effects it produces. For example, some of the more evident effects are:

* Extruded grains fall apart into segments. There may be shrinkage marks on some shapes and configurations, much like the shrinkage marks seen on injection-molded plastics. These marks indicate differences in the composition of the underlying material. Thermal shrinkage is, of course, greater for unfilled polymers, than for filled ones.

* Castable grains have visible non-uniformities in the color of the propellant, and sometimes will even have definite "wet" streaks or lines when demixing is pronounced. There are some cure systems which do not necessarily produce the softness, and tackiness of binder-rich places, and in these cases, there will usually be a visible shift in the color of the propellant. There may be localized indentations in the "as cast" surface of the propellant. If these are not associated with identifiable voids in the propellant, then the indentations often are associated with binder-rich areas for the same reason as extrudates will show non-uniform shrinkage upon cool-down.

* Thrust-time curves differ noticeably from theoretical --- sometimes dramatically. This effect is most readily seen when the theoretical thrust-time, or pressure-time, curve is supposed to be a straight line. Demising will show up as lower thrust or pressure in the early part of the curve, with a peak somewhere in the middle-part of the curve (so-called mid-web-hump), followed by a steady decrease to a lower than normal burn-out thrust or pressure. The tail-off may be extended, as a result of the lower pressure at burnout.

3.2 WHO SHOULD BE CONCERNED?

Every:

Ballistician

Stress Analyst

Tooling Designer

Propellant Formulator

Rocket motor hardware designer

Propellant process engineer and mix crew.

In other words: everyone!!!!

Simply stated, there is no room in designing, developing and in actually making successful rocket motors for anyone to not be concerned about the uniformity of the propellant. Just as the important parts of many chemical specifications is the level of the **IMPURITIES** because they cause many unwanted effects far out of relationship to their absolute magnitude within the chemical, the effects of demixing are much, much greater than the absolute percentages of change from the average, or nominal, composition of the propellant.

4. EXAMPLES OF DEMIXING FROM MY EXPERIENCE.

4.1 Rocket Power Inc. test motor

Rocket Power Inc. (RPI) worked with a test motor derived from a 12-pointed star grain used in a production motor that was a component of an aircrew escape system. This unit was bottom cast through four small diameter circular ports. Early use of this as a test motor was with the smaller mandrel, (shown by a dotted line in the sketch below) in order to provide a progressive geometry in the grain. The progressive geometry theoretically allowed the incremental calculation of real-world, motor burning rates over the entire, wide, pressure range. These calculations were expected to give good burning rate data over a significant range by firing only one motor at anyone temperature. The derived rate data typically had a plateau with an exponent nearly zero Because it was known that burning rate data from strands was of limited application in the design of rocket motors, it was hoped that these derived motor burning rates would be better. However, application of this derived data in the design of other motors was of limited success, which we now recognize was at least partially due to demixing, and the resulting mid-web-hump.

Decrease of the propellant web to only ½-inch continued to show the break in the derived rate curve. The reason for this break in the rate versus pressure curve was dramatically illustrated when some propellants began leaving slivers of pure polymer after the firing. These were located mid-way between the casting ports. Their length appeared to be a direct function of casting rate, which is what our present understanding of demixing says would happen.

4.2 RPI Hopi IV sounding rocket

The Hopi IV sounding rocket used a slow-burning polyurethane-AP propellant to lengthen the burning time, and to permit use of the rocket as a second-stage in addition to its first-stage use. The rocket motor was bottom-cast on an upward slope using only one relatively small casting port and cured in a horizontal position. The single casting port produced some remixing of the propellant stream, reducing the demixing. However, the horizontal curing position, and the relatively low solids loading allowed the solids to settle during the curing cycle, producing a grain with a continuous oxidizer-to-binder gradient from the top as cured, to the bottom as cured.

The result was a motor with the center-of-gravity not on the motor centerline. The rocket motor was designed to be roll-stabilized during flight, and therefore the off-center c.g. meant the rocket would develop a coning angle in flight. The coning effect meant that it had increased drag from the partially sideways attitude of the rocket. The increased drag resulted in failure to reach the target altitude.

4.3 Flow laminae and patterns.

The first of these two color photos below shows how laminae, created by a bottom casting process, remain in the same relative relationship to each other, even when passing through relatively sharp-edged, narrow clearances around a mandrel. Note that no visible remixing has occurred.

The second of the photos shows laminae present at locations within the tooling, where the tooling was not fully optimized for propellant flow.

Both of these photos emphasize the need to utilize proper casting tooling design as one of the ways to minimize demizing, and its effects upon all aspects of the rocket performance.

5. Summary and Conclusions:

5. 1 Everyone at all levels of involvement in the rocket motor design, development, and manufacturing process should be concerned about demixing.

5.2. All steps of the propellant manufacturing process are involved.

5. 3. No propellant is immune from demixing until it is in its final configuration, and within its service temperature range.

<u>The "Bottom line" is that if you allow the 'demon of demixing' the smallest opportunity, he can probably demix any propellant to the point that it will not meet the functional requirements.</u>

<u>The author's personal position</u>: The entire rocket motor and propellant creation process, from initial formulation work, all the way through to the final completed propellant grain is one, unified, integrated process, rather than a

series of isolated, unrelated activities, where the blame for non-ideality can be passed on to a different step in the series.

And, finally, two questions to this group:

1. How do we measure or define "good enough" mixing, recognizing that demixing will destroy the perfection we are seeking? The propellant creation process, from initial formulation work, all the way through the final processing of the grain into its desired configuration must be one integrated process.

2. How do we define a batch or lot when using a continuous process? Many propellant specifications now state that a batch is composed of all the ingredients in the mixer at one time. The author believes it is time, or even past time, to be addressing this aspect of continuous processing. Incorrectly worded specifications will invalidate all benefits of continuous processing, including the economies of continuous processing for large quantities, and the benefits of flexible manufacturing.

Thank you for the privilege of presenting these observations.

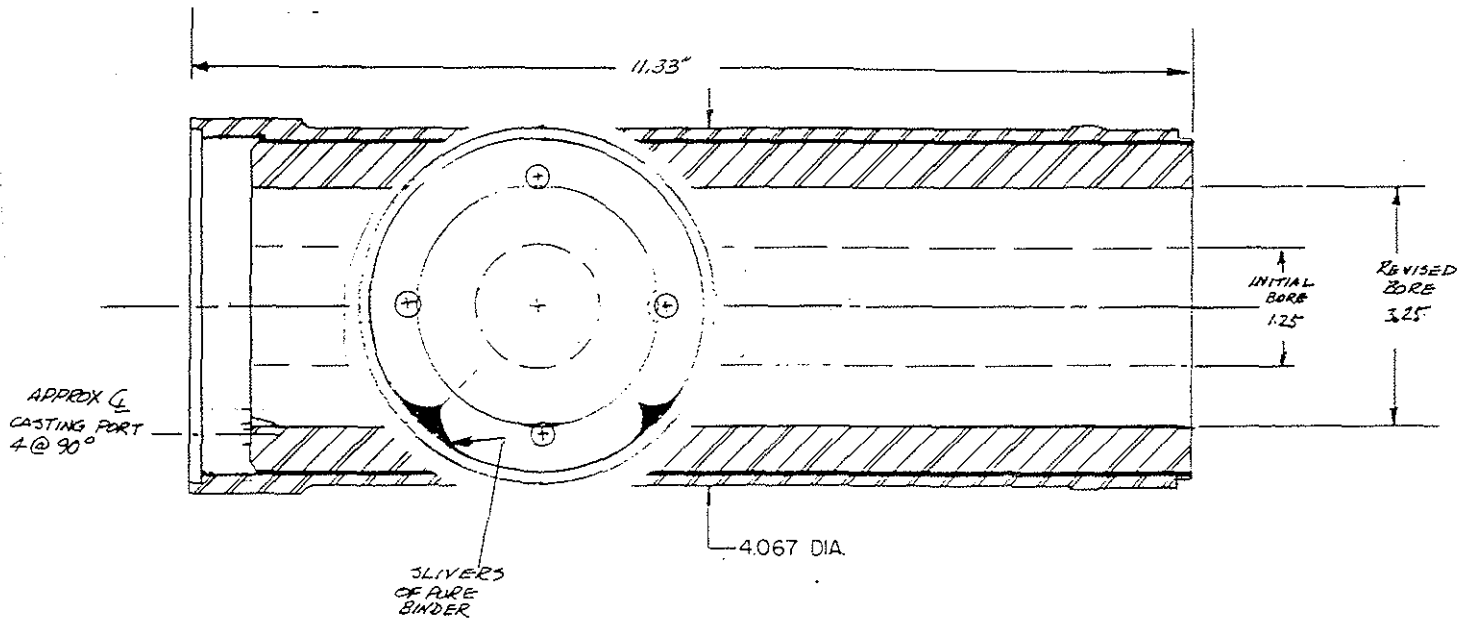
11.33"
INITIAL BORE 1.25
REVISED BORE 3.25
APPROX ℄ CASTING PORT 4 @ 90°
4.067 DIA.
SLIVERS OF PURE BINDER

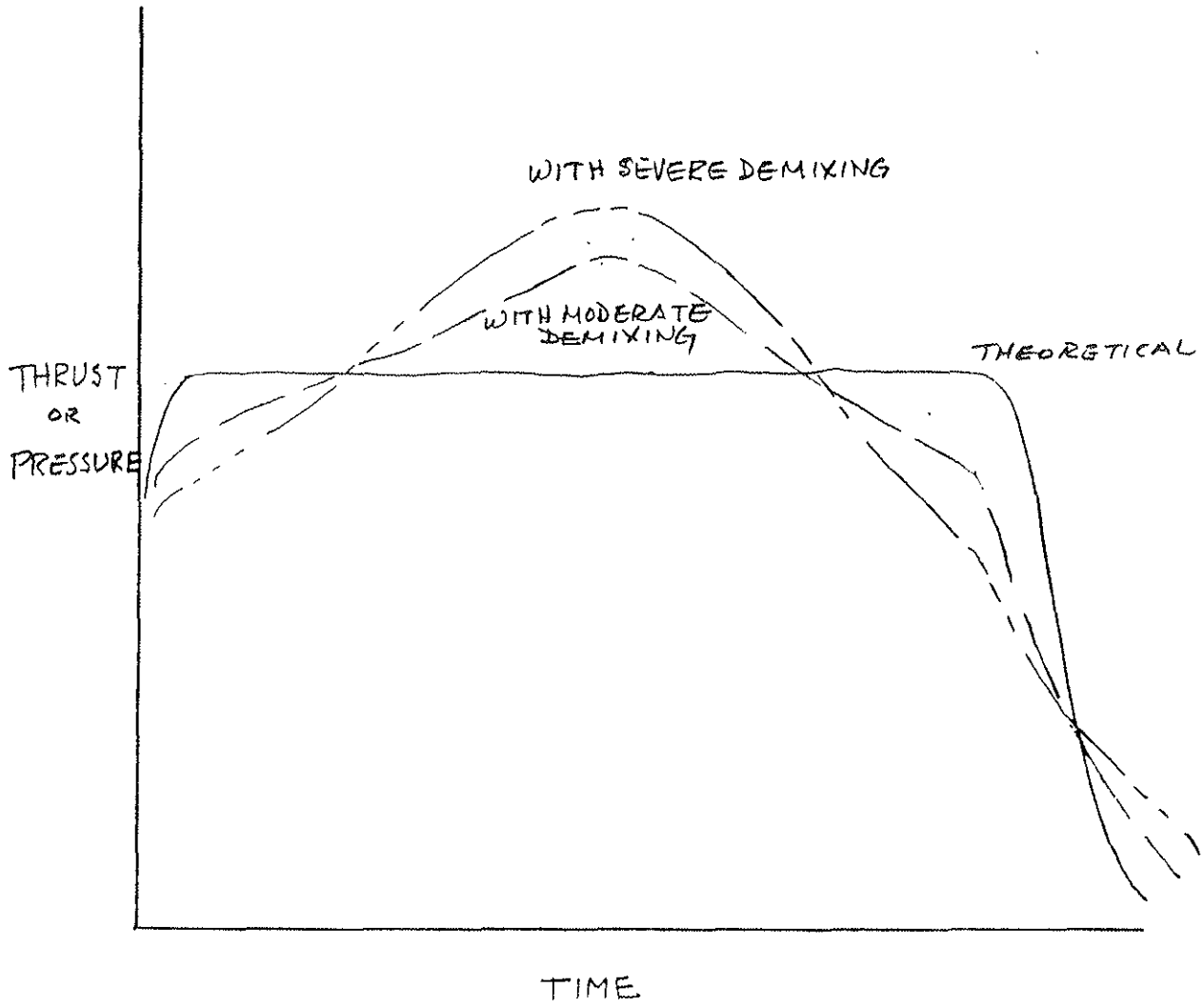
WITH SEVERE DEMIXING
WITH MODERATE DEMIXING
THEORETICAL
THRUST OR PRESSURE
TIME

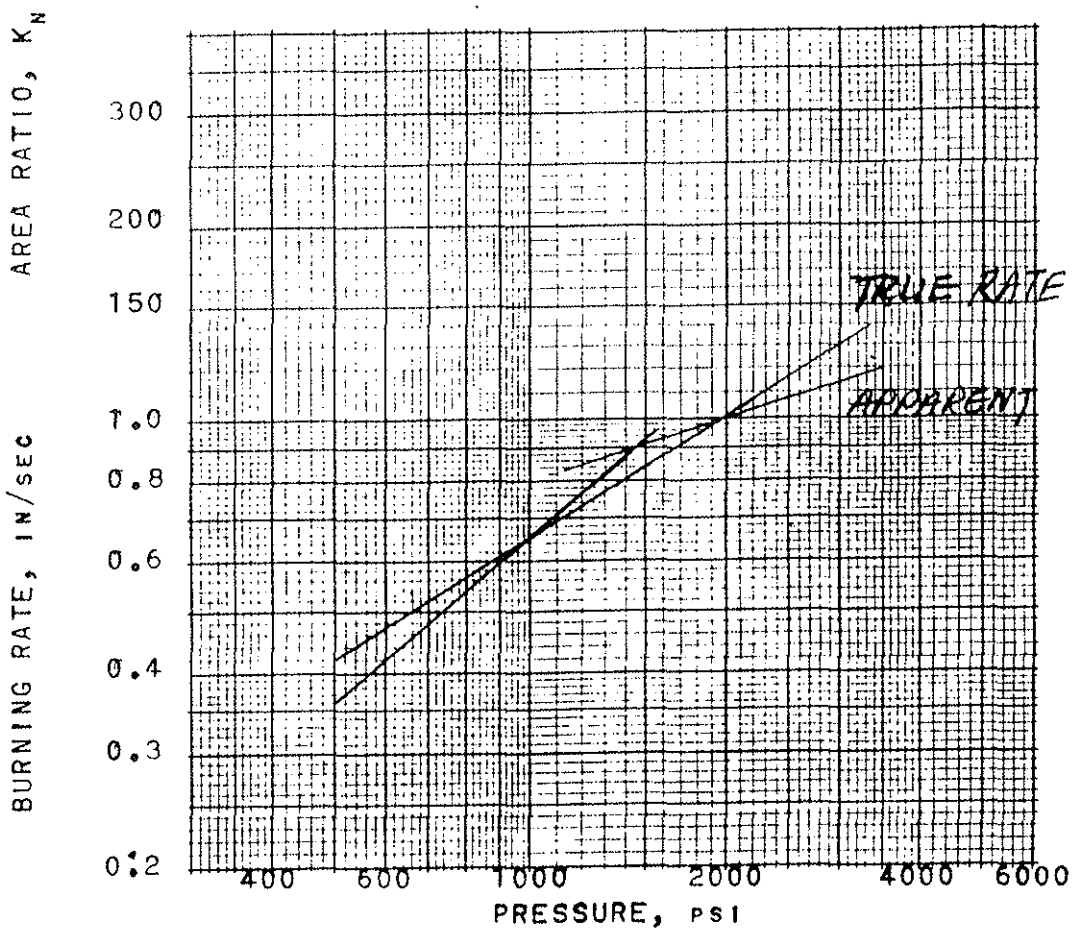
AREA RATIO, K_N
300
200
150
BURNING RATE, IN/SEC
1.0
0.8
0.6
0.4
0.3
0.2
400
600
1000
2000
4000
6000
PRESSURE, PSI
TRUE RATE
APPARENT

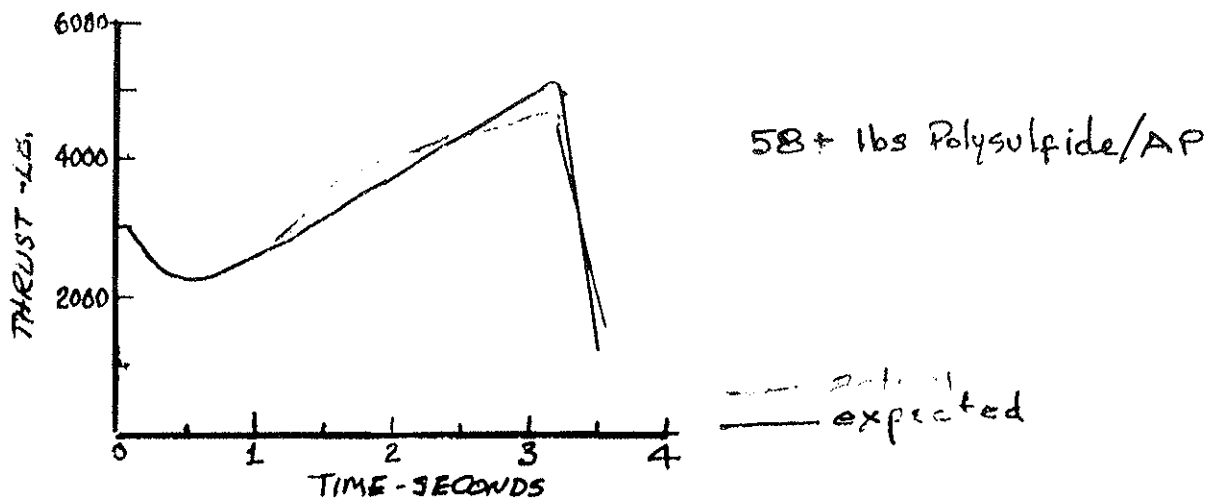

HOPI II 3.0 KS 4000

4.5 in. dia; 79.7 in. long

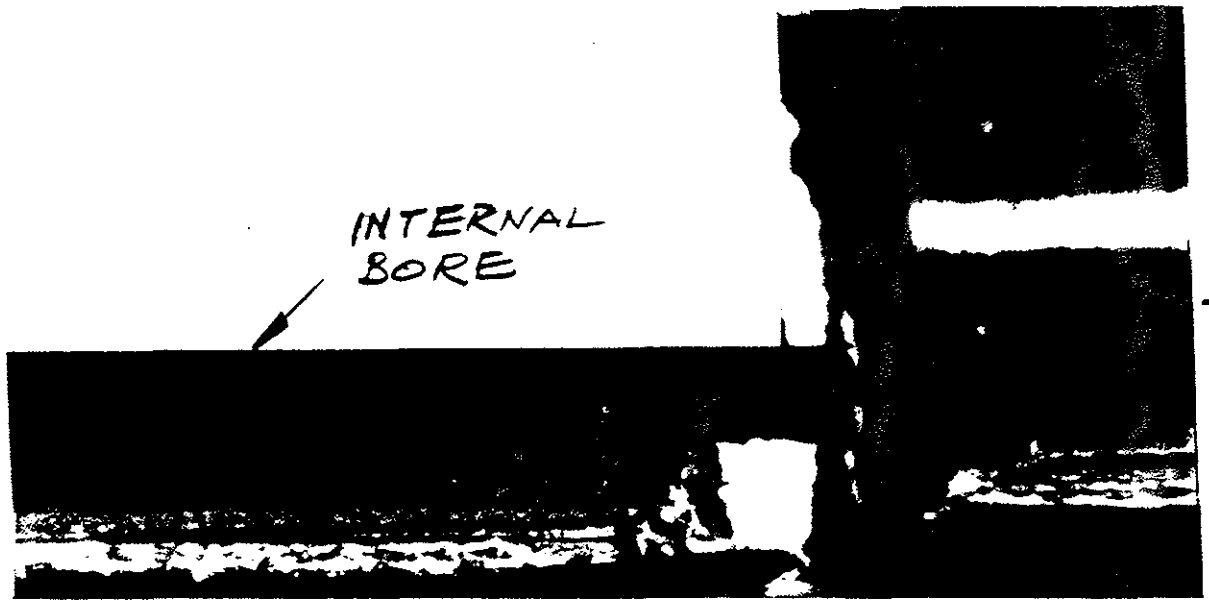

→ PROPELLANT FLOW

3M Flip-Frame
Transparency Protec
3M

3M

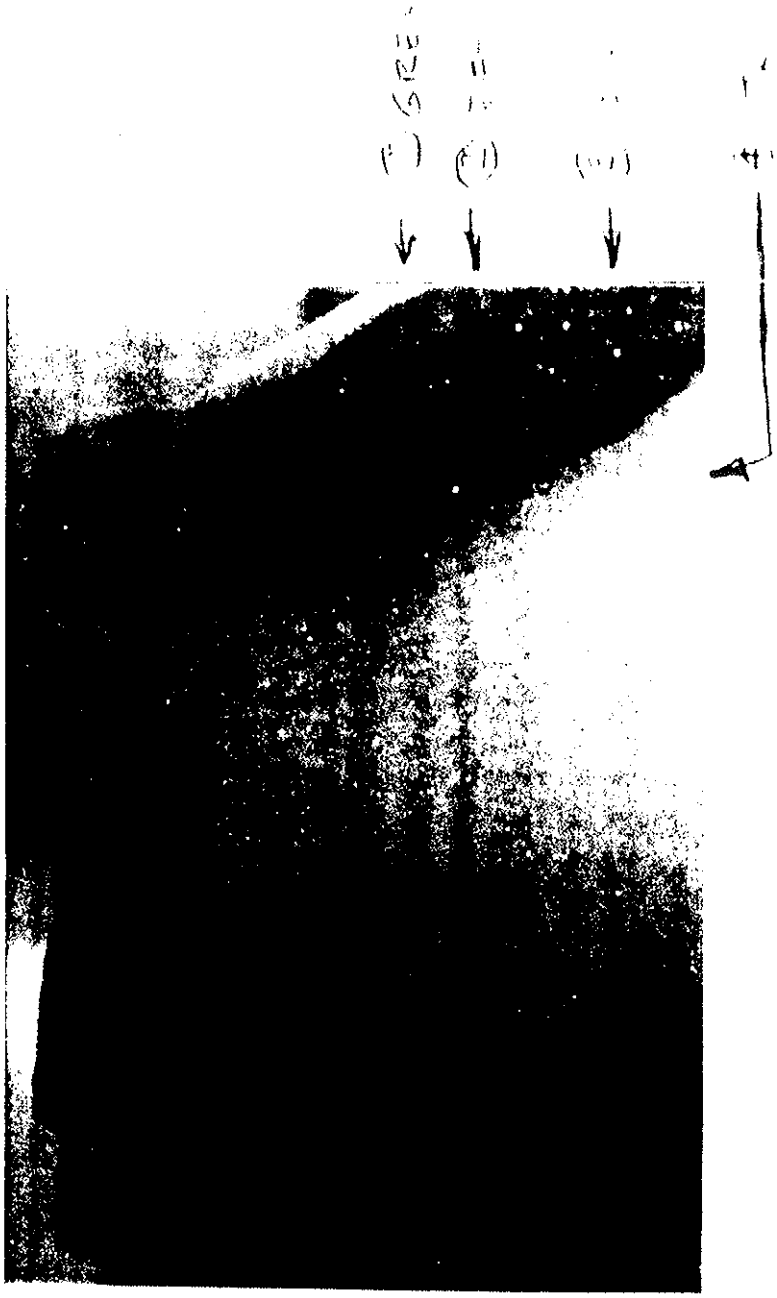

3M Flip-Fram
Transparency Prote